Plant Ecology and Evolution 143 (3): 365–377, 2010
doi:10.5091/plecevo.2010.420

REGULAR PAPER

Observations on the limnology and phytoplankton community of crater Lake Kyaninga (Uganda), with special attention to its diatom flora

Christine Cocquyt[1,2,*], Pierre-Denis Plisnier[3], Vanessa Gelorini[2], Bob Rumes[2] & Dirk Verschuren[2]

[1]National Botanic Garden of Belgium, Domein van Bouchout, BE-1860 Meise, Belgium
[2]Ghent University, Limnology Unit, K.L. Ledeganckstraat 35, BE-9000 Gent, Belgium
[3]Royal Museum for Central Africa, Leuvensesteenweg 13, BE-3080 Tervuren, Belgium
*Author for correspondence: christine.cocquyt@br.fgov.be

Background and aims – With a depth of at least 220 m, Lake Kyaninga is the deepest known maar crater lake in western Uganda. We studied its limnology and phytoplankton community to determine how the frequency and depth of water-column mixing influences nutrient cycling and seasonality in this aquatic ecosystem.
Methods – Water-column temperature was measured continuously during a full annual cycle between August 2007 and August 2008. Other physical and chemical variables as well as diatom and other phytoplankton communities were investigated on three occasions, namely during the dry season in August of 2007 and 2008, and during the main wet season in April 2009.
Key results and conclusions – The water column of Lake Kyaninga is permanently stratified (meromictic) below ~ 100 m depth. Above this depth, mixing frequency varies from daily (down to 8–12 m depth) over at least once per year (down to 39–47 m depth), to once in several years or decades (between 39–47 and ~ 100 m depth). Nutrient and chlorophyll concentrations as well as phytoplankton data classify the lake as low in aquatic productivity (oligotrophic). Its pelagic, open-water phytoplankton community is dominated by Cyanobacteria (blue-green algae) and Chlorophyta (green algae). Bacillariophyta (diatoms) contribute only a minor part of total phytoplankton biomass in both wet and dry seasons, and are characterized by an assemblage of small *Nitzschia* species. Epiphytic and epipelic diatoms are relatively few, because steep rocky crater slopes limit the littoral zone even though water-column transparency is high. The composition of recently deposited diatom assemblages preserved in offshore surface sediments gives a good, annually integrated representation of the present-day pelagic diatom community. The documented species richness of the diatom flora of Lake Kyaninga is moderate with about 150 taxa. Only ~ 17% of these are biogeographically restricted to tropical Africa; and most of these belong to the genus *Nitzschia*.

Keywords – Africa, crater lakes, diatoms, lake dynamics, phytoplankton, Uganda.

INTRODUCTION

Lake Kyaninga (00°41.85'N 30°17.86'E) is a relatively large (24 ha) and very deep (> 220 m) maar crater lake situated at 1530 m above sea level on the shoulder of the Edward-George extension of the western branch of the East African Rift System, in western Uganda. The local equatorial climate is tropical sub-humid (Fort Portal mean annual rainfall 1903–1980 = 1484 mm) with little seasonal variation in monthly temperature (T_{min}: 11.7–13.7°C; T_{max}: 24.5–26.8°C), and two wet seasons (March–May and late August to November) and two drier seasons (December–February and June to mid-August; fig. 1) associated with the twice-annual migration of the Intertropical Convergence Zone (ITCZ) over the area. The crater catchment of 42 ha is enclosed by a crater rim reaching up to 77 m above the present-day lake surface. The lake consists of a deep northern basin (> 220 m) and a shallower southern basin (58 m), both with mostly very steep sloping shores. Lake Kyaninga is one of 48 fresh crater lakes in western Uganda studied in the framework of the comprehensive research programme CLANIMAE (Climatic and Anthropogenic Impacts on African Ecosystems), which investigates the relationship between the limnological environment of these crater lakes and their vulnerability to water-quality loss caused by anthropogenic disturbance of their catchment vegetation and soils. Study lakes were selected along gradients

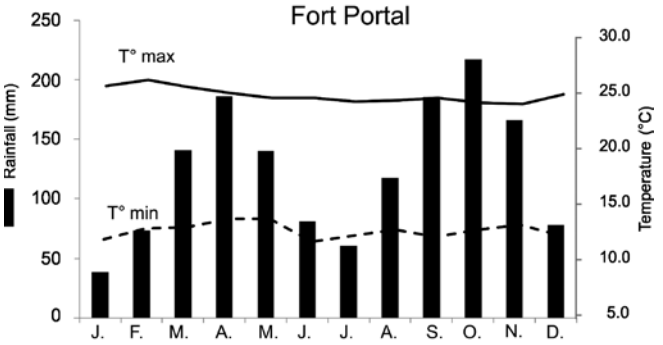

Figure 1 – Monthly rainfall (mm), and monthly average maximum (daytime) and minimum (nighttime) air temperature at Fort Portal, 7 km south of Lake Kyaninga.

from low to high primary productivity (oligotrophic to hypertrophic) and from virtually non-existent to intense human activity within their crater catchments. One aim is to develop a multivariate statistical transfer function for reconstruction of past changes in lake productivity based on the species composition of fossil diatom assemblages preserved in the bottom sediments of African lakes. Lake Kyaninga is among a subset of study sites where besides the diatom flora the entire phytoplankton community was examined during both dry and wet seasons, and where a direct comparison was made between the present-day diatom flora and its representation in recently deposited diatom assemblages preserved in the lake's sedimentary record.

MATERIAL AND METHODS

Physical and chemical limnology

Lake Kyaninga was visited three times between August 2007 and April 2009 to measure depth profiles of temperature (T in °C), pH, dissolved oxygen (DO in mg/l) and conductivity (K, specific conductivity in µS/cm at 25°C) through the water column. Measurements were obtained either continuously (with a Seabird®19 CTD profiler in August 2007 and April 2009), or at discrete 1-meter intervals (with a Hydrolab Quanta® multi-sensor probe in August 2008). Inter-calibration had previously shown the results from these instruments to be fully interchangeable. When DO content is low (< 0.5 mg/l), the DO sensors on both instruments may take ~ 10' to achieve the correct value even when providing continuous flow with a built-in propeller. Therefore, values dropping below 0.5 mg/l were assumed to reflect anoxic (0.0 mg/l) conditions. On 2 Aug. 2007 we installed a series of Vemco® automatic loggers to record temperature at 3, 15, 30 and 57 m water depth at 2h intervals, and from these data we derive the timing of deep seasonal mixing. The depth of daily, seasonal, and low-frequency water-column mixing was estimated from the mid-point of prominent inflections common to the vertical profiles of T, pH, K and DO.

Water transparency (SD, in cm) was measured with a standard white Secchi disc of 20 cm diameter. The depth of the euphotic zone (Z_{eu}, where light is 1% of that just below the water surface) was estimated as 1.9 times SD (Vollenweider 1974). We estimated water-column stability using the potential energy anomaly (PEA) for fresh water according to Simpson et al. (1982). The probability of nutrient-rich hypolimnetic water re-circulating to the surface is increased when PEA is low. The total stability of the lower water column is enhanced by the density increase due to accumulation of dissolved salts (K= 1585 µS/cm at 200 m), but unknown details of deep-water chemistry do not allow to quantify this additional chemical stability at this time.

For water sampling at depth we used a Hydrobios® Niskin-type bottle of 2 l volume. Water samples were kept cool (4°C) in the field, and nutrients were analysed the same day using a Hach Lange DR2800 spectrophotometer. Total phosphorus (TP, in mg/l) and total nitrogen (TN, in mg/l) concentrations were determined using quartz-cuvette tests following hydrolysis. Dissolved silica (Si, in mg/l) was analysed upon return to Belgium, using inductively-coupled plasma atomic emission spectrometry. Chlorophyll *a* (Chl *a*, in µg/l) concentrations were measured at the surface and at 10, 25 and 160 m depth. For this purpose between 400 and 700 ml of water was filtered using a Nalgene filtration unit and GF5 Macherey Nagel glass fiber filters of 45 mm diameter. The filter was extracted by placing it for 24 hours in a tube containing 5 ml of 90% acetone, at 4°C. The extracted solution was filtered using a syringe with encapsulated filter into a 5-cm spectrophotometric cell. The Chl *a* concentration was calculated from the absorption value at 665 nm with a DRELL 2800 spectrophotometer after zeroing with pure acetone.

Phytoplankton

The present-day living algal community of Lake Kyaninga was sampled by filling a 50 ml bottle, and fixed in situ with an alkaline lugol solution and formalin. These samples were analyzed quantitatively (excluding the picophytoplankton) following Uthermöhl (1931) using an Olympus CKX41 inverted microscope equipped with an Olympus Color View digital camera. We studied six quantitative phytoplankton samples: mid-lake pelagic phytoplankton from near the water surface collected on 2 Aug. 2007 and 18 Aug. 2008, and from near the water surface, 10 and 25 m water depth collected on 15 Apr. 2009; and a near-shore open-water phytoplankton sample also collected on 15 Apr. 2009. Additionally four samples for semi-qualitative diatom analyses (counts and identifications) were collected. Two are pelagic phytoplankton samples from a mid-lake location, collected with a phytoplankton net (mesh 10 µm) on 2 Aug. 2007 and 15 Apr. 2009. The others are a littoral epiphyton sample from submerged *Phragmites mauritianus* Kunth stems, and an epipelon sample scraped from submerged rocks, both collected on 15 Apr. 2009.

The time-integrated diatom assemblage preserved in recently deposited bottom sediments was analyzed in the 0–1, 1–3 and 3–5 cm intervals of two UWITEC gravity cores recovered on 10 Jan. 2007. Both cores were taken in the shallower southern basin, KYANINGA-07-1G at 58 m depth in the deepest part of this basin and KYANINGA-07-2G near the southern shore at 5 m depth; the cores were extruded upright in watertight plastic bags using a fixed-interval sectioning device (Verschuren 1993). The sediment samples were oxidized with peroxide to remove organic material, and embedded in Naphrax® to obtain permanent microscope slides.

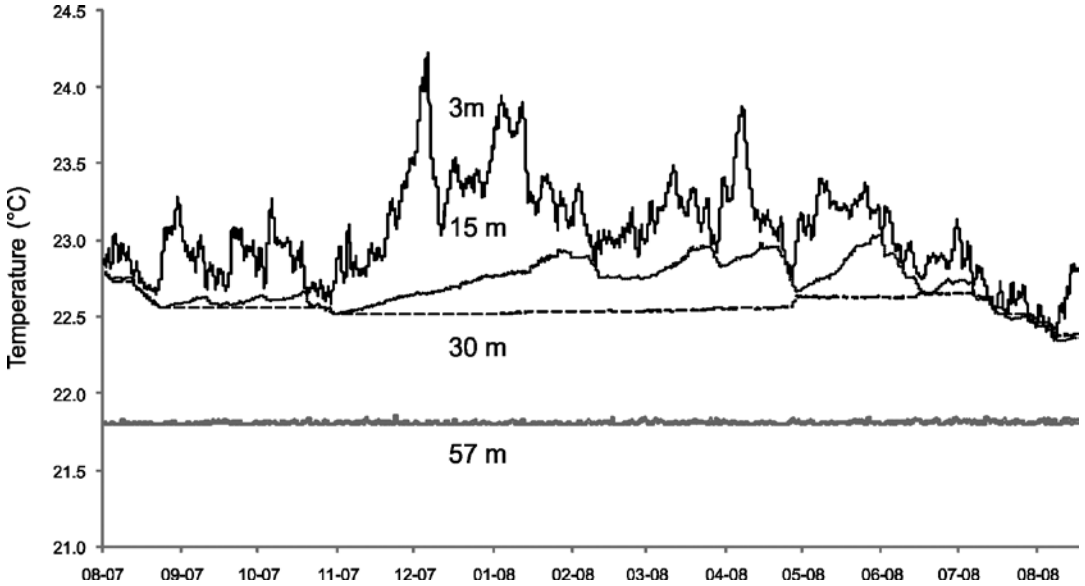

Figure 2 – Temperature measured by 4 temperature loggers every two hours from 2 Aug. 2007 to 18 Aug. 2008 at four depths (3m, 15 m, 30 m and 57 m) in the water column in the south basin of Lake Kyaninga.

Samples and permanent slides are kept at the herbarium of the National Botanic Garden of Belgium (BR). Identification of diatom taxa was performed using an Olympus BX 51 light microscope equipped with differential interference contrast at a magnification of 1000× and an Olympus Color View digital camera. For some problematic taxa, a small fraction of the oxidized suspension was gold-coated with a sputter coater SCD 020 and studied with a JEOL 5800 scanning electron microscope (SEM) operating at 25 KV. Identification of the phytoplankton taxa was done with reference to Compère (1974, 1976), Huber-Pestalozzi (1941, 1955), Huber-Pestalozzi & Fott (1968), Komárek (2008), Komárek & Fott (1983), Komárek & Anagnostidis (1999, 2005), Komárek & Jankovska (2001), Popovský & Pfiester (1990), Starmach (1985), Van Meel (1954) and other works. For diatoms we also referred to Cholnoky (1960, 1964, 1968, 1970a, 1970b), Cocquyt (1998, 2007), Gasse (1986), Hustedt (1949) and Müller (1905). The relative abundance of diatom taxa is expressed in percentages relative to total counts of 500 valves. Statistical data analysis, e.g. Pearson correlation coefficients on relative species abundances, was done using STATISTICA 6.0 software.

RESULTS

Water-column stratification and mixing

The water column of Lake Kyaninga displays both thermal and chemical density stratification (figs 2–4), and the typical multiple–thermocline structure of tropical lakes which reflects the decreasing frequency of water-column mixing with depth (Lewis 1983, 1987). Daytime temperature stratification due to solar heating of the water surface under wind-calm conditions was typically limited to the uppermost 2–4 m (fig. 3A), and very often followed by mixing due to wind-driven evaporative cooling and/or nighttime surface cooling followed by convection (fig. 2). The more or less daily cycle of this surface stratification and de-stratification typically extends to between 9 and 12 m water depth, as can be deduced from the near-constant pH values over at least this depth range on 18 Aug. 2008 and 15 Apr. 2009 (fig. 3D). This frequently mixed uppermost part of the water column is bounded below by a first and principal thermocline (fig. 3A), below which temperature varies only on longer time scales (fig. 2; 15 m). Physical separation of this uppermost water column (epilimnion) from deeper water is indicated by the notably reduced conductivity values in the uppermost 12 m on 15 Apr. 2009 (fig. 3B: 436 µS/cm vs. ~ 460 µS/cm deeper down). This lower surface conductivity is due to dilution of the epilimnion following significant rainfall over the crater catchment in the days (or less likely, weeks) before the profiling. Frequent complete mixing of the epilimnion also maintains high (> 5 mg/l) and often near-constant DO concentrations over this interval (fig. 3C). The DO profile of 15 Apr. 2009 displays a strong subsurface maximum between 9 and 12 m depth, suggesting elevated photosynthetic activity in that zone. This positive heterograde profile (Kalff 2002) may be related to the high water-column transparency on 15 Apr. 2009 compared with that in August of 2007 and 2008 (table 1: SD = 605 cm vs. 390–470 cm), causing the euphotic zone to extend to about 11.5 m rather than 7.4–8.9 m and allowing a sub-surface maximum in photosynthetic activity.

In the course of the annual cycle between August 2007 and August 2008, sustained warming of the epilimnion of Lake Kyaninga occurred only during a ~ two-month period from mid-November to mid-January, i.e. largely coincident with the dry season of December-January. Even then warming was limited to a modest 1.0–1.5°C (fig. 2) with peak surface temperature of 24.3°C reached in early December. Over this period also water below the principal thermocline warmed up gradually, by ~ 0.3°C at 15 m depth (fig. 2). From mid-January, surface cooling followed by convective and/or wind-driven mixing started to gradually erode the principal thermocline until around 10 February it was temporarily annihilated and deeper mixing cooled the upper water column

Table 1 – Limnological data at various depth (m).
Water temperature, pH, conductivity (K_{25}), dissolved oxygen (DO), anoxic depth, potential energy anomaly (P.E.A.), total phosphorous (TP), total nitrogen (TN), silica ($Si0_2$ as Si), alkalinity (as $CaCO_3$), chlorophyll a and Secchi disk transparency at Lake Kyaninga at three periods (< DL = below detection limit).

			2 Aug. 2007	18 Aug. 2008	15 Apr. 2009
temperature	° C	surface	23.10	22.40	24.25
		25 m	22.80	22.30	22.45
		160 m	-	-	21.00
pH		surface	8.20	7.99	8.50
		25 m	8.10	7.74	7.80
		160 m	-	-	6.00
K25	µS/cm	surface	429	462	436
		25 m	429	460	459
		160 m	-	-	1394
DO	mg/l	surface	5.10	6.30	9.10
		25 m	4.70	2.80	0.00
		160 m	-	-	0.00
anoxic depth	m		38	46	25
P.E.A.	J m^{-3}		0.102	0.217	0.835
TP	mg/l	surface	0.07	0.02	< DL
		160 m	-	0.50	0.58
TN	mg/l	surface	-	0.27	0.07
		160 m	-	1.03	1.74
SiO_2	mg/l	surface	12.90	15.60	14.02
		160 m	-	27.89	25.63
alkalinity	mg/l	surface	-	-	220
		10 m	-	236	223
		25 m	-	-	230
		160 m	-	748	753
Chl a	µg/l		5.24	9.27	3.49
Secchi depth	cm		470	390	605

to below 15 m depth (fig. 2). Similar cycles of epilimnetic stratification and de-stratification, and of gradual warming and abrupt cooling below the depth of the principal thermocline, were repeated through the main wet season from March to May. One particularly prominent but short-lived surface-cooling event to 22.7°C at the end of April even caused mixing to below 30 m, but stratification was restored soon after. After mid-June only weak stratification developed, such that when in mid-July, i.e. during peak dry season, the water-surface temperature consistently dropped below 22.6°C, a period of near-continuous deep mixing ensued. Ending on 10 August, this deep mixing set the water-column temperature at 30 m (and at 15 m) depth to 22.3°C, ~ 0.2 °C below its lowest value in the previous 12 months. However, this is still 0.5°C above the constant temperature of 21.8°C at 57 m depth. Our temperature-logger data show no evidence that Lake Kyaninga ever mixed to the bottom of the south basin between 2 Aug. 2007 and 18 Aug. 2008.

The temperature-logger data provide the context which helps to interpret the profiles of temperature and other physical variables measured at the start and end of the logging period, and in April 2009. With the exception of modest temperature stratification at the surface (fig. 3A), values for temperature, DO and pH on 2 Aug. 2007 are homogeneous down to ~ 35 m water depth; for temperature we note the identical value of 22.8°C at 15 and 30 m (fig. 2). This suggests that shortly before logging started an event of deep seasonal mixing occurred, which injected fresh oxygen to a depth of 37 m and created a distinct deep thermocline at 39 m (fig. 3A). Similarly, sustained deep mixing during the July-August 2008 dry season extended to at least 47 m (fig. 3A & C), but by 18 Aug. 2008 a new principal (seasonal) thermocline (and oxycline) had already formed around 9 m depth. The 0.5°C higher temperature of the water column from immediately above the deep (annual) thermocline in August 2007 compared to August 2008 suggests that the July–August dry season of 2007 was warmer, or less windy, than the 2008 dry season. This inference can also be drawn from the observation that water above the deep thermocline in August 2008 has higher conductivity and lower pH, i.e. more similar to values in the lower water column, consistent with the notion that 2008 mixing has entrained water from greater depths. This is confirmed by the greater depth of the deep thermocline in August 2008 (47 m), compared with August 2007 (39 m). The conductivity and pH of this mid-depth water column remained quite stable between August 2008 and April 2009.

During the rain-season profiling in April 2009, three thermoclines occurred within the upper water column of Lake Kyaninga (fig. 3A): one around 45 m that formed following the deepest mixing of the most recent dry season, a modest secondary thermocline at 21 m, and the principal thermocline at 12 m depth that separates the epilimnion from the deeper water column. Comparable to evidence for intermittent mixing in the logger data of the previous year, the secondary thermocline likely represents one or more occasional events of deeper mixing which occurred earlier during the March-to-May rain season, or at least after the main mixing phase of the previous dry season. Their effect on DO concentration within this depth zone is evident in fig. 3C. Below 20 m the water column was anoxic, because its supplies had not been replenished for up to eight months and had by then been exhausted by bacterial respiration. The DO gradient between 20 and 12 m is created by the shifting balance between the rate of oxygen consumption in the lower water column and the frequency of oxygen replenishment by down-welling of epilimnetic water.

The variable thermal structure of the upper 40 m of the Lake Kyaninga water column during our three surveys (fig. 3A) is translated in strikingly variable PEA values: upper-water thermal stability was four times stronger during the rain-season survey in April 2009 than in August 2008 and eight times stronger than in August 2007 (table 1).

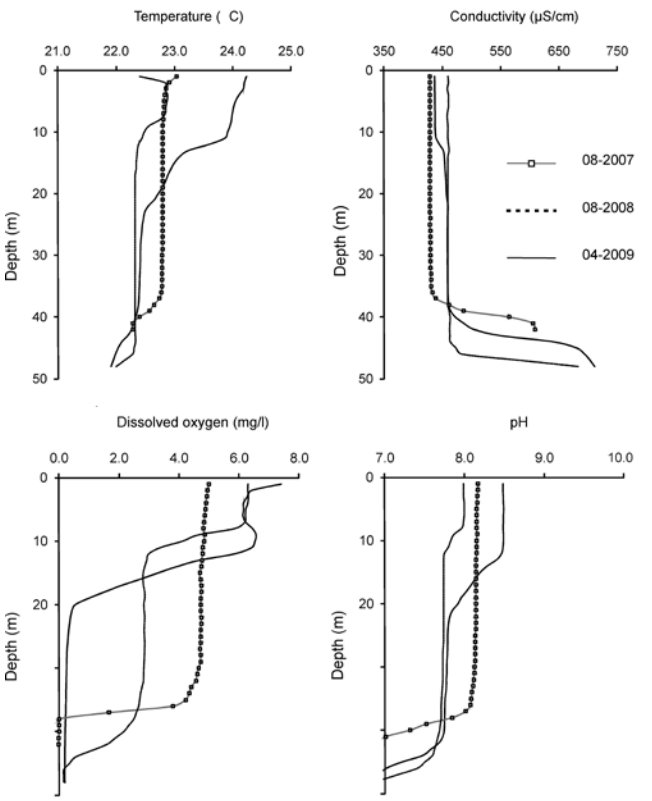

Figure 3 – Upper water-column (0 to 50 m) profiles of: A, temperature (°C); B, specific conductivity (µS/cm); C, dissolved oxygen (mg/l); D, pH. Measurements were made on 2 Aug. 2007, 18 Aug. 2008 and 15 Apr. 2009 at Lake Kyaninga.

During all three surveys a sharp increase in conductivity, from ~ 450 to 750 µS/cm, was observed between 40 and 47 m depth. Water temperature below this level drops below 22°C (see also fig. 2) and decreases further to a minimum of 20.8°C near 120 m depth (fig. 4). Below 75 m also conductivity further increases with depth, to cross 1000 µS/cm at ~ 120 m, reach a stable level of 1400 µS/cm between 160 and 185 m, and then rise again to ~ 1600 µS/cm at 200 m depth. Successful mixing of this deep water column requires downwelling water to overcome both the greater density due to low temperature (at 120 m, ~ 1.5°C below the present-day annual minimum of 22.3°C) and the greater density due to the higher concentration of dissolved substances. For example, the alkalinity of water at 160 m is 3.4 times higher than at the surface (table 1). Based on the entire temperature profile from the deep northern basin (fig. 4) we surmise that such very deep mixing occurs occasionally down to ~ 80 m (reflected in a modest thermocline at that depth), exceptionally even down to ~ 100 m. The recurrence frequency of these very deep mixing events is hard to estimate. Considering that the total density difference (i.e. due to both temperature and dissolved substances) between 40 and 80 m depth is equivalent to a reduction in surface-water temperature of ~ 3.0°C below the present-day annual minimum, we surmise that the frequency of such very deep mixing events is on the order of decades or even centuries, rather than years. It is certainly not a regular annual phenomenon, as testified by the strong H_2S smell of water brought up from below 50 m. Based on our observations we thus conclude that the water column of Lake Kyaninga is probably meromictic (permanently stratified) below ~ 100 m depth, oligomictic (mixing infrequently) down to 80–100 m, and mixing at least once each year down to between 39 and 47 m. Our logger data indicate that deepest mixing occurs during the main dry season of June to early August (fig. 1), and that intermittent deep mixing also punctuates the wet seasons of March to May and late August to November. During our year of observation, most pronounced lake-surface heating and stratification of the upper water column occurred during the dry season of December to February, notwithstanding low seasonal insolation and the lowest monthly day- and nighttime air temperatures (fig. 1).

Below 140 m water depth we measured a slight temperature increase, to a stable value of 21.0°C at 160–190 m and 21.2°C at 200 m. Corresponding with changes in conductivity and pH (fig. 4), this elevated near-bottom temperature is probably due to geothermally heated groundwater inflow into the lake. Geothermal activity has been reported to exist in the region, as close as 12 km from Lake Kyaninga (Bahati et al. 2005). Formation of bubbles upon recovery of water from 160 m is a probable consequence of its high dissolved CO_2 content. Echo-sounding of the lake's bathymetry also showed plumes of bubbles rising to the surface.

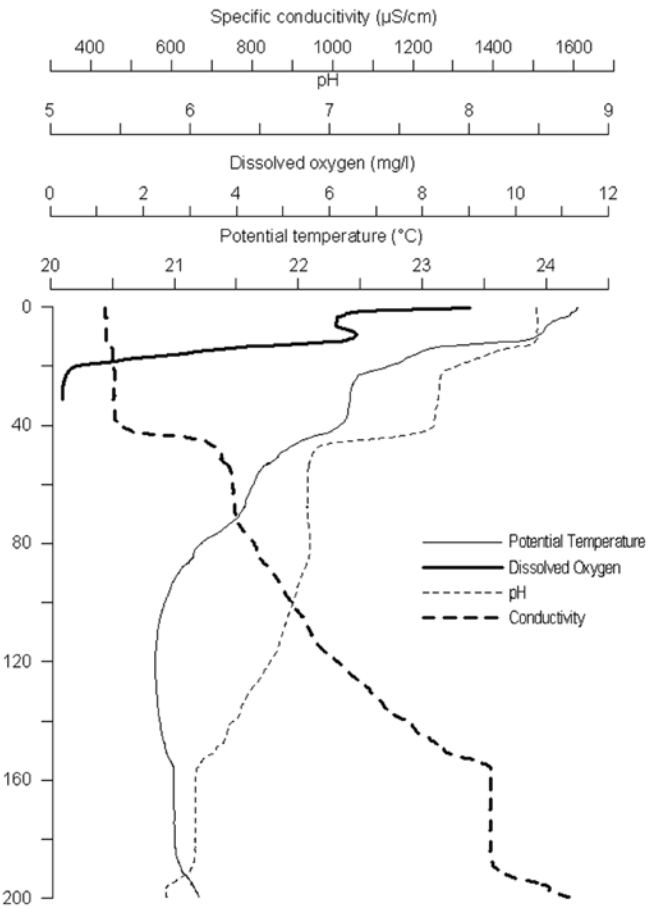

Figure 4 – Profiles (0 to 200 m) of temperature (°C), dissolved oxygen (mg/l), pH and specific conductivity (µS/cm) on 15 Apr. 2009 in the deep basin of Lake Kyaninga.

Table 2 – Phytoplankton abundance.
Expressed in cells/ml and in biomass (µg/l) from 3 differences depths (0, 10 and 25 m) on 15 Apr. 2009 at Lake Kyaninga, as derived from cell counts and biovolume calculations.

	cells/ml			biomass (µg/l)		
depth	0 m	10 m	25 m	0 m	10 m	25 m
Cyanobacteria	10000	11000	48000	8.22	1.125	2.07
Chlorophyta	700	800	2000	2.35	0.72	1.72
Euglenophyta	20	0	0	0.03	0	0
Dinophyta	70	0	0	1.03	0	0
Chrysophyta + Cryptophyta	30	0	300	0.12	0	0.47
Diatoms	50	20	0	0.24	0.15	0

Nutrient data show high TP, TN and Si values in the hypolimnion (table 1), consistent with their long-term accumulation in a stratified water column. The molar TP:TN ratio of the surface water (12.1) is slightly below the Redfield TP:TN ratio of 16 for phytoplankton (Redfield 1958, Teubner & Dokulil 2002), suggesting that algal productivity in Lake Kyaninga is limited by a shortage of nitrogen. Surface-water SiO_2 concentrations do not differ much between mixing and stratified seasons, and molar ratios TP:Si (0.001 to 0.005) and TN:Si (0.01 to 0.03) indicate no limitation of silica for diatom growth (Roberts et al. 2003).

Temporal variation in phytoplankton composition

Chlorophyll *a* measurements indicate that phytoplankton biomass in surface waters of Lake Kyaninga was low (3.49 µg/l) during the rain season in April 2009 and higher during the dry season of 2007 (5.24 µg/l) and particularly 2008 (9.27 µg/l). This is consistent with variation in water-column transparency being inversely proportional to Chl *a* values, and with the surface-water TN and TP concentrations, which are also lowest in April 2009 (table 1). Low algal productivity in April 2009 can be attributed to a shortage of essential nutrients due to their inefficient recycling from algae that decompose after sinking out of the stratified upper water column. Productivity was only modestly higher during deep water-column mixing on 2 Aug. 2007, but substantially higher in the period following deep mixing on 18 Aug. 2008. We propose two alternative explanations for this difference. During mixing events algal cells may spend too much time below the photic zone to allow rapid growth, whereas incipient stratification in the weeks following deep mixing (figs 2 & 3A) creates a stable sub-surface environment where algae can optimally benefit from the newly available nutrient supply. To the extent that our two dry-season surveys are representative, an alternative (or additional) reason for the observation of highest productivity in August 2008 may be the deeper mixing which occurred that year compared to the year before, and hence a greater supply of recycled nutrients being provided.

The depth distribution of pelagic phytoplankton in Lake Kyaninga was quantified only in April 2009, with volumetric cell counts near the surface and at 10 and 25 m water depth (tables 2 & 3). Since 25 m is well below the photic depth at that time (~ 11 m), the high abundance of (mostly small) cyanobacteria at that depth must represent dying cells sinking slowly into the cooler, and thus denser hypolimnion. The by far highest biomass (in µg/l) was observed near the surface; the lowest at 10 m depth. This result argues against the existence of a sub-surface phytoplankton maximum as principal explanation for the heterograde oxygen profile during that time (fig. 3C).

The phytoplankton of Lake Kyaninga is dominated by a Cyanobacteria-Chlorophyta community both in mid-lake and near-shore zones, and at mid-lake both during stratified and mixing seasons (table 3, based on biovolume calculations). Chlorophyta were the most important group during deep annual mixing in 2007, whereas Cyanobacteria dominated during the stratified season in April 2009; a few weeks after deep annual mixing in August 2008 the two groups' percent abun-

Table 3 – Phytoplankton abundance (%).
Relative abundance (%) of the algae groups in the pelagic zone of Lake Kyaninga in August 2007, August 2008 and April 2009, and in the near-shore zone in April 2009, derived from biomass calculations.

Date	2 Aug. 2007	18 Aug. 2008	15 Apr. 2009			
Depth	0 m	0 m	0 m	10 m	25 m	littoral
Cyanobacteria	33.6	30.9	68.7	92.7	48.6	73.7
Chlorophyta	63.7	44.3	19.6	6.0	40.5	18.9
Euglenophyta	0.2	0.0	0.2	0.0	0.0	0.0
Dinophyta	1.5	3.2	8.6	0.0	0.0	2.2
Chrysophyta	0.0	1.1	0.9	0.0	9.6	0.0
Cryptophyta	0.1	0.0	0.0	0.0	1.3	0.5
Diatoms	0.9	20.4	2.0	1.3	0.0	4.0

dance was more similar to each other. Diatoms were a minor component of the phytoplankton community, but contributed 20% to total biovolume in August 2008 when nutrients had just been replenished and the water column had started to stratify. The most important diatom taxa at this time were *Urosolenia* sp., *Nitzschia* spp. and *Cyclotella* spp. (see below). Excluding picocyanobacteria, which are not abundant in our samples, about eighteen taxa of Cyanobacteria were found. The most abundant of these are *Planktolyngbya limnetica* (Lemmerm.) Komárk.-Legn. & Cronberg, *Cylindrospermopsis raciborskii* (Wołosz.) Seenayya & Subbaraju, *Aphanizomenon* sp., *Aphanocapsa* sp. and *Aphanothece* sp. *Merismopedia minima* Beck, *Merismopedia tenuissima* Lemmerm. and *Snowella* cf. *lacustris* (Chodat) Komárk. & Hindák are less abundant, but still significant. The Chlorophyta are represented by about 25 taxa, among which *Tetraedron minimum* (A.Braun) Hansg., *Monoraphidum irregulare* (G.M.Sm.) Komárk.-Legn., *M. komarkovae* Nygaard and *M. circinale* (Nygaard) Nygaard are most abundant, and *Monoraphidium dybowkii* Hindák & Komárk.-Legn., *M. griffithii* (Berk.) Komárk.-Legn., *M. minutum* (Nägeli) Komárk.-Legn., *Chlorella* sp., *Crucigenia tetrapedia* (Kirchn.) W.West & G.S.West, *C. quadrata* C.Morren, *Quadrigula* sp., *Scenedesmus quadricauda* (Turpin) Bréb. and small *Cosmarium* spp. less abundant. The most common Dinophyta, Euglenophyta and Chrysophyta are respectively *Peridinium africanum* Lemmerm., *Euglena pisciformis* var. *minor* Hansg. and *Ochromonas variabilis* Meyer.

Diatoms

In total around 130 diatom taxa were identified in all ten living samples (phytoplankton, periphyton and epipelon) collected in Lake Kyaninga during 2007, 2008 and 2009. Scanning electron microscopic pictures of some of these taxa are given in fig. 5. The percent abundance of the twenty most important taxa, reaching 5% in at least one sample, is listed in table 4. Total diatom species richness in the five surface-sediment samples was about 75 taxa, of which 22 were not observed in the living samples. These additional taxa were all only sporadically observed, except *Sellaphora seminulum* which reaches 33.1% in the 1–3 cm interval of near-shore core 07-2G and *Staurosira construens* which amounts to 19% in the 3–5 cm interval of core 07-1G (table 4), and further *Epithemia sorex* Kutz. (1.6% in the 0–1 cm interval of near-shore core 07-2G) and *Nitzschia mediocris* Hust. (1.4% in the 0–1 cm interval of mid-lake core 07-1G). The diatom species richness of Lake Kyaninga is substantially higher than that found in Lake Kaitabarago, located about 4 km to the west, where in February 2008 only 28 taxa were found in living mid-lake and near-shore phytoplankton samples, and only seventeen taxa were recovered from a comparable volume of surface sediments (Cocquyt & Verschuren 2009).

Of the diatom taxa reported from Lake Kyaninga, only 22 (~ 17%) can be considered to have a tropical-African distribution. Most of these belong to the genus *Nitzschia*: *N. accomodata* Hust., *N. adapta* Hust., *N. bacata* Hust., *N. confinis*, *N. congolensis* Hust., *N. epiphytica* O.Müll., *N. epiphyticoides*, *N. lancettula*, *N. mediocris* Hust., *N. palea* var. *tropica* Hust., *N. spiculum* Hust., *N. tropica* Hust. and *N. vanoyei* Cholnoky. Other Lake Kyaninga taxa with tropical African distribution are *Caloneis aequatorialis* Hust., *Encyonema grossestriatum* (O.Müll.) D.G.Mann, *E. geisslerae* Krammer, *E. neomuelleri* Krammer, *Gomphonema affine* Kütz. var. *rhombicum* E.Reichardt, *Navicula zanonii* Hust., *Rhopalodia gracilis* O.Müll., *R. hirudiniformis*, *R. rhopala* (Ehrenb.) Hust. and [*Sellaphora*] *Navicula platycephala* O.Müll. One taxon, *Navicula zanonii*, has a broader distribution and is also reported from the temperate southern part of the African continent.

The fossil diatom assemblage preserved in recently deposited surface sediments showed reasonably high similarity in three successive depth horizons (0–1 cm, 1–3 cm and 3–5 cm) of deepwater core 07-1G and in two successive horizons (0–1 cm and 1–3 cm) of near-shore core 07-2G (table 5). In the deepwater core this annually integrated community is dominated by *Achnanthidium microcephalum*, *Cyclotella stelligera*, *Nitzschia epiphyticoides*, *N. fonticola* sensu Hustedt, *N. frustulum* and *Pseudostaurosira brevistriata* (table 4). Significant correlation can also be reported between the surface-sediment assemblages at mid-lake and near-shore localities, except for the somewhat deviating 1–3 cm layer of the mid-lake core (table 5).

The diatom assemblage in the uppermost sediment horizon (0–1cm) has a strongly significant similarity with the pelagic living diatom communities collected both in mid-lake and near-shore zones during both the 2007 dry season and the 2009 wet season; similarity is highest with the 2009 wet season community. The six taxa that dominate the sediment samples also rank among the diatom species most abundantly found in the living pelagic phytoplankton. However two common local taxa that are conspicuously missing in the surface-sediment assemblages are *Amphora pediculus* and *Urosolenia* sp. The latter species has very thin valves, dissolving rapidly in the water column. Also notable is that the surface-sediment assemblages at the near-shore locality do not show more affinity with living near-shore, epiphyton and epipelon samples than surface-sediment assemblages at the mid-lake locality. This can be attributed to the limited development of true littoral habitat, and the overall scarcity of epiphytic and epipelic substrate on an areal basis, in this steep-sided crater lake rather than to spatial integration of distinct near-shore and mid-lake diatom communities prior to burial. Not surprisingly, a significant positive correlation also exists between the species composition of epiphyton and epipelon diatom samples and all planktonic samples, with exception of the mid-lake sample of the dry season in 2007. This correlation is highest with the April 2009 wet season sample.

DISCUSSION

Deep seasonal mixing in tropical freshwater lakes occurs when a temporarily favourable combination of relatively low daytime insolation, wind-driven turbulence and evaporative heat loss break down the temperature-related density stratification of the water column (Talling 1969). The deepest annual water-column mixing typically occurs when surface-water temperature is lowest, but given limited seasonal variation in solar insolation (386–439 W/m^2, resp. in June and March; Berger & Loutre 1991) at the Equator, lowest surface-water temperature does not necessarily coincide with the seasonal insolation minimum or lowest near-surface air temperatures.

Table 4 – Relative abundances (%) of the most important diatom taxa, i.e. taxa representing > 5% in at least one sample, across all samples studied.

	living community							surface sediments				
	pelagic 2007	pelagic 2009	pelagic 2009	near-shore 2007	epiphyton (1) 2009	epiphyton (2) 2009	epipleon 2009	0–1cm (1G)	1–3cm (1G)	3–5cm (1G)	0–1cm (2G)	1–3cm (2G)
Achnanthidium exiguum (Grunow) Czarnecki	0.4	0.5	1.0	0.8	0.4	7.1	4.3	0.0	0.0	0.0	0.0	0.0
Achnanthidium microcephalum Kütz.	0.4	3.9	4.2	4.9	3.3	1.0	2.9	13.0	30.2	3.1	0.2	0.2
Amphora pediculus (Kütz.) Grunow	0.0	5.4	8.8	2.9	26.6	27.7	10.6	0.0	0.0	0.4	0.0	0.4
Cyclotella stelligera Cleve & Grunow	11.3	5.9	5.3	1.2	0.2	1.8	3.5	15.1	32.5	12.0	0.0	0.0
Eolimnia minima (Grunow) Lange-Bert.	0.0	0.5	0.6	0.2	0.0	0.6	3.1	2.5	0.0	0.6	6.5	4.4
Epithemia adnata (Kütz.) Breb.	0.8	1.6	1.9	2.1	9.5	1.4	0.2	0.0	0.8	1.4	0.0	0.0
Navicula seminuloides Hust.	0.0	0.5	0.6	0.2	0.0	0.6	3.1	2.5	0.0	0.6	6.5	4.4
Navicula cryptotenella Lange-Bert.	0.4	0.0	0.2	0.6	0.4	6.7	2.9	0.0	0.0	0.2	0.6	0.0
Nitzschia confinis Hust.	5.9	1.6	1.7	0.4	0.0	2.2	1.0	1.5	11.0	0.2	1.6	0.0
Nitzschia epiphyticoides Hust.	0.0	4.7	1.0	8.8	5.5	8.8	3.9	8.5	2.4	2.3	12.4	0.0
Nitzschia fonticola Grunow sensu Hustedt	60.9	13.7	9.9	3.5	7.9	9.2	6.5	13.2	0.0	1.2	14.8	7.6
Nitzschia frustulum (Kütz.) Grunow	0.8	15.2	21.1	4.9	9.5	8.1	16.2	10.1	0.0	19.0	16.9	17.3
Nitzschia lancettula Hust.	0.8	3.4	3.0	5.7	0.5	0.8	3.7	0.6	1.8	0.6	2.2	1.7
Placoneis gastrum (Ehrenb.) Mereschk.	0.0	1.3	1.5	9.2	1.1	1.6	0.8	0.0	0.2	0.0	0.0	0.2
Pseudostaurosira brevistriata (Grunow) D.M.Williams & Round	4.7	5.4	4.0	4.9	0.0	0.4	4.1	14.7	7.7	19.5	22.4	20.1
Rhopalodia gibberula var. *vanheurckii* O.Müll.	0.0	0.5	0.6	3.7	6.0	2.8	7.4	0.6	0.0	1.0	2.4	0.0
Rhopalodia hirudiniformis O.Müll.	0.8	1.0	0.8	2.5	8.2	0.4	0.6	0.0	0.0	0.0	0.0	0.0
Sellaphora seminulum (Grunow) D.G.Mann	0.0	0.0	0.0	0.0	0.0	0.0	0.0	0.0	1.2	0.0	0.0	33.1
Staurosira construens (Ehrenb.) Grunow	4.3	0.0	0.0	1.2	0.0	0.0	0.0	0.0	0.0	19.0	0.0	1.7
Urosolenia sp.	1.2	12.7	5.9	0.0	0.0	0.0	0.0	0.0	0.0	0.0	0.0	0.0
Subtotal	92.7	77.8	77.5	57.7	79.1	81.2	74.8	82.3	87.8	81.1	86.5	91.1

Table 5 – Pearson correlation coefficients between the % species compositions of diverse diatom samples from Lake Kyaninga.
Samples are from the living diatom community sampled in 2007 and 2009, and from recently deposited sediments in mid-lake (core KYANINGA-07-1G) and near-shore (core KYANINGA-07-2G) locations of the southern basin. Significant correlations are given in bold ($p < 0.001$).

		living community						surface-sediment assemblage				
		pelagic 2007	pelagic 2009	pelagic 2009	near-shore 2007	epiphyton 2009 (1)	epiphyton 2009 (2)	epipelon 2009	0–1cm (1G)	1–3cm (1G)	3–5cm (1G)	0–1cm (2G)	1–3cm (2G)
living community	pelagic 2007	1.00	**0.56**	**0.40**	0.19	0.22	0.27	0.28	**0.52**	0.15	0.16	**0.47**	0.19
	pelagic 2009		1.00	**0.90**	**0.50**	**0.47**	**0.48**	**0.69**	**0.67**	0.27	**0.49**	**0.64**	**0.37**
	pelagic 2009			1.00	**0.46**	**0.58**	**0.57**	**0.83**	**0.61**	0.24	**0.57**	**0.63**	**0.41**
	near-shore 2007				1.00	**0.46**	**0.40**	**0.54**	**0.49**	0.24	**0.35**	**0.44**	0.23
	epiphyton 2009 (1)					1.00	**0.87**	**0.69**	0.23	0.04	0.16	0.24	0.12
	epiphyton 2009 (2)						1.00	**0.72**	0.27	0.05	0.15	0.27	0.12
	epipelon 2009							1.00	**0.53**	0.18	**0.49**	**0.60**	**0.36**
surface-sediment assemblage	0–1cm (1G)								1.00	**0.69**	**0.65**	**0.71**	**0.40**
	1–3cm (1G)									1.00	**0.36**	0.10	0.07
	3–5 cm (1G)										1.00	**0.64**	**0.47**
	0–1 cm (2G)											1.00	**0.58**
	1–3 cm (2G)												1.00

Rather more important is the annual timing of weather systems moving across the region that cause sustained strong winds, from a direction allowing a long fetch across the lake surface. In East Africa this timing is mostly controlled by the twice-annual migration of the ITCZ to north and south of the Equator, and associated east-west movement of the Congo Air Boundary, the zone of surface air convergence separating Atlantic monsoon (and Congo Basin) influences from Indian Ocean monsoon influences. As a result, in our Fort Portal study region of south-western Uganda the highest monthly day-time (T_{max}) and nighttime (T_{min}) air temperatures (fig. 1) coincide only broadly with the insolation maximum in February–March, and the lowest monthly T_{max} and T_{min} values occur during a secondary insolation minimum in December–January instead of the primary insolation minimum in June (fig. 1). In the year of our continuous temperature monitoring at Lake Kyaninga and most probably also the year before, deepest water-column mixing (to 39–47 m depth) occurred in late July and early August, i.e. during the principal dry season and around the end of the primary insolation minimum. Strikingly, temperature stratification of the water column was strongest during the other dry season, even though this broadly coincides with the secondary insolation minimum. Further, the only other mixing events extending beyond 30 m depth occurred in late October and late April, i.e. in the middle of the two wet seasons. Our present data thus indicate that seasonal variation in the physical limnology of Lake Kyaninga is only modestly tied into the annual succession of climate variables such as air temperature and rainfall; and hence that significant inter-annual variability can be expected to occur in the timing of water-column stratification, mixing, and nutrient supply to the phytoplankton community.

Based on Chl *a* data, Lake Kyaninga had a lower phytoplankton biomass during the rain season of 2009 than during the northern summer dry seasons of 2007 and 2008, as can be expected when algal productivity mainly depends on nutrients regenerated from the hypolimnion during deep-mixing events. Still, phytoplankton biomass measured on 15 Apr. 2009 may have benefited from a secondary event of deep mixing in the weeks before our visit, such as occurred on at least one occasion during the rain season of 2008 (fig. 2). More frequent rain-season measurements of aquatic productivity are clearly needed to obtain a representative value, and from it determine Lake Kyaninga's mean trophic status.

We explained the elevated DO concentration at 10–12 m depth on 15 Apr. 2009 as reflecting an active phytoplankton community deeper in the water column, favoured by the increased transparency associated with limited algal production near the surface. In such circumstances the phytoplankton prefers to reside in sub-surface water to avoid the damaging UV radiation which penetrates relatively deep into the surface water. However the low algal biomass at 10 m depth indicates instead that the heterograde profile may have resulted because very low photosynthetic activity during peak stratification failed to compensate for oxygen consumption by zooplankton and fish concentrated in the 3–8 m depth range.

The marked difference in phytoplankton community between dry and rain seasons and the pronounced accumulation of nutrients below the thermocline during stratification adds to our arguments above that the productivity of Lake Kya-

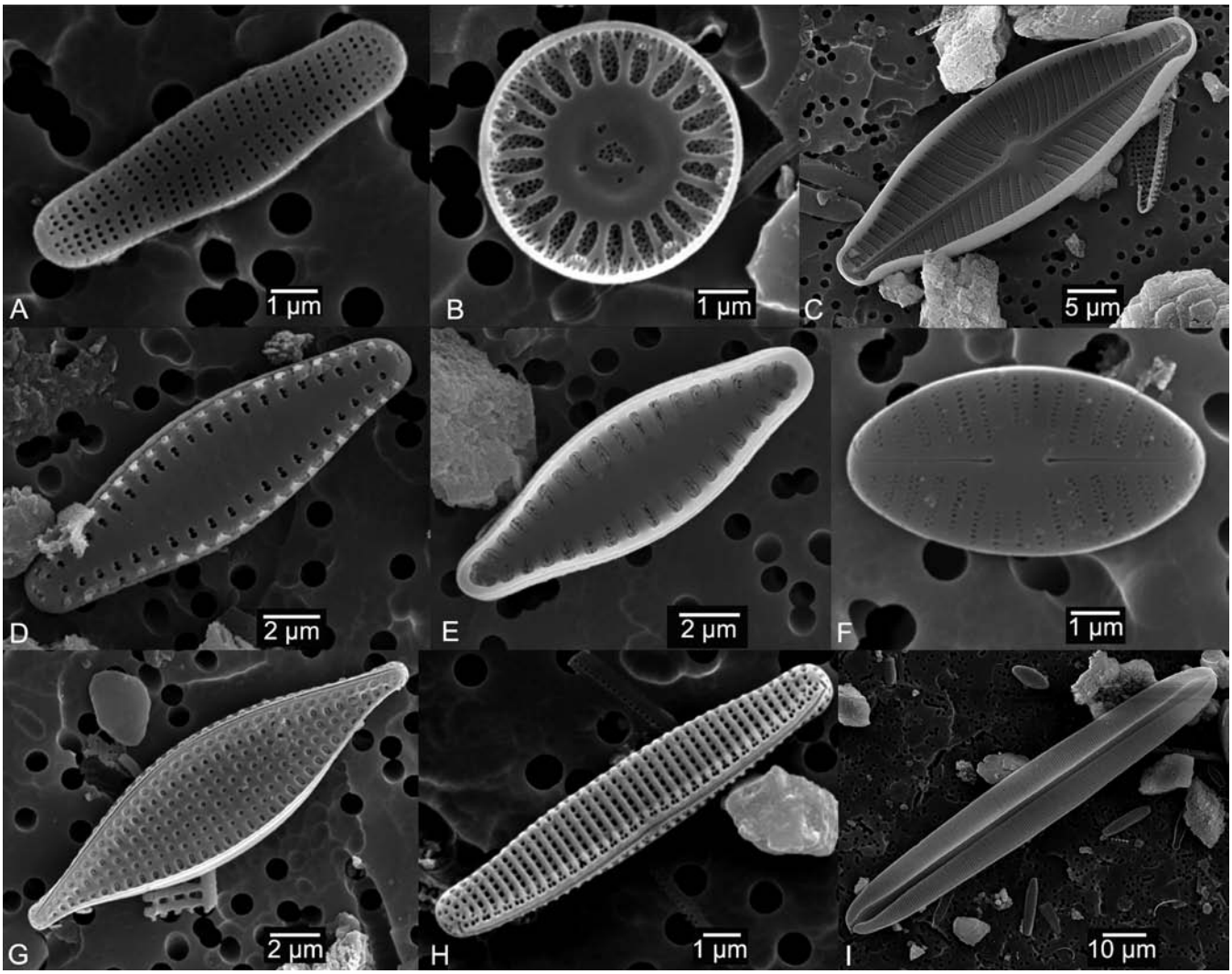

Figure 5 – Scanning electron microscopic photographs of diatom taxa: A, *Achnanthidium microcephalum*; B, *Cyclotella stelligera*; C, *Placoneis gastrum*; D–E, *Pseudostaurosira brevistriata*, external and internal valve view; F, *Navicula seminuloides*; G, *Nitzschia lancettula*; H, *Nitzschia epiphyticoides*; I, *Rhopalodia gracilis*.

ninga must be highly sensitive to variations in the timing and depth of seasonal mixing as controlled by inter-annual climate variability. Slight changes in air temperature and winds may cause significant thermic stability changes allowing variable quantities of hypolimnion water to reach the surface and influence rates of photosynthesis. Though the lake is meromictic, a great part of its lower water column can mix at rare occasions depending of specific climate conditions. Whether seasonal mixing extends to the typical depth of between 39 and 47 m (affecting a hypolimnetic volume of ~ 0.2 km^2 × 27–35 m = ~ 5.4–7.0 × 10^6 m^3) or the more extreme depth of 80 m (affecting a hypolimnetic volume of ~ 0.2 km^2 × 68 m = ~ 13.4 × 10^6 m^3) implies a 100% difference in nutrient supply.

This low-frequency, extreme deep mixing also brings a large quantity of anoxic water to the surface, potentially lowering DO concentration in Lake Kyaninga epilimnetic waters to below the limit tolerated by fish. As an indication of the frequency of extreme deep mixing events (not necessarily to 80 m depth), local fishermen reported fish kills to occur approximately every five years; the most recent fish kill appears to have taken place in 2006. The local population reports that during those periods a strong 'bubble' emerges from Lake Kyaninga, possibly reflecting ebullition and release of gases (CO_2, CH_4) accumulating in the lower water column. Such events may have importance in avoiding excessive build-up of dissolved gases in the lake. Multiple sites of on-land gas emission are reported to occur in the immediate vicinity of Lake Kyaninga, where dead animals such as birds, otters and python snakes have been found. This could be similar to the 'mazukus' phenomenon in the Nyaragongo area near Lake Kivu, D.R.Congo (Vaselli et al. 2004, Smets et al. 2010) where high concentrations of carbon dioxide are released.

Transparency, Chl *a*, TP and TN values classify Lake Kyaninga as oligotrophic (Forsberg & Ryding 1980, Carlson1977, Wetzel 1983). However, when mixing the lake may temporarily reach the lower mesotrophic level. Our preliminary measurements indicate that N seems to be more limiting to algal growth than P, consistent with Talling's (1966) general observation for tropical-African lakes. More measurements would be needed however to confirm this. The in-

creased biomass and percentual contribution of Cyanobacteria during stratification in April 2009 could be explained by their ability to circumvent N depletion by fixing atmospheric nitrogen.

The algal community of Lake Kyaninga also does not seem to fit one of the functional groups of phytoplankton defined by Reynolds et al. (2002), which "group together species with similar morphological and physiological traits and with similar ecologies" (Reynolds et al. 2002). On the one hand, the presence of *Urosolenia* spp. suggests affinity with functional group A, typical for clear lakes. But the lakes typified by functional group A are slightly acidic and often well-mixed, unlike Kyaninga. *Cyclotella comensis* Grunow, the other typical group A representative, is not observed in Lake Kyaninga but possibly replaced by another small *Cyclotella*, namely *C. stelligera*. This group A has nutrient deficiency tolerance but is sensitive to pH rise. On the other hand the presence of *Synechococcus* spp. points to a relationship with functional group Z, typical for a clear, well-mixed habitat with a tolerance for low nutrients and sensitive to light deficiency and grazing. Thus, the classification of Reynolds et al. (2002) is evidently problematic here, and may not be applicable to African lakes in general. Richardson (1968) proposed a diatom-based typology specifically for East and Central African lakes. This typology does not seem to be applicable here either, since the lake set used to calibrate it does not include any of the crater lakes located in the Edward-George extension of the East African Rift Valley, but only high-elevation in the Ruwenzori Mountains. Lake Kyaninga has a diatom assemblage dominated by small *Nitzschia* species, such as *N. fonticola* sensu Hustedt, *N.* aff. *frustulum* and *N. confinis*. In contrast, *Nitzschia* dominated lakes in Richardson's (1968) classification, such as Lake Tanganyika, are represented by large *Nitzschia* species such as *N. lacustris* Hust. With ~ 130 recorded taxa diatom species diversity in Lake Kyaninga is much higher than in Lake Kaitabarago (Cocquyt & Verschuren 2009), but rather moderate, compared to some other crater lakes in the area (CLANIMAE, unpubl. data). Literature data (e.g. Gasse 1986) on some Ugandan crater lakes typically involve single samples and are therefore not truly comparable. A maximal number of 32 species was reported for lakes Bisina (eastern Uganda) and Mwamba, a crater lake in the Kasenda area south of Fort Portal (treated as 'Rwenzori region' in Gasse, 1986).

The correlations between the composition of the actual planktonic diatom community and the sub-fossil diatom assemblage preserved in offshore surface sediments (upper 5 cm) reveals good representation of the annual pelagic diatom community of Lake Kyaninga in recent years (table 5). The lack of correlation between the 1–3 cm layer and living samples taken in 2007 and in 2009 suggests substantial inter-annual variability in the pelagic diatom community. Although the match between the 2007 and 2009 planktonic samples themselves is significant, the rather low Pearson values further reflect seasonal variability within the diatom community. Indeed, in April 2009 the pelagic diatom community was dominated by *Nitzschia frustulum* (small morphotype), *N. fonticola* sensu Hustedt, *Urosolenia* sp., *Cyclotella stelligera* and *Amphora pediculus* while in August 2007 *Nitzschia fonticola* sensu Hustedt and *Cyclotella stelligera* were the most important taxa. *Pseudostaurosira brevistriata* was co-dominant in both seasons (table 5).

In comparison with Lake Kaitabarago (Cocquyt & Verschuren 2009) the living diatom community of Lake Kyaninga is less well reflected in its surface-sediment assemblages. Where the Pearson's correlation between the percent abundances of living and recently buried taxa exceeded 0.90 in Lake Kaitabarago, for Lake Kyaninga the highest value is 0.67. We suggest that this difference can be explained by the much larger surface area of Lake Kyaninga (24 ha) vs. Kaitabarago (1.8 ha). Although the maximal height of the crater rim (77 m) is greater than for Lake Kaitabarago (46 m), Lake Kyaninga is more exposed to the wind than the strongly sheltered Lake Kaitabarago. By implication, seasonality in the diatom community may also be less pronounced in Lake Kaitabarago, but more research is needed. The small difference between the near-shore and offshore pelagic phytoplankton community of Lake Kyaninga is due to the mostly very steep crater slope below the waterline, causing the littoral euphotic zone to be highly restricted.

In summary, our present data indicate that the deepest known crater lake in western Uganda is permanently stratified below ~100 m depth, and mixes at least once per year to between 39 and 47 m depth when lake-surface temperatures are lowest. Based on our observations deep mixing is most likely to occur in July or early August towards the end of the dry season coinciding with the period of minimum solar insolation. Most strongly pronounced stratification occurs during the other dry season of December–January, despite its coincidence with lowest monthly day- and nighttime air temperatures. Near-daily mixing of the upper water column (epilimnion) extends to 8–12 m depth, and the photic zone to between 7.5 and 11.5 m. This high transparency is due to low phytoplankton biomass and production: nutrient and chlorophyll concentrations as well as phytoplankton composition classify Lake Kyaninga as oligotrophic, except that it may briefly reach mesotrophy after deep mixing has regenerated deep-water nutrient supplies to the surface. Its open-water phytoplankton community is dominated by Cyanobacteria and Chlorophyta. Bacillariophyta (diatoms) contribute only a minor part of total phytoplankton biomass in both wet and dry seasons, and are characterized by an assemblage of *Urosolenia* and small *Nitzschia* species. Steep rocky crater slopes limit the littoral zone even though water-column transparency is high. We report about 130 diatom taxa in the living community and recent surface-sediment assemblages, of which ~ 17% (most of them *Nitzschia* spp.) are biogeographically restricted to tropical Africa.

ACKNOWLEDGMENTS

This study was conducted in the framework of the CLANIMAE (Climatic and Anthropogenic Impacts on African Ecosystems) project SD/BD/03A, financed by the Science and Sustainable Development programme of the Belgian Science Policy (BelSPO). The fieldwork was conducted with permission of the Uganda National Council of Science and Technology (Uganda NCST research clearance NS 162) and the Uganda Wildlife Authority (permit UWA/TBDP/RES/50). The "Fondation pour favoriser la recherche scientifique en

Afrique" funded the field campaign of the first author. The authors are grateful to Johnson Bwambale and Maureen Fagot for field assistance, Myriam de Haan (NBGB) for technical assistance with scanning electron microscopy, Laurence Monin (RMCA) for laboratory assistance, and Harold Hughes and Nourdine Dahkani (RMCA) for dissolved Si determination using ICP-AES.

REFERENCES

Bahati G., Pang Z., Ármannsson H., Isabirye E., Kato V. (2005) Hydrology and reservoir characteristics of three geothermal systems in western Uganda. Geothermics 34: 568–591.

Berger A., Loutre M.-F. (1991) Insolation values for the climate of the last 10 million years. Quaternary Science Reviews 10: 297–317.

Carlson R.E. (1977) A trophic state index for lakes. Limnology and Oceanography 22: 361–369.

Cholnoky B.J. (1960) Diatomeen aus einem Teiche am Mt. Kenya in Mittelafrika. Österreichische Botanische Zeitschrift 107: 351–365.

Cholnoky B.J. (1964) Die Diatomeenflora einiger Gewässer der Ruwenzori-Gebirge in Zentralafrika. Nova Hedwigia 8: 55–101.

Cholnoky B.J. (1968) Die Ökologie der Diatomeen in Binnengewässern. Lehre, Cramer.

Cholnoky B.J. (1970a) Bacillariophyceae from the Bangweulu swamps. In: Symoens J.-J. (ed.) Hydrobiological survey of the Lake Bangweulu, Luapula River basin 5(1). Brussels, Cercle Hydrologique de Bruxelles.

Cholnoky B.J. (1970b) Hydrobiologischen Untersuchungen in Transvaal III. Die Fischteiche von Marble Hall. Botanica Marina 3 (suppl.): 5–44.

Cocquyt C. (1998) Diatoms from the northern basin of Lake Tanganyika. Bibliotheca Diatomologica 39: 1–275.

Cocquyt C. (2007) Diatom diversity in Hausburg Tarn, a glacial lake on Mount Kenya, East Africa. Diatom Research 22: 255–285.

Cocquyt C., Verschuren D. (2009) The algal flora of Lake Kaitabarago, a small Ugandan crater lake, with special attention to the diatoms. Proceedings of the Third Central European Diatom Meeting, Utrecht, The Netherlands, 7–13 March 2009. Diatomededelingen 33: 50–53.

Compère P. (1974) Algues de la région du lac Tchad. II Cyanophycées. Cahiers ORSTOM. Série Hydrobiologie 8(3–4): 165–198.

Compère P. (1976) Algues de la région du lac Tchad. V Chlorophycophytes. Cahiers ORSTOM. Série Hydrobiologie 10(2): 77–118.

Forsberg C., Ryding S.O. (1980) Eutrophication parameters and trophic state indices in 30 Swedish waste-receiving lakes. Archiv für Hydrobiologie 89: 189–207.

Gasse F. (1986) East African diatoms: taxonomy, ecological distribution. Bibliotheca Diatomologica 11: 1–201.

Huber-Pestalozzi G. (1941) Chrysophyceen, Farblose Flagellaten, Heterokonten. In: Huber-Pestalozzi G. (ed.) Das Phytoplankton des Süsswassers, Systematik und Biologie 2(1). Stuttgart, E. Schweizerbart.

Huber-Pestalozzi G. (1955) Euglenophyceen. In: Huber-Pestalozzi G. (ed.) Das Phytoplankton des Süsswassers, Systematik und Biologie 4. Stuttgart, E. Schweizerbart.

Huber-Pestalozzi G., Fott B. (1968) Cryptophyceae, Chloromonadophyceae, Dinophyceae. In: Huber-Pestalozzi G. (ed.) Das Phytoplankton des Süsswassers, Systematik und Biologie 3. Stuttgart, E. Schweizerbart.

Hustedt, F. (1949) Süsswasser-Diatomeen. In: Exploration du Parc National Albert, Mission H.Dumas (1935–1936) 8. Bruxelles, Institut des Parcs Nationaux du Congo Belge.

Kalff J. (2002) Limnology – Inland water ecosystems. New Jersey, Prentice Hall.

Komárek J. (2008) The cyanobacterial genus Macrospermum. Fottea 8: 79–86.

Komárek J., Anagnostidis K (1999) Cyanoprokaryota 1 – Chroococcales. In: Ettl H., Gärtner G., Heynig H., Mollenhauer D. (eds) Süsswasserflora von Mitteleuropa 19(1). Jena, Gustav Fischer.

Komárek J., Anagnostidis K (2005) Cyanoprokaryota 2 – Oscillatoriales. In: Büdel B., Gärtner G., Krienitz L., Schagerl M. (eds) Süsswasserflora von Mitteleuropa 19(1). München, Elsevier.

Komárek J., Fott B. (1983) Chlorophyceae (Grünalgen) Ordnung: Chlorococcales. In: Huber-Pestalozzi G. (ed.) Das Phytoplankton des Süsswassers, Systematik und Biologie 7(1). Stuttgart, E. Schweizerbart.

Komárek J., Jankovska V. (2001) Review of the green algal genus Pediastrum. Implication for pollen-ananlytical research. Bibliotheca Phycologica 108: 1–124.

Lewis W.M. (1983) A revised classification of lakes based on mixing. Canadian Journal of Fisheries and Aquatic Sciences 40: 1779–1787.

Lewis W.M. (1987) Tropical limnology. Annual Review of Ecology and Systematics 18: 159–184.

Müller O. (1905) Bacillariaceen aus dem Nyassalande und einigen benachbarten Gebieten. IV. Botanische Jahrbücher fur Systematik, Pflanzengeschichte und Pflanzengeographie 45: 66–122.

Popovský J., Pfiester L.A. (1990) Dinophyceaea (Dinoflagellida). In: Ettl H., Gerloff J., Heynig H., Mollenhauer D. (eds) Süsswasserflora von Mitteleuropa 6. Stuttgart, Gustav Fischer.

Redfield A.C. (1958) The biological control of chemical factors in the environment. American Scientist 46: 205–222.

Reynolds C.S., Huszar V., Kruk C., Naselli-Floresi L., Melo S. (2002) Towards a functional classification of freshwater phytoplankton. Journal of Plankton Research 24: 417–428.

Roberts E.C., Davidson K., Gilpin L.C. (2003) Response of temperate microplankton communities to N:Si ratio perturbation. Journal of Plankton Research 25: 1485–1495.

Richardson J.L. (1968) Diatoms and lake typology in East and Central Africa. Internationale Revue der gesamten Hydrobiologie und Hydrographie 53: 299–338.

Simpson J.H., Tett P.B., Argoteespinoza M.L., Edwards A., Jones K.J., Savidge G. (1982) Mixing and phytoplankton growth around an island in a stratified sea. Continental Shelf Research 1: 15–31.

Starmach K. (1985) Chrysophyceae und Haptophyceae. In: Ettl H., Gerloff J., Heynig H., Mollenhauer D. (eds) Süsswasserflora von Mitteleuropa 1. Stuttgart, Gustav Fischer.

Smets B.,Tedesco D., Kervyn F., Kies A., Vaselli O.,Yalire M.M. (2010) Dry gas vents (''mazuku") in Goma region (North-Kivu, Democratic Republic of Congo): Formation and risk assessment. Journal of African Earth Sciences. DOI:10.1016/j.jafrearsci.2010.04.008

Talling J.F. (1966) The annual cycle of statification and phytoplankton growth in Lake Victoria (East Africa). Internationale Revue der gesamten Hydrobiologie und Hydrographie 51: 545–621.

Talling J.F. (1969) The incidence of vertical mixing, and some biological and chemical consequences, in tropical African lakes.

Verhandlungen der Internale Vereinigung für Theoretische und Angewandte Limnologie 17: 998–1012.

Teubner K., Dokulil M.T. (2002) Ecological stoichiometry of TN:TP:SRSi in freshwaters: nutrient ratios and seasonal shifts in phytoplankton assemblages. Archiv für Hydrobiologie 154: 625–646.

Uthermöhl H. (1931) Neue Wege in der quantitativen Erfassung des Planktonts. Verhandlungen der internationale Vereinigung fur theoretische und angewandte Limnologie 5: 567–596.

Van Meel L. (1954) Le phytoplancton. In: Exploration, hydrobiologie du lac Tanganyika 4(1). Bruxelles, Institut Royal des Sciences Naturelles de Belgique.

Vaselli O., Capaccioni B., Tedesco D., Tassi F., Yalire M.M., Kasareka M.C. (2004) The "evil's winds" (mazukus) at Nyiragongo Volcano (Democratic Republic of Congo). Acta Vulcanologica 14–15: 123.

Verschuren D. (1993) A lightweight extruder for accurate sectioning of soft-bottom lake sediment in cores in the field. Limnology & Oceanography 38: 1796–1802.

Vollenweider R.A. (1974) A manual for measuring primary production in aquatic environments. IBP Handbook 12. 2nd Ed. Oxford, Blackwell Scientific Publishers.

Wetzel, R.G. (1983) Limnology. 2nd Ed. New York, CBS College Publishing.

Paper based on results presented during the Symposium "Diatom Taxonomy in the 21st Century" (Meise 2009). Manuscript received on 19 Jan. 2010; accepted in revised version 30 Sep. 2010.

Communicating Editor: Bart Van de Vijver.

Lake Katinda, a eutrophic Ugandan crater lake: limnology, phytoplankton composition and diatoms

Christine Cocquyt[1], Pierre-Denis Plisnier[2] & Dirk Verschuren[3]

[1]National Botanic Garden of Belgium, Domein van Bouchout, B-1860 Meise, Belgium; christine.cocquyt [at] br.fgov.be
[2]Royal Museum for Central Africa, Leuvensesteenweg 13, B-3080 Tervuren, Belgium; pierre-denis.plisnier [at] africamuseum.be
[3]Ghent University, Limnology Unit, K.L. Ledeganckstraat 35, B-9000 Gent, Belgium; dirk.verschuren [at] ugent.be

Introduction

Lake Katinda is a shallow crater lake (16 m max. depth) with a watershed strongly impacted by human settlements and agriculture. It is located in the Bunyaruguru district in western Uganda, southeast of Queen Elizabeth National Park, at an altitude of 1040 m asl in the Edward-George extension of the East African Rift Valley. The maximum height of the crater rim reaches 107 m, and encloses a crater basin of 45 ha surface area. Average annual rainfall in the area is about 800 mm. Lake Katinda is one of the 48 Ugandan freshwater crater lakes studied in the CLANIMAE (CLimatic and ANthropogenic IMpacts on African Ecosystems) project. These crater lakes were specifically chosen along a gradient from oligotrophic to eutrophic (natural as well as anthropogenic) with the aim to develop a diatom-based transfer function for reconstruction of the past trophic status (nutrient budget) of East African lakes.

Physical and chemical limnology

The transparency in Lake Katinda, measured during 3 missions between 2007 and 2008, was low (45 to 70 cm) while surface Chl a was always high: between 22.9 µg l^{-1} in August 2007 to 42.6 µg l^{-1} in January 2007 µg l^{-1} and 40.6 in August 2008 (compared with the oligotrophic Lake Kyaninga where 2.2 µg l^{-1} was measured in February 2007, 5.2 µg l^{-1}, in August 2007 and 9.3 µg l^{-1} in August 2008, Cocquyt et al. submitted). Total phosphorus in the surface waters was variable but always high: 43 µg l^{-1} PO_4-P in January 2007 and 126 µg l^{-1} in August 2007. Total nitrogen values were also high: 768 µg l^{-1} in August 2007 to 1660 µg l^{-1} in August 2008. Lake Katinda is an alkaline lake with a pH between 8.9 and 9.1 at the surface and decreasing with depth but remaining high (between 7.9 and 8.6). Total alkalinity measured in 2007 was 381 mg l^{-1} $CaCO_3$. Those mentioned parameters indicated clearly that Lake Katinda is a eutrophic lake. The lake is not a saline lake but a high conductivity was observed: 752 µS cm^{-1} at the surface to 803 µS cm^{-1} at the bottom. The temperature stratification was weak in August 2007 (24.7°C at the surface to 24.4°C at 15 m depth). A very low potential energy anomaly was observed in 2007 (PEA = 0.012 j m^{-3}). The thermal gradient was quite similar in August 2008 but slightly more developed. Anoxic waters were observed at around 5 m depth in January 2007 and August 2008. In August 2007, when the stability in the water-column was very low, the anoxia was observed already at 70 cm. It could have been linked with a very recent mixing fish mortality reported by some local fishermen to occur generally during 3 days twice every year. The shallowness of Lake Katinda and

those frequent observations of fish kills events indicate that this lake is probably polymictic.

Phytoplankton: Results of the quantitative phytoplankton analysis (method following Utermöhl 1931), showed that the Lake Katinda was dominated by a Cyanobacteria community, which most important taxa are: *Planktolyngbya limnetica* (Lemmerm.) Komárk.-Legn. & Cronberg, *P. contorta* (Lemmerm.) Anagn. & Komárek and *Chroococcus* sp.. Chlorophytes were less important and were represented by *Schroederia setigera* (Schrïd.) Lemmerm., *Tetraedron minium* (A.Braun) Hansg., *T. triangulare* O.Korshikov, *Monoraphidium flexuosum* Komárek. Some Dinophyte cells were present (*Peridinium* cf. *africanum* Lemmerm.) while no diatoms at all were observed in the phytoplankton counts.

Diatoms

By means of concentrated phytoplankton net samples (mesh width of 10 µm), the diatoms living in the actual water-column were studied. The diversity was low: 31 taxa in 500 counted valves. Besides in phytoplankton samples, diatoms were studied in recently deposited diatoms in bottom sediments (0-5 cm), where 45 taxa in 500 counted valves were observed. The valves were well preserved in the upper sediments; up to 77.5 % of them were intact. The most important diatoms with a relative abundance ≥ 5.0 in the actual water-column were: *Diadesmis contenta* (Grunow ex Van Heurck) D.G.Mann (5.7 %), *Gomphonema* spp. (49.7 %), *Hantzschia amphioxys* (Ehrenb.) Grunow (13.7 %) and *Luticola mutica* (Kütz.) D.G.Mann (7.2 %); and in the surface sediments: *Amphora pediculus* (Kütz.) Grunow (5.0) %, *Diadesmis contenta* (10.5 %), *Gomphonema spp.* (8.7 %), *Hantzschia amphioxys* (25.8 %), *Luticola mutica* (16.1 %), *Navicula cryptotenella* Lange-Bert. (5.4 %), *Navicula* cf. *monoculata* var. *omissa* Lange-Bert. (6.4 %). Correlation between the diatom assemblages in the actual and the recent deposited sediments was low, 0.308, compared to other crater lakes in Western Uganda, e.g. Lake Kaitabarogo between 0.898 and 0.999 (Cocquyt & Verschuren 2009) and Lake Kyaninga 0.670 (Cocquyt et al. submitted). Looking at the geographical distribution of the diatoms we found that Afrotropical species were restricted to 12.5 % (6 of the 48 observed taxa): *Amphora minutissima* var. *africana* Levkov, *Encyonema grossestriatum* (O.Müll.) D.G.Mann, *Encyonema neomuelleri* Krammer, *Gomphonema affine* var. *rhombicum* Reichardt, *Nitzschia confinis* Hust. and *Nitzschia epiphyticoides* Hust.

Conclusions

Lake Katinda is a eutrophic lake, with anoxic water rapidly observed below the surface. The lake is highly impacted by human activities and its phytoplankton is dominated by a Cyanobacteria community. Its shallowness and the observations of frequent fish mortalities are probably signs of frequent mixing resulting in whole water anoxia. Although diatoms are restricted in the plankton, they are well preserved in the sediments of the lake and can be used to reconstruct the past history of the lake.

References

Cocquyt C. & Verschuren D. 2009: The algal flora of Lake Kaitabarago, a small Ugandan crater lake, with special attention to the diatoms. Proceedings of the 3th Central European Diatom Meeting, Utrecht, The Netherlands, 7-13 March 2009. – Diatomededelingen **33:** 50-53.

Cocquyt C., Plisnier P.-D., Gelorini V., Rumes B. & Verschuren D. 2010: Observations on the limnology and phytoplankton community of crater Lake Kyaninga (Uganda), with special attention to its diatom flora. – Plant Ecol. & Evol. **1:** submitted.

Utermöhl, H.: Neue Wege in der quantitativen Erfassung des Planktons (mit besonderer Berücksichtigung des Ultraplanktons). – Int. Vereinigung Theor. Limnol. Verh. **5:** 567-595.

De bijdrage van fossiele diatomeeën aan multi-disciplinair onderzoek naar de lange-termijn dynamiek van Afrikaanse aquatische ecosystemen onderhevig aan klimaatverandering en historische antropogene invloed

Christine Cocquyt[1] en Dirk Verschuren[2]

[1] Nationale Plantentuin van België, Domein van Bouchout, B-1860 Meise, België
c.cocquyt@telenet.be
[2] Universiteit Gent, Vakgroep Biologie, Onderzoeksgroep Limnologie , K.L. Ledeganckstraat 35, B-9000 Gent, België
Dirk.Verschuren@UGent.be

INLEIDING

Onderzoek naar globale patronen van historisch landgebruik focust op grootschalige landschapsmodificatie welke een significante invloed kan hebben gehad op het wereldklimaat. Dergelijke analyses veronderstellen een zeer beperkte verstoring van het Afrikaans landschap door pre-koloniale culturen, wegens de zeer lage geschatte bevolkingsdichtheid (~3% tov vandaag in 1700 AD). Dit is in tegenstelling tot de gangbare opvattingen in de archaeologie waar aangenomen wordt dat menselijke voorouders al van in het Paleolithicum het landschap van Oost-Afrika modifieerden, en dat significante ontbossing ongeveer 2500 jaar geleden op gang kwam.

Enkel een multidisciplaire studie kan aan deze tegenstrijdende opvattingen een einde stellen. Een dergelijke studie zal uitgevoerd worden in het kader van CLANIMAE (Climatic and Anthropogenic Impacts on African Ecosystems), een multidisciplinair project (Tabel 1), gefinancieerd door BELSPO (Belgian Science Policy) in het kader van het Belgische duurzame ontwikkelingbeleid, dat een lange-termijn perspectief wil geven voor hedendaagse interacties tussen mens, klimaat en natuur in Oost-Afrika. Dit zal gebeuren aan de hand de reconstructie van enerzijds (pre-) historische klimaatvariaties en veranderingen in het terrestrisch landschap en anderzijds van de waterkwaliteit van meren, door middel van multi-disciplinaire analyses van gedateerde meersedimenten. De klimaatreconstructie zal gebruik maken van biologische en sedimentologische datasets en van geochemische proxy-indicatoren van fluctuaties in de waterbalans van een aantal geselecteerde meren. Samengevat zijn de voornaamste objectieven van dit project 1) een onderscheid te maken tussen de invloeden van natuurlijke klimaatverandering en antropogene activiteit op terrestrische ecosystemen in Oost-Afrika; 2) de precieze timing en relatieve omvang te bepalen van historische (pre-20ste eeuwse) kaalkap en landschapsverstoring in relatie tot die welke zich in de laatste decaden heeft afgespeeld; en 3) het verlies aan waterkwaliteit (eutrofiëring, hoge turbiditeit) te bepalen welke kan worden gelinkt aan bodemerosie en nutriëntenexport veroorzaakt door ontbossing en landbouw, eerder dan het gevolg van natuurlijke lange-termijn variatie in waterbalans.

Diatomeeën zijn een belangrijk onderdeel van de geïntegreerd multi-disciplinaire onderzoeksmethode van het CLANIMAE project. Vooreerst zal aan de hand van diatomeeënanalyses in oppervlaktesedimenten een transferfunctie voor nutriënten (hoofdzakelijk TP, Total phosphorus) worden opgesteld voor Oost-Afrika. Daarna wordt dit inferentiemodel toegepast op fossiele diatomeeën-assemblages in sedimentkernen om zo historische veranderingen in de trofiegraad van een aantal Oegandese kratermeren te reconstrueren, welke van natuurlijke aard kunnen zijn dan wel het gevolg van menselijke verstoring van het landschap in hun stroomgebied.

STUDIEGEBIED

De meren die zullen bestudeerd worden in het kader van het CLANIMAE project zijn gesitueerd in zuidwest-Oeganda, in het laaglandgebied dat in het westen grenst aan het Ruwenzori gebergte en in het zuiden aan het Virunga vulkanengebied (Fig. 1). Dit gebied ligt in de zone waar antropogene invloed duidelijke sporen heeft nagelaten. De oorspronkelijke vegetatie bestond uit loofwoud en gras- of boomsavannes in een subhumied tot semi-aried klimaat. Een eerste groep van meren, o. a. de meren Kanyamukali, Kisibendi, Kyaninga, Mahuhura en Nyantonde, is gelegen nabij Fort Portal in het noordelijk gedeelte van het studiegebied. Een tweede groep meren, o.a. de meren Chibwera, Katinda, Mirambi en Nyamusingere, liggen meer zuidelijk in de Kikorongo-Bunyaruguru regio. In beide groepen komen zowel oligotrofe (vb. Mahuhura) als eutrofe meren (vb. Kisibendi, Mirambi) voor.

Tabel 1. Overzicht van de partners van het CLANIMAE project met vermelding van de onderzoeksinstellingen, de projectmedewerkers en de onderzoeksitems.

Partner 1 (coördinator)	Universiteit Gent Prof. Dr. Dirk Verschuren Drs. Vanessa Gelorioni Drs. Bob Rumes	palynologie sporen van fungi resten van zoöplankton chl a bepalingen
Partner 2	Koninklijk Museum voor Midden Afrika Prof. Dr. Luc André Dr. Pierre-Denis Plisnier	Si isotopen fysische en chemische wateranalyses
Partner 3	Faculté universitaire des Sciences agronomiques de Gembloux Prof. Dr. Gregory Mahy Prof. Dr. Laurent Bock Drs. Julie Lebrun	resten van aquatische macrofieten
Partner 4	Nationale Plantentuin van België Dr. Christine Cocquyt	diatomeeën
Partner 5	York Institute for Tropical Ecosystem Dynamics Prof. Dr. R.A. Marchant	palynologie

MATERIAAL EN METHODEN

Oppervlaktesedimenten werden genomen met een UWITEC valboor in een groot aantal kratermeren gesitueerd langsheen de moderne regionale gradiënt in nutriëntaanrijking en turbiditeit. In een voorbereidende expeditie begin 2007 werden een 50-tal meren bemonsterd. Een vijftiental van deze meren zullen in juli/augustus 2007 opnieuw bemonsterd worden waarbij tevens uitgebreide fysische en chemische analyses van het water zullen worden uitgevoerd. Intacte oppervlaktesedimenten worden bekomen door de bovenste 5 cm van de sedimentboorkern rechtopstaand te extruderen (Verschuren 1993), namelijk 0-1 cm voor de reconstructie van de actuele diatomeeënsamenstelling in het meer, 1-3 cm en 3-5 cm, voor de reconstructie van de diatomeeëngemeenschap zoals die fossiel terug te vinden is.

Alle meren die zullen onderzocht worden in het kader van het CLANIMAE project zijn zoetwatermeren. Meren die onderhevig zijn aan fluctuaties in saliniteit zijn eerder geschikt voor

reconstructies van het waterniveau en worden gebruikt voor de studie van klimaatveranderingen (veranderingen in neerslag en verdamping, de hydrologische balans). Voor Oost Afrika is een transferfunctie voor saliniteit aan de hand van diatomeeënassemblages reeds beschikbaar (Gasse et al. 1995). Het CLANIMAE project daarentegen wil historische veranderingen in nutriëntenrijkdom te wijten aan anthropogene invloed opsporen en loskoppelen van klimaatverandering.

Het geheel van diatomeeënanalyses, uitgedrukt als procentuele abundanties van individuele taxa per staal, vormen samen met de chemische samenstelling van de bemonsterde meren een dataset voor calibratie van de verspreiding van diatomeeënsoorten in relatie tot de belangrijkste nutriënten en andere abiotische omgevingsfactoren (Fig.2).

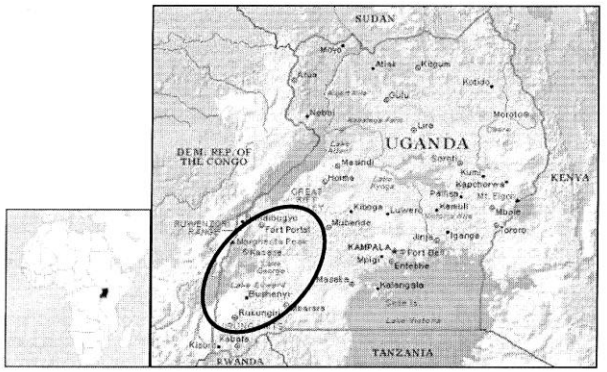

Fig. 1. Localisatie van het studiegebied in zuidwest-Oeganda

Als tweede onderdeel van het project zullen fossiele diatomeeën in sedimentboorkernen geanalyseerd worden. De resultaten van de diatomeeënanalyse zullen samen met de opgestelde transferfunctie gebruikt worden voor reconstructie van historische veranderingen in waterkwaliteit, en meer bepaald veranderingen in de trofiegraad. Daarvoor werdeneerder reeds sedimentboorkernen genomen in het Kanyamukalimeer uit de noordelijke groep meren, en in het Chibwerameer uit de zuidelijke groep.

RESULTATEN

Een aantal diatomeeënanalyses van oppervlaktesedimenten, genomen begin 2007, werden reeds uitgevoerd. Hieruit blijken duidelijke verschillen in de diatomeeëngemeenschappen van de onderzochte meren. Zo zijn in het oligotrofe Kyaningameer *Fragilaria construens* var. *venter*, *Nitzschia fonticola* en *Nitzschia epiphyticoides* de dominante soorten, terwijl in het eutrofe Mirambimeer *Gomphonema clavatum* en *Nitzschia amphibia* dominant zijn. Het onderzoek is echter pas gestart zodat geen verdere resultaten kunnen gegeven of besproken worden.

Hetzelfde geldt voor de analyses van de sedimentboorkernen. Reeds een gedeelte van de diatomeeënanalyses van de sedimentboorkernen uit het Chibwera- en het Kanyamulimeer zijn uitgevoerd, maar zijn niet volledig genoeg om hier resultaten weer te geven of te bespreken.

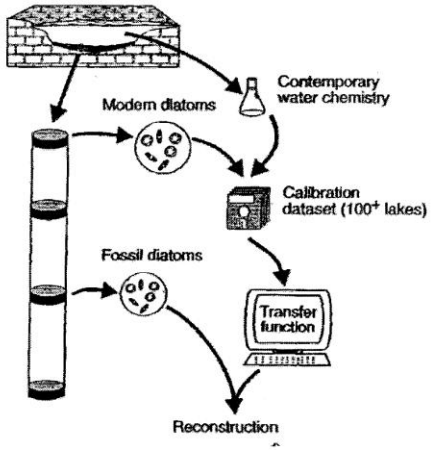

Fig. 2. Schematisch overzicht van de werkwijze die zal gebruikt worden in het diatomeeënonderzoek in het kader van het CLANIMAe project (naar Smol 2002).

VOORLOPIGE CONCLUSIES.

1. De onderzochte meren vertonen een grote taxonomische diversiteit aan diatomeeën.
2. De diatomeeëngemeenschappen zijn verschillend in oligotrofe en eutrofe meren.
3. De diatomeeëngemeenschappen zijn variabel tussen meren met eenzelfde trofiegraad.

BEDANKINGEN

CLANIMAE wordt gefinancierd wordt door het Belgisch Federaal Wetenschapsbeleid (BELSPO project nr. SD/BD/03A). Hartelijke dank is verschuldigd aan Hilde Eggermont voor de informatie over de transferfuncties, Bob Rumes voor het nemen van oppervlaktesedimenten tijdens de expeditie begin 2007 en aan Miriam De Haan voor de hulp bij de preparatie van de diatomeeën.

REFERENTIES

Gasse F., S. Juggins & L.B. Khelifa (1995). Diatom-based transfer functions for inferring past hydrochemical characteristics of African lakes. Palaeogeography, palaeoclimatology, palaeoecology 117: 31-54.

Smol J.P. (2002). Pollution of Lakes and Rivers: A Paleoenvironmental Perspective. Arnold Publishers, London. 280 pp.

Verschuren D. 1993. A lightweight extruder fro accurate sectioning of soft-bottom lake sediment cores in the field. Limnology and Oceanography 38: 1796-1802.

The algal flora of Lake Kaitabarago, a small Ugandan crater lake, with special attention to the diatoms

Cocquyt, C.[1], Verschuren, D.[2]

[1]National Botanic Garden of Belgium, 1860 Meise, Belgium; e-mail: christine.cocquyt@br.fgov.be
[2]Ghent University, Limnology Unit, K.L. Ledeganckstraat 35, B-9000 Gent, Belgium

Introduction

Lake Kaitabarago (Fig. 1) is a small (1.8 ha) but deep (45 m) maar crater lake in the region of Fort Portal, western Uganda situated at an altitude of 1554 m asl on the shoulder of the Edward-George extension of the East African Rift Valley. The maximum height of the crater rim reaches 46 m, and encloses a crater basin of 9 ha surface area. Average annual rainfall is 1400 mm. The lake's major physical and chemical characteristics are given in Table 1.

Lake Kaitabarago is one of 48 Ugandan freshwater crater lakes studied in the CLANIMAE project. These crater lakes were specifically chosen along a gradient from oligotrophic to eutrophic (natural as well as anthropogenic) with the aim to develop a diatom-based transfer function for reconstruction of the past trophic status (nutrient budget) of East African lakes. The broader objective of the project is to resolve the controversy between research on global patterns of historical land-use, which supposes low population density (~3% of today in 1700 AD) and low anthropogenic impact on the landscape in pre-colonial Africa; and the traditional paradigm from archaeology stating that landscape modification and significant deforestation was important from at least 2500 years ago. This research question will be addressed with paleoecological techniques through reconstruction of lake history using fossil diatoms, chironomids and aquatic macrophyte remains in the sediment record (indicating lake-level and water-quality changes due to natural climate variability), and though reconstruction of historic land use using fossil pollen, fungal spores, and phytoliths (indicating landscape changes due to anthropogenic impact).

Materials and Methods

Quantitative phytoplankton analyses of all algal groups from one pelagic and one littoral sample, taken on 6 February 2008, were done following Uthermöhl (1931) with an Olympus CKX41 inverted microscope.

Diatoms were studied in three types of samples: a pelagic and a littoral phytoplankton sample taken with a phytoplankton net (mesh width 10 µm) on 6 February 2008 and a surface-sediment sample containing dead diatoms recently settled on the lake bottom. This sample was collected with a UWITEC gravity corer on 22 January 2007. The three samples were oxidized with peroxide and embedded in Naphrax; and the analyses were executed using an Olympus BX 51 light microscope equipped with differential interference contrast and a color view digital camera. A JEOL 5800 scanning electron microscope was used for the determination of critical taxa.

Table 1. *Physical and chemical characteristics of Lake Kaitabarago after Rumes (2007) and Gelorini, Cocquyt & Lebrun (2008).*

		22-01-2007	06-02-2008
temp. (°C)	surface	24.98	22.87
	bottom	21.56	21.56
pH	surface	8.03	8.2
	bottom	6.04	6.04
Conductivity (µS/cm)	surface	489	502
	bottom	1373	1427
dissolved oxygen	surface	5.23	6.91
	bottom	0.00	0.00
anoxic (< 0.5 mg/L) depth (m)		8.0	7.0
TP (mg/L)	surface	65	-
TN (mg/L)	surface	416	-
Chl a (µg/L)	surface	4.7	-
Secchi depth (cm)		-	172

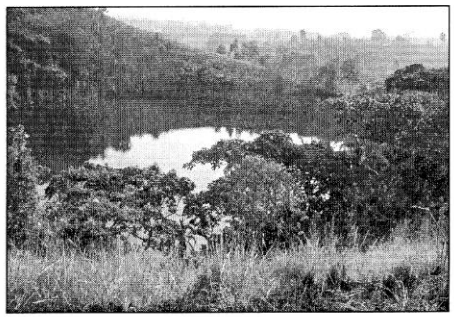

Figure 2. *Lake Kaitabarago.*

Results

Phytoplankton

The quantitative phytoplankton analyses (Tables 2 & 3) revealed that the Cyanobacteria, represented by 11 taxa, is the most important algal group in the pelagic as well as in the littoral. Although less numerous in cell numbers, the large biovolume of *Peridinium* spp. (Dinophyta), makes this group the second most important, followed by the Chlorophyta (12 taxa). Only seven diatom taxa were observed, of which *Achanthidium minutissimum* and *Nitzschia confinis* (Fig. 2) are the most numerous.

Diatoms

Diatom taxonomic diversity was very low: in 500 valves only 9 taxa were observed in the pelagic, 13 taxa in the littoral and 12 taxa in the surface sediments. In all these samples the dominant taxa were *Nitzschia confinis* and *Achnanthidium minutissimum* (Table 4).

Only some minor differences were found between the three samples; the Pearson's correlation coefficient between the percent abundances of the represented taxa varied between 0.898 and 0.999. The highest correlation exists between the pelagic and surface-sediment samples.

Total diatom species richness is low in Lake Kaitabarago: less than 30 diatom taxa were observed. A small number of taxa were observed separate to the counts: *Cymatopleura solea* var. *clavata*,

Gomphonema clevei, G. gracile, Placoneis gastrum, Rhopalodia gibberula. Only three species (corresponding to 10 % of the total species richness) have a distribution restricted to tropical Africa: *Nitzschia confinis, N. obsoleta* and *N. tropica*.

Table 2. *Percent abundance of phytoplankton groups in Lake Kaitabarago on 6 February 2008, derived from cell counts and biovolume calculations.*

	Pelagic	Littoral
Cyanobacteria	38.6	36.1
Chlorophyta	17.0	9.7
Euglenophyta	0.0	5.3
Dinophyta	23.6	36.2
Chrysophyta	0.0	0.0
Cryptophyta	6.9	8.3
Diatoms	13.9	4.4
Total	100.0	100.0

Table 3. Most *important phytoplankton taxa in the pelagic and littoral of Lake Kaitobarago.*

	Pelagic	Littoral
Cyanobacteria	*Ananaenopsis* cf. *raciborskii*	*Ananaenopsis* cf. *raciborskii*
	Anabaenopsis circularis	*Anabaenopsis circularis*
	Synechococcus elongatus	*Synechococcus elongatus*
Chlorophyta	*Monoraphidium komarkovae*	*Monoraphidium komarkovae*
	Tetraedron minimum	*Tetraedron minimum*
Euglenophyta		*Trachelomonas volvocinopsis*

Discussion

The crater basin of Lake Kaitabarago is very steep, both above and below the waterline. Consequently the littoral zone (substrate within the illuminated surface water) is restricted to a very small area nearshore, notwithstanding the relatively high transparency (Table 1). Therefore also the nearshore phytoplanktonic community has a strongly pelagic character. Conversely, due to the small size of the lake also species that normally live attached to a substrate (e.g. *Cocconeis plancentula*) are recovered in net samples from the central part of the lake.

The very high similarity between the diatom assemblages recovered from surface sediments and in the actual live pelagic plankton of Lake Kaitabarago partly reflects the scarcity of littoral epiphytic habitat, but also indicates that diatom preservation is very good, and that the single living phytoplankton sample collected in February 2008 is representative for the local algal community. Good preservation of the thinly silicified Nitzschia confinis in the surface sediment confirms limited dissolution of diatom valves in the lower water column and the sediments. Only a monitoring of the algal composition in Lake Kaitabarago over an entire year can give information on seasonal variability in the diatom community; however the congruence between the surface-sediment assemblage and the live sample from February may indicate that in Lake Kaitabarago this seasonal variability is relatively low compared to other tropical African lakes.

Conclusion

The surface-sediment death assemblage of Lake Kaitobarago, composed of a *Nitzschia confinis-Achnanthidium minutissimum* association, is a perfect reflection of the living pelagic diatom community collected in February 2008 because its littoral zone is poorly developed, diatom preservation is excellent, and seasonal variability in the diatom community is limited. Diatom species richness is low in the plankton, the littoral and in the surface-sediments of the lake. Ten percent of observed taxa, all belonging to the genus *Nitzschia*, have a distribution restricted to tropical Africa.

Acknowledgements

The present study is part of the CLANIMAE (CLimatic and ANthropogenic IMpacts on African Ecosystems) project SD/BD/03A, financed by the Belgian Science Policy. Thanks are due to Bob Rumes for collecting the surface-sediment sample and physical and chemical field data in 2007, and to Vanessa Gelorini and Julie Lebrun for helping with field measurements in 2008. Participation of the first author in February 2008 field work was possible thanks to sponsoring by the "Stichting tot Bevordering van het Wetenschappelijk Onderzoek in Afrika".

References

Uthermöhl, H. (1931) Neue Wege in der quantitativen Erfassung des Planktonts. Verh. Int. Verein. Theor. Angew. Limnol. 5: 567-596.

Table 4. *Percent abundance of diatoms in the littoral, pelagic and surface-sediment samples of Lake Kaitabarago (x= valve observed in the sample, but not present in the counts).*

	Littoral	Pelagic	Surface sediments
Achnanthidium minutissimum	32.6	14.9	4.5
Amphora copulta	0.0	0.0	0.2
Amphora pediculus	0.2	0.0	0.0
Cocconeis placentula var.	0.8	0.4	0.6
Cymatopleura solea var. *clavata*	0.0	0.0	x
Cymbella naviculoides	0.0	0.0	0.6
Diadesmis contenta	0.0	2.4	0.0
Encyonema muelleri	0.8	0.2	0.0
Epithemia adnata	0.4	0.0	0.0
Fragilaria cf. *tenera*	1.2	0.6	0.0
Gomphonema affine	0.4	0.0	0.0
Gomphonema clevei	0.0	0.0	x
Gomphonema gracile	0.0	0.0	x
Gomphonema sp.	0.8	0.8	0.0
Navicula cryptotenella	0.0	0.0	0.6
Nitzschia acicularis	0.0	0.0	0.2
Nitzschia confinis	60.4	80.2	89.5
Nitzschia fonticola	0.0	0.0	0.4
Nitzschia epiphyticoides	0.0	0.0	0.2
Nitzschia cf. *frustulum*	0.0	0.2	0.0
Nitzschia lancettula	0.0	0.4	0.0
Nitzschia obsoleta	0.2	0.0	0.0
Nitzschia tropica	1.2	0.0	0.2
Placoneis gastrum	0.0	0.0	x
Rhopalodia gibberula	0.0	0.0	x
Rhopalodia rhopala	0.4	0.0	0.0
Ulnaria acus	0.0	0.0	0.2
Ulnaria ulna	0.6	0.0	2.6

Poster

The diatom flora of Lake Kyaninga, a freshwater crater lake in Western Uganda

Christine Cocquyt[1], Dirk Verschuren[2] & Pierre-Denis Plisnier[3]
christine.cocquyt@br.fgov.be

[1] National Botanic Garden of Belgium, Belgium
[2] Ghent University, Belgium
[3] Royal Museum for Central Africa, Belgium

Lake Kyaninga is a deep crater lake situated at an altitude of 1530 m asl on the shoulder of the Edward-George extension of the East African Rift Valley, Western Uganda. It has a surface area of 24 ha, and is enclosed by a crater catchment of 42 ha with maximum rim height of 77 m above the lake surface. Lake Kyaninga is among the 48 Ugandan fresh crater lakes studied in the CLANIMAE project (Climatic and anthropogenic impacts on African ecosystems). These lakes represent a productivity gradient from oligotrophic to hyper-eutrophic (natural as well as anthropogenic), and their modern diatom flora is studied in order to make a diatom-based inference model for the past trophic status of East African lakes.
Permanently stratified with a maximum depth of more than 220 m and Secchi-disk transparency between 3.9 and 6 meter, Lake Kyaninga is among the least productive crater lakes of western Uganda. In August 2008 a chlorophyll a content of 5.2 µg/l was measured in surface waters. Quantitative phytoplankton analyses of the pelagic zone during the dry season in August 2008 and during the wet season in April 2009 showed that diatoms contribute only a minor part of the total phytoplankton biomass in this lake during the studied periods: in August 2008 only 0.9 % of the total biomass, in April 2009 at the surface 2.0 % and 1.3 % at 10 m depth. *Nitzschia fonticola*, *Ulnaria acus* and *Urosolenia* sp. were the dominant species. Analysis of the sub-fossil diatom assemblage preserved in offshore surface sediments (upper 5 cm) gives a good representation of the annual pelagic diatom community of Lake Kyaninga in recent years. It is composed by a *Pseudostaurosira brevistriata* - *Nitzschia fonticola* assemblage in the upper first cm, switching to a ***Pseudostaurosira brevistriata*** - *Achanthidium minutissimum* - *Cyclotella* cf. *stellligera* assemblage in the next four cm. *Nitzschia frustulum*, comprising several morphotypes, is also fairly important. Diatom species richness in the surface sediments is moderate, about 75 taxa. Only a small number of the diatom species inhabiting Lake Kyaninga have a distribution restricted to tropical Africa: *Nitzschia bacata*, *N. confinis*, *N. congolensis*, *N. epiphyticoides*, *N. lancettula*, *N. tropica*, *Rhopalodia gracilis* and *R. rhopala*.

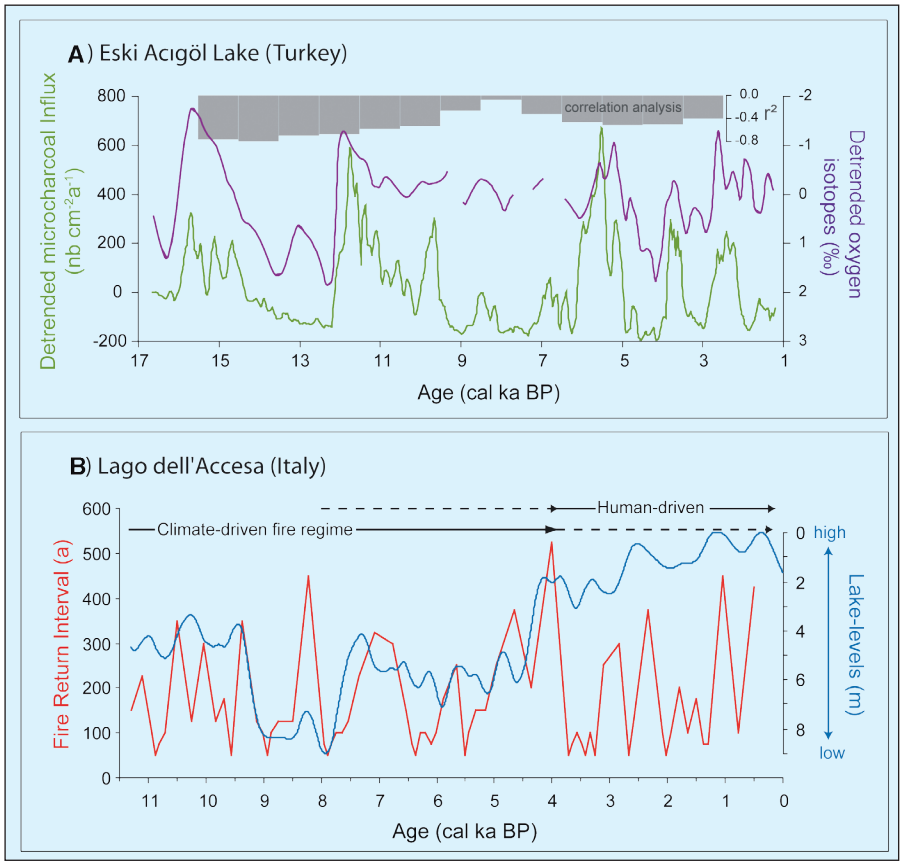

*Figure 2: **A**) Detrended microscopic charcoal (green line) and oxygen isotope record (purple line) for Eski Acıgöl Lake (Turkey). Correlation analysis (gray bars) shows statistically significant correlations between microscopic charcoal influx (particles cm^{-2} a^{-1}) and $\delta^{18}O$ (‰) for most of the record (modified from Turner et al., 2008); **B**) Lago dell'Accesa (Tuscany, Italy) lake-level fluctuations (blue line; modified from Magny et al., 2007) and the fire-return interval (red line) reconstructed from fire-event detection based on sedimentary macroscopic charcoal (modified from Vannière et al., 2008). Peaks in the fire-return interval curve correspond with high lake-level stands before 4 cal ka BP.*

across the Mediterranean (Carrión et al., 2003, 2007; Sadori et al., 2008).

Conclusion

The paleofire record from the Mediterranean is paradoxical. Climatic variations have certainly acted as one of the main pacemakers of fire regimes, particularly in the first half of the Holocene. Under different climate conditions (e.g., seasonality of precipitation), the southern and northern Mediterranean may have been differentially impacted by fire. Similarly, human actions (e.g., directly via ignition or indirectly via fuel management) have both increased and decreased fire activity during the Holocene. Increased sedimentary charcoal influx is often associated with pre- and proto-historic forest clearance but in the late Holocene, wildfire frequency often reached a maximum during phases of land abandonment and secondary scrub-woodland development, e.g., during the last century in much of Mediterranean Europe. Even apparently well-established relationships, such as evergreen oaks being favored by fire, turn out to be wrong when viewed over decadal to centennial timescales. These complex long-term responses are significant in the context of increasing aridity and warming, as well as major regional land-use changes linked to agricultural and tourism development around the Mediterranean Sea. Understanding them will help us to better manage and preserve one of the most fire-prone regions of the world, characterized by extraordinary plant diversity.

Data

The data are submitted to the Global Palaeofire Working Group Database (http://www.gpwg.org) and are available by contacting B. Vannière (boris.vanniere@univ-fcomte.fr)

Acknowledgements

We are greatly indebted to M. Magny, M. Power, W. Tinner and R. Turner who have contributed to these results and for enriching discussions about paleofire. Many thanks also to all contributors to the Mediterranean part of the Global Charcoal Database.

References

Colombaroli, D., Tinner, W., van Leeuwen, J.F.N., Noti, R., Vescovi, E., Vannière, B., Magny, M., Schmidt, R. and Bugmann, H., 2009: Response of broad-leaved evergreen Mediterranean forest vegetation to fire disturbance during the Holocene: insights from the peri-Adriatic region, *Journal of Biogeography*, **36**: 314-326.

Colombaroli, D., Vannière, B., Chapron, E., Magny, M. and Tinner, W., 2008: Fire-vegetation interactions during the Mesolithic-Neolithic transition at Lago dell'Accesa, Tuscany, Italy, *The Holocene*, **18**: 679-692.

Turner, R., Roberts, N. and Jones, M.D., 2008: Climatic pacing of Mediterranean fire histories from lake sedimentary microcharcoal, *Global and Planetary Change*, **63**: 317-324.

Vannière, B., et al., in press: Circum-Mediterranean fire activity and climate changes during the mid Holocene environmental transition (8500-2500 cal yr BP), *The Holocene*.

Vannière, B., Colombaroli, D., Chapron, E., Leroux, A., Tinner, W. and Magny, M., 2008: Climate versus human-driven fire regimes in Mediterranean landscapes: the Holocene record of Lago dell'Accesa (Tuscany, Italy), *Quaternary Science Reviews*, **27**: 1181-1196.

For full references please consult:
http://www.pages-igbp.org/products/newsletters/ref2010_2.html

Tropical fire ecology across the African continent: A paleoecological perspective

Daniele Colombaroli[1,2] and Dirk Verschuren[2]

[1]*Institute of Plant Sciences and Oeschger Center for Climate Change Research, University of Bern, Switzerland; daniele.colombaroli@ips.unibe.ch*
[2]*Limnology Unit, Department of Biology, Ghent University, Belgium*

High-resolution charcoal records from African lake sediments provide new insights for longstanding research questions on fire-climate-human interactions in tropical and subtropical ecosystems.

Every year, the tropics experience more fire than any other region in the world (Fig. 1). Tropical grassland (savannah) fires are the dominant source of carbon from biomass burning and provide more than 60% of the global total (Mouillot and Field, 2005). However, much of what is known about tropical fire ecology is based on monitoring programs started within the last decade, with highly fragmentary historical data extending only to the early 20th century. These data do not allow us to assess whether recent trends in fire frequency and magnitude are unusual in the context of natural long-term ecosystem dynamics (Gillson and Willis, 2004).

Natural or anthropogenic fire regime?

Seventy percent of tropical and subtropical areas worldwide are considered to have ecologically degraded fire regimes (Shlisky et al., 2007). In Africa, the recent increase in fire frequency is attributed to human ecosystem disturbance associated

with intensifying agriculture (Fig. 2; Davidson et al., 2003). For instance, in the lowland rainforests of West Africa and in moist montane forests at higher elevations in East Africa, natural fire is uncommon (Goldammer, 1990). Yet widespread clearance of natural vegetation has converted large, formerly forested areas into highly flammable grasslands (Roberts, 2000; Goldewijk, 2001). Studies of global-scale patterns in historical land use (e.g., Archibald et al., 2005) tend to assume that human impact on tropical African ecosystems was limited before 1700 AD because population densities of indigenous people were low (Goldewijk, 2001; Ramankutty and Foley, 1999). This perspective contrasts with archeological and paleoecological evidence that indicates that anthropogenic forest clearance in parts of East Africa started at least 2.5 ka ago, in association with the introduction of iron smelting technology (Robertshaw and Taylor, 2000). Other authors suggest that humans have altered African forest ecosystems over a longer time (Willis et al., 2004). If increasing fire activity during the Holocene was indeed related to intensifying human impact (Lejju et al., 2005; Ryner et al., 2008), the timing and extent to which humans altered local ecosystems varied regionally and among ecosystems. For instance, recent studies indicate that deforestation associated with sedentary agriculture started only ~0.35 ka ago in the moist highlands of central Kenya (Lamb et al., 2003) but at least ~0.8–1 ka ago in sub-humid western Uganda (Ssemmanda et al., 2005; Russell et al., 2009). In drier environments, agricultural activity often began ~0.12 ka ago, during colonial times, yet landscapes may have been significantly modified by pastoralist cultures well before then. Detailed charcoal studies with adequate spatial coverage are needed to determine whether current fire regimes are within the range of historic variability (Willis and Birks, 2006), or whether fire frequency has increased in response to the different types and intensities of human impact associated with pastoralist and agriculturalist societies.

Fire regime response & feedback to past climate variability

High-resolution charcoal studies have shown how fire can be a "catalyst" for climate-change effects on vegetation. For instance, moist conditions limit fire to spread in present tropical forests, but during drier periods in the past wildfire was likely more common, causing changes in ecosystem structure and degradation (e.g., Willis and Birks, 2006; Bush et al., 2008; Fig. 2). Climate-proxy information from the sediments of East African lakes document major variations in moisture balance. For example, in the late 18th century, an episode of severe drought completely desiccated all but one lake in the Eastern Rift Valley of Kenya, south of Lake Turkana (Verschuren, 2004; Bessems et al., 2008). In the last few millennia, century-long periods of both significantly drier and wetter conditions than today have occurred over most of equatorial East Africa. There have also been periods (e.g., from ~1500 to 1750 AD) when climate was unusually dry in the normally sub-humid western parts of the region while remaining unusually wet in semi-arid regions further east (Verschuren et al., 2000; Russell and Johnson, 2007). Research documenting the response of terrestrial ecosystems to this climate variability reveals the high sensitivity of vegetation transition zones, such as the forest/savannah ecotone, to even modest decadal-scale variations in rainfall (Lamb et al., 2003; Ngomanda et al., 2007). Additional charcoal records of high temporal resolution are needed to show how fire regimes have responded to contrasting climate trends at the regional scale (Fig. 1b).

Tropical ecosystems resilience to fire

In the seasonally dry climate regime prevailing throughout most of East Africa, fire is the dominant direct control on vegetation distribution (Bond et al., 2005; Gillson and Duffin, 2007) but natural fire frequency decreases from semi-arid central and eastern Kenya to sub-humid western Uganda. How does fire control the landscape-scale ecotone between savannah and forest? Recent studies postulate that tropical rainforests and grass savannah may exist as "stable states" in which a grass-dominated ecosystem is maintained by frequent fires while a tree-dominated ecosystem helps create a wet microclimate and low ground cover/fuel load that limits fire (Sankaran et al., 2005; Gillson and Duffin, 2007; Gillson, 2008). A shift from small patchy fires set by indigenous peoples to the larger fires characteristic of European land management has strongly altered the savannah-forest ecotone, by favoring highly flammable annual grasses. Thus, by increasing the flammability of grass communities, this historical change in fire management may have caused a positive feedback with fire (Cochrane, 2009). This hypothesis needs to be rigorously tested

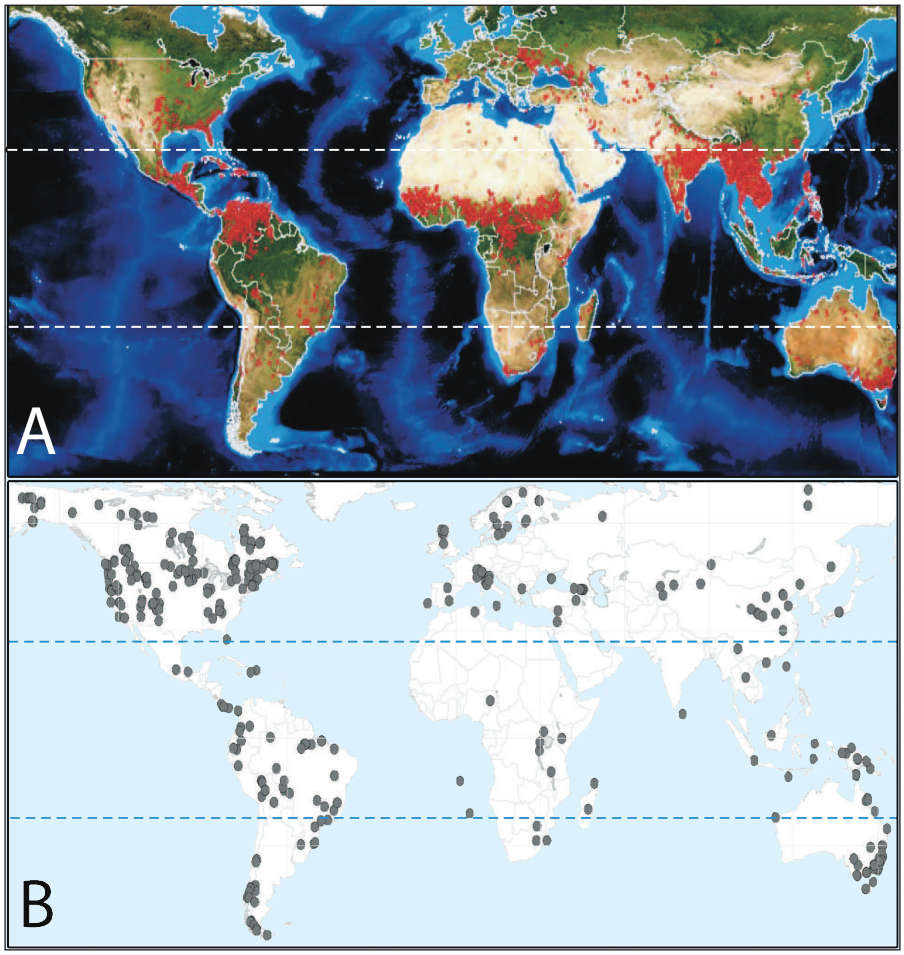

*Figure 1: **A**) Satellite image of world fire activity detected by MODIS in the early spring of 2010 (red dots, data from Fire Information for Resource Management System FIRMS, http://maps.geog.umd.edu/firms). **B**) Worldwide geographical distribution of paleoecological fire-regime records currently in the Global Charcoal Database (modified from Power et al., 2008). Despite the great fire activity in tropical and subtropical ecosystems, few paleofire records are available from regions such as Africa. Dashed lines delimit the tropical region, bounded by latitudes 23.5°N and S.*

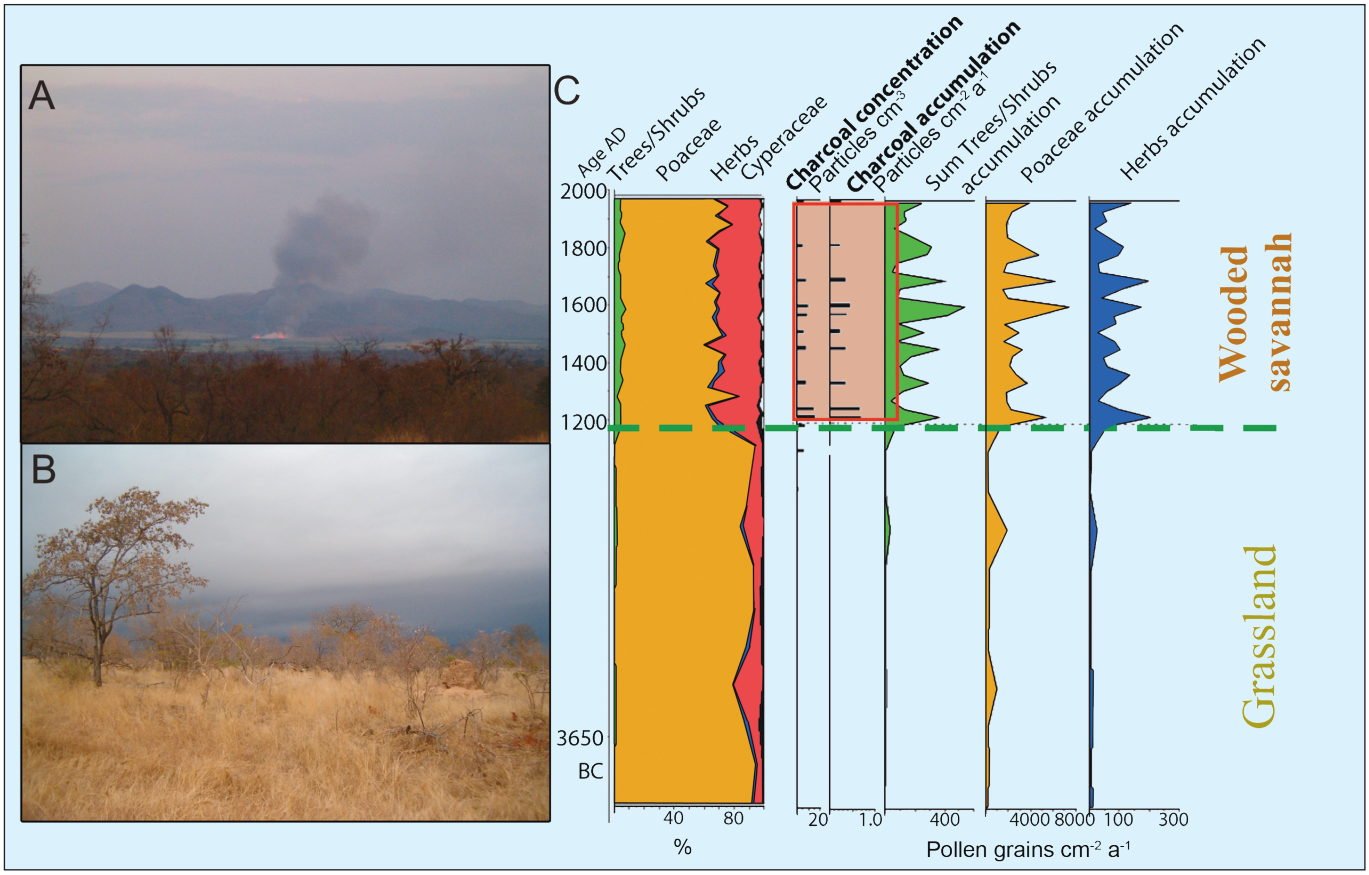

*Figure 2: **A**) Human-set fire in a rural area close to Mozambique border. Here, fire is used to clear land for agriculture and livestock ranching. **B**) Wooded savannah stand in Kruger National Park (South Africa). During the dry season (Apr-Oct), most of the biomass dries, increasing the fire hazard. (Photos by D. Colombaroli). **C**) Pollen and charcoal record from Malahlapanga Lake (Kruger National Park) showing the transition from grassland to a fire-maintained wooded savannah after 1100 AD (modified from Gillson and Ekblom, 2009). The authors suggested that increased regional rainfall promoted biomass production (i.e., wooded savannah), allowing fire activity to increase.*

on long timescales and in multiple regions to determine whether this feedback is characteristic of presently highly disturbed conditions, or whether it also occurred during natural cycles of long-term hydrological change. Paleoinformation on the resilience of tropical moist forests to occasional fire and, specifically, the rate at which rainforests recover from destructive fire would also be highly instructive for future conservation (Cochrane, 2003). New reconstructions of past fire regimes based on fossil charcoal analysis that quantify the local frequency of fire (e.g., Whitlock and Larsen, 2001; Gavin et al., 2006; Higuera et al., 2008), combined with modern calibration studies (Duffin et al., 2008), should reveal how African ecosystems respond to fire variability at decadal to century timescales.

Research outlook

Coupled atmosphere/ocean/biosphere climate models project future temperatures across tropical Africa to increase from 0.2 to 0.5°C per decade, and precipitation in East Africa to increase during the short rainy season (Northern Hemisphere winter) and decrease during the main rainy season (Northern Hemisphere spring) (Hulme et al., 2001; IPCC, 2007). In addition, changes in the teleconnected El Niño/Southern Oscillation (ENSO) are projected to cause pronounced drought in some regions and increased risk of flooding in others (Wara et al., 2005). If mean annual precipitation over East Africa does increase (IPCC, 2007), its beneficial effect on forest ecosystems will likely be lost in areas with frequent anthropogenic fires and increasing demographic pressure. Insights into how Africa's forest and savannah ecosystems will respond to the multiple stressors of future global climate change requires an understanding of past ecosystem responses to large-magnitude environmental changes. Currently still very rare in Africa and elsewhere in the tropics, high-resolution paleoecological records of (pre-)historical human impact, fire and vegetation can provide such holistic information.

Acknowledgements

We thank Lindsey Gillson for useful comments and Mitchell J. Power for the global map of sites in the Global Charcoal Database. The project "Fire, climate change and human impact in tropical ecosystems: paleoecological insights from the East African region" is funded by the Swiss National Science Foundation (FNS "Ambizione" Project no. PZ00P2_126573).

References

Cochrane, M.A., 2003: Fire science for rainforests, *Nature*, **421**: 913-919.

Duffin, K.I., Gillson, L. and Willis, K.J., 2008: Testing the sensitivity of charcoal as an indicator of fire events in savanna environments: quantitative predictions of fire proximity, area and intensity, *The Holocene*, **18**: 279-291.

Gillson, L. and Ekblom, A., 2009: Resilience and thresholds in savannas: nitrogen and fire as drivers and responders of vegetation transition, *Ecosystems*, **12**: 1189-1203.

Sankaran, M., Hanan, N. and Scholes, R., 2005: Determinants of woody cover in African savannah, *Nature*, **438**: 846-849.

Willis, K.J., Gillson, L. and Brncic, T.M., 2004: How "virgin" is virgin rainforest? *Science*, **304**: 402-403.

For full references please consult:

http://www.pages-igbp.org/products/newsletters/ref2010_2.html

Full list of references

Archibald, S., Bond, W.J., Stock, W.D. and Fairbanks, D.H.K., 2005: Shaping the landscape: Fire-grazer interactions in an African savanna, *Ecological Applications*, **15:** 96-109.

Bessems, I., Verschuren, D., Russell, J.M., Hus, J., Mees, F. and Cumming, B.F., 2008: Palaeolimnological evidence for widespread late 18th century drought across equatorial East Africa, *Palaeogeography, Palaeoclimatology, Palaeoecology*, **259** (2-3): 107-120.

Bond, W.J., Woodward, F.I. and Midgley, G.F., 2005: The global distribution of ecosystems in a world without fire, *New Phytologist*, **165:** 525-537.

Bush, M.B., Silman, M.R., McMichael, C. and Saatchi, S., 2008: Fire, climate change and biodiversity in Amazonia: a Late-Holocene perspective, *Philosophical Transactions of the Royal Society B-Biological Sciences*, **363:** 1795-1802.

Cochrane, M.A., 2003: Fire science for rainforests, *Nature*, **421**: 913-919.

Cochrane, M.A., 2009: Tropical Fire Ecology, *Climate change, Land use and ecosystems dynamics*, Springer-Verlag, Berlin, 645.

Davidson, O., Halsnaes, K., Huq, S., Kok, M., Metz, B., Sokona, Y. and Verhagen, J., 2003: The development and climate nexus: the case of sub-Saharan Africa, *Climate Policy*, **3:** 97-113.

Duffin, K.I., Gillson, L. and Willis, K.J., 2008: Testing the sensitivity of charcoal as an indicator of fire events in savanna environments: quantitative predictions of fire proximity, area and intensity, *The Holocene*, **18**: 279-291.

Gavin, D.G., Hu, F.S., Lertzman, K. and Corbett, P., 2006: Weak climatic control of stand-scale fire history during the late Holocene, *Ecology*, **87:** 1722-1732.

Gillson, L., 2008: Resilience, thresholds and dynamic landscapes, *South African Journal of Botany*, **74:** 357-358.

Gillson, L. and Duffin, K.I., 2007: Thresholds of potential concern as benchmarks in the management of African savannahs, *Philosophical Transactions of the Royal Society B-Biological Sciences*, **362:** 309-319.

Gillson, L. and Willis, K.J., 2004: 'As Earth's testimonies tell': wilderness conservation in a changing world, *Ecology Letters*, **7:** 990-998.

Gillson, L. and Ekblom, A., 2009: Resilience and thresholds in savannas: nitrogen and fire as drivers and responders of vegetation transition, *Ecosystems*, **12:** 1189-1203.

Goldammer, J.G., 1990: Fire in the Tropical Biota, *Ecosystem Processes and Global Challenges*, Springer-Verlag, Berlin, 497.

Goldewijk, K.K., 2001: Estimating global land use change over the past 300 years: The HYDE Database, *Global Biogeochemical Cycles*, **15:** 417-433.

Higuera, P.E., Brubaker, L.B., Anderson P.M., Brown, T.A., Kennedy, A.T. and Hu, F.S., 2008: Frequent Fires in Ancient Shrub Tundra: Implications of Paleorecords for Arctic Environmental Change, *PLoS ONE*, **3**(3): e1744.

Hulme, M., Doherty, R., Ngara, T., New, M. and Lister, D., 2001: African climate change: 1900-2100, *Climate Research*, **17:** 145-168.

IPCC, 2007: Climate Change 2007: The Physical Science Basis. Contribution of Working Group I to the Fourth Assessment Report of the Intergovernmental Panel on Climate Change [Solomon, S., D. Qin, M. Manning, Z. Chen, M. Marquis, K.B. Averyt, M.Tignor and H.L. Miller (eds.)]. Cambridge University Press, Cambridge, United Kingdom and New York, NY, USA.

Lamb, H., Darbyshire, I. and Verschuren, D., 2003: Vegetation response to rainfall variation and human impact in central Kenya during the past 1100 years, *The Holocene*, **13**: 285-292.

Lejju, B.J., Taylor, D. and Robertshaw, P., 2005: Late-Holocene environmental variability at Munsa archaeological site, Uganda: a multicore, multiproxy approach, *The Holocene*, **15**: 1044-1061.

Mouillot, F. and Field, C.B., 2005: Fire history and the global carbon budget: a 1 degrees x 1 degrees fire history reconstruction for the 20th century, *Global Change Biology*, **11:** 398-420.

Ngomanda, A., Jolly, D., Bentaleb, I., Chepstow-Lusty, A., Makaya, M., Maley, J., Fontugne, M., Oslisly, R. and Rabenkogo, N., 2007: Lowland rainforest response to hydrological changes during the last 1500 years in Gabon, Western Equatorial Africa, *Quaternary Research*, **67**: 411-425.

Power, M. J., et al., 2008: Changes in fire regimes since the Last Glacial Maximum: an assessment based on a global synthesis and analysis of charcoal data, *Climate Dynamics*, **30**: 887-907.

Ramankutty, N. and Foley, J.A., 1999: Estimating historical changes in global land cover: Croplands from 1700 to 1992, *Global Biogeochemical Cycles*, **13**: 997-1027.

Roberts, S.J., 2000: Tropical fire ecology, *Progress in Physical Geography*, **24**: 281-288.

Robertshaw, P. and Taylor, D., 2000: Climate change and the rise of political complexity in western Uganda, *Journal of African History*, **41**: 1-28.

Russell, J.M. and Johnson, T.C., 2007: Little Ice Age drought in equatorial Africa: ITCZ migrations and ENSO variability, *Geology*, **35**: 21-24.

Russell, J.M., McCoy S.J., Verschuren, D., Bessems, I. and Huang, Y., 2009: Human Impacts, Climate Change, and Aquatic Ecosystem Response during the past 2000 years at Lake Wandakara, Uganda, *Quaternary Research*, **72**: 315-324.

Ryner, M., Holmgren, K. and Taylor, D., 2008: A record of vegetation dynamics and lake level changes from Lake Emakat, northern Tanzania, during the last c. 1200 years, *Journal of Paleolimnology*, **40**: 583-601.

Sankaran, M., Hanan, N. and Scholes, R., 2005: Determinants of woody cover in African savannah, *Nature*, **438**: 846-849.

Ssemmanda, I., Ryves, D.B., Bennike, O. and Appleby, P.G., 2005: Vegetation history in western Uganda during the last 1200 years: a sediment-based reconstruction from two crater lakes, *Holocene*, **15**: 119-132.

Shlisky, A., et al., 2007: Fire, ecosystems and people: threats and strategies for global biodiversity conservation. GFI Technical Report 2007-2, The Nature Conservancy, Arlington, VA.

Verschuren, D., 2004: Decadal to century-scale climate variability in tropical Africa during the past 2000 years, In: R.W. Battarbee, et al., (Eds.) *Past climate variability through Europe and Africa*, Kluwer, Dordrecht, 139-158.

Verschuren, D., Laird, K.R. and Cumming, B.F., 2000: Rainfall and drought in equatorial East Africa during the past 1100 years, *Nature*, **403**: 410-414.

Wara, M.W., Ravelo, A.C. and Delaney, M. L., 2005: Permanent El Nino-like conditions during the Pliocene warm period, *Science*, **309**: 758-761.

Whitlock, C. and Larsen, C.P.S., 2001: Charcoal as a Fire Proxy, In Smol J. P., Birks H. J. B. and Last W. M.. *Tracking Environmental Change Using Lake Sediments*, Kluwer Academic Publishers, Dordrecht, 75-97.

Willis, K.J., Gillson, L. and Brncic, T.M., 2004: How "virgin" is virgin rainforest? *Science*, **304:** 402-403.

Willis, K.J. and Birks, H.J.B., 2006: What is Natural? The need for a long-term perspective in biodiversity conservation, *Science*, **314**: 1261-1265.

Review of Palaeobotany and Palynology 164 (2011) 143–173

Contents lists available at ScienceDirect

Review of Palaeobotany and Palynology

journal homepage: www.elsevier.com/locate/revpalbo

Research papers

Modern non-pollen palynomorphs from East African lake sediments

Vanessa Gelorini [a,*], Annemieke Verbeken [b], Bas van Geel [c], Christine Cocquyt [d], Dirk Verschuren [a]

[a] Limnology unit, Department of Biology, Ghent University, K.L. Ledeganckstraat 35, B-9000 Gent, Belgium
[b] Research Group Mycology, Department of Biology, Ghent University, K.L. Ledeganckstraat 35, B-9000 Gent, Belgium
[c] Institute for Biodiversity and Ecosystem Dynamics, Research Group Paleoecology and Landscape Ecology, Universiteit van Amsterdam, Science Park 904, P.O. Box 94248, 1090 GE Amsterdam, The Netherlands
[d] National Botanic Garden of Belgium, Domein van Bouchout, B-1860 Meise, Belgium

ARTICLE INFO

Article history:
Received 8 July 2010
Received in revised form 6 December 2010
Accepted 8 December 2010
Available online 15 December 2010

Keywords:
tropical Africa
non-pollen palynomorphs (NPPs)
fungal spores
biodiversity
taxonomy
palaeoecology
palaeolimnology

ABSTRACT

This paper presents an illustrated guide to the identification of non-pollen palynomorphs (NPPs) preserved in lake-sediment archives from equatorial East Africa. Modern NPPs were recovered from recently deposited surface sediment in 20 small crater lakes in western Uganda, located along environmental gradients of vegetation (moist evergreen and semi-deciduous forest, wooded and open grass savannah), land use (pastoralism, crop agriculture, plantations) and lake characteristics (basin morphometry, water chemistry and aquatic production). We analyzed 9700 NPP specimens, which could be assigned to 265 distinct morphotypes, of which 239 belong to six major taxonomic groups: spores and other remains of fungi (198 morphotypes), spores of ferns and mosses (19 morphotypes), microscopic zoological remains (14 morphotypes), colonies, coenobia or zygo-/aplanospores produced by filamentous algae (7 morphotypes) and microscopic aquatic plant remains (1 morphotype). The remaining 26 morphotypes could not be assigned to a specific taxonomic category. Using primary taxonomic and molecular phylogenetic literature, 73 (28%) of the recovered morphotypes could be identified at the species, genus or family level, thereby conferring ecological indicator value to them. This study may facilitate the use of fossil NPPs to help reconstruct past climatic and anthropogenic impacts on African ecosystems, as already broadly established in other study regions outside Africa.

1. Introduction

The study of fossil non-pollen palynomorphs (NPPs) was introduced to the research discipline of palynology by van Geel (1978), who in the late 1970s analyzed a heterogeneous group of non-pollen microfossils found in pollen preparations from Holocene peat-bog sections in Germany and the Netherlands. These microfossils included remains of vascular plants as well as a great variety of degradation-resistant remains of fungi, algae and invertebrates. Van Geel (1978) provided descriptions, identifications and/or morphotype code numbers and, when available, ecological information on the taxa concerned. Since then palynologists have exploited the palaeoenvironmental indicator value of these microfossils, resulting in the established use of NPPs as a palaeoecological tool supplementary to palynology all over Europe (Kuhry, 1985; van Smeerdijk, 1989; Ralska-Jasiewiczowa and van Geel, 1992; López Sáez et al., 1998; Carrión and Navarro, 2002). During the most recent decade, NPP reference literature has expanded remarkably (including a special issue of the *Review of Palaeobotany and Palynology*: van Geel, 2006 and Vegetation history and Archaeobotany: Haas, 2010), and many newly described NPPs have been added to the morphotype list, which now counts in excess of 1000 types. NPP analysis recently also started to develop in other parts of the world such as North America (van Geel et al., 2007), Asia (Limaye et al., 2007; Zong et al., 2007; van Geel et al., 2008), the Subantarctic (Yeloff et al., 2007), and tropical South America (Berrío et al., 2006; Ledru et al., 2006; Rull et al., 2008).

The use of NPPs to help reconstruct tropical African palaeoenvironments has, thus far, been very modest in comparison. The first African NPP studies by Wolf (1966, 1967a,b) assessed the diversity of fungal spores preserved in the bottom sediments of some East African lakes sampled by D. A. Livingstone: Lake Naivasha in Kenya, Lake Chishi in Zambia, Lake Rukwa in Tanzania, and Lakes Kitandara and Mahoma in the Rwenzori Mountains of Uganda. Wolf identified a sizable number of fungal spores from these deposits, but their reference value remained limited due to their representation by pencil drawings with little detail, and lack of diagnostic descriptions and ecological information. Jarzen and Elsik (1986) studied fungal palynomorphs from recent river deposits in Zambia, mostly referring to the taxonomy and inferred ecology of Tertiary fossil fungi, to constrain the environmental conditions associated with certain fungal assemblages recovered from Neogene sediments. All later studies on fossil African NPPs (Carrión et al., 2000; Burney et al., 2003; Lejju et al., 2005; Mumbi et al., 2008) were fully

* Corresponding author.
E-mail address: Vanessa.Gelorini@UGent.be (V. Gelorini).

0034-6667/$ – see front matter © 2010 Elsevier B.V. All rights reserved.
doi:10.1016/j.revpalbo.2010.12.002

integrated into analyses of fossil pollen and spore assemblages, and African NPP morphotypes were identified with near-exclusive reference to European NPP morphotypes. This procedure evidently cannot derive much useful ecological information from NPP morphotypes not previously encountered in European contexts. Also it carries the risk that similarly looking European and African NPP morphotypes, many of which have not been positively attributed to a particular biological taxon, may occupy distinctly different ecological niches, such that transfer of ecological information from the European to the African taxon may be invalid. A first step towards scientifically sound application of NPPs in African palaeoecology was recently made by van Geel et al. (in press, 2011-this issue) through analysis of NPP diversity and biostratigraphy in relation to regional climate and vegetation history in a 25,000-year lake-sediment record from Lake Challa in southeastern Kenya. These authors imaged and described 61 NPP morphotypes, and related the stratigraphic distribution of some spore types to past changes in rainfall and the regional distribution of vegetation biomes.

A key requirement of understanding past environmental dynamics is to successfully link the fossil record to the distributions, tolerances and associations of living organisms in modern-day ecosystems (Birks and Birks, 1980; Blackford and Innes, 2006); i.e., the uniformitarian principle that is the foundation of geology and paleontology. However, the ecological indicator value of individual NPP morphotypes has traditionally been derived from their stratigraphic association with certain environmental conditions inferred from other palaeoecological indicators, documented in other research or geographical contexts (Blackford and Innes, 2006). This procedure carries the risk that the stratigraphic association with those other indicators is fortuitous, and hence that palaeoecological inferences based on the occurrence of those NPPs in a new context are erroneous. A regressive methodological approach, which starts from the association between modern-day NPP assemblages and actual environmental conditions and/or taphonomical processes, is only recently being explored in earnest. Nevertheless, the number of ecological studies focussing on modern NPP diversity and distribution in various substrates is rising (Pinto da Luz et al., 2002; Mulder et al., 2003; Prager et al., 2006; Blackford and Innes, 2006; Medeanic, 2006; Cugny et al., 2010) and reveals their true potential as a means to elucidate past vegetation changes and human activity in the landscape. With regard to tropical Africa, Carreta et al. (1998, 1999) studied the modern-day diversity of filamentous fungi on stems and leaves of grassland vegetation, and the presence of coprophilous fungi on wild animal dung (e.g., antilope, buffalo, zebra) from Marula Estate in Kenya. The significance of these studies for palaeoecological applications is unfortunately limited by the lack of diagnostic morphological descriptions.

This paper is the first of three contributions on a collection of modern NPPs recovered from recently deposited bottom sediments in western Ugandan crater lakes. Here we provide best-possible identifications, descriptions and images of all NPP morphotypes encountered, and we evaluate the observed NPPs against taphonomic processes and the species richness of the corresponding living organisms reported in tropical East Africa. The second paper will assess the effects of land use intensity and habitat differentiation on the observed fungal spore diversity in the study lakes and the third paper will validate the ecological indicator value of predominant African NPP morphotypes in relation to climate- and human-related terrestrial and aquatic environmental variables.

2. Material and methods

2.1. Environmental setting of the study lakes

The Lake Edward-George branch of the East African Rift System in western Uganda (0°43′ N-0°15′ S, 29°50′–30°21′ E) comprises about 80 maar-crater lakes, distributed over four lake districts identified as Fort Portal, Kasenda, Katwe-Kikorongo and Bunyaruguru (Melack, 1978). Intensifying land use, mainly based on small-scale subsistence farming, has reduced the area covered by natural forest vegetation (tropical high forests and savanna woodlands), to only 20.3% of the total land area (Andrua, 2002). Gently sloping crater walls surrounding the lakes are generally occupied by plantations (banana, coffee, *Eucalyptus*, pine and cotton), annual food crops (*Sorghum*, millet, maize), mixed vegetable gardens (potatoes, beans, cabbage) and meadows (grazed by cows, sheeps and goats). On steeper crater slopes the natural vegetation of some succulent species (such as *Euphorbia dawii*), shrubs and light-demanding ferns has often remained more or less intact. Also a fair number of crater lakes are located in the pristine savannah of Queen Elisabeth National Park, and in the partially pristine, partially secondary forest of Kibale National Park. Until a few years ago, only few of these lakes had been the subject of limnological or biological studies (e.g., Beadle, 1932; Kilham, 1971; Melack, 1978; Kizito et al., 1993). More recently their great number and diversity is being exploited to develop regional calibration data sets for a range of palaeoecological proxies (Eggermont and Verschuren, 2004a,b; Rumes et al., 2005; Eggermont et al., 2006, 2010), and some lakes have been the site of palaeohydrological or palaeoecological reconstruction (Ssemmanda et al., 2005; Russell et al., 2007, 2009; Bessems et al., 2008).

During two field campaigns in January–February and August–September 2008 we surveyed 41 Ugandan crater lakes to map the distribution of natural and disturbed vegetation, various types of human land use, patterns and intensity of human occupation, and the abundance ratio of livestock versus large wild herbivores within the crater catchments. The present inventory of NPP diversity in East African lake sediments is based on processed samples from 20 of these 41 surveyed crater lakes (Fig. 1), selected to cover the main landscape gradients from moist evergreen forest to grass savannah, and from pristine to severely impacted by human activity. Also taken into account are limnological characteristics such as basin morphometry, water chemistry and aquatic production (Table 1). The study lakes are all small (surface area 0.01–0.92 km^2), but have a surface-water salinity ranging from 56 μS/cm (freshwater) to 61,100 μS/cm (hypersaline); a trophic status ranging from oligothrophic to hypertrophic; and water-column mixing regimes ranging from shallow polymictic to deep and permanently stratified (Verschuren et al., 2009).

2.2. Sampling and analytical procedures

Surface sediments were collected from the deep, central part of each lake using a UWITEC gravity corer, and extruded upright with a fixed-interval sectioning device (Verschuren, 1993) in 1-cm to 5-cm increments depending on local sedimentation conditions. Samples were prepared for NPP analysis according to standard pollen extraction techniques (Faegri et al., 1989) which included sieving at mesh size 212 μm, KOH (10%) treatment, acetolysis, heavy liquid separation (density: 2.0) with sodium polytungstate, and mounting in glycerin jelly. For routine scanning and counting of NPPs an Olympus CX 31 light microscope was used at 400× and 1000× magnification. Identification of known NPP morphotypes was based on comparison with descriptions and illustrations in Wolf (1966, 1967a,b), van Geel (1978, 2001), van Geel and van der Hammen (1978), Pals et al. (1980), Bakker and van Smeerdijk (1982), van Geel and Aptroot (2006), Prager et al. (2006) and van Geel et al. (in press, 2011-this issue). NPP morphotypes with no apparent analogue in the European NPP literature were identified by reference to primary taxonomic literature, including Ellis (1971, 1976), Ellis and Ellis (1985), Hanlin (1990), Vánky (1994) and Bell (1983) for fungal remains; Hires (1965, 1978) and Tryon and Lugardon (1990) for fern and moss spores; Haas (1996) for microscopic zoological remains and Van Meel (1954), Batten and Grenfell (1996), Komárek and Jankovská (2001)

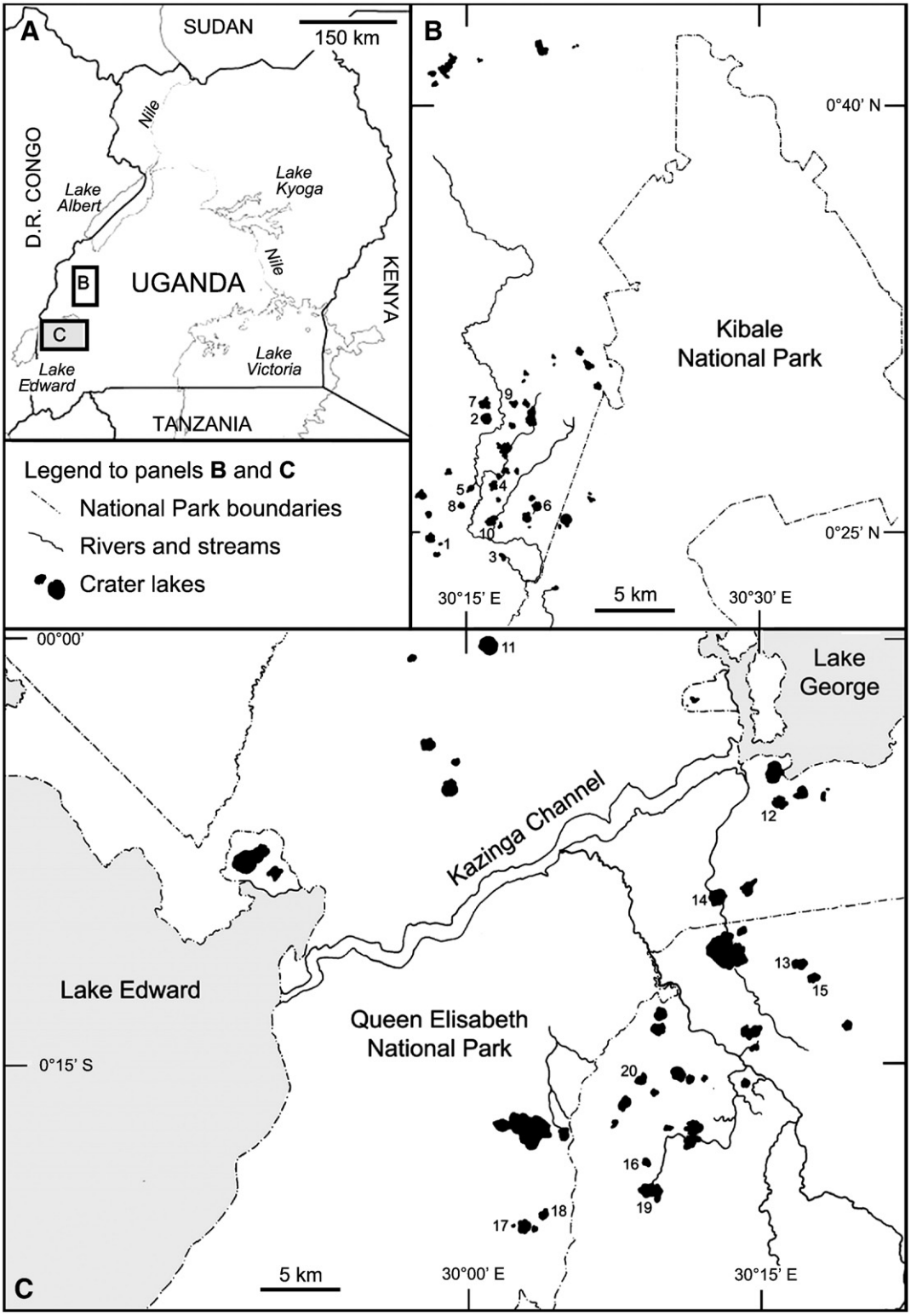

Fig. 1. Location of the 20 study lakes in western Uganda (modified from Rumes et al., 2005). Kasenda-cluster: 1. Kanyamukali, 2. Katanda, 3. Kitere, 4. Mahuhura, 5. Mubiro, 6. Murusi, 7. Mwengenyi, 8. Nyarayabana, 9. Nyantonde, 10. Wankenzi; Kikorongo-cluster: 11. Kikorongo; Bunyaruguru-cluster: 12. Bagusa, 13. Bugwagi, 14. Chibwera, 15. Ibamba, 16. Kako, 17. Kyogo, 18. Murabyo, 19. Nkugute, 20. Nyungu.

and John et al. (2002) for algal remains; and specialized tropical taxonomic literature (e.g. Dennis, 1961; Goh et al., 1997; Goh et al., 1998; Sivichai et al., 1998; Mibey and Kokwaro, 1999).

Since the taxonomy of fungi is in a state of constant flux due to increasing phylogenetic research, there is still no unique generally accepted system at the higher taxonomic level. However, multiple effort in establishing a consistent nomenclature based on molecular phylogenies is currently in progress under the auspices of the '*Assembling the Fungal Tree of Life*' (AFTOL; Celio et al., 2006) project, and the Deep Hypha Research Coordination network (Hibbett et al., 2007). Therefore, all identified fungal remains were classified with reference to the latest taxonomic developments, implemented in the

Table 1
Selected limnological and land use data of the 20 study lakes. Abbreviations: SA (surface area), Scond (conductivity), MAT (mean annual temperature), TOC (total organic carbon), HI (human index), Fo (forest), Sa (savannah), Per agri (perennial agriculture), Tree pl (tree plantation), Fa (fallow land), An agri (annual agriculture), Pa (pasture), B (bare land).

	Lake/Cluster	SA (km²)	Elevation (m asl)	Scond (µS/cm)	MAT (°C)	TOC (mg/l)	pH	Chl a (µg/l)	HI	Fo (%)	Sa (%)	Per agri (%)	Tree pl (%)	Fa (%)	An agri (%)	Pa (%)	B (%)
B	**Kasenda**																
1	Kanyamukali	0.02	1150	920	23.16	8.21	8.60	8.23	3.36	18	0	3	15	45	1	18	0
2	Katanda	0.37	1340	419	21.62	3.30	8.51	1.86	2.03	65	0	4	0	0	23	3	5
3	Kitere	0.10	1160	711	23.07	5.07	8.97	16.76	1.64	65	0	4	0	16	2	10	3
4	Mahuhura	0.19	1254	600	22.31	2.30	8.97	6.66	1.85	55	0	1	13	16	1	13	1
5	Mubiro	0.16	1208	718	22.69	4.55	9.02	1.79	2.81	40	0	2	0	20	1	37	0
6	Murusi	0.21	1226	382	22.54	8.61	8.54	1.32	3.4	25	0	6	2	34	1	30	2
7	Mwengenyi	0.29	1397	352	21.15	3.85	8.43	1.57	3.78	25	0	21	7	5	9	20	13
8	Nyarayabana	0.12	1179	857	22.92	11.23	8.84	9.22	1.72	60	0	0	0	34	5	0	1
9	Nyantonde	0.12	1387	501	21.24	2.90	8.76	2.27	4.74	18	0	9	2	0	41	0	30
10	Wankenzi	0.16	1158	496	23.09	7.59	8.65	13.71	2.44	55	0	11	5	0	14	0	15
C	**Katwe-Kikorongo**																
11	Kikorongo	0.92	915	22400	25.06	51.30	9.58	3.54	0	0	100	0	0	0	0	0	0
C	**Bunyaruguru**																
12	Bagusa	0.33	905	61100	25.14	228.38	10.62	670.65	0	0	100	0	0	0	0	0	0
13	Bugwagi	0.60	1048	441	23.98	3.23	9.02	3.84	3.85	25	0	45	0	5	5	10	10
14	Chibwera	0.76	971	457	24.60	1.91	8.91	6.74	0	100	0	0	0	0	0	0	0
15	Ibamba	0.01	1073	104	23.78	23.13	6.55	7.51	4.86	0	0	59	5	20	1	0	15
16	Kako	0.17	1396	89	21.16	1.50	8.18	1.19	4.87	0	0	40	6	25	24	5	0
17	Kyogo	0.02	1113	56	23.45	3.67	6.87	2.04	0	100	0	0	0	0	0	0	0
18	Murabyo	0.27	1098	141	23.58	6.27	8.42	5.94	0	100	0	0	0	0	0	0	0
19	Nkugute	0.89	1409	121	21.06	5.24	8.72	15.85	4.05	3	0	32	43	3	4	10	5
20	Nyungu	0.14	1172	430	22.98	6.60	9.40	47.10	4.66	0	0	64	0	35	1	0	0

Index fungorum (CABI database, Index Fungorum Partnership, 2004). Besides this, fungal species can also have multiple scientific names depending on their life cycle and mode of reproduction. Especially in tropical regions, the anamorphs (asexual states) of fungi are far better represented than teleomorphs (sexual states); often the latter are totally lacking. This frequently hampers the recognition of taxa, since anamorphs often do not contain sufficient diagnostic features to guarantee unambiguous identification (Whalley, 1993). When dealing with anamorphic states of known teleomorphs, we added the scientific name of the teleomorph to the taxonomic description.

The biotic richness and taxonomic complexity encountered in the study material necessitated rigorous application of standard taxonomic principles, to avoid mis-identification and mis-classification. Morphotypes were attributed to known species or genera only when published literature allowed a high degree of taxonomic precision (e.g., *Pediastrum angulosum*) and the taxon's biogeographical distribution in tropical regions could be confirmed. We used 'cf. (conferatur)' when a morphotype resembled a known species or genus (e.g., from the European NPP inventory) but positive association could not be made due to the fragmentary knowledge of the distribution of tropical species (e.g., *Curvularia* cf. *comoriensis*). When morphological resemblance was superficial or ambiguous, 'type' was added to the genus name (e.g., *Cercophora* type). Such morphotypes mostly represent not accurately identifiable but more or less homogeneous entities, based on conservative distinction of general morphological features of shape, size, and surface texture. Thus the word 'type' does not confer the taxonomic significance of a holotype on the described and photographed specimen, but is rather a provisional, not formally named form-species (van Geel, 1978). All morphotypes were photographed with a high-resolution Nikon DMX1200 digital camera. They were assigned to an existing type number (HdV) when already described previously by van Geel and others. Due to the affiliation with van Geel et al. (in press, 2011-this issue), first recorded African NPP morphotypes were given a new number, following the numbering system of van Geel et al. (in press, 2011-this issue), preceded by our lab initials UG (*Universiteit Gent*). Each assigned morphotype was classified in a broad taxonomic group, except for spores of ferns and mosses, which were assembled in a single morphological group. This is because both ferns (Pteridophyta) and mosses (Bryophyta) can produce trilete spores, which cannot properly be discerned from each other when identification is uncertain.

To facilitate morphological classification within a broad taxonomic category, some subgroups were formed on the basis of general diagnostic character states such as the presence and number of apertures (pores), germ slits and septa, and surface sculpture (smooth or ornamented). When fungal spores could not accurately be classified into conidia or ascospores, they were simply described as spores. Fungal morphotypes of which the total number of septa or pores was unclear due to fragmentation or unfavourable orientation were classified in the category corresponding with the visible features. Also to enhance consistency in classification, every division between two cavities was defined as a septum. Size differences between the single cells of a spore are described by terms of equality, while the geometry of the spore itself is expressed by terms of symmetry. The reported mean/modal length and width of each morphospecies were based on measurements of one to three intact (if present) and straight specimens from each lake where it was recovered. All descriptive botanical and nomenclatural terms follow the glossary of the Flora of Tropical East Africa (Beentje and Cheek, 2003) and some botanical (Stearn 2004) and fungal standard dictionaries (Kirk et al., 2008). Abbreviations of the authorities for all botanic groups, including fungi and algae follow the Brummitt and Powell (1992) standard for botanical names.

3. Results

The 20 surface-sediment samples processed for this study yielded a total of 9700 NPP specimens, which could be attributed to 265 distinct morphotypes. Most of these belong to one of six major taxonomic groups: spores and other remains of fungi (198 morphotypes, 74.7%), fern and moss spores (19 morphotypes, 7.2%), microscopic zoological remains (14 morphotypes, 5.3%), colonies, coenobia or zygo-/aplanospores of algae (7 morphotypes, 2.6%) and microscopic aquatic plant remains (1 morphotype, 0.4%). The

taxonomic affinity of the remaining 26 morphotypes (9.8%) is at present unknown, but many of them are nevertheless included in the analysis because of their sizable combined contribution to total NPP diversity, and their possible value as palaeoecological indicator once their distribution in relation to relevant environmental variables is established. We also illustrate and provide short diagnoses for NPP taxa (17 types) presented by van Geel et al. (in press, 2011-this issue), to better convey the level of morphological discrimination which we applied when NPP morphotypes are considered identical or distinct, and to allow the possibility that western Ugandan and south-eastern Kenyan populations are eventually found to be distinct. In the following overview, 78 unidentified NPP morphotypes which have only occasionally been observed (≤ 3 specimens) and lacked clear diagnostic characters are not included in the text or illustrations. Table 2 categorizes all 187 described morphotypes into the four broad abundance classes 'abundant', 'common', 'uncommon' or 'rare', based on their representation in our collection of 9700 recent NPP specimens from western Uganda. In all, 73 of the 265 morphotypes (about 28%) recovered from this Ugandan material could be identified at the family, genus or species level.

Table 2
Representation of each described morphotype (in ascending order) in our collection of 9700 recent NPP specimens from western Uganda, categorized into four broad abundance classes 'abundant' (>10% of all specimens), 'common' (>1–10%), 'uncommon' (0.1–1.0%) and 'rare' (<0.1%).

a. Abundant (>10%)
UG-1208: *Coniochaeta* spp.

b. Common (>1–10%)
HdV-1013: *Cercophora* type, UG-1068, UG-1073, UG-1099: *Brachysporium* spp., UG-1231: *Botryococcus* cf. *neglectus*, UG-1233: *Coelastrum reticulatum*, UG-1236: *Pediastrum boryanum* var. *brevicorne*, UG-1237: *Pediastrum boryanum* cf. var. *Forcipatum*, UG-1274, UG-1315: monoletes undiff.

c. Uncommon (0.1–1%)
HdV-89: *Tetraploa aristata*, HdV-1002: *Sporoschisma* spp., HdV-1005: *Brachydesmiella* sp., HdV-1029A: *Curvularia* cf. *intermedia*, HdV-1043: cf. *Lasiodiplodia theobromae*, HdV-1048, HdV-1052: Xylariaceae, HdV-1053: *Dictyosporium* cf. *heptasporum*, UG-1066: *Delitschia* spp., UG-1070: Xylariaceae, UG-1072, UG-1077: cf. Xylariaceae/Sordariaceae/Coniochaetaceae, UG-1078: *Sporidesmium* spp., UG-1080: *Sordaria* spp., UG-1084, UG-1087, UG-1091: *Bactrodesmium* type, HdV-1093: *Gelasinospora* cf. *cratophora*, UG-1098, UG-1103: *Glomus* sp., UG-1104, UG-1106, UG-1109, UG-1110, UG-1145: cf. *Fusarium* sp., UG-1148, UG-1151, UG-1153, UG-1155, UG-1173, UG-1174: *Rosellinia* sp., UG-1176, UG-1178: *Sordaria* type, UG-1180, UG-1185, UG-1223, UG-1224, UG-1235: *Pediastrum angulosum*, UG-1241: Epidermis of *Nymphaea nouchali*, UG-1243: cf. *Asplenium* sp., UG-1245: *Diporotheca* sp., UG-1246: *Isoetes* type, UG-1253: Polypodiaceae, UG-1254: *Phaeoceros* cf. *carolianus*, UG-1259: *Pteridium aquilinum*, UG-1260: *Coniogramme africana* type, UG-1261: cf. *Pteris/Actiniopteris* sp., UG-1262: *Canalisporium pulchrum*, UG-1277, UG-1286, UG-1303, UG-1307, UG-1309, UG-1311, UG-1316: *Asplenium* type, UG-1319, UG-1320

d. Rare (<0.1%)
HdV-1018A: *Spegazzinia tessarthra*, HdV-1018B: *Spegazzinia tessarthra*, HdV-1022: *Clasterosporium* sp., HdV-1030: cf. *Byssothecium* sp., HdV-1032, HdV-1049: cf. *Mitteriella ziziphina*, HdV-1058A, UG-1065: Xylariaceae, UG-1071: cf. *Amphirosellinia* sp., UG-1075, UG-1076, UG-1079: *Urocystis* sp., UG-1081, UG-1082, UG-1083, UG-1085, UG-1089, UG-1090: *Sporidesmium* cf. *macrurum*, UG-1092, UG-1095, UG-1096, UG-1097, UG-1101, UG-1105, UG-1107, UG-1111, UG-1112: *Phaeosphaeria* type, UG-1113: *Meliola* sp., UG-1114, UG-1115, UG-1118: cf. *Savoryella lignicola*, UG-1120: *Savoryella curvispora*, UG-1121, UG-1122: cf. *Cookeina* sp., UG-1123, UG-1124, UG-1125, UG-1126, UG-1127, UG-1128: cf. *Kretzschmaria clavus/K. cetrarioides*, UG-1129, UG-1130, UG-1134, UG-1135: cf. Xylariaceae, UG-1137: *Meliola* sp., UG-1138, UG-1139: *Gelasinospora* sp., UG-1141, UG-1142, UG-1144, UG-1147, UG-1150, UG-1157: *Rosellinia* sp., UG-1158, UG-1159, UG-1162, UG-1168, UG-1171: *Apiosordaria* type, UG-1172, UG-1177, UG-1179, UG-1182, UG-1183: cf. *Cercophora* sp., UG-1187, UG-1188, UG-1191, UG-1192, UG-1194, UG-1195, UG-1197, UG-1199, UG-1203, UG-1204, UG-1206: cf. *Acroconidiellina loudetiae*, UG-1211, UG-1216: *Diporotheca* sp., UG-1217, UG-1221, UG-1222, UG-1225, UG-1229, UG-1230, UG-1239: *Scenedesmus* sp., UG-1240: *Spirogyra* sp., UG-1242: *Dryopteris* subg. *Dryopteris*, UG-1247, UG-1248, UG-1249: cf. *Ctenitis/Lastreopsis* sp., UG-1250: *Curvularia* cf. *comoriensis*, UG-1252, UG-1255: *Ophioglossum* subg. *Ophioglossum*, UG-1258, UG-1263: cf. *Grammitis* sp., UG-1264: *Pteris* sp., UG-1268: *Canalisporium variabile*, UG-1276, UG-1280, UG-1281, UG-1282, UG-1284, UG-1285: cf. *Ascodesmis* sp., UG-1288, UG-1291: *Glomus* type, UG-1300, UG-1306, UG-1310, UG-1312, UG-1326, UG-1329: cf. Xylariaceae, UG-1330, UG-1331, UG-1332, UG-1333, UG-1334, UG-1340, UG-1342, UG-1343: cf. *Cirrenalia* sp., UG-1346, UG-1352

3.1. Descriptions and illustrations of African non-pollen palynomorphs

3.1.1. Spores and other remains of fungi

3.1.1.1. Septated spores

3.1.1.1.1. Uniseptate

Type HdV-1043: cf. *Lasiodiplodia theobromae* (Pat.) Griffon & Maubl. (Plate I)

Conidia ellipsoid, subequally and subsymmetrically 2-celled, reddish brown, 27 × 14 μm, slightly thick-walled, not constricted at the septum, with longitudinal ridges (3–4 on surface view). It is not always clear that it concerns conidia because the point of attachment can be indistinct due to unfavourable orientation. This morphotype strongly resembles *Lasiodiplodia theobromae*. It also resembles *Cainia desmazieri* C. Moreau & E. Müll. (syn. *Cainia incarcerata* (Desm.) E. Müll. & Arx), but *C. desmazieri* ascospores are smaller (22 × 7 μm), clearly constricted at the septum and not strictly ellipsoid (Moreau and Müller, 1963). Furthermore, the latter species is restricted to more temperate regions (Krug, 1978), whereas *Lasiodiplodia theobromae* has a worldwide distribution in tropical and subtropical regions. It has a very wide range of host plants, mainly woody plants including fruits and tree crops such as mango, peach, avocado, cacao and *Eucalyptus* (Mohali et al., 2005; Mbenoun et al., 2008).

Type UG-1066: *Delitschia* spp. (Plate I)

Ascospores ellipsoid to broadly fusiform, unequally and unsymmetrically 2-celled, brown to dark brown, 20–30(37) × 9–10(15) μm, smooth, thick-walled, often constricted at the septum; each cell with a straight germ slit parallel to the long axis of the ascospores. Based on differences in size of the ascospores and position of the germ slits (centred or not), this morphotype may include some *Delitschia* species. *Delitschia* species are mostly coprophilous, occurring worldwide on various kinds of dung (Bell, 1983; Hanlin, 1990).

Type UG-1081 (Plate I)

Spores ellipsoid, equally and symmetrically 2-celled, brown, 33 × 26 μm, smooth, very thick-walled, slightly constricted at the short (pseudo-)septum, with two points of attachment (truncate ends).

Type UG-1083 (Plate I)

Spores ellipsoid, equally and symmetrically 2-celled, brown, 52 × 30 μm, smooth, thick-walled, not constricted at the septum, with two points of attachment (truncate ends).

Type UG-1096 (Plate I)

Spores fusiform and slightly curved, subequally and subsymmetrically 2-celled, yellow, 86 × 10 μm, smooth, thick-walled, constricted at the septum, with nearly rounded ends.

Type UG-1105 (Plate I)

Ascospores ellipsoid, equally and symmetrically 2-celled, yellowish brown, 32 × 12 μm, smooth, thick-walled, constricted at the septum, with nearly rounded ends.

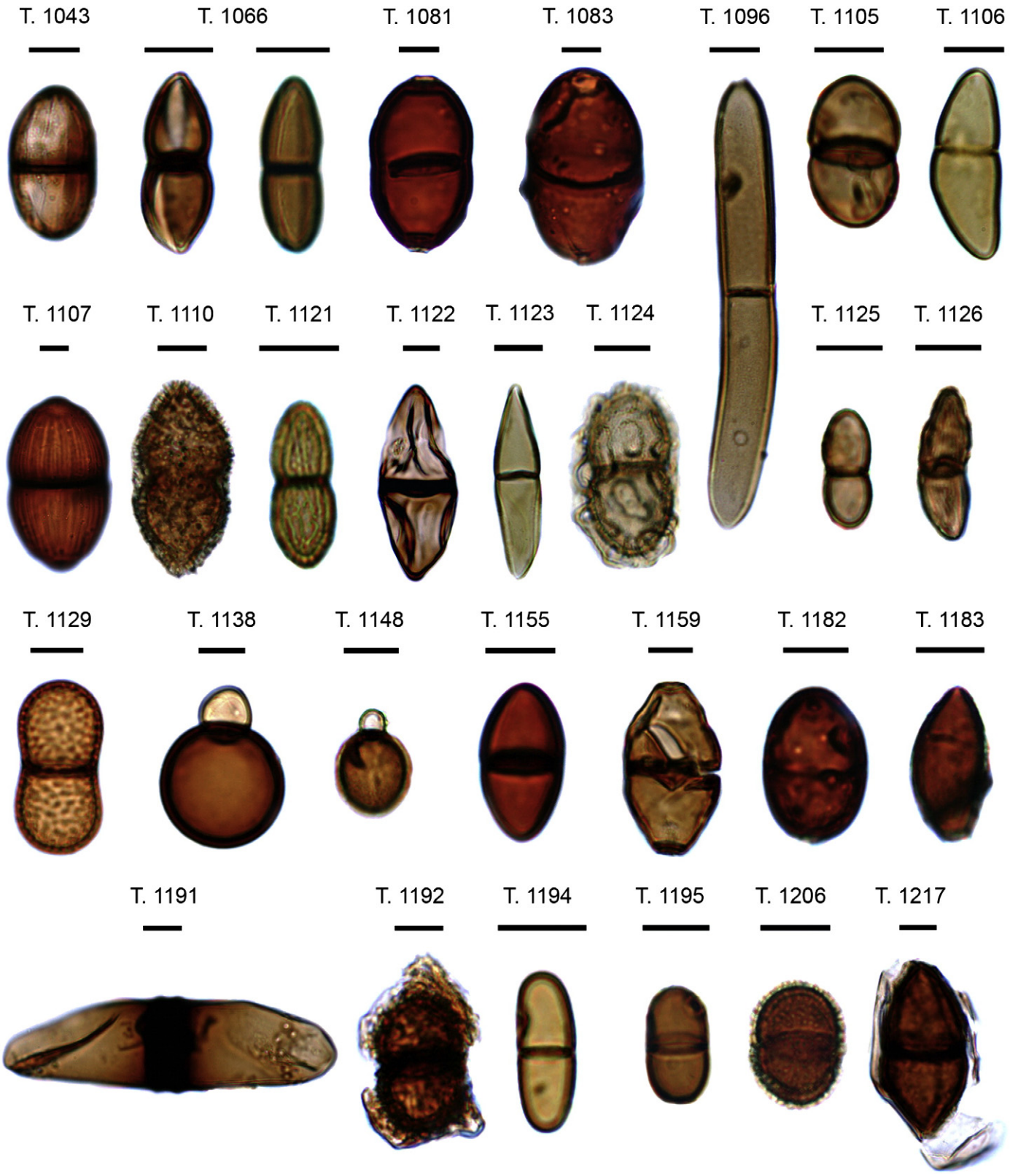

Plate I. Septate fungal spores: uniseptate: T. HdV-1043: cf. *Lasiodiplodia theobromae*, T. UG-1066: *Delitschia* spp., T. UG-1081, T. UG-1083, T. UG-1096, T. UG-1105, T. UG-1106, T. UG-1107, T. UG-1110, T. UG-1121, T. UG-1122: cf. *Cookeina* sp., T. UG-1123, T. UG-1124, T. UG-1125, T. UG-1126, T. UG-1129, T. UG-1138, T. UG-1148, T. UG-1155, T. UG-1159, T. UG-1182, T. UG-1183: cf. *Cercophora* sp., T. UG-1191, T. UG-1192, T. UG-1194, T. UG-1195, T. UG-1206: cf. *Acroconidiellina loudetiae*, T. UG-1217. All scale bars are 10 μm.

Type UG-1106 (Plate I)

Ascospores ellipsoid, (un)equally and (a)symmetrically 2-celled, yellow, 24–32 × 8–11 μm, smooth, slightly thick-walled, constricted at the septum, with slightly tapering ends. Based on small differences in the morphology of the single cells (symmetrical versus asymmetrical, small versus large), this type probably includes different species or genera.

Type UG-1107 (Plate I)

Spores ellipsoid, equally and symmetrically 2-celled, brown, 67×38 μm, finely striate, thick-walled, constricted at the septum, with bulged and rounded ends.

Type UG-1110 (Plate I)

Spores ellipsoid, equally and symmetrically 2-celled, yellowish brown, 37–39×15–17 μm, densely covered with small, cylindrical free standing processes, thick-walled, constricted at the septum, with slightly tapering ends.

Type UG-1121 (Plate I)

Spores ellipsoid, subequally and subsymmetrically 2-celled, yellow, 22×5 μm, covered with a pattern in which parallel or subparallel *individual dots* are cross-linked to form a reticulum in the grooves (striato-reticulate), thick-walled, constricted at the septum, nearly rounded ends.

Type UG-1122: cf. *Cookeina* sp. (Plate I)

Ascospores ellipsoid to fusiform, equally and symmetrically 2-celled, pale brown, 52×30 μm, slightly thick-walled, not constricted at the septum, with tapering ends. *Cookeina* is commonly distributed in the tropics and subtropics, and can be found on fallen angiosperm branches, trunks and occasionally on fruits (Weinstein et al., 2002; Bera et al., 2008).

Type UG-1123 (Plate I)

Spores fusiform, unequally and asymmetrically 2-celled, pale yellow, 42×9 μm, smooth, slightly thick-walled, slightly constricted at the septum, with tapering ends.

Type UG-1124 (Plate I)

Spores ellipsoid, subequally and subsymmetrically 2-celled, pale yellow, 32×15 μm, smooth, thick-walled, constricted at the septum, and with microreticulate hyaline sheath/coat, ornamented with circular and curving ridges, which are often hollow.

Type UG-1125 (Plate I)

Spores ellipsoid, subequally and subsymmetrically 2-celled, yellow, 19–32×6–11 μm, smooth, thick-walled, constricted at the septum. This rather nondescript morphotype probably includes several species or genera.

Type UG-1126 (Plate I)

Spores ellipsoid to fusiform, equally and symmetrically 2-celled, yellow, 24×7 μm, finely striate, slightly thick-walled, constricted at the septum, with slightly tapering ends.

Type UG-1129 (Plate I)

Spores ellipsoid to slightly dumbbell-shaped, equally and symmetrically 2-celled, brown, 34×14 μm, coarsely reticulate, thick-walled, constricted at the septum.

Type UG-1138 (Plate I)

Spores flask-shaped, unequally and asymmetrically 2-celled, brown to yellow, 37×28 μm, smooth, one cell large (28 μm in diameter), dark and thick-walled; other cell small (9 μm in diameter), pale and thin-walled.

Type UG-1148 (Plate I)

Spores flask-shaped, unequally and asymmetrically 2-celled, pale brown to yellow, 20×15 μm, smooth, one cell dark, large (15 μm in diameter) and very thick-walled; other cell pale, small (5 μm in diameter) and thin-walled; large cell surrounded by hyaline sheath (present or not) with scabrate pattern.

Type UG-1155 (Plate I)

Spores ellipsoid, equally and symmetrically 2-celled, brown, 23–32×12–15 μm, smooth, thick-walled, constricted at the septum; with slightly tapering ends; small opening/pore at one end (only visible in strictly polar or equatorial orientation).

Type UG-1159 (Plate I)

Spores fusiform, equally and symmetrically 2(4?)-celled (end cells may be missing), yellowish brown, 39–45×18–22 μm, smooth, thick-walled, constricted at the septum; single cells trapezoidal.

Type UG-1182 (Plate I)

Ascospores ellipsoid, subequally and subsymmetrically 2-celled, dark brown, 25×17 μm, smooth, thick-walled, not constricted at the septum; with pale septum.

Type UG-1183: cf. *Cercophora* sp. (Plate I)

Ascospores ellipsoid, unequally and asymmetrically 2-celled, dark brown, 23×12 μm, smooth, thick-walled, not constricted at the septum, truncated at one end but tapering at the other, pale septum not truly median; covered with slightly ribbed subhyaline sheath; with apical pore. *Cercophora* species occur worldwide on dung or on decaying wood, culms and other plant debris (Bell, 1983; Hanlin, 1990).

Type UG-1191 (Plate I)

Spores ellipsoid, equally and symmetrically 2-celled, yellowish brown, 88×26 μm, smooth, relatively thick-walled, not constricted at the septum; central zone very dark; septum only visible with overexposure to light.

Type UG-1192 (Plate I)

Spores ellipsoid, equally and symmetrically 2-celled, brown, 38×18 μm, smooth, thick-walled, slightly constricted at the septum; with subhyaline verrucate sheath/coat.

Type UG-1194 (Plate I)

Spores ellipsoid, equally and asymmetrically 2-celled, yellow, 18×7 μm, smooth, thick-walled, slightly constricted at the septum, with point of attachment.

Type UG-1195 (Plate I)

Spores ellipsoid, equally and asymmetrically 2-celled, yellowish brown, 18×10 μm, smooth, thick-walled, not constricted at the septum, with thickened point of attachment.

Type UG-1206: cf. *Acroconidiellina loudetiae* M.B.Ellis (Plate I)

Conidia ellipsoid, subequally and subsymmetrically 2-celled, brown, 16–20×13 μm, with small echinae (~1 μm), thick-walled, sometimes slightly constricted at the septum. It is not always clear that it concerns conidia because the point of attachment can be indistinct due to unfavourable orientation. *Acroconidiellina loudetiae* occurs in Tanzania and can be found on leaves of *Loudetia arundinacea* (Hochst. ex A. Rich.) Steud. in grassland vegetation (Ellis, 1976).

Type UG-1217 (Plate I)

Ascospores ellipsoid, equally and symmetrically 2-celled, brown, 50×23 μm, smooth, thick-walled, constricted at the septum; with hyaline sheath (present or not).

Type UG-1252 (Plate II)

Ascospores ellipsoid, equally and symmetrically 2-celled, yellowish brown, 24×13 μm, smooth, thick-walled, not constricted at the septum.

Type UG-1333 (Plate II)

Conidia club-shaped, unequally and asymmetrically 2-celled, brown, 28–37×18 μm, smooth, not constricted at the septum, slightly ribbed in the central part of the large and thick-walled cell (23–29×18 μm), end cell subhyaline, small (5–8×5 μm) and thin-walled.

Type UG-1340 (Plate II)

Conidia inversely club-shaped, unequally and asymmetrically 2-celled, brown, 42×17 μm, smooth, thick-walled, not constricted at the septum, end cell subhyaline, small (3×8 μm) and trapezoidal.

Type UG-1352 (Plate II)

Ascospores fusiform, unequally and asymmetrically 2-celled, yellowish brown, 37×15 μm, finely reticulate, slightly thick-walled, slightly constricted at the septum, more tapering towards one end, one cell slightly broader than the other.

3.1.1.1.2. Diseptate

Type HdV-1005: *Brachydesmiella* sp. (Plate II)

Conidia lemon-shaped, unequally and symmetrically 3-celled, pale brown to brown, 30–47×13–18 μm, smooth, thick-walled; central cell larger (20–37×13–18 μm) and darker than end cells (5×7 μm), which are broadly trapezoidal. See also van Geel et al. (in press, 2011-this issue). *Brachydesmiella biseptata* has previously been reported from temperate regions (e.g. France, Japan, Canada, United Kingdom), but three *Brachydesmiella* (sub)species (*Brachydesmiella anthostomelloidea* Goh & K.D. Hyde, *B. biseptata* var. *orientalis* V. Rao & de Hoog and *B. caudata* V. Rao & de Hoog) are particularly known from submerged wood in tropical freshwater environments (Sivichai et al., 1998). Based on spore characters, this East African morphotype may refer to *B. anthostomelloidea* or *B. biseptata* var. *orientalis*.

Type HdV-1048 (Plate II)

Ascospores ellipsoid to fusiform, unequally and symmetrically 3-celled, dark brown, 30–32(52)×15–19(22) μm, smooth, thick-walled, surrounded by a hyaline sheath, central cell larger (22–24(48)×15–19(22) μm) than end cells (4×8 μm), which are paler and conical to tapering. See also van Geel et al. (in press, 2011-this issue).

Type HdV-1049: cf. *Mitteriella ziziphina* Syd. (Plate II)

Conidia club-shaped, unequally and asymmetrically 3-celled, smooth, very thick-walled, with two pale to dark brown larger cells and one more subhyaline smaller and narrower basal cell, 27×13 μm, central zone very dark, septum only visible with overexposure to light, other (parts of) cells paler. See also van Geel et al. (in press, 2011-this issue). The genus *Mitteriella*, the anamorphic state of *Schiffnerula*, is parasitic on different species of *Ziziphus*, a genus of spiny shrubs and small trees in the family of Rhamnaceae (Tandon, 1935).

Type UG-1076 (Plate II)

Spore s ellipsoid, unequally and subsymmetrically 3-celled, pale brown to brown, 38×18 μm, smooth, very thick-walled; two (pseudo-)septa almost invisible; not constricted at the septa; central cell large, end cells small and tapering.

Type UG-1084 (Plate II)

Spores inversely egg-shaped, unequally and asymmetrically 3-celled, 38–50×29–30 μm, smooth, thick-walled, slightly constricted at the septa; two cells dark brown and broad; basal cell paler and narrow.

Type UG-1085 (Plate II)

Spores ellipsoid, unequally and asymmetrically 3-celled, dark brown, 36–40×24–28 μm, smooth, not constricted at the septa; basal cell paler and thinner. This morphotype may be related to Type UG-1084 (Plate II).

Type UG-1142 (Plate II)

Spores ellipsoid to slightly curved, unequally and asymmetrically 3-celled, brown, 38×13 μm, smooth, thick-walled, slightly constricted at the septa, surrounded by a hyaline sheath; cells differing in size; basal cell small, conical to tapering.

Type UG-1151 (Plate II)

Spores flask-shaped, unequally and asymmetrically 3-celled, 21–25×14 μm, smooth, thick-walled, constricted at the septa, cells differing in size; one cell very large and almost globose, brown; basal cell subhyaline, small and conical.

Type UG-1199 (Plate II)

Spores flask-shaped, unequally and asymmetrically 3-celled, 46×34 μm, smooth, very thick-walled, constricted at the septa, cells

Plate II. Septate fungal spores: uniseptate: T. UG-1252, T. UG-1333, T. UG-1340, T. UG-1352; Diseptate: T. HdV-1005: *Brachydesmiella* sp., T. HdV-1048, T. HdV-1049: cf. *Mitteriella ziziphina*, T. UG-1076, T. UG-1084, T. UG-1085, T. UG-1142, T. UG-1151, T. UG-1199, T. UG-1230, T. UG-1331, T. UG-1332, T. UG-1334; Triseptate: T. HdV-1029A: *Curvularia* cf. *intermedia*, T. HdV-1030: cf. *Byssothecium* sp., T. UG-1068, T. UG-1080, T. UG-1082, T. UG-1089, T. UG-1090: *Sporidesmium* cf. *macrurum*, T. UG-1091: *Bactrodesmium* type, T. UG-1092, T. UG-1098, T. UG-1111. All scale bars are 10 μm.

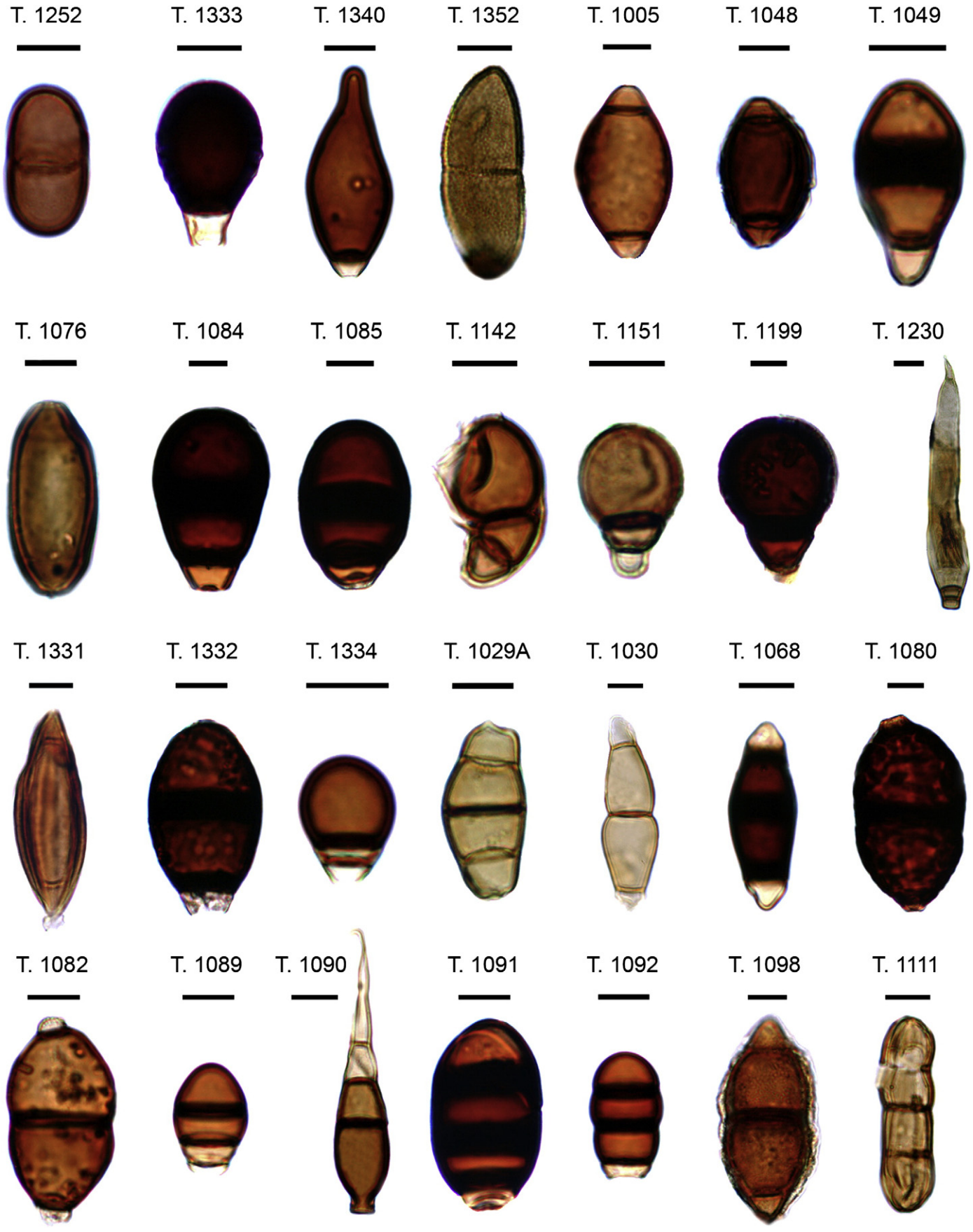

differing in size, one cell dark brown, very large and almost globose, basal cell (partly broken) subhyaline and small.

Type UG-1230 (Plate II)

Spores awl-shaped, unequally and asymmetrically 3-celled, yellow, 87×10 μm, smooth, thick-walled, with 2 septa at one end and an apiculate appendage at the other end.

Type UG-1331 (Plate II)

Ascospores ellipsoid to fusiform, unequally and subsymmetrically 3-celled, pale brown, 48×17 μm, smooth, very thick-walled (thickest in the center), with a small hyaline projection at the base forming a so-called foot cell, not constricted at the septa; (pseudo-)septa thickened.

Type UG-1332 (Plate II)

Conidia ellipsoid, unequally and asymmetrically 3-celled, brown, 34–50×21–28 μm (length dependent on the number of preserved cells), smooth or verrucate, thick-walled, not constricted at the septa; zone around widest septum dark; basal cell subhyaline, small and tapering (often missing or partly broken).

Type UG-1334 (Plate II)

Spores inversely egg-shaped, unequally and asymmetrically 3-celled, 18×13 μm, smooth, thick-walled, not constricted at the septa; one cell brown, large and almost globose; basal cells subhyaline and tapering.

3.1.1.1.3. Triseptate

Type HdV-1029A: *Curvularia* cf. *intermedia* Boedijn (Plate II)

Conidia ellipsoid to fusiform, unequally and asymmetrically 4-celled, yellow, 25–39×13–19 μm, smooth, not constricted at the septa, middle septum usually positioned along the median; slightly thick-walled. This *Curvularia* species has currently been differentiated from the Types HdV-1029A-B (see van Geel et al., in press, 2011-this issue), which include a symmetrical (i.e. Type HdV-1029A) and asymmetrical (i.e. Type HdV-1029B) 4-celled *Curvularia* species. *Curvularia intermedia*, an anamorphic state of *Cochliobolus*, has been reported from Australia, Papua-New Guinea, Tanzania and the USA, and occurs on *Triticum*, *Zea*, *Oryza* and *Cynodon* (Ellis, 1971).

Type HdV-1030: cf. *Byssothecium* sp. (Plate II)

Ascospores fusiform, oblong and slightly curved, unequally and asymmetrically 4-celled, pale yellow, 60×13 μm, smooth, constricted at the middle septum; one central cell more elongated and slightly broader than the other; central cells with thickened walls; end cells subhyaline, with thinner wall. See also van Geel et al. (in press, 2011-this issue). *Byssothecium* can be found on (submerged) wood (Crane et al., 1992).

Type UG-1068 (Plate II)

Spores fusiform, unequally and subsymmetrically 4-celled, 30–38×14–15 μm, smooth, not constricted at the septa; central cells dark brown and thick-walled; end cells subhyaline and thinner (frequently absent).

Type UG-1080 (Plate II)

Ascopores ellipsoid, unequally and asymmetrically 4-celled, 45–50 (65)×27–30(40) μm, verrucate, slightly constricted at the septa; central cells large (17–20(27)×27–30(40), dark brown and thick-walled; end cells 5 μm long, 7–9 μm wide, subhyaline and thin-walled. This morphotype resembles *Savoryella verrucosa* Minoura & T.Muroi, but the ascospores of the latter species are clearly smaller (Ho et al., 1997).

Type UG-1082 (Plate II)

Ascospores ellipsoid, unequally and asymmetrically 4-celled, 42×18 μm, smooth (but some protuberances may be caused by corrosion, see Plate II), constricted at the septa; central cells brown, large (18×18 μm) and thick-walled; end cells subhyaline, small (3×5 μm) and thin-walled. This morphotype may be related to Type UG-1080 (Plate II), which is ornamented, larger and thick-walled. Also some resemblance with Type HdV-1001 (see van Geel et al., in press, 2011-this issue) is apparent, but Type UG-1082 is slightly smaller and thin-walled.

Type UG-1089 (Plate II)

Spores ellipsoid to narrowly inversely club-shaped, unequally and asymmetrically 4-celled, pale brown, 23×14 μm, smooth, not constricted at the septa, thick-walled; basal cell subhyaline and thin-walled.

Type UG-1090: *Sporidesmium* cf. *macrurum* (Sacc.) M.B.Ellis (Plate II)

Conidia straight, curved or inversely club-shaped to beaklike; conico-truncate and protuberant at the base, unequally and asymmetrically 4-celled, 63–36×13–12 μm, smooth, slightly constricted at the septa, thick-walled; cells brown and gradually decreasing in size and colour towards apical part of conidia; end cell subhyaline and strongly tapering. *Sporidesmium macrurum* is mainly distributed in tropical areas (e.g., Brazil, Ceylon, Papua) and occurs on the leaves and leaf-stalks of palms such as *Areca*, *Borassus*, *Cocos*, *Elaeis*, *Licuala*, *Mauritia* and *Phoenix* (Ellis, 1971).

Type UG-1091: *Bactrodesmium* type (Plate II)

Conidia ellipsoid, unequally and asymmetrically 4-celled, 30–45×17–30 μm, smooth, thick-walled, slightly constricted at the septa, rounded at one end; septa dark; one central cell often darker than other cells; basal cell subhyaline, truncate and slightly thin-walled. Based on size and morphological variation, this morphotype probably includes different *Bactrodesmium* species, and maybe also other representatives of unknown but similarly looking genera. *Bactrodesmium* can be found worldwide on the wood and bark of various deciduous trees (Ellis, 1971).

Type UG-1092 (Plate II)

Spores ellipsoid, unequally and asymmetrically 4-celled, brown, 25×13 μm, smooth, thick-walled, constricted at the septa; basal cell much paler and subhyaline, somewhat smaller and thin-walled.

Type UG-1098 (Plate II)

Ascospores lemon-shaped, unequally and subsymmetrically 4-celled, smooth, dark yellow to pale brown, 50×20 μm, slightly constricted at the septa, thick-walled; with microreticulate hyaline sheath; central cells dark and large; end cells paler, conical and rather acute.

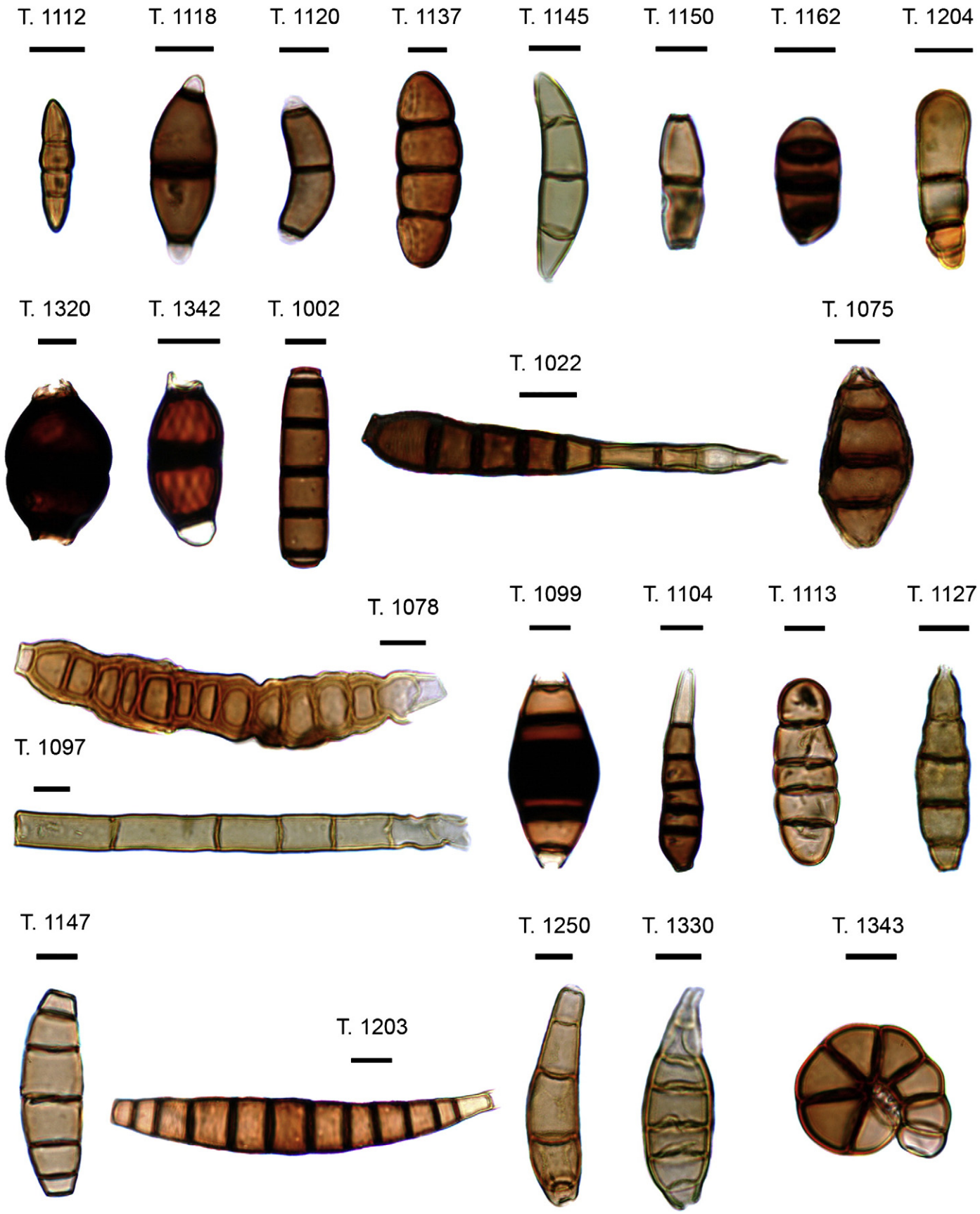

Plate III. Septate fungal spores: triseptate: T. UG-1112: *Phaeosphaeria* type, T. UG-1118: cf. *Savoryella lignicola*, T. UG-1120: *Savoryella curvispora*, T. UG-1137: *Meliola* sp., T. UG-1145: cf. *Fusarium* sp., T. UG-1150, T. UG-1162, T. UG-1204, T. UG-1320, T. UG-1342; Multiseptate: T. UG-1002: *Sporoschisma* spp., T. HdV-1022: *Clasterosporium* sp., T. UG-1075, T. UG-1078: *Sporidesmium* spp., T. UG-1097, T. UG-1099: *Brachysporium* spp., T. UG-1104: cf. *Podosporium rigidum*, T. UG-1113: *Meliola* sp., T. UG-1127, T. UG-1147, T. UG-1203, T. UG-1250: *Curvularia* cf. *comoriensis*, T. UG-1330, T. UG-1343: cf. *Cirrenalia* sp. All scale bars are 10 μm.

Type UG-1111 (Plate II)

Ascospores cylindrical to slightly dumbbell-shaped, unequally and asymmetrically 4-celled, yellow, 38–45 × 10–11 μm, striate, thick-walled, slightly constricted at the septa, end cells slightly broader and swollen.

Type UG-1112: *Phaeosphaeria* type (Plate III)

Ascospores narrowly fusiform, unequally and asymmetrically 4-celled, brown, 25 × 6 μm, longitudinally and finely striate, thick-walled, slightly constricted at the septa; one central cell enlarged; end cells tapering. This morphotype resembles *Phaeosphaeria*, in which one central cell is commonly enlarged (Shoemaker and Babcock, 1989), but may also be related to other genera, which have similarly looking ascospores (such as *Lophiostoma* and *Leptosphaeria*) (Ellis and Ellis, 1985). Species of *Phaeosphaeria* are known as pathogens on cereals, wild grasses, sedges and rushes (Shoemaker and Babcock, 1989).

Type UG-1118: cf. *Savoryella lignicola* E.B.G.Jones & R.A.Eaton (Plate III)

Ascospores ellipsoid to fusiform, unequally and asymmetrically 4-celled, 27–30 × 11–12 μm, smooth, slightly constricted at the septa; central cells brown, large (12–18 × 11–12 μm) and thick-walled; end cells subhyaline, small (2 μm long, 5 μm wide) and thin-walled. Based on shape and the length to width ratio this morphotype may refer to *Savoryella lignicola*, which was first reported from a water cooling tower, but has now been recorded from natural habitats throughout the world (e.g., Australië, Brunei, Hong Kong, Sri Lanka, and United Kingdom). It appears to be the only *Savoryella* species encountered in both marine and freshwater habitats, although it is doubtful at the molecular level if the similarly looking ascospores from both habitats in fact belong to the same species (Ho et al., 1997).

Type UG-1120: *Savoryella curvispora* W.H.Ho, K.D.Hyde & Hodgkiss (Plate III)

Ascospores curved, unequally and symmetrically 4-celled, 30 × 8 μm, smooth; central cells yellow to brown, relatively large and thick-walled; end cells subhyaline, small and thin-walled. This type may be related to the European type HdV-715. *Savoryella curvispora* has been reported from submerged wood in Mauritius, Taiwan, Malaysia, Philippines and South Africa (Ho et al., 1997).

Type UG-1137: *Meliola* sp. (Plate III)

Ascospores ellipsoid to oblong, unequally and asymmetrically 4-celled, slightly curved, brown, 53 × 16 μm, smooth, thick-walled, slightly constricted at the septa. *Meliola* species are found as parasites on leaves and stems of a wide range of hosts in the tropics. In East Africa they have been found on *Acacia*, *Cynanchum*, *Periploca*, *Secamone*, *Tylophora*, *Perguleria* and *Warburgia* (Mibey and Kokwaro, 1999).

Type UG-1145: cf. *Fusarium* sp. (Plate III)

Conidia narrowly fusiform, slightly curved, unequally and asymmetrically 4-celled, pale yellow, 37–42 × 9 μm, smooth, thick-walled, slightly constricted at the middle septum, and often with a small hyaline projection at the base forming a so-called foot cell. *Fusarium* species are anamorphic states of *Gibberella* sp. and commonly found on dead herbaceous plants (Ellis and Ellis, 1985). They occur in the normal mycoflora of staple foods such as rice, maize, bean and soybean. While most species are more frequent in tropical and subtropical areas, some inhabit soil in cold climates (Pitt et al., 1994).

Type UG-1150 (Plate III)

Ascospores fusiform, subequally and symmetrically 2(4)-celled, 28 × 9 μm, smooth, slightly constricted at the septa; two central cells pale brown and thick-walled; subhyaline end cells probably absent. This morphotype may be related to Type UG-1068 (Plate II), but the wall of Type UG-1150 is thin-walled.

Type UG-1162 (Plate III)

Spores ellipsoid, unequally and subsymmetrically 4-celled, brown, 22 × 11 μm, smooth, slightly thick-walled, not constricted at the septa.

Type UG-1204 (Plate III)

Conidia narrowly club-shaped to oblong, unequally and asymmetrically 4-celled, yellow, 32 × 9 μm, smooth, thick-walled, slightly constricted at the septa; basal cells somewhat paler.

Type UG-1320 (Plate III)

Spores ellipsoid to lemon-shaped, unequally and subsymmetrically 4-celled, 50–57 × 29–31 μm, smooth, constricted at the septa; central cells dark brown, large and very thick-walled; end cells subhyaline, small and thin-walled (often damaged or absent). This morphotype may be related to Type UG-1080 (Plate II).

Type UG-1342 (Plate III)

Spores ellipsoid, unequally and asymmetrically 4-celled, 27 × 13 μm, striate in a slightly spiralic pattern, slightly constricted at the septa; central cells brown, large and thick-walled; end cells subhyaline, small and thin-walled (often damaged or absent).

3.1.1.1.4. Multiseptate

Type UG-1002: *Sporoschisma* spp. (Plate III)

Conidia cylindrical with flattened ends, unequally and subsymmetrically 4- or 6-celled, 50–61 × 12–14 μm, smooth, thick-walled, slightly constricted at the septa; central cells pale to dark brown, almost of equal size; end cells paler, short, discoid or somewhat truncate, flattened or slightly rounded at free ends (often absent). These conidia probably belong to *Sporoschisma saccardoi*. Specimens of which the end cells are missing, are possibly fragmented conidia of the same species (due to decay) or 3-septate conidia of other *Sporoschisma* species (e.g., *S. juvenile* Boud., *S. mirabile* Berk. & Broome). *Sporoschisma saccardoi* is distributed in tropical (e.g., Indonesia, Taiwan, Ecuador, and South Africa) and more temperate regions (e.g., Europe). It is mainly found on submerged wood in freshwater habitats (Goh et al., 1997).

Type HdV-1022: *Clasterosporium* sp. (Plate III)

Conidia straight, curved or inversely club-shaped to beaklike; conico-truncate and protuberant at the base, unequally and asymmetrically 5- or more celled, ca. 40–75 × 8–9 μm (length dependent on the number of septa), striate, thick-walled, slightly constricted at the septa; cells brown and gradually decreasing in size and colour towards apical part of conidia; end cell subhyaline and strongly tapering. See also van Geel et al. (in press, 2011-this issue). *Clasterosporium* can be found on

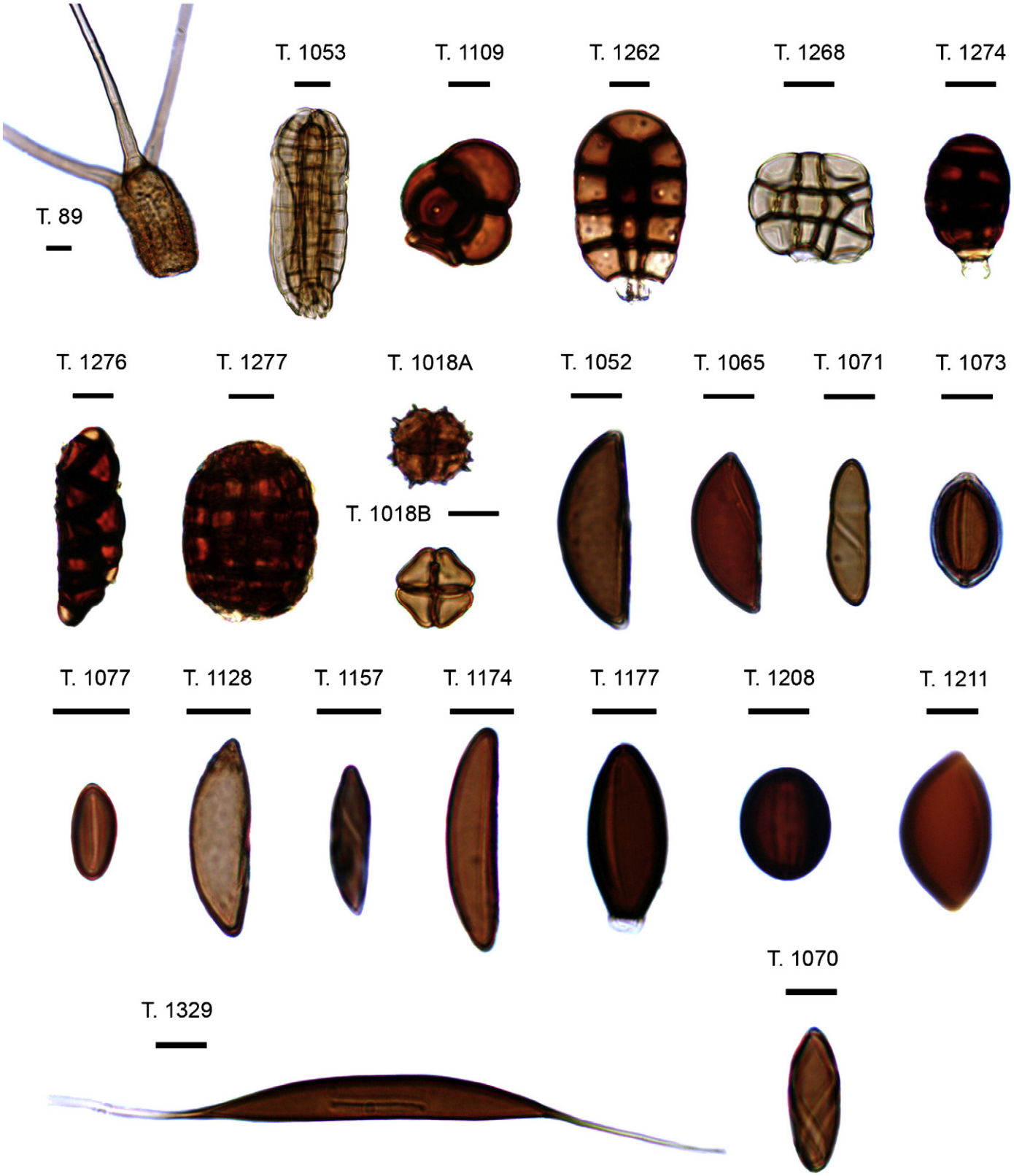

Plate IV. Septate fungal spores: muriform: T. HdV-89: *Tetraploa aristata*, T. HdV-1053: *Dictyosporium* cf. *heptasporum*, T UG-1109, T. UG-1262: *Canalisporium pulchrum*, T. UG-1268: *Canalisporium variabile*, T. UG-1274, T. UG-1276, T. UG-1277; Tetrads: T. HdV-1018A–B: *Spegazzinia tessarthra*; Non-septated spores/Amerosporae: with one or more germ slits: one germ slit: T. HdV-1052: Xylariaceae, T. UG-1065: Xylariaceae, T. UG-1071: cf. *Amphirosellinia* sp., T. UG-1073, T. UG-1077: cf. Xylariaceae/Sordariaceae/Coniochaetaceae, T. UG-1128: cf. *Kretzschmaria clavus/cetrarioides*, T. UG-1157: *Rosellinia* sp., T. UG-1174: *Rosellinia* sp., T. UG-1177, T. UG-1208: *Coniochaeta* spp., T. UG-1211, T. UG-1329: cf. Xylariaceae; two germ slits: T. UG-1070: Xylariaceae. All scale bars are 10 μm.

different plants, of which some are frequently subjected to periodic flooding, such as sedges (Ellis, 1971, Ellis and Ellis, 1985).

Type UG-1075 (Plate III)

Spores ellipsoid to broadly fusiform, unequally and subsymmetrically 5-celled, dark yellow to pale brown, 37–50 × 16–20 μm, microreticulate, thick-walled, costricted at the septa; with hyaline sheath (present or not).

Type UG-1078: *Sporidesmium* spp. (Plate III)

Conidia straight, slightly curved and narrower towards the ends, unequally and asymmetrically 11- or more celled (often broken), dark yellow to pale brown, ca. 47–105 × 8–13 μm (length dependent on the number of septa), smooth, very thick-walled, constricted at the septa. This morphotype probably includes different *Sporidesmium* species. *Sporidesmium* has a worldwide distribution (e.g., Australia, England, India, Tanzania, and United States) and is common on (fallen) leaves, rotten wood and dead culms of temperate (e.g., *Tilia*, *Sambucus*, *Alnus*) and tropical plants (e.g., *Cissus*, *Cordia*, *Cajanus*, *Eucalyptus, Jasminum*, and *Terminalia*) (Ellis, 1976).

Type UG-1097 (Plate III)

Spores (or hypha?) rod-shaped, pale yellow, unequally and asymmetrically 6- or more celled (partly broken), 125 × 10 μm, smooth, thick-walled, not constricted at the septa; individual cells variable in length.

Type UG-1099: *Brachysporium* spp. (Plate III)

Conidia broadly fusiform, unequally and subsymmetrically 5(6)-celled, 30–52 × 17–27 μm, smooth, thick-walled, not constricted at the septa; central cell dark brown and very large; other cells progressively paler and smaller towards the end. Younger conidia are generally paler than maturing ones. Based on size differences, this morphotype can probably be attributed to different (tropical) *Brachysporium* species, in which Type HdV-1024 (see van Geel et al., in press, 2011-this issue) is included. *Brachysporium* is distributed worldwide and is commonly isolated from rotten wood and bark of various trees and shrubs (Ellis, 1971).

Type UG-1104: cf. *Podosporium rigidum* Schwein. (Plate III)

Conidia straight, curved or inversely club-shaped to beaklike; funnel-shaped at the base, unequally and asymmetrically 5- or more celled (often broken), ca. 50–62 × 12 μm (length dependent on the number of septa), smooth, thick-walled, slightly constricted at the septa; cells brown and gradually decreasing in size and colour towards apical part of conidia; end cell subhyaline and strongly tapering. *Podosporium rigidum* can be found on dead stems and branches of plants, such as *Ampelopsis* and *Rhus* (Ellis, 1971).

Type UG-1113: *Meliola* sp. (Plate III)

Ascospores oblong to rarely subellipsoid, unequally and asymmetrically 5-celled, brown, 38–45 × 12–18 μm, smooth, thick-walled, constricted at the septa. For distribution and ecology of *Meliola* see Type UG-1137 (1.1.3.).

Type UG-1127 (Plate III)

Conidia inversely club-shaped, unequally and asymmetrically 5-celled, yellow, 33–41 × 6–11 μm, microreticulate, thick-walled, slightly constricted at the septa.

Type UG-1147 (Plate III)

Spores fusiform, unequally and symmetrically 6- or more celled (partly broken), pale yellow, 50 × 15 μm, smooth, thick-walled, slightly constricted at the septa; middle septum median.

Type UG-1203 (Plate III)

Conidia fusiform and slightly curved, unequally and asymmetrically 7- or more celled (partly broken), 99 × 13 μm, finely striate, thick-walled, slightly constricted at the septa; cells pale brown and large at the basis, subhyaline and smaller towards the ends.

Type UG-1250: *Curvularia* cf. *comoriensis* Bouriquet & Jauffret ex M.B. Ellis (Plate III)

Conidia inversely club-shaped and slightly curved, unequally and asymmetrically 5-celled, yellow, 45–60 × 13–15 μm, smooth, thick-walled, not constricted at the septa. *Curvularia comoriensis* has previously been found on *Cymbogon* in Congo and on the Comoro Islands (Ellis, 1971).

Type UG-1330 (Plate III)

Conidia inversely club-shaped, slightly curved, unequally and asymmetrically 7- or more celled, pale yellow, 50 × 15 μm, smooth, thick-walled, not constricted at the septa.

Type UG-1343: cf. *Cirrenalia* sp. (Plate III)

Conidia spiral-shaped, subglobose, unequally and asymmetrically 8-celled, brown, 31 μm in diameter, smooth, thick-walled, slightly constricted at the septa; cells increasing in diameter from base to end. Fourteen species are described in the genus *Cirrenalia*, of which 7 species are marine lignicolous and 7 are terrestrial, mostly occurring on bark and wood and often in wet habitats. This morphotype probably refers to one of the seven known terrestrial species (Ellis, 1976; Somrithipol et al., 2002, Zhao and Liu, 2005)

3.1.1.1.5. Muriform

Type HdV-89: *Tetraploa aristata* Berk. & Broome (Plate IV)

Conidia ellipsoid to rectangular, 3–4 columns with 4 cells to each column, yellowish brown, 35–40 × 20–25 μm, verruculose, thick-walled; terminating in septate appendages, 12–80 μm long (frequently broken), 5–8 μm wide. See also van Geel et al. (in press, 2011-this issue). *Tetraploa aristata* is widespread, usually found on leaf bases and stems of host plants (such as *Andropogon*, *Carex*, *Cyperus*, *Juncus*, *Musa*, *Phaseolus*, *Phoenix*, *Phragmites* and *Zea*) just above the soil (Ellis, 1971).

Type HdV-1053: *Dictyosporium* cf. *heptasporum* (Garov.) Damon (Plate IV)

Conidia broadly ellipsoid, composed of ca. 7 rows of cells, pale yellow, 42–71 × 21–25 μm, smooth, slightly thick-walled, slightly constricted at the septa. See also van Geel et al. (in press, 2011-this issue). Contrary to other *Dictyosporium* species, the conidia of *Dictyosporium heptasporum* are not flattened in one plane. *Dictyosporium heptasporum* has been observed on decaying and submerged wood and stems in Europe, India and North America (Ellis, 1971).

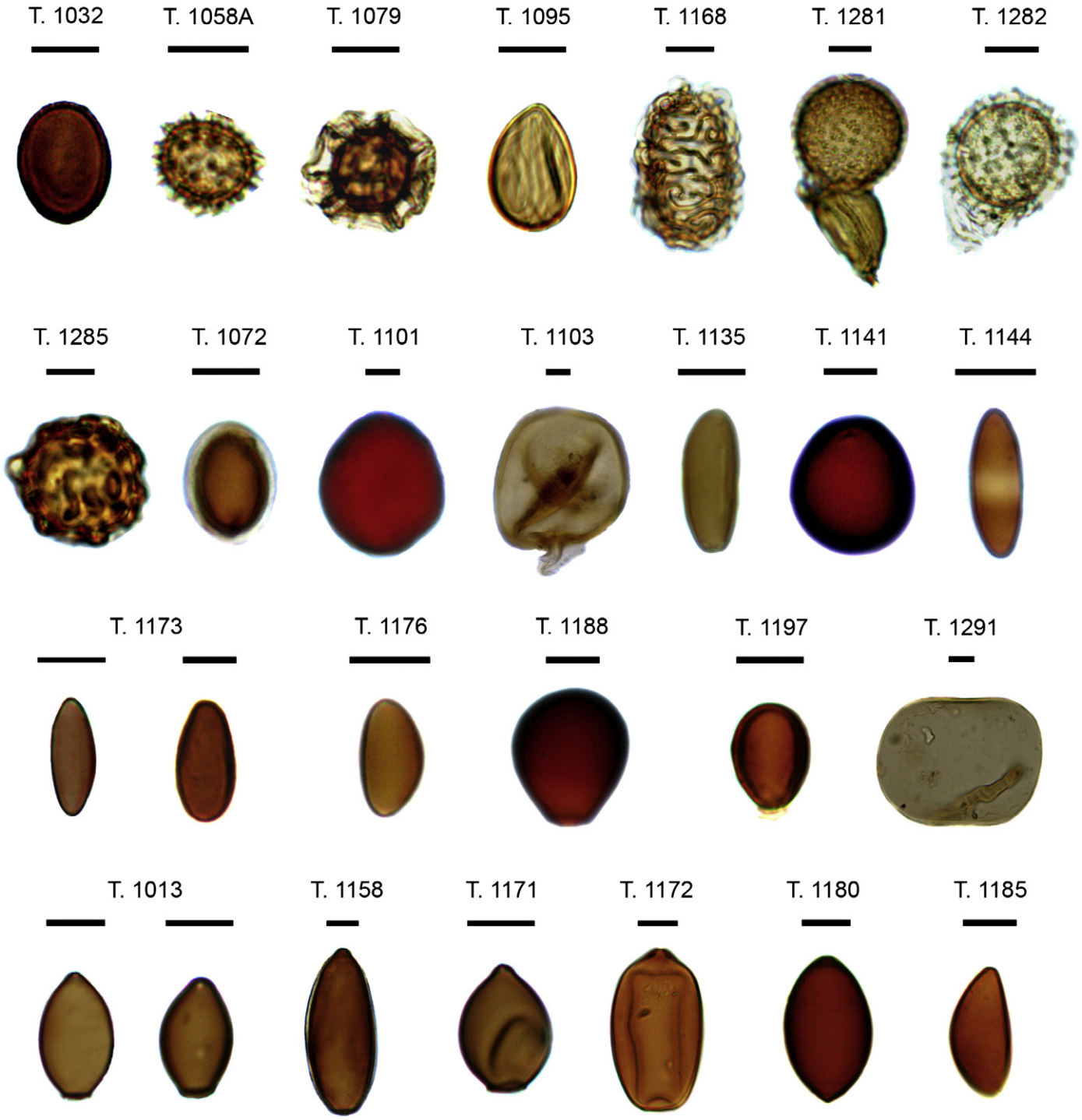

Plate V. Non-septated spores/Amerosporae: without germ slit: aporate: ornamented: T. HdV-1032, T. HdV-1058A, T. UG-1079: *Urocystis* sp., T. UG-1095, T. UG-1168, T. UG-1281, T. UG-1282, T. UG-1285: cf. *Ascodesmis* sp.; Aporate: not ornamented: T. UG-1072, T. UG-1101, T. HdV-1103: *Glomus* sp., T. UG-1135: cf. Xylariaceae, T. UG-1141, T. UG-1144, T. UG-1173, T. UG-1176, T. UG-1188, T. UG-1197, T. UG-1291: *Glomus* type; Porate: monoporate: T. HdV-1013: *Cercophora* type, T. UG-1158, T. UG-1171: *Apiosordaria* type, T. UG-1172, T. UG-1180: *Sordaria* spp., T. UG-1185. All scale bars are 10 μm.

Type UG-1109 (Plate IV)

Cluster of 5–10 globose fungal cells, brown, 34×30 μm, smooth, thick-walled; individual cells variable in size. This type may be related to the European Type HdV-200, which suggests the presence of relatively dry microhabitats (van Geel et al., 1989).

Type UG-1262: *Canalisporium pulchrum* (Hol.-Jech. & Mercado) Nawawi & Kuthub. (Plate IV)

Conidia ellipsoid to inversely egg-shaped, pale to dark brown, 48–68×25–32 μm, smooth, thick-walled, slightly constricted at the septa; some septa strongly pigmented and heavily

accentuated (septal canals often badly visible); with 3 columns of septa, and 4–6 rows of septa, and a single subhyaline basal cell (sometimes missing). Species of *Canalisporium* are common saprophytes on rotten and submerged wood (e.g., on bamboo culms, palm rachis) and have a pan-tropical distribution. The genus has previously been recorded in Cuba, India, Kenya, Malaysia, Uganda and Australia. (Goh et al., 1998, see also table I in Goh and Hyde, 2000).

Type UG-1268: *Canalisporium variabile* Goh & K.D.Hyde (Plate IV)

Conidia cubical, pale brown, 25×23 μm, smooth, thick-walled, moderately to strongly constricted at conidial septa (cells appear to bulge in outline); septa unpigmented, thin and septal canals clearly visible; with 2(–3) major columns of septa, 2 rows of septa, and a single basal cell, which is subhyaline and thin-walled. *Canalisporium variabile* is a recently described *Canalisporium* species, found on submerged wood and decaying palm raches in Australia (Goh and Hyde, 2000).

Type UG-1274 (Plate IV)

Conidia ellipsoid, subglobose or club-shaped, with more than 10 septated pale to dark brown cells (slightly variable in size and shape), and subhyaline basal cell(s) (sometimes missing), 26–33×17–22 μm, smooth, thick-walled, constricted at the septa. This morphotype may correspond with several different species due to its scarcity of diagnostic features.

Type UG-1276 (Plate IV)

Spores cylindrical, formed by a cluster of ~12 cells or more, variable in size and shape, dark brown, 50×17 μm, smooth, thick-walled, constricted at the septa; basal cells often slightly paler than central cells.

Type UG-1277 (Plate IV)

Spores globose to subglobose, 40–57×40–43 μm, smooth, with more than 20 brown, thick-walled septated cells (slightly variable in size and shape), and some subhyaline, thin-walled basal cell(s) (may be missing), slightly constricted at the septa. This morphotype differs from Type UG-1274 (Plate IV) by its bigger size and higher amount of cells. Type UG-1274 and UG-1277 may be produced by (morphologically) related species.

3.1.1.1.6. Tetrads

Type HdV-1018A–B: *Spegazzinia tessarthra* (Berk. & M.A.Curtis) Sacc. (Plate IV)

This fungal morphotype occurs in two more or less distinct types. Conidia of Type A are cruciately (cross-shaped) septate, equally and symmetrically 4-celled, brown, 10–16 μm in diameter, echinate (spines up to 3 μm long), thick-walled. Conidia of Type B are cruciately septate, equally and symmetrically 4-celled, brown, 14–18 μm in diameter, smooth, thick-walled. See also van Geel et al. (in press, 2011-this issue). *Spegazzinia tessarthra* is widespread in tropical and subtropical regions. It is particularly common on dead leaves and stems of various monocotyledonous plants, such as maize, grasses and *Andropogon* (Ellis, 1971; Subramanian, 1971).

3.1.1.2. Non-septated — Amerosporae

3.1.1.2.1. With one or more germ slits

3.1.1.2.1.1. One germ slit. Type HdV-1052: Xylariaceae (Plate IV)

Ascospores ellipsoid to subfusiform, inequilaterally one-celled, yellowish brown, 37–40×13–16 μm, smooth, thick-walled and with tapering ends; germ slit nearly straight and running over the entire spore-length near the flattened side. See also van Geel et al. (in press, 2011-this issue). This morphotype belongs to the family Xylariaceae, but further identification at the genus and species level is currently difficult because of possible affiliation with different genera (such as *Rosellinia* and *Hypoxylon*) or tropical species, which are still unknown. Xylariaceae are widely spread in temperate and tropical regions throughout the world. Apart from their endophytic existence, they are best known as saprotrophic wood-rotting fungi, as inhabitants of dung or litter and pathogens of a range of plants (Whalley, 1993).

Type UG-1065: Xylariaceae (Plate IV)

Ascospores slightly ellipsoid, inequilaterally one-celled, dark brown, 33–35×14–17 μm, smooth, thick-walled and with tapering ends; germ slit sigmoid and running over the entire spore-length near the less convex side (not always visible). For distribution and ecology see Type HdV-1052 (Section 3.1.1.2.1.1).

Type UG-1071: cf. *Amphirosellinia* sp. (Plate IV)

Ascospores ellipsoid to cylindrical, inequilaterally one-celled, pale brown to brown, 29–30×8 μm, smooth, thick-walled and with narrowly to broadly rounded ends; germ slit sigmoid and running transversally over the entire width of the spore. Based on its size and the position and length of the germ slit on the ventral/transversal side, this morphotype may possibly refer to *Amphirosellinia*, a new Xylariaceae genus which currently includes two former *Rosellinia* species (*R. evansii* Læssøe & Spooner and *R. americana* (Petr.) Rappaz) and three new species, growing inside the bark of dicotyledonous trees (Ju et al., 2004).

Type UG-1073 (Plate IV)

Ascospores globose to ellipsoid, equilaterally one-celled, brown, 17–24×13–17 μm, smooth, thick-walled, covered by a hyaline sheath (of which the slit may be a part); germ slit straight and running over the entire spore-length. This morphotype is probably strongly related to Type UG-1072 (Plate V).

Type UG-1077: cf. Xylariaceae/Sordariaceae/Coniochaetaceae (Plate IV)

Ascospores ellipsoid, equilaterally one-celled, brown to dark brown, 14–30×7–12 μm, smooth, thick-walled; germ slit straight and running over the entire spore-length. Based on size variability, this morphotype may include several species which possibly belong to the families Coniochaetaceae, Sordariaceae or Xylariaceae (Dennis, 1961; Hanlin, 1990; Lu et al., 2000; Petrini, 2003).

Type UG-1128: cf. *Kretzschmaria clavus* (Fr.) Sacc./*Kretzschmaria cetrarioides* (Welw. & Curr.) Sacc. (Plate IV)

Ascospores ellipsoid to subfusiform, inequilaterally one-celled, pale brown, 32×10 μm, smooth, thick-walled and with tapering ends; germ slit straight and running about 1/2 of the spore-length near the flattened side. *Kretzschmaria* (syn. *Ustulina*) species are found worldwide throughout temperate and tropical regions and occur

Plate VI. Non-septated spores/Amerosporae: without germ slit: diporate: ornamented: T. HdV-1093: *Gelasinospora* cf. *cratophora*, T. UG-1179, T. UG-1187, T. HdV-1245: *Diporotheca* sp.; Diporate: not ornamented: T. UG-1087, T. UG-1153, T. UG-1178: cf. *Sordaria* sp., T. UG-1216: *Diporotheca* sp.; Multiporate: T. UG-1139: *Gelasinospora* sp. All scale bars are 10 μm.

on plant debris and dead wood (Rogers and Ju, 1998). Only two distinct species, *Kretzschmaria clavus* and *Kretzschmaria cetrarioides*, seem to be distributed in tropical Africa (Dennis, 1961).

Type UG-1157: *Rosellinia* sp. (Plate IV)

Ascospores ellipsoid to fusiform, inequilaterally one-celled, brown to dark brown, 25×6 μm, smooth, thick-walled and with tapering ends; germ slit sigmoid and running about 3/4 of the spore-length. This morphotype resembles *Rosellinia dingleyae* L.E.Petrini, a new *Rosellinia* species encountered in New Zealand (Petrini, 2003), but the East African ascospores are slightly smaller and may thus represent an unknown tropical *Rosellinia* species. *Rosellinia* is widespread in temperate and tropical regions, and commonly found on decaying herbaceous stems and wood. In the tropics some species (such as *Rosellinia necatrix* Berl. ex Prill.) are particularly known as root pathogens, exclusively in plantations of cultivated trees and shrubs (Petrini, 1993).

Type UG-1174: *Rosellinia* sp. (Plate IV)

Ascospores ellipsoid to fusiform, inequilaterally one-celled, dark brown, 30–38×8–10 μm, smooth, with nearly rounded to slightly tapering ends, thick-walled; germ slit straight and running over the entire spore-length near the flattened side. For distribution and ecology see Type UG-1157 (Section 3.1.1.2.1.1).

Type UG-1177 (Plate IV)

Ascospores ellipsoid, inequilaterally one-celled, dark brown, 29×12 μm, smooth, thick-walled, truncate at one end but tapering at the other, covered by two polar hyaline caps, of which only the pedicel is clearly visible; germ slit straight and running over the entire spore-length.

Type UG-1208: *Coniochaeta* spp. (Plate IV)

Ascospores ellipsoid to globose, equilaterally one-celled, dark brown, 20–24×18–24 μm, smooth, thick-walled; germ slit straight, running over the entire spore-length and enclosed by a pale brown zone. When seen in polar view or a particular side view, the germ slit may be invisible; often the ascospore is also disrupted by a weakening of the germ slit. Based on small differences in size and shape, this morphotype may include *Coniochaeta ligniaria* (Grev.) Massee (Type HdV-172, see van Geel et al., in press, 2011-this issue) and several other *Coniochaeta* species (Hawksworth and Yip, 1981). *Coniochaeta* species are common on dung and dead wood (Hanlin, 1990).

Type UG-1211 (Plate IV)

Ascospores ellipsoid to lemon-shaped, inequilaterally one-celled, dark brown, 35–30×17–20 μm, smooth, very thick-walled, with slightly tapering ends; germ slit straight and running over the entire spore length. When seen from one particular side, the germ slit may be invisible.

Type UG-1329: cf. Xylariaceae (Plate IV)

Ascospores fusiform, inequilaterally one-celled, brown, smooth and thick-walled, cell 68 μm long, 10 μm wide, extremities needle-shaped and 35 μm long; germ slit (17 μm) short and centred near the flattened side. Apart from the atypical extremities, this morphotype appears to be affiliated with the family of Xylariaceae, and perhaps with the genus *Rosellinia* (Petrini, 2003).

3.1.1.2.1.2. Two germ slits

Type UG-1070: Xylariaceae (Plate IV)

Ascospores ellipsoid, inequilaterally one-celled, yellow, 18–21×7–9 μm, smooth, slightly thick-walled and with nearly rounded ends; two spiral germ slits running over the entire spore-length each at one side. This morphotype, which resembles the European Type EMA-55 (apart from the presence of one spiral germ slit, see Barthelmes et al., 2006), is probably affiliated with the Xylariaceae. For distribution and ecology see Type HdV-1052 (Section 3.1.1.2.1.1).

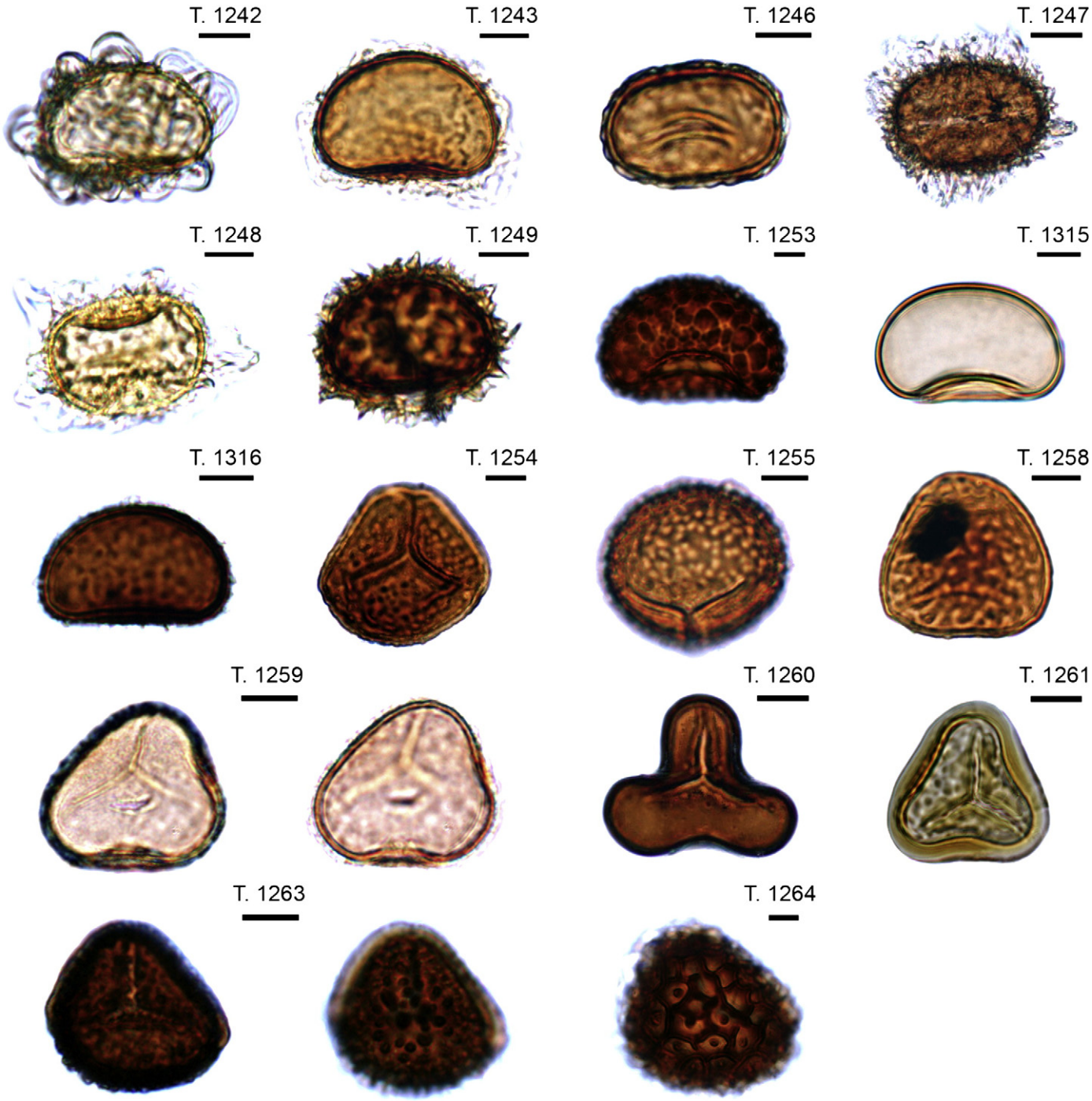

Plate VII. Fern and moss spores: monoletes: T. UG-1242: *Dryopteris* subg. *Dryopteris*, T. UG-1243: cf. *Asplenium* sp., T. UG-1246: *Isoetes* type, T. UG-1247, T. UG-1248, T. UG-1249: cf. *Ctenitis*/*Lastreopsis* sp., T. UG-1253: Polypodiaceae, T. UG-1315: monoletes undiff., T. UG-1316: *Asplenium* type; Triletes: T. UG-1254: *Phaeoceros* cf. *carolianus*, T. UG-1255: *Ophioglossum* subg. *Ophioglossum*, T. UG-1258, T. UG-1259: *Pteridium aquilinum*, T. UG-1260: *Coniogramme africana* type, T. UG-1261: cf. *Pteris*/*Actiniopteris* sp., T. UG-1263: cf. *Grammitis* sp., T. UG-1264: *Pteris* sp. All scale bars are 10 μm.

3.1.1.2.2. Without germ slit

3.1.1.2.2.1. Aporate

3.1.1.2.2.1.1. Ornamented

Type HdV-1032 (Plate V)

Ascospores ellipsoid, equilaterally one-celled, brown, 20 × 14 μm, microreticulate, slightly thick-walled.

Type HdV-1058A (Plate V)

Spores globose to subglobose, equilaterally one-celled, yellowish brown, 12 μm in diameter, coarsely echinate (spines ~1–2 μm), thick-walled. See also van Geel et al. (in press, 2011-this issue).

Type UG-1079: *Urocystis* sp. (Plate V)

Spore balls globose, composed of one yellowish brown spore, 11–14 μm in diameter, surrounded by small subhyaline cells, 3 μm in

diameter, attached to the dark central cell; spore balls often preserved as clusters of two or more specimens. *Urocystis* is widespread, mostly found in leaves and stems, and less often in flowers, seeds and roots of different host plants within the families Cyperaceae, Brassicaceae, Poaceae, Ranunculaceae, etc. (Vánky, 1994; van Geel et al., in press, 2011-this issue).

Type UG-1095 (Plate V)

Spores ellipsoid, inequilaterally one-celled, yellow, 19×14 μm, thick-walled, tapering at one end, ornamented with a fingerprint pattern running predominantly in the longitudinal direction.

Type UG-1168 (Plate V)

Spores ellipsoid, inequilaterally one-celled, yellowish brown, 32×15 μm, thick-walled, with subhyaline sheath/coat forming high curving ridges which are partially anastosmosing.

Type UG-1281 (Plate V)

Conidia globose, equilaterally one-celled, yellowish brown, 18–20 μm in diameter, verrucose, thick-walled.

Type UG-1282 (Plate V)

Spores globose to subglobose, equilaterally one-celled, yellow, 15–20 μm in diameter, thick-walled, with the subhyaline sheath/coat developed into fairly high, coarse ridges which may or may not anastomose, and with small spines present on the tops of the ridges.

Type UG-1285: cf. *Ascodesmis* sp. (Plate V)

Ascospores subglobose, inequilaterally one-celled, dark brown, 38 μm in diameter, irregularly and coarsely verrucose (individual knobs ~7 μm thick), thick-walled. *Ascodesmis* is widespread on dung of both wild and domesticated animals (Hanlin, 1990).

3.1.1.2.2.1.2. Not ornamented

Type UG-1072 (Plate V)

Ascopores globose to ellipsoid, equilaterally one-celled, brown, 14–22×10–17 μm, smooth, thick-walled, mostly covered with a hyaline sheath. This morphotype may be strongly related to Type UG-1073 (Plate IV), which has a slit running over the entire spore-length (probably as part of the hyaline sheath).

Type UG-1101 (Plate V)

Spores subglobose, subequilaterally one-celled, brown to dark brown, 45×39 μm, smooth and thick-walled, often covered by a hyaline sheath.

Type HdV-1103: *Glomus* sp. (Plate V)

Chlamydospores globose to subglobose, subequilaterally one-celled, yellow, 55×50 μm, smooth and thick-walled, mostly with hyphate attachment. This East African type is almost certainly not *Glomus* cf. *fasciculatum* (Thaxt.) Gerd. & Trappe (European Type HdV-207), which occurs in more temperate regions (van Geel et al., 1989) and is probably also related to Type UG-1291 (Plate V). The genus *Glomus* includes some 132 known species, which are hard to distinguish on the basis of their chlamydospores. *Glomus* is the largest genus of arbuscular mycorrhizal fungi, occurring on a variety of host plants and indirectly indicative for soil erosion when recorded in a lake deposit (van Geel et al., 1989; van Geel et al., in press, 2011-this issue).

Type UG-1135: cf. Xylariaceae (Plate V)

Conidia ellipsoid, inequilaterally one-celled, yellow, 22×9 μm, smooth and thick-walled, truncate at one end but tapering at the other. This morphotype may be the anamorphic state of a Xylariaceae species. For distribution and ecology see Type HdV-1052 (1.2.1.1.).

Type UG-1141 (Plate V)

Spores globose to subglobose, subequilaterally one-celled, dark brown, 19–27×19–24 μm, smooth, very thick-walled (3–4 μm thick).

Type UG-1144 (Plate V)

Ascospores ellipsoid to fusiform, subequilaterally one-celled, pale brown, 20×7 μm, smooth and slightly thick-walled, tapering at both ends; with the paler and thinner girdle running transversally over the entire width of the spore.

Type UG-1173 (Plate V)

Ascospores ellipsoid to fusiform, (in)equilaterally one-celled, yellow to brown, 15–24×6–12 μm, smooth, slightly thick-walled and slightly tapering at both ends.

Type UG-1176 (Plate V)

Ascospores ellipsoid to fusiform, inequilaterally one-celled, yellow to brown, 11–27×4–10 μm, smooth, slightly thick-walled, slightly tapering at both ends, with one side flattened. Judging by observed variability in morphology and size, this morphotype probably represents various species.

Type UG-1188 (Plate V)

Conidia slightly pyriform, inequilaterally one-celled, brown to dark brown, 24–27×17–23 μm, smooth, thick-walled and truncate at one end.

Type UG-1197 (Plate V)

Spores ellipsoid, inequilaterally one-celled, brown, 12–17×8–12 μm, smooth and thick-walled, often covered by hyaline sheath at truncate end.

Type UG-1291: *Glomus* type (Plate V)

Chlamydospores broadly ellipsoid, equilaterally one-celled, yellow, 72×57 μm, smooth, slightly thin-walled, with hypha-like attachment/appendix. This morphotype probably belongs to the mycorrhizal fungi, and may represent *Glomus* or a related tropical genus. It differs from the common *Glomus* chlamydospores (see Type HdV-1103, Plate V) by its distinctly ellipsoid shape and thinner wall. For distribution and ecology see Type HdV-1103 (1.2.2.1.).

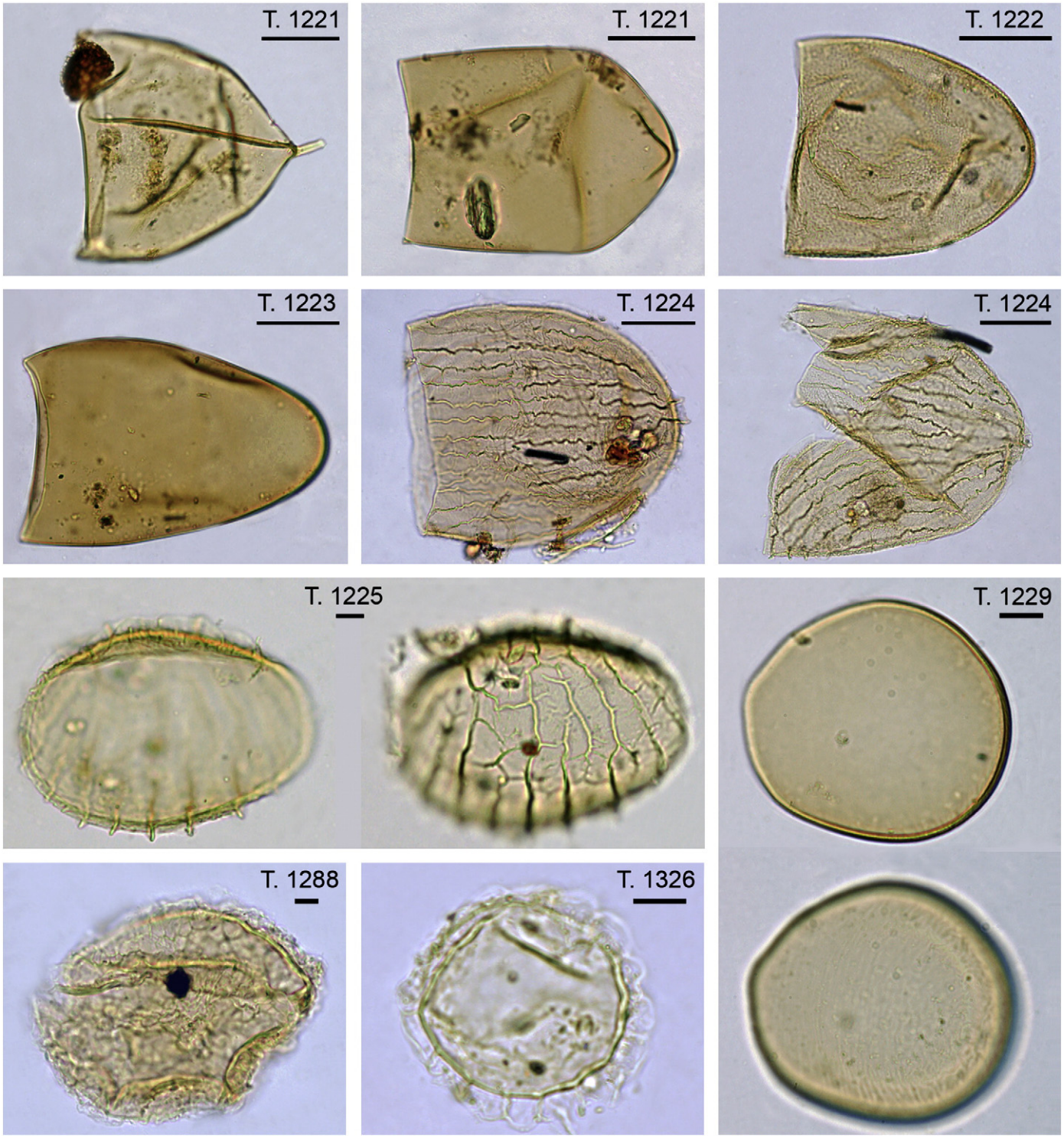

Plate VIII. Microscopic zoological remains: oocytes from Neorhabdocoela (flatworm) species: T. UG-1221, T. UG-1222, T. UG-1223, T. UG-1224; external cases of diapausing eggs (cysts) of unknown aquatic invertebrates: T. UG-1225, T. UG-1229, T. UG-1288, T. UG-1326. All scale bars are 10 μm, except for the Nheorhabdocoela oocytes, which are 50 μm.

3.1.1.2.2.2. Porate

3.1.1.2.2.2.1. Monoporate

Type HdV-1013: *Cercophora* type (Plate V)

Ascospores ellipsoid, inequilaterally one-celled, brown, 15–30×10–15 μm, smooth and thick-walled, tapering at one end but truncate at the other, often with one less convex side; pore often in a subpolar position and slightly protruding. See also van Geel et al. (in press, 2011-this issue). This morphotype differs from *Apiosordaria* type (Type UG-1171) by its more ellipsoid and often asymmetrically oblong form. This type probably represents different species which may be attributed to different genera such as *Cercophora*, *Podospora, Triangularia*, *Tripterospora* and *Zopfiella*. All of these genera are difficult to distinguish by their single ascospores (Bell, 1983; Khan and Krug, 1989b).

Type UG-1158 (Plate V)

Ascospores ellipsoid, inequilaterally one-celled, brown, 54×23 μm, smooth and thick-walled, tapering at one end but truncate at the other; pore slightly protruding.

Type UG-1171: *Apiosordaria* type (Plate V)

Ascospores broadly ellipsoid to subglobose, inequilaterally one-celled, brown, 20–30×15–20 μm, smooth and thick-walled, tapering at porate end but truncate at the other (originally with hyaline appendage); pore slightly protruding. This morphotype differs from *Cercophora* type (Type HdV-1013) by its more globose and shortened form. It superficially resembles the temperate-region species *Apiosordaria verruculosa* (C.N.Jensen) Arx & W.Gams (Type HdV-169, see van Geel and Aptroot, 2006), but ascospores of the latter are usually smaller. This East African type may therefore represent a tropical *Apiosordaria* species or an unknown tropical species of the Sordariales. *Apiosordaria* is particularly known from soil isolates, dung and plant debris (Bell, 1983; Hanlin, 1990).

Type UG-1172 (Plate V)

Ascospores ellipsoid, inequilaterally one-celled, brown, 32–35×14–19 μm, smooth and thick-walled, tapering at porate end but truncate at the other; pore slightly protruding.

Type UG-1180: *Sordaria* spp. (Plate V)

Ascospores ellipsoid, equilaterally one-celled, brown, 17–36×11–24 μm, smooth and thick-walled, tapering at both ends; pore slightly protruding. Based on size variability, this type may include several Sordaria species. *Sordaria* mainly occurs on dung substrates, but it can also been found on seeds and in soil (Bell, 1983; Hanlin, 1990).

Type UG-1185 (Plate V)

Ascospores broadly fusiform, inequilaterally one-celled, yellowish brown to brown, 20–28×10–13 μm, smooth and thick-walled,

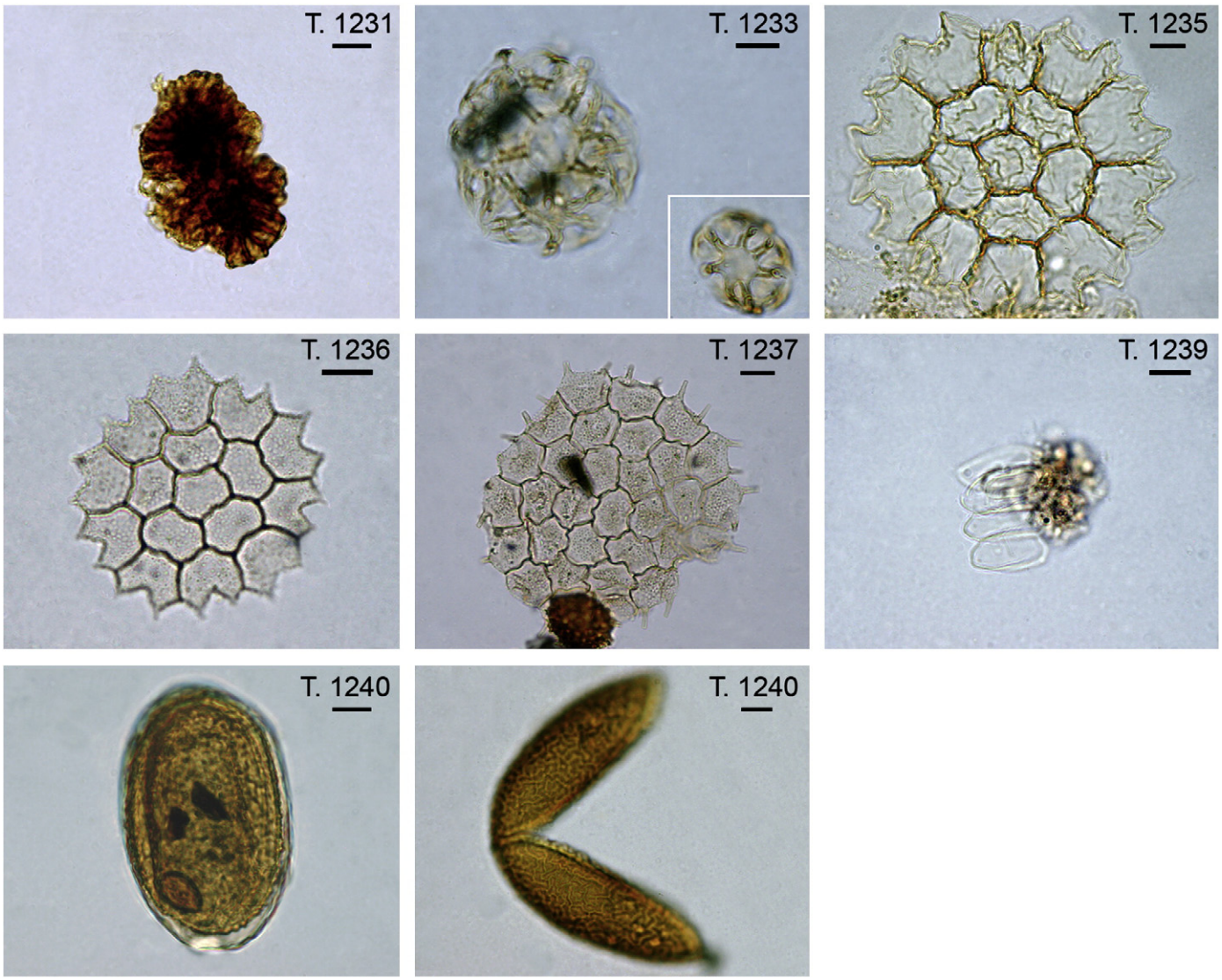

Plate IX. Algal zygospores, coenobia and colonies: T. UG-1231: *Botryococcus* cf. *neglectus*, T. UG-1233: *Coelastrum reticulatum*, T. UG-1235: *Pediastrum angulosum*, T. UG-1236: *Pediastrum boryanum* var. *brevicorne*, T. UG-1237: *Pediastrum boryanum* var. *forcipatum*, T. UG-1239: *Scenedesmus* sp., T. UG-1240: *Spirogyra* sp. All scale bars are 10 μm.

tapering at both ends, often with one side flattened; pore slightly protruding. Based on small differences in size and morphology, this morphotype may represent several unknown species.

3.1.1.2.2.2. Diporate. Ornamented

Type HdV-1093: *Gelasinospora* cf. *cratophora* R.S.Khan & J.C.Krug (Plate VI)

Ascospores ellipsoid to subglobose, equilaterally one-celled, dark brown, 30–33 × 20–22 μm, covered by hyaline pits about 1 μm in diameter, thick-walled; with one or two slightly protruding pores, concentrated near both ends. See also van Geel et al. (in press, 2011-this issue). *Gelasinospora* is widely reported from both coprophilous and soil habitats. Judging from the available records it is more widely distributed in tropical and subtropical regions than in temperate climate zones (Krug et al., 1994). Based on morphological features (size, form, surface pattern), this type may possibly belong to *Gelasinospora cratophora*, found on herbivore dung in Tanzania (Khan and Krug, 1989a).

Type UG-1179 (Plate VI)

Ascospores ellipsoid, equilaterally one-celled, brown, 28 × 14 μm, small longitudinal grooves (striae) alternating and running sub-parallel with lines of minute spheroidal projections (papillae), thick-walled; tapering ends with two protruding pores; surrounded by a hyaline sheath.

Type UG-1187 (Plate VI)

Ascospores ellipsoid, equilaterally one-celled, brown, 35 × 17 μm, longitudinal sub-parallel striae running over the entire spore-length, thick-walled; tapering ends with two protruding pores; surrounded by a hyaline sheath. This morphotype superficially resembles *Hypoxylon chestersii* J.D.Rogers & Whalley, but the latter species' ascospores are generally much smaller (14–17 × 6–7 μm) (Rogers and Whalley, 1978).

Type HdV-1245: *Diporotheca* sp. (Plate VI)

Ascospores broadly fusiform, equilaterally one-celled, pale brown to dark brown, 34–45 × 24–30 μm, with thick anastomosing ribs that are often broadly reticulate, very thick-walled; tapering ends with pores. It is previously known from European palaeoecological studies that a single *Diporotheca* fruitbody may include ascospores which are morphologically very divers (van Geel et al., 1986). This is also true for the East African *Diporotheca* findings, in which small morphological differences between specimens hamper solid classification of species. Contrary to the *Diporotheca* specimens found in the fossil record of lake Challa (see van Geel et al., in press, 2011-this issue), most ascospores reported from the Ugandan lake surface sediments are characterized by the absence of two (pale) septa. In temperate regions this parasitic genus of Meliolaceae regularly occurs in Holocene deposits formed in eutrophic to mesotrophic moist conditions (van Geel et al., 1986).

Not ornamented

Type UG-1087 (Plate VI)

Ascospores ellipsoid, equilaterally one-celled, dark brown, 31 × 25 μm, smooth, very thick-walled; two protruding pores located in the center.

Type UG-1153 (Plate VI)

Ascospores ellipsoid to lemon-shaped, inequilaterally one-celled, dark brown, 23 × 14 μm, smooth and thick-walled; tapering ends with two protruding pores of which one is located is a more subpolar position.

Type UG-1178: *Sordaria* type (Plate VI)

Ascospores ellipsoid, equilaterally one-celled, pale brown to dark brown, 29–35 × 17–19 μm, smooth, thick-walled; slightly rounded ends with two protruding pores. This type differs from Type HdV-1012 (see van Geel et al., in press, 2011-this issue) by its larger size and more pronounced pores, and may include different Sordariaceous ascospores from genera, such as *Sordaria* and *Arnium*. Both genera have a worldwide distribution and have most frequently been encountered on dung (Bell, 1983).

Type UG-1216: *Diporotheca* sp. (Plate VI)

Ascospores broadly fusiform, equilaterally one-celled, pale brown to brown, 43 × 18 μm, smooth, thick-walled; tapering ends with two slightly protruding pores, covered by small hyaline end caps. *Diporotheca* ascospores with very diverse morphology (see above: Type HdV-1245, Plate VI) have also been recorded from Holocene deposits in more temperate regions (van Geel et al., 1986). For distribution and ecology see Type HdV-1245 (1.2.2.2.).

3.1.1.2.2.3. Multiporate

Type UG-1139: *Gelasinospora* sp. (Plate VI)

Ascospores ellipsoid to subglobose, inequilaterally one-celled, dark brown, 37 × 25 μm, surface sculpture reticulate (ridges and hollows of about 1 μm), thick-walled; at least three germ pores visible, concentrated near both ends. From an evolutionary perspective the occurrence of *Gelasinospora* spores with multiple germ pores is thought to be a recent development. Given that this genus is primarily known from tropical latitudes, and largely from Africa, the evolutionary origin of the genus may be situated in this continent (Krug et al., 1994). *Gelasinospora* is mainly known from dung and dead wood (Hanlin, 1990).

3.1.2. Fern and moss spores

3.1.2.1. Monoletes

Type UG-1242: *Dryopteris* subg. *Dryopteris* Ching (Plate VII)

Spores bean-shaped, yellow, 40–45 × 15–18 μm, smooth, covered with perisporium forming curving and twisting subhyaline ridges and sacci (winglike compressed inflated folds). *Dryopteris* is distributed nearly worldwide in both temperate and tropical regions. Most African taxa, such as *Dryopteris kilemensis* (Kuhn) Kuntze, *Dryopteris inaequalis* (Schltdl.) Kuntze and *Dryopteris pentheri* (Krasser) C. Chr., have a smooth perine surface and typically inflated sacci with superficial ridges (Tryon and Lugardon, 1990). *Dryopteris* species are mainly found in shaded habitat along forest margins and streams in evergreen forest (Burrows, 1990).

Type UG-1243: cf. *Asplenium* sp. (Plate VII)

Spores bean-shaped, yellow to brown, 42–55 × 28–38 μm, smooth, covered with perisporium developed into fairly high and coarse,

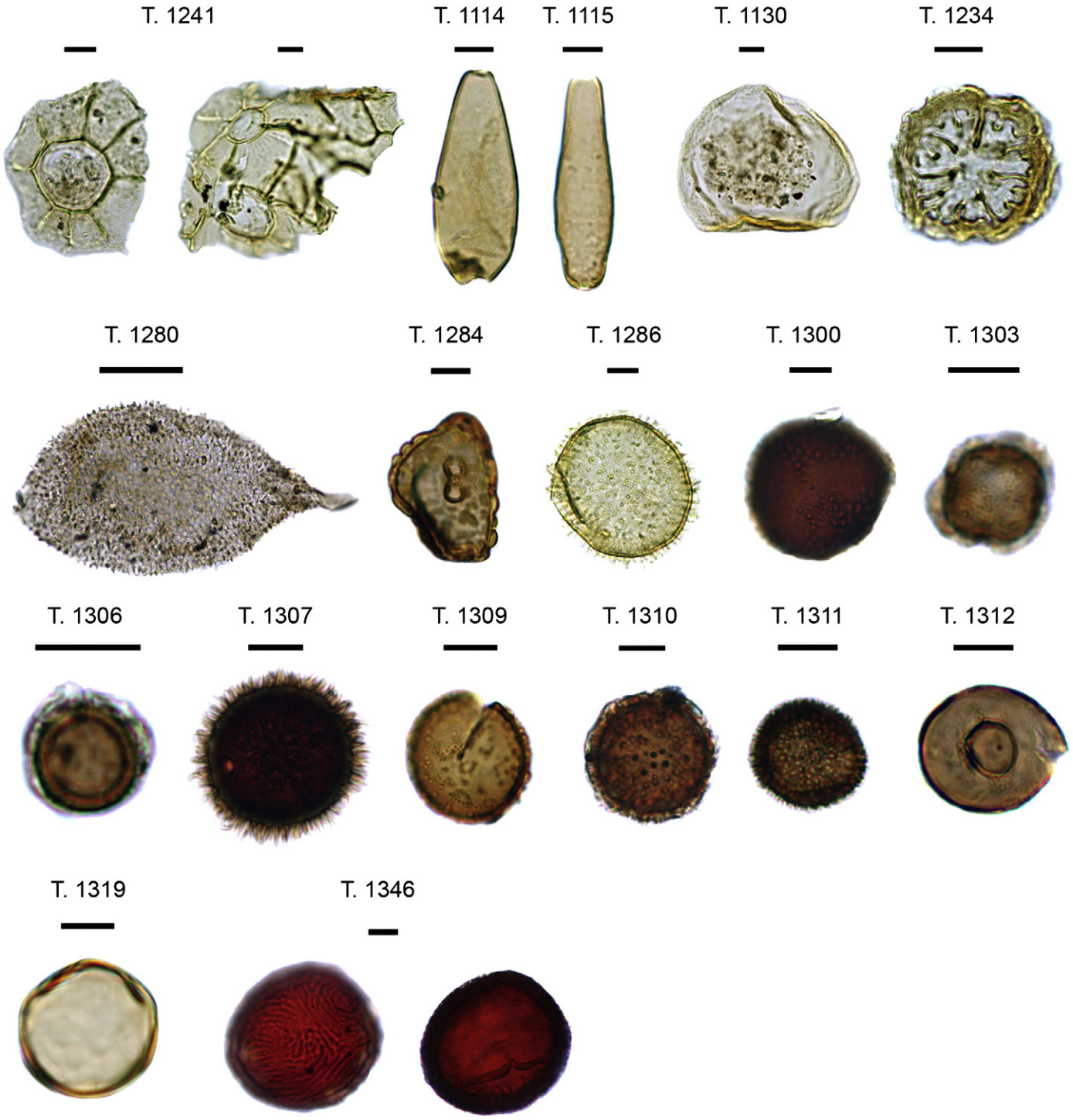

Plate X. Microscopic aquatic plant remains: T. UG-1241: epidermis of *Nymphaea nouchali*; unknown microfossils: T. UG-1114, T. UG-1115, T. UG-1130, T. UG-1234, T. UG-1280, T. UG-1284, T. UG-1286, T. UG-1300, T. UG-1303, T. UG-1306, T. UG-1307, T. UG-1309, T. UG-1310, T. UG-1311, T. UG-1312, T. UG-1319, T. UG-1346. All scale bars are 10 μm, except for T. UG-1280, which is 50 μm.

subhyaline ridges. These ridges anastomose or not, bear small echinae (spines) on top and columella-like structures underneath. *Asplenium* is one of the largest fern genera, distributed worldwide from Greenland and Europe to South America and New Zealand (Tryon and Lugardon, 1990). It occurs in a wide variety of exposed or partly shaded habitats, e.g., on rocks, in low-altitude semi-deciduous woodland, wet evergreen forest and (sub)montane rain forest (Burrows, 1990; Hemp, 2002).

Type UG-1246: *Isoetes* type (Plate VII)

Spores bean-shaped, brown, 32–37 × 15–28 μm, low, surface covered with broad disconnected muri mostly wider than high, and irregularly pitted. This morphotype may refer to *Isoetes*, which has similarly looking microspores. *Isoetes* is a heterosporous, usually lacustrine genus, occuring in aquatic habitats or saturated soils (Tryon and Lugardon, 1990).

Type UG-1247 (Plate VII)

Spores bean-shaped, brown, 40×33 μm, smooth, covered with perisporium forming subhyaline to pale yellow echinae (~ 5 μm), densely arranged in a fimbriate (curtain-like) pattern.

Type UG-1248 (Plate VII)

Spores bean-shaped, brown, 45×30 μm, smooth, covered with perisporium forming large subhyaline folds with local wing-like extensions, areas between folds microreticulate to perforate.

Type UG-1249: cf. *Ctenitis*/*Lastreopsis* sp. (Plate VII)

Spores bean-shaped, yellow to brown, 33×23 μm, surface covered with coarse and irregularly distributed echinae, varying in size but up to 5 μm tall. This spore strongly resembles both *Ctenitis* and *Lastreopsis*, which besides similar spore morphology have similar articulated trichomes on the leaves (Tryon and Lugardon, 1990). *Ctenitis* is widespread in tropical and south-temperate regions, such as Venezuela, Argentina and tropical Africa, and scattered in north-warm temperate regions of Asia, such as Ceylon. It usually occurs in mesic to wet forests. *Lastreopsis* has nearly the same distribution range, and occurs in tropical/subtropical forests and moist lowlands (Tryon and Lugardon, 1990).

Type UG-1253: Polypodiaceae (Plate VII)

Spores bean-shaped, brown, 54–92×23–55 μm, surface covered with large and undulating, solid wart-like projections. Polypodiaceae are widely distributed throughout the world, with highest species diversity in tropical and subtropical regions. However, in Africa only 11 genera (*Belvisia*, *Drynaria*, *Loxogramme*, *Lepisorus*, *Microgramma*, *Microsorum*, *Phytomatosorus*, *Platecyrium*, *Pleopeltis*, *Polypodium*, and *Pyrrosia*) are encountered, of which most species occur in forested areas, such as mixed evergreen forest, riverine forest, rainforest, gallery forest and woodland (Verdcourt, 2001).

Type UG-1315: monoletes undiff. (Plate VII)

Spores bean-shaped, yellow to brown, strongly varying in size from approximately 30×15 to 95×55 μm, smooth. This type comprises all monolete filicales without perispore.

Type UG-1316: *Asplenium* type (Plate VII)

Spores bean-shaped, brown, 35–45×22–26 μm, with smooth surface except low subhyaline plain folds. These type of spores are very common within the *Asplenium* genus, but affiliation with other genera is also apparent. For distribution and ecology see Type UG-1243 (2.1.).

3.1.2.2. Triletes

Type UG-1254: *Phaeoceros* cf. *carolianus* (Plate VII)

Spores tetrahedral-obtuse, brown, 37–50×23–37 μm, surface covered with small echinae, not joined by reticulum, some echinae forked and bent; arms of the trilete scar long (3/4 the radius) and appearing as prominent ridges. *Phaeoceros* is distributed nearly worldwide, growing in diverse open habitat such as moist slopes, cleared areas and (often) fallow land (Proskauer, 1951). Only *P. carolianus* (L.) Prosk. appears to have been reported from Uganda so far (Hodgetts, 2004).

Type UG-1255: *Ophioglossum* subg. *Ophioglossum* Linnaeus (Plate VII)

Spores globose, brown, 35×30 μm, surface covered with fine ridges developed into a dense reticulum, and irregularly spaced, depressed areolae (halos) underneath; trilete scar with short arms (1/2 to 2/3 the radius). The subgenus *Ophioglossum* is widely distributed in both tropical and temperate regions at low altitudes. It occurs in a wide range of habitats, from woodland and the margins of evergreen forest to wet grassland and sandy soils overlying granite sheet-rock (Burrows and Johns, 2001).

Type UG-1258 (Plate VII)

Spores tetrahedral-globose, brown, 36×34 μm, surface pitted and wrinkled with low coalescent ridges, trilete scar with long arms (3/4 the radius).

Type UG-1259: *Pteridium aquilinum* (L.) Kuhn (Plate VII)

Spores tetrahedral-globose, usually with concave sides, yellow, 30–38×20–28 μm, surface diffusely and irregularly granulate, trilete scar with relatively short arms (2/3 the radius). In subfossil specimens the sculptured perispore is often missing. *Pteridium aquilinum* has a worldwide distribution and occurs in a large variety of habitats (forest margins, grassland, woodland, rocky places and disturbed areas) in lowland to high mountain regions (Friis and Vollesen, 1998; Verdcourt, 2000). It is definitely the most common African fern, often forming vast stands in eastern parts of southern Africa, and frequently becoming an invasive weed following land-clearance and fire (Burrows, 1990).

Type UG-1260: *Coniogramme africana* type (Plate VII)

Spores tetrahedral-globose, often deeply curved, yellow to brown, 37–30×30 μm, surface faintly patterned (rugate or irregularly papillate), trilete scar with relatively short arms (2/3 the radius). This type may be affiliated with *Coniogramme africana* Hieron., which occurs in tropical Africa and Madagascar in submontane and subalpine zones at altitudes ranging from ~1100 to 2200 m (Tryon and Lugardon, 1990; Hemp, 2002).

Type UG-1261: cf. *Pteris*/*Actiniopteris* sp. (Plate VII)

Spores tetrahedral-globose, yellow to brown, 43–48×40–45 μm, with prominent equatorial flange/rib, surface covered with low tubercles, trilete scar with long arms (3/4 the radius). This spore resembles some species of *Pteris* and *Actiniopteris*, which can be morphologically similar. *Pteris* is distributed in the tropics, subtropics and warm temperate regions, whereas *Actiniopteris* is primarily restricted to Africa, Madagascar and the adjacent islands extending northeastward to Afghanistan, Nepal, India and Sri Lanka (Tryon and Lugardon, 1990). Both taxa occur in a wide variety of habitats (rock outcrops, woodland, bushland), but *Actiniopteris* is apparently more favoured by dry conditions (Verdcourt, 1999, 2002).

Type UG-1263: cf. *Grammitis* sp. (Plate VII)

Spores tetrahedral-globose, brown, 32×30 μm, surface covered with prominent tubercles, with papillae near the aperture, and a trilete scar with long arms (1/3 to 3/4 the radius). *Grammitis* has a pantropic distribution across tropical, subtropical and warm temperate regions. These are small, often epiphytic ferns, usually growing in mossy substrates on trees (Tryon and Lugardon, 1990).

Type UG-1264: *Pteris* sp. (Plate VII)

Spores tetrahedral-globose, brown, 62×52 μm, surface covered with a very distinct coarse reticulum, with ridges (up to 2.5 μm tall) partly connected to each other and large papillae (2.5 μm in diameter) within areolae, trilete scar with long arms (3/4 the radius). The large papillae or tubercles within the aureolae of some *Pteris* spores (e.g., *P. vittata* L. and *P. longifolia* L.) are remarkably similar to those of *Onychium* species. However, *Pteris* is far more common in East Africa than *Onychium*, which is mostly distributed in the Sikkim–Himalayan area and southwest China. *Pteris* is widespread in tropical, subtropical and warm temperate regions and occurs in diverse habitat ranging from river banks, wet evergreen forest and stream-side vegetation to drier areas on limestone outcrops (Tryon and Lugardon, 1990; Verdcourt, 2002).

3.1.3. Microscopic zoological remains

Type UG-1221, UG-1222, UG-1223 and UG-1224 (Plate VIII) are oocytes with a size of ~100–190 μm belonging to various Neorhabdocoela (flatworm) species, which can be found worldwide in (semi-) aquatic habitats such as ponds, marshy pools, ditches, peat trenches and lakes (Haas, 1996). Type UG-1221, UG-1222 and UG-1223 are probably related to the oocyte types *Gyratrix hermaphroditus* Ehrenberg 1831 (Type UG-1221) and *Microdalyellia armigera* O.Schmidt 1861 (Types UG-1222 and UG-1223) described by Haas (1996). However, since the oocyte morphology of these species is currently not well differentiated from those of other species, and since their palaeoecological significance is completely based on local Central European ecological conditions, we made no attempt to link the East African oocytes to these previously described types.

Type UG-1221 (Plate VIII)

Oocyte without operculum, yellow, funnel-shaped or oval, 125–150×120–150 μm, with smooth surface, smooth, stalk typical but often only partly or not preserved, with articulation just beneath the body.

Type UG-1222 (Plate VIII)

Oocyte without operculum, yellow, ellipsoid, 112–125×85–100 μm, with finely reticulated surface.

Type UG-1223 (Plate VIII)

Oocyte without operculum, yellow, oval to ellipsoid, 98–155×86–120 μm, with smooth surface.

Type UG-1224 (Plate VIII)

Oocyte without operculum, yellow, oval to ellipsoid, 137–188×110–150 μm, surface smooth or microreticulate, with parallel but slightly undulating, longitudinal ribs.

Types UG-1225, UG-1229, UG-1288 and UG-1326 (Plate VIII) are probably the external cases of diapausing eggs (cysts) of various aquatic invertebrates, excluding Rotifera and Branchiopoda. Considering the great variety of possible source organisms (microcrustaceans, arthropods, etc.) and an enormous number of possible genera within each of these broad taxa we made no attempt to attribute these NPP types to a specific taxon. Their inclusion here mostly serves to help distinguish such NPP types from the spores of fungi, mosses and ferns.

Type UG-1225 (Plate VIII)

Cyst ellipsoid, hyaline to pale yellow, 110×85 μm, surface smooth with slightly undulating, transversely ribs, partly connected to each other and ornamented with regularly placed spines.

Type UG-1229 (Plate VIII)

Cyst subglobose, subhyaline to pale yellow, 64–73×55–61 μm, surface covered with striae finely arranged in a barely visible fingerprint pattern.

Type UG-1288 (Plate VIII)

Cyst ellipsoid, subhyaline to pale yellow, 110×85 μm, surface ornamented with low reticulated flanges (honeycomb structure).

Type UG-1326 (Plate VIII)

Cyst globose, subhyaline, 41 μm in diameter, surface smooth but ornamented with rounded flanges (~4 μm).

3.1.4. Algal zygo-/aplanospores, coenobia and colonies

Type UG-1231: *Botryococcus* cf. *neglectus* (W.West & G.S.West) (Plate IX)

Colonies (cells are arranged in a three-dimensional structure) yellow-brown to brown with irregularly sculpted surface, composed of sub-colonies (25–50 μm) connected by very short and thin undulating strings; cells (2 μm) obovoid, usually radially stacked up to a layer of larger (9 μm) and modified peripheral cells. Peripheral cells slightly distant one from another. This species of green alga (Chlorophyceae, Chlorococcales) strongly resembles *Botryococcus neglectus,* which is characteristic for small oligotrophic and mesotrophic aquatic environments in more temperate regions (Komárek and Marvan, 1992). However, the colonies and individual cells of this East African morphotype are more regularly arranged, which suggests it is a distinct *B. neglectus* variety or a *Botryococcus* species with more tropical ecological requirements. The genus *Botryococcus* is widely distributed in temperate and tropical regions, but the taxonomic classification of the species within the genus is still open for revision (Jankovská and Komárek, 2000).

Type UG-1233: *Coelastrum reticulatum* (P.A.Dang) Senn (Plate IX)

Coenobia (cells are arranged in a single layer) globose to ovoid, hyaline to pale yellow, 30–41×25–39 μm, covered by a hyaline envelope and built from 2, 4 or 8 cells that are globose to ellipsoid, each measuring up to 10 μm; neighbouring cells connected by 5–7 long, slender processes (up to 8 μm); intercellular spaces large. *Coelastrum reticulatum* (Chlorophyceae, Chlorococcales) has a worldwide distribution, and is common in the tropics. It mainly occurs planktonic in warm ponds and productive lakes (Jankovská and Komárek, 2000; John et al., 2002).

Type UG-1235: *Pediastrum angulosum* (Ehrenb. ex) Menegh. (Plate IX)

Coenobia circular, slightly oval or irregular in outline, hyaline, 79–190×79–125 μm, comprised of 16–64 tightly packed cells. Peripheral cells with two short, conical processes flanking a U-shaped concave margin, cell wall with distinct irregular net-like sculpture. Peripheral and inner cells resp. 27 and 23 μm. *Pediastrum angulosum* is a cosmopolitan but not very common planktonic species with numerous varieties in need of taxonomic revision. Based on fossil records in temperate regions (Denmark, Finland, Germany, Russia), it seems indicative for both large and small lake habitats with slightly alkaline water and abundant submerged macrophyte vegetation (Komárek and Jankóvska, 2001). However, the specific ecological requirements of tropical populations is uncertain.

Type UG-1236: *Pediastrum boryanum* var. *brevicorne* A.Br. (Plate IX)

Coenobia circular, pale yellow, diameter 50–83 μm, comprised of 16–32 tightly packed cells. Peripheral cells with two triangular lobes flanking a wide V-shaped concave margin, processes very short cylindrical and hyaline, cell wall regularly granular. Peripheral and inner cells resp. 12 and 8 μm. *P. boryanum* var. *brevicorne* is a planktonic thermophilic taxon, occurring in tropical regions and warmer areas of temperate zones (Komárek and Jankóvska, 2001).

Type UG-1237: *Pediastrum boryanum* cf. var. *forcipatum* (Corda) Chod. (Plate IX)

Coenobia nearly circular to irregular in outline, hyaline to pale yellow, 50–100 μm in diameter, comprised of 32–64 tightly packed cells. Peripheral cells with two long, narrow, hyaline processes on little developed lobes, margin between them shallowly concave, cell wall densely and distinctly granular. All cells 12–22 μm. *Pediastrum boryanum* var. *forcipatum* is a rare taxon and taxonomically not clearly defined, but probably more thermophilic than other *P. boryanum* varieties. It is mainly distributed in tropical and warm-temperate zones (Komárek and Jankóvska, 2001). In Africa it has previously been reported from Chad (Compère, 1970).

Type UG-1239: *Scenedesmus* sp. (Plate IX)

Colonies linear, hyaline, 26(30) × 17 μm, with four ellipsoid to oblong cells, arranged subparallel to each other, broadly rounded or slightly truncate, and with a smooth surface. Cells 5–8 × 17–22 μm. *Scenedesmus* species typically occur in freshwater ponds, lakes and/or slow-moving rivers, most abundantly in slightly eutrophic waters. The joint occurrence of *Scenedesmus* and *Pediastrum* species in small water bodies (wells, ditches, watering holes, etc.) and as fossils in lake deposits is indicative of eutrophication caused by human activities, and therefore has occasionally been used to infer past organic pollution (Cronberg, 1986).

Type UG-1240: *Spirogyra* sp. (Plate IX)

Zygo-/aplanospores yellow to dark yellow, 70–75 × 40–45 μm, oval, ellipsoid, ovoid or cylindrical-ovoid in shape, often split along its periphery. Surface with fine striate-rugulate pattern, smooth coating of the outer wall is occasionally present. This African green algae resembles Type 773 reported from a late-Holocene sediment record in The Netherlands (Bakker and van Smeerdijk, 1982). Species of *Spirogyra* have a worldwide distribution, and commonly occur in stagnant, shallow waters of mesotrophic to eutrophic small lakes and pools, or in the littoral zones of larger lakes. Many species seem to prefer rather extreme conditions, such as ephemeral standing waters, or strong daily fluctuations in pH and temperature. The sexual reproduction during which these zygospores are formed requires high temperatures, which can best be reached in shallow waters directly exposed to strong solar radiation. The optimum growth conditions for *Spirogyra* species lie above 20 °C (Hoshaw, 1968).

3.1.5. Microscopic aquatic plant remains

Type UG-1241: Epidermis of *Nymphaea nouchali* Burm. f. (Plate X)

Globose to shaped like a rounded square in outline, subhyaline to pale yellow, 38–58 μm in diameter, consisting of 7–8 cells, each 17–25 × 14–22 μm. Cell walls covered by a very fine, wavy net-like sculpture, central cell globose, marginal cells tetragonal. Only occasionally found in assembled condition. This morphotype belongs to the epidermis of *Nymphaea nouchali*, which is the only living *Nymphaea* species found in the 20 lakes studied (Lebrun, unpublished CLANIMAE data), and can easily be mistaken for coenobia of the coccal green alga *Pediastrum privum* (Printz) E.Hegewald (see Komárek and Jankóvska, 2001). *Nymphaea nouchali* is a common macrophyte in tropical regions, occuring in shallow waters (Verdcourt, 1989).

3.1.6. Unknown microfossils

Type UG-1114 (Plate X)

Inversely club-shaped to broadly fusiform, yellow, 50–57 × 20 μm, smooth, thick-walled, truncate at both ends (partly broken off).

Type UG-1115 (Plate X)

Inversely club-shaped, yellow, 54 × 15 μm, smooth, thick-walled, at one end obliquely truncate with an aperture covered by a hyaline membrane (present or not), other end possibly broken off. This morphotype is probably related to Type UG-1114.

Type UG-1130 (Plate X)

Subglobose, subhyaline to pale yellow, 59–80 × 47–67 μm, slightly thin-walled, microreticulate.

Type UG-1234 (Plate X)

Globose, unicellular, pale yellow to yellow, 40 × 38 μm, smooth, consisting of 2 intricately lobed semi-cells with concave margins between them and a star-like pattern of projections pointing towards the center. This African morphotype superficially resembles *Micrasterias* (Chlorophyceae, Desmidiales) which is distinctly larger and of which the semi-cells are more complex and intricately lobed. However, experiments show that the size of some *Micrasterias* species, such as *Micrasterias rotata* Ralfs, consistently decreases at high temperatures, and the morphology is less elaborate than in cells grown at low temperature (Neustupa et al., 2008). This NPP type may represent one or more tropical species of *Micrasterias*, but identification is severely hampered by the lack of a centrally placed nucleus, a typical feature of Desmidiaceae.

Type UG-1280 (Plate X)

Ellipsoid, yellow to brown, 100 × 187 μm, with small spines densely arranged across the surface. Possibly this is a swollen hair from an aquatic insect larva.

Type UG-1284 (Plate X)

Nearly triangular to obtuse, yellow to brown, 38 × 27 μm, covered with microreticulate knobs, thick-walled; two centrally located circular apertures are provided with annuli.

Type UG-1286 (Plate X)

Subglobose, yellow, 49–53 μm, with irregularly arranged linear and T-shaped appendages (1 to 3 μm), thick-walled.

Type UG-1300 (Plate X)

Globose, brown to dark brown, surface locally smooth but partly covered with small verrucae (~1 μm) grouped and restricted to some areas, 45 μm in diameter, thick-walled; with a long slit-like aperture.
Type UG-1303 (Plate X)

Globose, shaped like a rounded square, yellow to brown, 15 μm in diameter, thick-walled; with subhyaline outer coat covered with small protuberances (~1 μm).

Type UG-1306 (Plate X)

Globose, yellow to brown, 10 μm in diameter, very thick-walled (~2 μm); with a subhyaline net-like outer coat.

Type UG-1307 (Plate X)

Globose, brown, 25–15 μm in diameter, thick-walled, surface densely covered with long hairy appendages (3 to 5 μm); characteristic aperture/pore (~5 μm) with costa.

Type UG-1309 (Plate X)

Globose, brown, 25–20 μm in diameter, thick-walled, with minute spheroidal protuberances (papillae, 0,5–1 μm tall) irregularly distributed across the surface.

Type UG-1310 (Plate X)

Globose, brown, 28 μm in diameter, tthick-walled, with echinae (~3 μm tall) densely distributed.

Type UG-1311 (Plate X)

Globose, brown, 19–12 μm in diameter, thick-walled, with small protuberances (~1 μm tall) evenly distributed across the surface. This microfossil superficially resembles *Michrystridium* (Acritarcha, European NPP type HdV-115), which was first reported in lake sediment deposited on a subsoil of marine clay in The Netherlands (Pals et al., 1980; Bakker and van Smeerdijk, 1982).

Type UG-1312 (Plate X)

Globose, yellow, 22 μm in diameter, smooth, slightly thick-walled; with a possible circular central aperture/hole (~10 μm). This microfossil superficially resembles the testate amoeba *Arcella*, which is clearly larger (~100–130 μm) and has a nucleus (Chardez, 1964).

Type UG-1319 (Plate X)

Globose, yellow, 20–26 μm in diameter, smooth, slightly thick-walled (~1 μm thick), often split. This microfossil resembles the European NPP type HdV-119, which is restricted to lake deposits (Pals et al., 1980), but since its morphology is rather simple and nondescript we use a new type number.

Type UG-1346 (Plate X)

Subglobose, brown to dark brown, 50–55 μm, very thick-walled, with striae (~1 μm wide) arranged in a finger-print pattern; with thick and elongated V-shaped furrow (~3 μm wide); covered by a smooth subhyaline outer coat.

4. Discussion

In this early stage of NPP research in tropical Africa, it is not surprising that the taxonomic affinity of many NPP morphotypes remains unknown. Our ~28% success rate of identification in this Uganda crater-lake collection is, in fact, comparable to that achieved in studies of modern NPP assemblages elsewhere (Prager et al., 2006). In part this is because identification of any microfossil to species or genus level is generally difficult when the range of possible source organisms is very wide. Most biological analysts have expertise in only a single group of organisms, and it already requires a much specialized study and accumulated experience to recognise (micro-) fragments of those organisms preserved in sediment samples. Often a single NPP morphotype can originate from different taxa, and depending on growth differentiation or body fragments a single organism can produce several NPP morphotypes (Prager et al., 2006).

The fraction of identified morphotypes in this collection differs greatly among the main taxonomic groups, from ~26% in the fungi and ~68% in the ferns and mosses to 100% in the algae. The modest success rate in the fungi certainly can be attributed partly to the fact that only an estimated 5% of the 1.5 million fungal species worldwide have been formally described (Hawksworth, 1991, 1993). Smith and Waller (1992) even consider this total number as unrealistically low, and suggested that perhaps 1 million undescribed fungi exist on tropical plants alone. Based on summaries of plant species richness by floristic regions (White, 1983) and an estimated vascular plant-to-fungus species ratio of 1:6 (Hawksworth, 1991), up to 18,000 species of fungi may occur in the Lake Victoria regional mosaic (occupying most of Uganda, eastern Rwanda and Burundi, small parts of D.R. Congo, Kenya and Tanzania, and a small exclave in the Rusizi Valley north of Lake Tanganyika). However, this estimate may be susceptible to over-generalization, since the degree of host specificity in fungi likely differs between regions and between host plants (Lodge, 1997). For example, on tropical palms the mean ratio of host-specific fungi to palm species is 33:1 (Fröhlich and Hyde, 1999), much higher than the 6:1 ratio considered by Hawksworth (1991). Also other environmental factors (e.g., substrate, altitude, rainfall, seasonality) will certainly create regional variation in fungal diversity. The species diversity of non-lichenized fungi is known to be highest in sub-humid to humid tropical regions at low to middle elevation (Lodge et al., 1995), i.e. the broad characteristics of our study area. A similar latitude effect in species richness has also been noted in the coprophilous mycobiota (Richardson, 2001), which are also present in our dataset (e.g., the Sordariales with *Sordaria*, *Gelasinospora* and *Coniochaeta* and possibly representatives of *Cercophora*, *Podospora, Zopfiella* or other morphologically related coprophilous fungi). In contrast, the diversity of fern and moss NPPs in our African collection (19 distinct types) is rather poor compared with other world areas. Some authors point to the scarcity of high-mountain habitats and the paucity of the continent's rain forest flora, as the main reason for the overall low diversity of Pteridophyta and Bryophyta in tropical Africa (Kornás, 1993; Moran, 1995; Pócs, 1998). Africa's total known species diversity in these groups is also strongly influenced by rich fern and moss communities in the Eastern Arc Mountains of Tanzania (Schelpe, 1983; Pócs, 1998; Aldasoro et al., 2004), quite distant from our study area in western Uganda.

The true richness of a regional species pool can hardly be estimated *a priori*, but requires comprehensive investigation of the number of morphospecies in representative ecosystems (Foissner, 2006). Thus, given the wide range of both pristine and disturbed ecosystems present near our lake sites, and the size of our fungal NPP collection (~7430 specimens), it seems fair to assume that the 198 fungal morphotypes reported here represent a reasonable score of overall NPP diversity, which may occur in fossil assemblages of East African lake deposits. This may also be true for the 19 fern and moss morphotypes recognized in 725 specimens. In the other taxonomic groups the recovered diversity (e.g., 7 morphotypes in 1115 specimens of algal NPPs) significantly underestimates regional species diversity because only a small fraction of species in those groups are composed of refractive organic materials (such as sporopollenine and thick chitine) which survive the chemically harsh palynological sample preparation. The preliminary results of phytoplankton

analyses of 29 western Ugandan crater lakes, of which 12 of the lakes are also included in this present study, revealed a total species richness of approximately 220 algal taxa (Cocquyt, unpublished CLANIMAE data) which is in sharp contrast to the 7 morphotypes found in our NPP dataset of 20 study lakes. Representation of these microfossil groups in NPP collections is highly selective and incomplete; other, more appropiate sample-processing techniques are required to reveal their full species diversity and to optimally exploit their palaeoecological indicator value.

Overall NPP taxon richness is certainly also affected by *in situ* decay processes, since after burial in bottom sediments the microfossils are differentially sensitive to chemical (oxidation), mechanical (abrasion) and biological (feeding) degradation. Differential preservation is well known in pollen (Dimbleby, 1957; Havinga, 1984), but to our knowledge it has not been experimentally studied in a wide range of fungal spores. Nevertheless, the results of the present study clearly indicate that pigmented, thick-walled fungal spores are far better preserved in (East African) lake sediments than hyaline, thin-walled species, which are totally absent. Since thin-walled fungal spores can mainly be attributed to species with airborne dispersal, it would seem that fungal NPP assemblages in lake sediments mainly reflect the local aquatic ecosystem and any immediately surrounding terrestrial ecosystems. Among the zoological remains, we recovered both smooth or modestly ornamented eggs of Neorhabdocoela (flatworms) and more strongly ornamented diapausing eggs (cysts) attributable to various groups of aquatic arthropods (copepods, ostracods, etc.). Cyst ornamentation (honeycombing, flanges, spines, etc.) in aquatic invertebrates is thought to help protect against predation (Dumont et al., 2002), consequently the relative abundance of aquatic invertebrate groups recorded in fossil NPP assemblages is biased in favour of those groups producing ornamented cysts.

Finally, experimental studies on modern NPP origin and deposition (Gaillard et al., 1994; Wilmshurst and McGlone, 2005; Prager et al., 2006) also reveal differences in microfossil diversity between substrate types (e.g., lake sediments, moss cushions, terrestrial soils). The high diversity of pollen and spore types typically found in lake sediments compared to terrestrial substrates (Wilmshurst and McGlone, 2005) has been attributed to a more diverse biotic influx from multiple lakeshore habitats and substrates, supplemented by important wind dispersal (see also Prentice, 1985; Sugita, 1993; DeBusk, 1997). However, at our study sites at least, wind dispersal appears to contribute less to lake-bottom NPP assemblages than entrainment from the surrounding landscape by water flow across it; and a significant portion of total NPP diversity is derived from local, (semi-)aquatic saprotrophic fungi, algae and aquatic invertebrates. We estimate that at least 24% of the 73 identified African NPPs in our data set are (semi-)aquatic species, but even these two fundamental ecological groups of terrestrial versus aquatic biota cannot be reliably separated. The group of algal NPPs and most zoological NPPs are fully aquatic, whereas the fern and moss NPPs are presumably mostly derived from terrestrial or riparian habitats. The terrestrial or aquatic affinity of fungal remains, however, is less tractable. Of the 53 fungal NPP taxa that could be (tentatively) identified to species, genus or family level, about 20% have worldwide distributions in both terrestrial environments and (sometimes fortuitously) freshwater environments. Terrestrial and aquatic fungi do not form separate monophyletic groups, but each comprise a diverse assemblage of species with representatives from various orders. Among the predominantly terrestrial fungi, Sordariales (e.g., *Apiosordaria*, *Coniochaeta*, *Cercophora*, *Gelasinospora* and *Sordaria*), Pleosporales (e.g., *Byssothecium*, *Curvularia*, *Delitschia* and *Sporidesmium*) and Xylariales (e.g. *Rosellinia*, *Kretzschmaria* and a few other unknown Xylariaceae) are well represented, whereas Chaetosphaeriales (e.g., *Sporoschisma*), Glomerales (*Glomus*), Phyllachorales (e.g., *Bactrodesmium* and *Clasterosporium*) and Ustilaginales (e.g., *Urocystis*) are less well represented. Only four or five (~10%) of the identified fungal genera in our dataset have previously been reported from tropical freshwater habitats (Goh, 1997; Hyde et al., 1997). Among the Ascomycota and Hyphomycetes, it is known that some species within genera such as *Brachydesmiella*, *Clasterosporium, Dictyosporium, Sporidesmium, Sporoschisma* and *Tetraploa* live on (partially) submerged dead stems, leaves and wood. Unfortunately, tropical Africa remains one of the least studied biogeographical regions for fungal diversity in aquatic habitats (Shearer et al., 2007). This problem of differentiation between aquatic NPPs (reflecting habitat conditions in the local lake system) and terrestrial NPPs (reflecting habitat conditions in the surrounding landscape), together with the biologically heterogeneous nature of NPP assemblages, hampers quantitative evaluation of the ecological parameters controlling the distribution of individual taxa, on the basis of which their palaeoecological indicator value must be established.

Acknowledgements

This study was funded by the 'Science for a Sustainable Development' programme of the Belgian Federal Science Policy (project SD/BD/03 CLANIMAE). The fieldwork was conducted with permission of the Uganda National Council of Science and Technology (NS 162) and the Uganda Wildlife Authority (UWA/TBDP/RES/50), with additional sponsoring by the Research Foundation — Flanders (*FWO Vlaanderen-Belgium*) and the Leopold III Fund for Nature Exploration and Conservation (*Belgium*). We thank Johnson Bwambale, Pierre-Denis Plisnier, Bob Rumes and Julie Lebrun for field assistance, Martine Hagen for sample preparation, Kay Van Damme and Olivier Leroux for graphical advice, and the following experts for help with identifications: Jiri Komárek and Vlasta Jankovská (algae); Jean Nicolas Haas, Henri Dumont, Lynda Beladjal and S.S.S. Sarma (zoological remains); Jacqueline van Leeuwen (spores); Elke Bellefroid and Ronnie Viane (ferns and moss spores); Fabienne Marret (dinoflagellates); and Andre Aptroot and Bernard Declercq (fungal spores). We are also grateful to the referees for valuable comments on the manuscript.

References

Aldasoro, J.J., Cabezas, F., Aedo, C., 2004. Diversity and distribution of ferns in sub-Saharan Africa, Madagascar and some islands of the South Atlantic. Journal of Biogeography 31, 1579–1604.

Andrua, H.J., 2002. Tropical Secondary Forest Management in Africa: Reality and Perpectives, Uganda Country paper. Ministry of Water, Lands, and Environment, Kampala. http://www.fao.org/DOCREP/006/J0628E/J0628E65.htm#TopOfPage.

Bakker, M., van Smeerdijk, D.G., 1982. A paleoecological study of a late Holocene section from "Het Ilperveld", western Netherlands. Review of Palaeobotany and Palynology 36, 95–163.

Barthelmes, A., Prager, A., Joosten, H., 2006. Palaeoecological analysis of *Alnus* wood peats with special attention to non-pollen palynomorphs. Review of Palaeobotany and Palynology 141, 33–51.

Batten, D.J., Grenfell, H.R., 1996. Chapter 7D. *Botryococcus*. In: Jansonius, J., McGregor, D.C. (Eds.), Palynology: Principles and Applications. Principles, Volume 1. American Association of Stratigraphic Palynologists Foundation, Dallas-Texas-USA, pp. 205–214.

Beadle, L.C., 1932. Scientific results of the Cambridge expedition to the East African lakes, 1930–1931. 4. The waters of some East African lakes in relation to their fauna and flora. Journal of the Linnean Society (Zoology) 38, 157–211.

Beentje, H.J., Cheek, M., 2003. Glossary. In: Beentje, H.J., Ghazanfar, S.A. (Eds.), Flora of Tropical East Africa. A.A. Balkema, Lisse.

Bell, A., 1983. Dung Fungi. An Illustrated Guide to the Coprophilous Fungi in New Zealand. Victoria University Press, Wellington.

Bera, S.K., Dixit, S., Basumatary, S.K., Gogoi, R., 2008. Evidence of biological degradation in sediments of Deepor Beel Ramsar Site, Assam as inferred by degraded palynomorphs and fungal spores. Current Science 95, 178–180.

Berrío, J.C., Hooghiemstra, H., van Geel, B., Ludlow-Wiegers, B., 2006. Environmental history of the dry forest biome of Guerrero, Mexico, and human impact during the last c. 2700 years. The Holocene 16, 63–80.

Bessems, I., Verschuren, D., Russell, J.M., Hus, J., Mees, F., Cumming, B.F., 2008. Palaeolimnological evidence for widespread late 18th century drought across equatorial East Africa. Palaeogeography, Palaeoclimatology, Palaeoecology 259, 107–120.

Birks, H.J.B., Birks, H.H., 1980. Quaternary Palaeoecology. Cambridge University Press, Cambridge.

Blackford, J.J., Innes, J.B., 2006. Linking current environments and processes to fungal spore assemblages: surface NPM data from woodland environments. Review of Palaeobotany and Palynology 141, 179–187.
Brummitt, R.K., Powell, C.E., 1992. Authors of Plant Names. Royal Botanic Gardens, Kew. http://www.ipni.org/index.html.
Burney, D.A., Robinson, G.S., Burney, L.P., 2003. *Sporormiella* and the late Holocene extinctions in Madagascar. PNAS 100 (19), 10800–10805.
Burrows, J.E., 1990. Southern African Ferns & Fern Allies. Frandsen Publishers, Sandton.
Burrows, J.E., Johns, R.J., 2001. Ophioglossaceae. In: Beentje, H.J., Smith, S.A.L. (Eds.), Flora of Tropical East Africa. A.A. Balkema, Rotterdam-Brookfield.
Carreta, G., Piontelli, E., Savino, E., Bulgheroni, A., 1998. Some coprophilous fungi from Kenya. Mycopathologia 142, 125–134.
Carreta, G., Piontelli, E., Picco, A.M., Del Frate, G., 1999. Some filamentous fungi on grassland vegetation from Kenya. Mycopathologia 145, 155–169.
Carrión, J.S., Navarro, C., 2002. Cryptogam spores and other non-pollen microfossils as sources of palaeoecological information: case-studies from Spain. Annales Botanici Fennici 39, 1–14.
Carrión, J.S., Scott, L., Huffman, T., Dreyer, C., 2000. Pollen analysis of Iron Age cow dung in southern Africa. Vegetation History and Archaeobotany 9, 239–249.
Celio, G.J., Padamsee, M., Dentinger, B.T.M., Bauer, R., McLaughlin, D.J., 2006. Assembling the Fungal Tree of Life: constructing the Structural and Biochemical Database. Mycologia 98, 850–859.
Chardez, D., 1964. Thécamoebiens (Rhizopodes testacés). In: Symoens, J.-J. (Ed.), Exploration Hydrobiologique du Bassin du Lac Bangweolo et du Luapula. : Résultats scientifiques, Thécamoebiens, 10(2). Cercle Hydrobiologique de Bruxelles, Bruxelles, pp. 1–77.
Compère, P., 1970. Contribution à l'étude des eaux douces de l'Ennedi, VI. Algues. Bulletin de l'Institut Fondamental d'Afrique Noire 32 (1), 18–72.
Crane, J.L., Shearer, C.A., Huhndorf, S.M., 1992. A new species of *Byssothecium* (Loculoascomycetes) from wood in freshwater. Mycologia 84, 235–240.
Cronberg, G., 1986. Blue-green algae, green algae and chrysophyceae in sediments. In: Berglund, B.E. (Ed.), Handbook of Holocene Palaeoecology and Palaeohydrology. John Wiley and sons, Chichester, pp. 507–526.
Cugny, C., Mazier, F., Galop, D., 2010. Modern and fossil non-pollen palynomorphs from the Basque mountains (western Pyrenees, France): the use of coprophilous fungi to reconstruct pastoral activity. Vegetation history and Archaeobotany 19, 391–408.
DeBusk Jr., G.H., 1997. The distribution of pollen in the surface sediments of Lake Malawi, Africa, and the transport of pollen in large lakes. Review of Palaeobotany and Palynology 97, 123–153.
Dennis, R.W.G., 1961. Xylarioideae and Thamnomycetoideae of Congo. Bulletin du Jardin Botanique de l'État à Bruxelles 31, 109–154.
Dimbleby, G.W., 1957. Pollen analysis of terrestrial soils. New Phytologist 56, 12–28.
Dumont, H.J., Nandini, S., Sarma, S.S.S., 2002. Cyst ornamentation in aquatic invertebrates: a defence against egg-predation. Hydrobiologia 486, 161–167.
Eggermont, H., Verschuren, D., 2004a. Subfossil Chironomidae from East Africa. 1. Tanypodinae and Orthocladiinae. Journal of Paleolimnology 32, 383–412.
Eggermont, H., Verschuren, D., 2004b. Subfossil Chironomidae from East Africa. 2. Chironomini and Tanytarsini. Journal of Paleolimnology 32, 413–455.
Eggermont, H., Heiri, O., Verschuren, D., 2006. Subfossil Chironomidae (Insecta: Diptera) as quantitative indicators for past salinity variation in African lakes. Quaternary Science Reviews 25, 1966–1994.
Eggermont, H., Heiri, O., Russell, J., Vuille, M., Audenaert, L., Verschuren, D., 2010. Chironomidae (Insecta: Diptera) as paleothermometers in the African tropics. Journal of Paleolimnology 43, 413–435. doi:10.1007/s10933-009-9339-2.
Ellis, M.B., 1971. Dematiaceous Hyphomycetes. Commonwealth Mycological Institute, Kew, Surrey.
Ellis, M.B., 1976. More dematiaceous Hyphomycetes. Commonwealth Mycological Institute, Kew, Surrey.
Ellis, M.B., Ellis, J.P., 1985. Microfungi on Land Plants. Croom Helm Ldt, Kent.
Faegri, K., Kaland, P.E., Krzywinski, K., 1989. Textbook of Pollen Analysis by Knut Faegri and Johs. Iversen, IV edition. John Wiley and sons Ltd, Chichester.
Foissner, W., 2006. Biography and dispersal of micro-organisms: a review emphasizing protists. Acta Protozoologica 45, 111–136.
Friis, I., Vollesen, K., 1998. Flora of the Sudan–Uganda Border Area East of the Nile: I. Catalogue of vascular plants, 1st part. Det Kongelige Danske videnskabernes Selskabs Biologiske Skrifter 51, 1–389.
Fröhlich, J., Hyde, K.D., 1999. Biodiversity of palm fungi in the tropics: are global fungal diversity estimates realistic? Biodiversity and Conservation 8, 977–1004.
Gaillard, M.J., Hicks, S., Ritchie, J.C. (Eds.), 1994. Modern Pollen Rain and Fossil Pollen Spectra. : Review of Palaeobotany and Palynology, 82 (1–2). Elsevier, Amsterdam.
Goh, T.K., 1997. Tropical freshwater Hyphomycetes. In: Hyde, K.D. (Ed.), Biodiversity of Tropical Microfungi. University Press, Hong Kong, pp. 189–227.
Goh, T.K., Hyde, K.D., 2000. A new species of *Canalisporium* from Australia. Mycologia 92, 589–592.
Goh, T.K., Ho, W.H., Hyde, K.D., Umali, T.E., 1997. New records and species of *Sporoschisma* and *Sporoschismopsis* from submerged wood in the tropics. Mycological research 101, 1295–1307.
Goh, T.K., Ho, W.H., Hyde, K.D., Whitton, S.R., Umali, T.E., 1998. New records and species of *Canalisporium* (Hyphomycetes), with a revision of the genus. Canadian Journal of Botany 76, 142–152.
Haas, J.N., 1996. Neorhabdocoela oocytes — paleoecological indicators found in pollen preparations from Holocene freshwater lake sediments. Review of Palaeobotany and Palynology 91, 371–382.
Haas, J.N. (Ed.), 2010. Fresh insights into the palaeoecological and palaeoclimatological value of Quaternary non-pollen palynomorphs. Vegetation history and Archaeobotany, 19 (5–6). Springer, New York.
Hanlin, R.T., 1990. Illustrated Genera of Ascomycetes, Volume I & II. The American Phytopathological Society, St. Paul, Minnesota.
Havinga, A.A., 1984. A 20 year experimental investigation into the differential corrosion susceptibility of pollen and spores in various soil types. Pollen et Spores 26, 541–558.
Hawksworth, D.L., 1991. The fungal dimension of biodiversity: magnitude, significance, and conservation. Mycological Research 95, 641–655.
Hawksworth, D.L., 1993. The tropical fungal biota: census, pertinence, prophylaxis, and prognosis. In: Isaac, S., Frankland, J.C., Watling, R., Watling, A.J.S. (Eds.), Aspects of Tropical Mycology. Cambridge University Press, Cambridge, pp. 265–293.
Hawksworth, D.L., Yip, H.Y., 1981. *Coniochaeta angustispora* sp. nov. from roots in Australia, with a key to the species known in culture. Australian Journal of Botany 29, 377–384.
Hemp, A., 2002. Ecology of the pteridophytes on the southern slopes of Mt. Kilimanjaro: I. Altitudinal distribution. Plant Ecology 159, 211–239.
Hibbett, D.S., Binder, M., Bischoff, J.F., Blackwell, M., Cannon, P.F., Eriksson, O.E., Huhndorf, S., James, T., Kirk, P.M., Lücking, R., Thorsten Lumbsch, H., Lutzoni, F., Matheny, P.B., McLaughlin, D.J., Powell, M.J., Redhead, S., Schoch, C.L., Spatafora, J.W., Stalpers, J.A., Vilgalys, R., Aime, M.C., Aptroot, A., Bauer, R., Begerow, D., Benny, G.L., Castlebury, L.A., Crous, P.W., Dai, Y.C., Gams, W., Geiser, D.M., Griffith, G.W., Gueidan, C., Hawksworth, D.L., Hestmark, G., Hosaka, K., Humber, R.A., Hyde, K.D., Ironside, J.E., Kõljalg, U., Kurtzman, C.P., Larsson, K.H., Lichtwardt, R., Longcore, J., Miadlikowska, J., Miller, A., Moncalvo, J.M., Mozley-Standridge, S., Oberwinkler, F., Parmasto, E., Reeb, V., Rogers, J.D., Roux, C., Ryvarden, L., Sampaio, J.P., Schüssler, A., Sugiyama, J., Thorn, R.G., Tibell, L., Untereiner, W.A., Walker, C., Wang, Z., Weir, A., Weiss, M., White, M.M., Winka, K., Yao, Y.J., Zhang, N., 2007. A higher-level phylogenetic classification of the Fungi. Mycological Research 111, 509–547.
Hires, C.S., 1965. Spores, ferns: microscopic illusions analyzed. : Varied Plant Groups Introduce True Ferns Through Spore Tetrad Structure, XXIV, Volume I. Mistaire Laboratories, Milburn, New Jersey.
Hires, C.S., 1978. Spores, Ferns: Microscopic Illusions Analyzed. : Representative Species with Spore Cases that Differ from "True Fern" Sporangia, XXIV, Volume II. Mistaire Laboratories, Milburn, New Jersey.
Ho, W.H., Hyde, K.D., Hodgkiss, I.J., 1997. Ascomycetes from tropical freshwater habitats: the genus *Savoryella*, with two new species. Mycological Research 101, 803–809.
Hodgetts, N., 2004. Mosses and liverworts of Uganda (MALOU). Checklist of hepatics and hornworts. U.K. Natural History Museum. http://tring.naturalhistory.museum/hosted_sites/bbstbg/ugaheps.htm.
Hoshaw, R.W., 1968. Biology of filamentous conjugating algae. In: Jackson, D.F. (Ed.), Algae, man and the environment. Syracuse Univ. Press, New York.
Hyde, K.D., Wong, S.W., Jones, E.B.G., 1997. Freshwater Ascomycetes. In: Hyde, K.D. (Ed.), Biodiversity of Tropical Microfungi. University Press, Hong Kong, pp. 179–187.
Index Fungorum Partnership, 2004. http://www.indexfungorum.org/Index.htm.
Jankovská, V., Komárek, J., 2000. Indicative value of *Pediastrum* and other coccal green algae in palaeoecology. Folia Geobotanica 35, 59–82.
Jarzen, D.M., Elsik, W.C., 1986. Fungal palynomorphs recovered from recent river deposits, Luangwa Valley, Zambia. Palynology 10, 35–60.
John, D.M., Whitton, B.A., Brook, A.J., 2002. The freshwater algal flora of the British Isles. An identification guide to freshwater and terrestrial algae. Cambridge University Press and the Natural Museum, Cambridge.
Ju, Y.-M., Rogers, J.D., Hsieh, H.-M., Vasilyeva, L., 2004. *Amphirosellinia* gen. nov. and a new species of *Entoleuca*. Mycologia 96, 1393–1402.
Khan, R.S., Krug, J.C., 1989a. New species of *Gelasinospora*. Mycologia 81, 226–233.
Khan, R.S., Krug, J.C., 1989b. New records of the Sordariaceae from East Africa. Mycologia 81, 862–869.
Kilham, P., 1971. Biochemistry of African lakes and rivers. Ph. D. Thesis, Duke University, Durham, North Carolina.
Kirk, P.M., Cannon, P.F., Minter, D.W., Stalpers, J.A., 2008. Dictionary of Fungi, 10th edition. CBS, The Netherlands.
Kizito, Y.S., Nauwerck, A., Chapman, L.J., Koste, W., 1993. A limnological survey of some western Uganda crater lakes. Limnologica 23, 335–347.
Komárek, J., Jankovská, V., 2001. Review of the green algal genus *Pediastrum*. Implication for pollen-analytical research. Bibliotheca Phycologia 108, 1–127.
Komárek, J., Marvan, P., 1992. Morphological differences in natural populations of the genus *Botryococcus* (Chlorophyceae). Archiv für Protistenkunde 141, 65–100.
Kornás, J., 1993. The significance of historical factors and ecological preference in the distribution of African pteridophytes. Journal of Biogeography 20, 281–286.
Krug, J.C., 1978. The genus *Cainia* and a new family, Cainiaceae. Sydowia 30, 122–133.
Krug, J.C., Khan, R.S., Jeng, R.S., 1994. A new species of *Gelasinospora* with multiple germ pores. Mycologia 86, 250–253.
Kuhry, P., 1985. Transgression of a raised bog across a coversand ridge originally covered with an oak-lime forest. Paleoecological study of a Middle Holocene local vegetational succession in the Amtsven (northwest Germany). Review of Palaeobotany and Palynology 44, 303–353.
Ledru, M.P., Ceccantini, G., Gouveia, S.E.M., López-Sáez, J.A., Pessenda, L.C.R., Ribeiro, A.S., 2006. Millenial-scale climatic and vegetation changes in a northern Cerrado (Northeast Brazil) since the Last Glacial Maximum. Quaternary Science Reviews 25, 1110–1126.
Lejju, B.J., Taylor, D., Robertshaw, P., 2005. Late-Holocene environmental variability at Munsa archaeological site, Uganda: a multicore, multiproxy approach. The Holocene 15, 1044–1061.
Limaye, R.B., Kumaran, K.P.N., Nair, K.M., Padmalal, D., 2007. Non-pollen palynomorphs as potential palaeoenvironmental indicators in the Late Quaternary sediments of the west coast of India. Current Science 92, 1370–1382.

Lodge, J.D., Chapela, I., Samuels, G., Uecker, F.A., Desjardin, D., Horak, E., Miller, O.K., Hennebert, G.L., Decock, C.A., Ammirati, J., Burdsall, H.H., Kirk, P.M., Minter, D.W., Halling, R., Læssoe, T., Mueller, G., Huhndorf, S., Oberwinkler, F., Pegler, D.N., Spooner, B., Petersen, R.H., Rogers, J.D., Ryvarden, L., Watling, R., Turnbull, E., Whalley, A.J.S., 1995. A survey of patterns of diversity in non-lichenized fungi. Mitteilungen aus dem Eidgenössische Forschunganstalt für Wald-, Schnee- und Landwirtschaft 70, 157–173.
Lodge, J.D., 1997. Factors related to diversity of decomposer fungi in tropical forests. Biodiversity and Conservation 6, 681–688.
López Sáez, J.A., van Geel, B., Farbos-Texier, S., Diot, M.F., 1998. Remarques paléoécologiques à propos de quelques palynomorphes non-polliniques provenant de sédiments quaternaires en France. Revue de Paléobiologie 17, 445–459.
Lu, B.-S., Hyde, K.D., Liew, E.C.Y., 2000. Eight new species of *Anthostomella* from South Africa. Mycological Research 104, 742–754.
Mbenoun, M., Momo Zeutsa, E.H., Samuels, G., Nsouga Amougou, F., Nyasse, S., 2008. Dieback due to *Lasiodiplodia theobromae*, a new constraint to cocoa production in Cameroon. Plant Pathology 57, 381.
Medeanic, S., 2006. Freshwater algal palynomorph records from Holocene deposits in the coastal plain of Rio Grande do Sul, Brazil. Review of Palaeobotany and Palynology 141, 83–101.
Melack, J.M., 1978. Morphometric, physical and chemical features of the volcanic crater lakes of western Uganda. Archiv für Hydrobiologie 84, 430–453.
Mibey, R.K., Kokwaro, J.O., 1999. Two new species of *Meliola* (Ascomycetes) from Kenya. Fungal Diversity 2, 153–157.
Mohali, S., Burgess, T.I., Wingfield, M.J., 2005. Diversity and host association of the tropical tree endophyte *Lasiodiplodia theobromae* revealed using simple sequence repeat markers. Forest Pathology 35, 385–396.
Moran, R.C., 1995. The importance of mountains to Pteridophytes, with emphasis on Neotropical montane forests. In: Churchill, S.P., Balslev, H., Forero, E., Luteyn, J.L. (Eds.), Biodiversity and Conservation of Neotropical Montane Forests. The New York Botanical Garden, New York, pp. 359–363.
Moreau, C., Müller, E., 1963. Sur deux ascomycètes phaeodidymés du *Spartium junceum* L. Revue de Mycologie 28, 19–26.
Mulder, Ch., Breure, A.M., Joosten, J.H.J., 2003. Fungal functional diversity inferred along Ellenberg's abiotic gradients: palynological evidence from different soil microbiota. Grana 42, 55–64.
Mumbi, C.T., Marchant, R., Hooghiemstra, H., Wooller, M.J., 2008. Late Quaternary vegetation reconstruction from the Eastern Arc Mountains, Tanzania. Quaternary Research 69, 326–341.
Neustupa, J., Šťastný, J., Hodač, L., 2008. Temperature-related phenotypic plasticity in the green microalga *Micrasterias rotata*. Aquatic Microbial Ecology 51, 77–86.
Pals, J.P., van Geel, B., Delfos, A., 1980. Paleoecological studies in the Klokkeweel bog near Hoogkarspel (prov. of Noord Holland). Review of Palaeobotany and Palynology 30, 371–418.
Petrini, L.E., 1993. *Rosellinia* species of the temperate zones. Sydowia 44, 169–281.
Petrini, L.E., 2003. *Rosellinia* and related genera in New Zealand. New Zealand Journal of Botany 41, 71–138.
Pinto da Luz, C.F., De Souza Nogueira, I., Barth, O.M., Silva, C.G., 2002. Differential sedimentation of Algae Chlorococcales (*Scenedesmus*, *Coelastrum* and *Pediastrum*) in Lagao de Cima, Campos dos Goitacazes Municipality (Rio de Janeiro, Brazil). Pesquisas em Geociências 29, 65–75.
Pitt, J.I., Hocking, A.D., Bhudhasamai, K., Miscamble, B.F., Wheeler, K.A., Tanboon-Ek, P., 1994. The normal mycoflora of commodities from Thailand. 2. Beans, rice, small grains and other commodities. International Journal of Food Microbiology 23, 35–43.
Pócs, T., 1998. Bryophyte diversity along the Eastern Arc. Journal of East African Natural History 87, 75–84.
Prager, A., Barthelmes, A., Theuerkauf, M., Joosten, H., 2006. Non-pollen palynomorphs from modern Alder carrs and their potential for interpreting microfossil data from peat. Review of Palaeobotany and Palynology 14, 7–31.
Prentice, I.C., 1985. Pollen representation, source area and basin size: toward a unified theory of pollen analysis. Quaternary Research 23, 76–86.
Proskauer, J., 1951. Studies on Anthocerotales. III. Bulletin of the Torrey Botanical Club 78, 331–349.
Ralska-Jasiewiczowa, M., van Geel, B., 1992. Early human disturbance of the natural environment recorded in annually laminated sediments of Lake Gościaź, central Poland. Vegetation History and Archaeobotany 1, 33–42.
Richardson, M.J., 2001. Diversity and occurrence of coprophilous fungi. Mycological Research 105, 387–402.
Rogers, J.D., Ju, Y.-M., 1998. The genus *Kretzschmaria*. Mycotaxon 68, 345–393.
Rogers, J.D., Whalley, A.J.S., 1978. A new *Hypoxylon* species from Wales. Canadian Journal of Botany 56, 1346–1348.
Rull, V., Lopéz-Sáez, J.A., Vegas-Vilarrúbia, T., 2008. Contribution of non-pollen palynomorphs to the paleolimnological study of a high-altitude Andean lake (Laguna Verde Alta, Venezuela). Journal of Paleolimnology 40, 399–411.
Rumes, B., Eggermont, H., Verschuren, D., 2005. Representation of aquatic invertebrate communities in subfossil death assemblages sampled along a salinity gradient of western Uganda crater lakes. Hydrobiologia 542, 297–314.
Russell, J., Verschuren, D., Eggermont, H., 2007. Spatial complexity of 'Little Ice Age' climate in East Africa: sedimentary records from two crater lake basins in western Uganda. The Holocene 17, 183–193.
Russell, J., McCoy, S.J., Verschuren, D., Bessems, I., Huang, Y., 2009. Human impacts, climate change, and aquatic ecosystem response during the past 2000 yr at Lake Wandakara, Uganda. Quaternary Research 72, 315–324.
Schelpe, E.A.C.L.E., 1983. Aspects of phytogeography of African Pteridophyta. Bothalia 14, 417–419.
Shearer, C.A., Descals, E., Kohlmeyer, B., Kohlmeyer, J., Marvanová, L., Padgett, D., Porter, D., Raja, H.A., Schmit, J.P., Thorton, H.A., Voglmayr, H., 2007. Fungal biodiversity in aquatic habitats. Biodiversity and Conservation 16, 49–67.
Shoemaker, R.A., Babcock, C.E., 1989. Phaeosphaeria. Canadian Journal of Botany 67, 1500–1599.
Sivichai, S., Goh, T.K., Hyde, K.D., Hywel-Jones, N.L., 1998. The genus *Brachydesmiella* from submerged wood in the tropics, including a new species and a new combination. Mycoscience 39, 239–247.
Smith, D., Waller, J.M., 1992. Culture collections of microorganisms: their importance in tropical plant pathology. Fitopatologia Brasileira 17, 1–8.
Somrithipol, S., Chatmala, I., Jones, E.B.G., 2002. *Cirrenalia nigrospora* sp. nov. and *C. tropicalis* from Thailand. Nova Hedwigia 75, 477–485.
Ssemmanda, I., Ryves, D.B., Bennike, O., Abbleby, P.G., 2005. Vegetation history in western Uganda during the last 1200 years: a sedimentbased reconstruction from two crater lakes. The Holocene 15, 119–132.
Stearn, W.T., 2004. Botanical Latin, 4th edition. Redwood Books, Trowbridge.
Subramanian, C.V., 1971. Hyphomycetes. An Account of Indian Species, Except Cercosporae. Indian Council of Agricultural Research, New Delhi.
Sugita, S., 1993. A model of pollen source area for an entire lake surface. Quaternary Research 39, 239–244.
Tandon, R.N., 1935. A note on the genus *Mitteriella*. Current Science 3, 613–614.
Tryon, A.F., Lugardon, B., 1990. Spores of the Pteridophyta. Surface, wall structure, and diversity based on Electron Microscope Studies. Springer-Verlag, New York.
van Geel, B., 1978. A paleoecological study of Holocene peat bog sections in Germany and the Netherlands. Review of Palaeobotany and Palynology 25, 1–120.
van Geel, B., 2001. Non-pollen palynomorphs. In: Smol, J.P., Birks, H.J.B., Last, W.M. (Eds.), Tracking Environmental Change Using Lake Sediments. Terrestrial, Algal and Silicaceous Indicators, Volume 3. Kluwer, Dordrecht, pp. 99–119.
van Geel, B. (Ed.), 2006. Quaternary Non-Pollen Palynomorphs. Review of Palaeobotany and Palynology, 141 (1–2). Elsevier, Amsterdam.
van Geel, B., Aptroot, A., 2006. Fossil ascomycetes in Quaternary deposits. Nova Hedwigia 82, 313–329.
van Geel, B., van der Hammen, T., 1978. Zygnemataceae in Quaternary Colombian sediments. Review of Palaeobotany and Palynology 25, 377–392.
van Geel, B., Klink, A.G., Pals, J.P., Wiegers, J., 1986. An upper Eemian lake deposit from Twente, eastern Netherlands. Review of Palaeobotany and Palynology 47, 31–61.
van Geel, B., Coope, G.R., van der Hammen, T., 1989. Palaeoecology and stratigraphy of a Lateglacial type section at Usselo (The Netherlands). Review of Palaeobotany and Palynology 60, 25–129.
van Geel, B., Zazula, G.D., Schweger, C.E., 2007. Spores of coprophilous fungi from under the Dawson tephra (25, 300 14 C years BP), Yukon Territory, northwestern Canada. Palaeogeography, Palaeoclimatology, Palaeoecology 252, 481–485.
van Geel, B., Aptroot, A., Baittinger, C., Birks, H.H., Bull, I.D., Cross, H.B., Evershed, R.P., Gravendeel, B., Kompanje, E.J.O., Kuperus, P., Mol, D., Nierop, K.G.J., Pals, J.P., Tikhonov, A.N., van Reenen, G., van Tienderen, P.H., 2008. The ecological implications of a Yakutian mammoth's last meal. Quaternary Research 69, 361–376.
van Geel, B., Dale Guthrie, R., Altmann, J.G., Broekens, P., Bull, I.D., Gill, F.L., Jansen, B., Nieman, A.M., Gravendeel, B., in press. Mycological evidence of coprophagy of an Alaskan Late Glacial Mammoth. Quaternary Science Reviews. doi:10.1016/j.quascirev.2010.03.008.
van Geel, B., Gelorini, V., Lyaruu, A., Aptroot, A., Rucina, S., Marchant, R., Sinninghe Damsté, J.S., Verschuren, D., 2011-this issue. Diversity and ecology of tropical African fungal spores from a 25,000-year palaeoenvironmental record in southeastern Kenya. Review of Palaeobotany and Palynology 164, 174–190.
Van Meel, L., 1954. Le phytoplancton: Etat actuel de nos connaissances sur les grands lacs est-africains et leur phytoplancton, A. Texte et B. Atlas. Musée royal de l'Afrique Centrale, Bruxelles.
van Smeerdijk, D., 1989. A paleoecological and a chemical study of a peat profile from the Assendelver polder (The Netherlands). Review of Palaeobotany and Palynology 58, 231–288.
Vánky, K., 1994. European Smut Fungi. Gustav Fischer Verlag. Stuttgart, Jena, New York.
Verdcourt, B., 1989. In: Polhill, R.M. (Ed.), Nymphaeaceae. Flora of Tropical East Africa. A.A. Balkema, Rotterdam-Brookfield.
Verdcourt, B., 1999. Actiniopteridaceae. In: Beentje, H.J., Smith, S.A.L. (Eds.), Flora of Tropical East Africa. A.A. Balkema, Rotterdam-Brookfield.
Verdcourt, B., 2000. Dennstaedtiaceae. In: Beentje, H.J., Smith, S.A.L. (Eds.), Flora of Tropical East Africa. A.A. Balkema, Rotterdam-Brookfield.
Verdcourt, B., 2001. Polypodiaceae. In: Beentje, H.J., Smith, S.A.L. (Eds.), Flora of Tropical East Africa. A.A. Balkema, Rotterdam-Brookfield.
Verdcourt, B., 2002. Pteridaceae. In: Beentje, H.J., Ghanzanfar, S.A. (Eds.), Flora of Tropical East Africa. A.A. Balkema, Rotterdam-Brookfield.
Verschuren, D., 1993. A lightweight extruder for accurate sectioning of soft-bottom lake sediment cores in the field. Limnology and Oceanography 38, 1796–1802.
Verschuren, D., Plisnier, P.-D., Hugues, H., Lebrun, J., Gelorini, V., Cocquyt, C., Mahy, G., 2009. CLANIMAE: climatic and anthropogenic impacts on African ecosytems. Belspo final report Phase I (2007–2008). 62 pp.
Weinstein, R.N., Pfister, D.H., Iturriaga, T., 2002. A phylogenetic study of the genus *Cookeina*. Mycologia 94, 673–682.
Whalley, A.J.S., 1993. Tropical Xylariaceae: their distribution and ecological characteristics. In: Isaac, S., Frankland, J.C., Watling, R., Whalley, A.J.S. (Eds.), Aspects of Tropical Mycology. Cambridge University Press, Cambridge, pp. 103–119.
White, F., 1983. The vegetation of Africa, a descriptive memoir to accompany the UNESCO/AETFAT/UNSO vegetation map of Africa. Natural Resources Research 20, 1–356.
Wilmshurst, J.M., McGlone, M.S., 2005. Origin of pollen and spores in surface lake sediments: comparison of modern palynomorph assemblages in moss cushions,

surface soils and surface lake sediments. Review of Palaeobotany and Palynology 136, 1–15.
Wolf, F.A., 1966. Fungus spores in East African lake sediments. Bulletin of the Torrey Botanical Club 93, 104–113.
Wolf, F.A., 1967a. Fungus spores in East African lake sediments. IV. Bulletin of the Torrey Botanical Club 94, 31–34.
Wolf, F.A., 1967b. Fungus spores in East African lake sediments. VII. Bulletin of the Torrey Botanical Club 94, 480–486.
Yeloff, D., Mauquoy, D., Barber, K., Way, S., van Geel, B., Turney, C.S.M., 2007. Volcanic ash deposition and long-term vegetation change on subantarctic Marion Island. Arctic, Antarctic, and Alpine Research 39, 500–511.
Zhao, G.Z., Liu, X.Z., 2005. A review of *Cirrenalia* (hyphomycetes) and a new species. Fungal Diversity 18, 201–209.
Zong, Y., Chen, Z., Innes, J.B., Chen, C., Wang, Z., Wang, H., 2007. Fire and flood management of coastal swamp enabled first rice paddy cultivation in east China. Nature 449, 459–462.

Ecology, 00(0), 0000, pp. 000–000

Priority effects and species sorting in a long paleoecological record of repeated community assembly through time

Joachim Mergeay,[1,2,5] Luc De Meester,[2] Hilde Eggermont,[3,4] and Dirk Verschuren[4]

[1]*Research Institute for Nature and Forest, Gaverstraat 4, 9500 Geraardsbergen, Belgium*
[2]*Laboratory of Aquatic Ecology and Evolutionary Biology, Katholieke Universiteit Leuven, Charles Deberiotstraat 32, 3000 Leuven, Belgium*
[3]*Royal Belgian Institute of Natural Sciences, Freshwater Biology, Vautierstraat 29, 1000 Brussels, Belgium*
[4]*Limnology Unit, Department of Biology, Ghent University, K.L. Ledeganckstraat 35, 9000 Ghent, Belgium*

Abstract. We studied the relative roles of environmental species sorting and priority effects in the assembly of ecological communities on long time scales, by analyzing community turnover of water fleas (*Daphnia*) in response to strong and recurrent environmental change in a fluctuating tropical lake. During the past 1800 years, Lake Naivasha (Kenya) repeatedly fluctuated between a small saline pond habitat during lowstands and a large freshwater lake habitat during highstands. Starting from a paleoecological reconstruction, we estimated the role of priority effects in *Daphnia* community assembly across 16 of these habitat turnovers, and compared this with the response of the community to reconstructed changes in three environmental variables important for species sorting.

Our results indicate that the best predictor of *Daphnia* community composition during highstands was the community composition just prior to the transition from lowstands to highstands. This reflects a long-lasting priority effect of late lowstand communities on highstand communities, arising when remnant lowstand populations fill newly available ecological space in the rapidly expanding lake habitat. Species sorting and priority effects had a comparable but relatively small influence on community composition during the lowstands. Moreover, these priority effects decayed rapidly with time as *Daphnia* communities responded to environmental change, in contrast with the highstand communities where priority effects lasted for several decades.

Key words: community assembly; Daphnia *spp.*; *Lake Naivasha, Kenya; mass effect; metacommunity; niche; paleoecology; priority effect; propagule pressure; restoration ecology; storage effect.*

Introduction

A fundamental goal of community ecology is to understand the processes that influence species distributions, how they operate, and how deterministic they are. Many different mechanisms have been proposed, with a special focus during the last decade on the relative roles of local and regional processes (Leibold et al. 2004). The species-sorting paradigm of metacommunity ecology, in particular, focuses on the local interaction between differences in patch quality (environmental heterogeneity) and dispersal into the patch. When dispersal is not limiting, environmental sorting of species according to their respective ecological traits is expected to be maximal; as a result, there is a perfect match between the occurrence of a species and the environment. As a consequence, species sorting with nonlimiting dispersal rates is generally viewed as a highly deterministic process (Cottenie and De Meester 2004). The general importance of species sorting is illustrated by a meta-analysis of 158 studies (Cottenie 2005), which showed that the majority of the analyzed ecological communities were affected primarily by species sorting. Deviations from expectations under species sorting are variously attributed to dispersal limitation, excessive dispersal (mass effects), colonization–extinction dynamics, or neutral processes (Leibold et al. 2004, Cottenie 2005). However, one other deterministic process that may interact with community assembly is the priority effect. Priority effects occur when a species attains higher relative abundances in a local community because it arrived first (Lockwood et al. 1997). Local residents exert a priority effect because they preempt niche space at the expense of later immigrants, even those that may be intrinsically better competitors (Begon et al. 2006, Louette and De Meester 2007).

Demonstration of priority effects has often focused on spatial occupancy at the individual level in sessile or territorial organisms, such as trees or coral reef fishes (Shulman et al. 1983, Hubbell and Foster 1986). However, priority effects can also be considered at the community level in a defined locality (sensu Leibold et al. 2004). Individuals that colonize empty habitat space and reproduce locally, fill with their progeny the

Manuscript received 6 September 2010; revised 31 March 2011; accepted 16 May 2011; final version received 15 June 2011. Corresponding Editor: K. L. Cottingham.
[5] E-mail: Joachim.mergeay@inbo.be

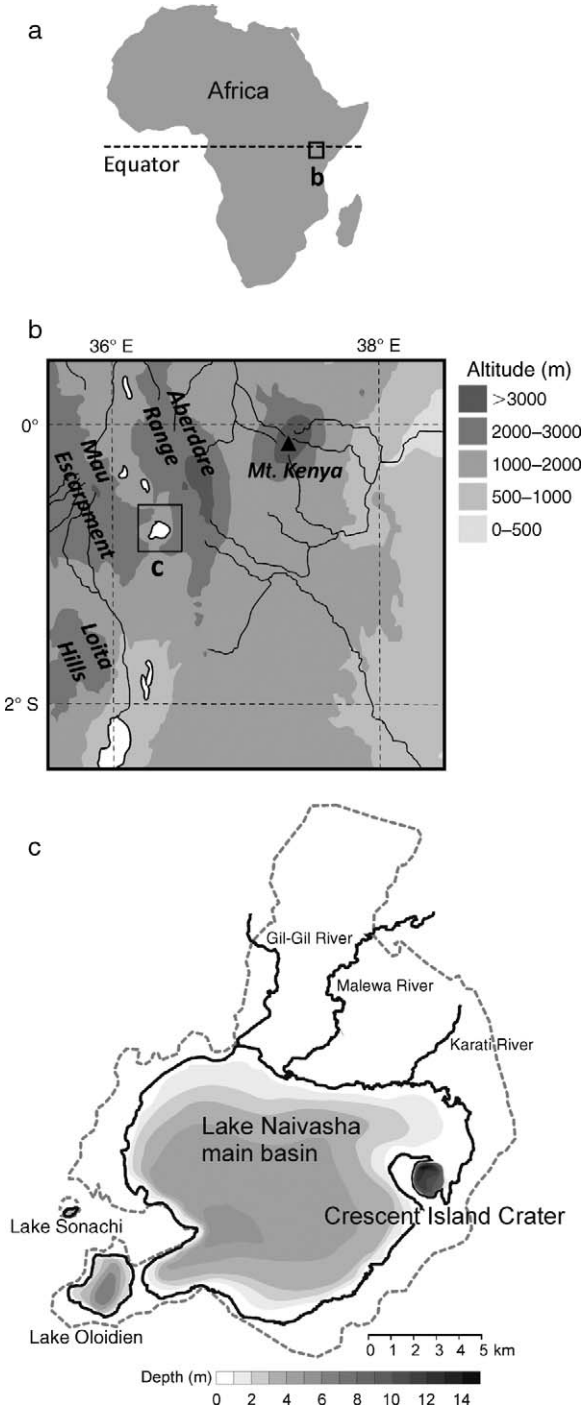

FIG. 1. The location of Lake Naivasha in Africa and the Eastern Rift Valley, showing its catchment and bathymetry. (a) Map of Africa showing the inset (labeled b) . (b) Expanded inset, with altitudinal map of the Eastern Rift Valley showing the locations of the Rift Valley lakes (in white) and the main rivers (black). Lake Naivasha, draining the Aberdare range, is enclosed within a box (c). (c) Detailed bathymetric map of Lake Naivasha and its satellite basins Sonachi, Oloidien, and Crescent Island Crater. The dashed line shows the water level during the 18th century highstand mega-lake conditions (a large, deep freshwater lake of 150–250 km^2), with a maximum lake depth of ~40 m. During lowstands (when the lake was reduced to a shallow, most often saline remnant pond) water was limited to Crescent Island Crater (~1 km^2).

available ecological niche space. As a result, later colonizers have reduced establishment success, because competition for resources (e.g., space, light and nutrients) increases among the individuals of the growing community. Once the habitat is at carrying capacity or has a stable population size, new arrivers are considered immigrants instead of founders.

The magnitude of a priority effect is expected to depend on (1) the number of founders, (2) the order, timing, and frequency of colonization attempts (creating propagule pressure) relative to the growth rate of the local population, (3) the difference in niche occupancy between and among founders and later immigrants, and (4) the occurrence of local genetic adaptation (Belyea and Lancaster 1999, De Meester et al. 2002, Louette and De Meester 2007, Urban and De Meester 2009). In itself, propagule pressure is strongly influenced by the relative density of each species across a region. In organisms with long-lived dormant propagule banks (seeds, resting eggs, statoblasts, and so forth), however, propagule pressure may also arise from within the system by the emergence of local dormant propagules produced during previous periods, representing dispersal and colonization in time. Due to the massive number of propagules involved (in zooplankton, annual production can easily reach 10^3–10^4 propagules/m^2 [Cáceres 1998]), dormant propagule banks can be more important sources of immigrants than regional communities (Mergeay et al. 2007).

Although studies on priority effects have a long history in ecology, both theoretical (e.g., Connell and Slatyer 1977, Law and Morton 1993, Gerla et al. 2009, Urban and De Meester 2009) and empirical (e.g., Shulman et al. 1983, Robinson and Dickerson 1987, Louette and De Meester 2007), few empirical studies have involved time series exceeding a few years. Consequently, very little is known on the long-term impact of priority effects. Sometimes, priority effects are little more than transient lags in the species sorting within communities that occur in response to relatively rapid environmental change. In addition, little is known on the interaction between priority effects and other deterministic processes such as species sorting (Kitching 1987, Louette and De Meester 2007).

Paleoecology offers unique opportunities to study these interactions empirically, by providing long, linked time series of both the target communities and various components of their living environment. In this study, we exploit the detailed paleoecological record of Lake Naivasha, a climate-sensitive tropical lake in Kenya (Fig. 1a, b), to study the degree to which priority effects contributed to the assembly and persistence of *Daphnia* (water flea) communities across repeated ecological crises associated with natural, climate-driven lake-level

fluctuations. Over the past 1800 years, Lake Naivasha fluctuated eight times between lowstands when the lake was reduced to a shallow, most often saline remnant pond inside a ~1 km^2 crater basin, and highstand "mega-lake" phases when it was a large and deep freshwater lake of 150–250 km^2 (Fig. 1c and Verschuren 2001). Transition periods with intermediate ecological conditions were relatively short lived, typically lasting less than a decade (Verschuren et al. 2004). As a result of these drastic and recurrent events of habitat turnover between lowstands and highstands, the process of community assembly following each ecological crisis can be reconstructed from the paleoecological archive. This replication in time, when combined with detailed reconstructions of the paleoenvironment, allows us to test specific hypotheses with regard to the relative role of species sorting and priority effects on decadal to centennial time scales.

Priority effects typically stem from differences among species or genotypes in the rate at which unoccupied niche space is colonized (Begon et al. 2006). In our study system, priority effects are expected to be strongest at the onset of a highstand, when resident populations that persisted in the small crater basin until the end of the lowstand colonized the rapidly expanding lake habitat and monopolized resources at the expense of later immigrants. In that case, highstand communities should be strongly influenced by the species composition of the lowstand community that existed just before the large new lake habitat became available for colonization. Conversely, lowstand communities are expected to be less influenced by priority effects, and relatively more by species sorting, when the habitat available to them was contracting. We specifically tested for such priority effects, and also estimated the role of environmental variation over time in determining community structure (species sorting). To distinguish persistent priority effects from temporal lags in the response of communities, we also tested to what extent priority effects persisted in time.

Methods

Study system

Lake Naivasha (LN) is today a large but shallow freshwater lake (~135 km^2, maximum depth 5 m in 2001) situated in Kenya's Central Rift Valley (Fig. 1). Crescent Island Crater (CIC) is a small (1.9 km^2) and deep (15 m in 2001) crater basin submerged in the northeast sector of LN (Fig. 1c). CIC is the only part of the lake that never desiccated completely in the past 1800 years, thereby preserving an intact sediment record of the lake's environmental history. In contrast, the main lake basin desiccated completely during lowstands, as indicated by the paleoenvironmental evidence (Verschuren 2001) and oral traditions of Maasai tribesmen reporting on episodes of 19th century drought (Hemsing 1987).

We tracked the process of community assembly and change in the *Daphnia* inhabiting LN throughout its 1800-year history of eight lowstand and eight highstand phases. *Daphnia* species are pelagic filter feeders of phytoplankton and other microorganisms, and occupy a central position in most freshwater food webs (Carpenter and Kitchell 1993). Their dormant egg capsules (ephippia) are well preserved in sediment accumulating on the bottom of lakes, providing a detailed historical archive of community change over time. These dormant eggs can remain viable up to at least 100 years (Cáceres 1998), creating a storage effect that provides an extensive buffer against fluctuations in the quality of their local environment (Chesson 1983, Cáceres 1997). Although *Daphnia* species clearly vary in their ecological preferences, there is marked overlap in the fundamental niche of many species, especially with regard to feeding ecology, tolerance for elevated salinity, and antipredator responses (Brooks 1965, Lampert 1987, Benzie 2005, Colbourne et al. 2006).

Reconstruction of Daphnia *community change through time*

In July 2001 two overlapping sediment cores (NC01-1S: 0–152 cm depth; NC01-D: 88–764 cm depth) were retrieved from the deepest point of CIC to construct a continuous 1800-year record of the population history of local *Daphnia* species (Fig. 2a–g), from the stratigraphy of their fossil ephippia. An earlier study on fossil *Daphnia* ephippia in four shorter sediment cores from different locations in CIC showed highly concordant patterns of community change through time over the last ~200 years (Mergeay et al. 2004). Moreover, the resulting reconstruction of 20th-century *Daphnia* population dynamics was highly congruent with patterns of zooplankton abundance in historical surveys (Lowndes 1936, Mavuti and Litterick 1981, Harper 1987, Uku and Mavuti 1994), indicating that fossil ephippia abundances in our sediment cores are a trustworthy representation of community history. Sediment chronology was established by detailed lithostratigraphic correlation to cores from the same location that had been dated directly by ^{210}Pb and ^{14}C (Verschuren 2001, Mergeay et al. 2004). The composite sediment core was sliced in consecutive 2-cm intervals, resulting in 383 sediment slices of ~35 cm^3. The temporal resolution of our analysis thus averaged 4.4 years per sampled interval, varying between about two years in the most recent, uncompacted muds and 25 years during the most extreme lowstand, when the rate of sediment accumulation was most reduced (Verschuren 2001). The sediment slices were washed and sieved through 150-μm mesh to retain *Daphnia* ephippia and the fossil remains of fish. Abundances of *Daphnia* and fish fossils were expressed as the number of remains per gram of dry sediment per year (i.e., their production flux) to correct for both changes in sedimentation rate and sediment compaction with depth. The *Daphnia* were identified to species morphologically and/or genetically (Mergeay et al. 2005, 2006*b*). Variation in temporal resolution between sampled intervals was not correlated

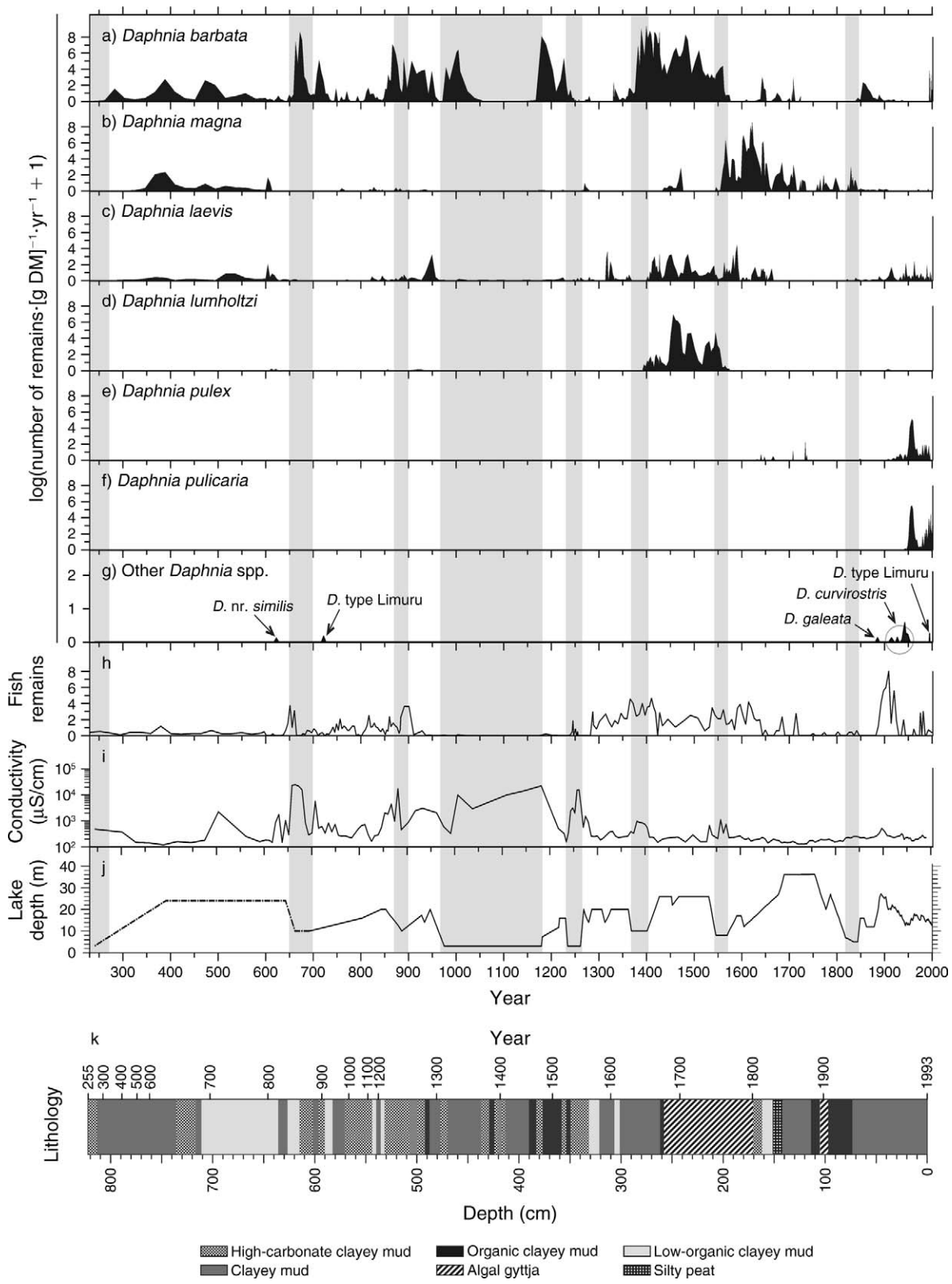

FIG. 2. (a–g) Abundance changes over time in the *Daphnia* species inhabiting Lake Naivasha in the past 1800 years (DM represents dry mass) in relation to (h) reconstructed changes in fish abundance, (i) lake water salinity (represented by the conductivity of dissolved salts), and (j) lake depth, as well as (k) the stratigraphic variation in sediment composition that allowed

with *Daphnia* species richness (Pearson product-moment correlation, $r = 0.053$, $P = 0.296$) or Shannon diversity ($r = 0.071$, $P = 0.163$). The fish fossils primarily consisted of scales and vertebrae of Cichlidae and Poeciliidae, of which the local representatives are known to be zooplanktivorous (Mavuti 1990).

Paleoenvironmental reconstruction

Abundance changes in fossil *Daphnia* ephippia were linked to the environmental history of Lake Naivasha through reconstruction of three ecologically relevant habitat variables (Fig. 2h–j). First, we inferred lake depth from lithological characteristics reflecting the lake-bottom environment at the time of sediment deposition (see Verschuren 2001). In this fluctuating tropical water body, lake depth is a proxy for lake size and water-column mixing regime, which in turn determine oxygen distribution, nutrient dynamics, and primary production (Verschuren et al. 2000*b*). Second, we inferred the past salinity of lake water (commonly measured as conductivity, i.e., the electrical conductance of dissolved salts) from the composition of fossil diatom assemblages (Verschuren et al. 2000*a*; supplemented by unpublished data of K. R. Laird and B. F. Cumming, Queen's University, Kingston, Ontario, Canada). Third, we reconstructed relative fish density using the log ($x + 1$) abundance of fossil fish remains. This may not represent a quantitative estimate of actual fish predation, but likely provides an indication of order-of magnitude changes in fish predation pressure. Lake depth and salinity together capture key environmental conditions that ultimately determine the physiological and ecological suitability of the local open-water (pelagic) habitat for separate *Daphnia* species (Benzie 2005). In addition, zooplanktivorous fish are important predators of *Daphnia* and often incite strong community changes (Kerfoot and Sih 1987). The combined lake depth and water conductivity data (Fig. 2i–j) define two main habitat types alternating through time. Highstand phases of relative hydrological stability were characterized by a large freshwater pelagic habitat across the main basin of LN and a full complement of nearshore and offshore bottom habitats. Lowstand phases were characterized by a lack of pelagic habitat, substantial seasonal hydrological variability, and often a critical episode of salinity increase above 1000 or even 3000 μS/cm, which is beyond what many freshwater macrophytes and aquatic invertebrates can tolerate (Hammer 1986, Frey 1993). We demarcated lowstand phases (gray bands in Fig. 2) by the stratigraphic occurrence of high-carbonate mud or silty peat (Fig. 2k), which is most often associated with rapid change in diatom-inferred salinity (Fig. 2i).

Priority effects

During a prominent lake-level rise, LN expands from a remnant pond inside CIC to a large freshwater lake within just a few years (Verschuren et al. 2004). Priority effects may arise when local populations that persisted in CIC until the end of the lowstand colonize this expanding lake habitat. Consider that CIC at its smallest was a pond of 1 km^2. With average local densities typically between 1 and 10 *Daphnia*/L (Mavuti and Litterick 1981) and an average depth of 5 m, this represents a local community of at least five billion individuals that can colonize the main basin following a lake-level rise. Resident populations thus have a massive numerical advantage compared to immigrants.

To test for the role of priority effects and the time scale of their persistence, we first performed a principal component analysis (PCA) in CANOCO 4.5 (Ter Braak and Smilauer 2002) on the *Daphnia* community data set. We performed Hellinger transformation of species abundance data to standardize behavior of data across ordinations (Legendre and Gallagher 2001). We used a Horn's parallel analysis (Glorfeld 1995) to decide how many PCA axes should be retained for further interpretation. We then used regression analysis (StatSoft 2007) to establish to what extent the community value along each of the retained PCA axes of the last lowstand interval (Low_{end}) was able to predict the respective PCA score of the highstand community 10, 25, and 50 years later, as well as the reciprocal analysis of the influence of "end-of-highstand" communities ($High_{end}$) on subsequent lowstand communities. Due to issues of temporal resolution, we approximated these intervals to the closest possible value allowed by the data. For lowstands lasting <50 years, we used the last sampled interval representing that lowstand. In two cases this was the interval for the time lag of 25 years. If priority effects are only transient, i.e., representing a lagged species-sorting response to environmental change, we expected a decay over time in the predictive power of $High_{end}$ or Low_{end} community values.

←
delimitation of successive low- and highstand phases. Light gray bars are lake phases when aquatic habitat was likely restricted to a shallow remnant pool in Crescent Island Crater. (k) Core lithostratigraphy is plotted against a linear depth scale (lower axis); indication of sediment age at depth (upper axis) highlights variation in sediment compaction and accumulation rate down-core. *Daphnia pulex* refers to European *D. pulex* Leydig, whereas *D. pulicaria* represents a single clone of hybrid origin of the North American *D. pulicaria* complex (Mergeay et al. 2006*b*), which is often incorrectly named *D. pulex* (Mergeay et al. 2008). *D. laevis* here refers to a cryptic East African endemic lineage of the *D. laevis* Birge species complex. *D.* nr. *similis* is probably a cryptic species of the *D. similis* Claus complex, and *D.* type Limuru is an East African endemic lineage of the *D. dolichocephala* G.O. Sars complex. All other taxa are genetically similar (<5% sequence divergence at the barcoding gene *Cox1*) to counterparts from their respective type localities or regions (J. Mergeay, *unpublished data*). Years are CE (Common Era).

TABLE 1. Results of regression analyses (regression coefficients and significance values) between principal components analysis (PCA) scores of *Daphnia* species data from Lake Naivasha, Kenya, Africa.

Predictor	Response	PCA1 r^2	P	PCA2 r^2	P
Low_{end}	$High_{10}$	0.927	0.000	0.892	0.000
Low_{end}	$High_{25}$	0.626	0.019	0.800	0.003
Low_{end}	$High_{50}$	0.625	0.046	0.769	0.004
$High_{end}$	Low_{10}	0.804	0.006	0.516	0.069
$High_{end}$	Low_{25}	0.068	0.573	0.340	0.169
$High_{end}$	Low_{50}	0.003	0.909	0.327	0.180

Notes: The scores are determined along axes PCA1 and PCA2, with either end-of-lowstand intervals (Low_{end}) or end-of-highstand intervals ($High_{end}$) as predictors for highstand/lowstand intervals 10, 25, and 50 years after the transition. These results represent the degree to which highstand communities are influenced by the preceding Low_{end} communities, and to which lowstand communities are influenced by the preceding $High_{end}$ communities, and how this changes over time. Highstand represents a mega-lake (large, deep freshwater lake ~150–250 km^2); during lowstands, the lake was reduced to a shallow, usually saline pond ~1 km^2.

We then tested whether Low_{end} and "highstand q years later" ($High_q$) communities were more similar to each other than $High_{end}$ and "lowstand q years later" (Low_q) communities, with the value of q set to 10, 25, and 50 years. This allows us to test whether priority effects are indeed significantly stronger from lowstands to highstands (expanding lake habitat) than from highstands to lowstands (contracting lake habitat). For this we used Bray-Curtis similarity scores of $\log(x + 1)$ transformed species data (Primer 5) in a Student's t test. Data were log-transformed to reduce the impact of samples with extremely high *Daphnia* abundances.

Explanatory power of environment vs. priority effects

We then tested to what extent community structure could be explained either by priority effects (P) or by environmental variation and species sorting (E). For this we used redundancy analysis (RDA) on Hellinger-transformed species data in CANOCO 4.5 (Ter Braak and Smilauer 2002) and variance partitioning (Borcard et al. 1992). We thus estimated the total explained variance, the unique contributions of environmental variation ($E|P$) and priority effects ($P|E$), and the intersection between them ($P \cap E$). Negative values of the intersection indicate that P and E together explain the species data better than the sum of their individual effects (Legendre and Legendre 1998). To assess the role of priority effects during particular highstands and lowstands, we used as explanatory variables the PCA axis 1 and axis 2 scores of *Daphnia* species data for the last interval of the previous lowstand or highstand, respectively. The significance of each full model (including all variables) was established with 499 Monte Carlo permutations. Variance partitioning was performed separately on lowstand and highstand intervals, to establish whether lowstand and highstand communities were differently affected by environmental variation and priority effects.

RESULTS

In total, we found 10 species of *Daphnia* in the 1800-year record of Lake Naivasha (Fig. 2a–g), among which 6 were frequently present (>10% of the 383 observations) and abundant (at least 1% of the overall fossil inventory). This species diversity amounts to all *Daphnia* taxa known from East Africa, apart from the *Daphnia obtusa* complex, which in Africa is restricted to high-mountain environments (Mergeay et al. 2005).

PCA axis 1 (PCA1) explained 40.9% of the variance in species data, compared to 27.6% for PCA2, 16.4% for PCA3, and 15.1% for PCA4. A Horn's parallel analysis indicated that eigenvalues for PCA3 and PCA4 were too low to be retained for further analyses. Regression analyses using the values of PCA1 and PCA2 to explain the corresponding PCA values 10, 25, and 50 years after a lowstand–highstand transition showed that Low_{end} communities were significant predictors for ensuing highstand communities ($High_{10}$, $High_{25}$, and $High_{50}$), with r^2 values between 0.625 and 0.927 (Table 1). Conversely, $High_{end}$ PCA values were only strong and significant predictors of lowstand PCA values 10 years later (Low_{10}), but not of those 25 and 50 years later (Low_{25} and Low_{50}; Table 1).

Bray-Curtis similarity scores between Low_{end} and $High_{10}$, $High_{25}$, and $High_{50}$ communities were higher than those between $High_{end}$ and Low_{10}, Low_{25}, and Low_{50} communities (Fig. 3). A t test showed that these differences were significant for the last two comparisons (t test for independent samples, df = 13; 10 years, $P = 0.211$; 25 years, $P = 0.010$; 50 years, $P = 0.013$, respectively). This shows that, in the long run, priority effects were significantly stronger when the lake expanded and new habitat became available, than when it contracted.

The full RDA model considered three environmental explanatory variables (lake depth, salinity, log[fish remains abundance]) and two explanatory variables representing priority effects (Low_{end} PCA1 and PCA2 scores for highstand periods, and $High_{end}$ PCA1 and PCA2 scores for lowstand periods). This full RDA explained 43.7% of the species variance during highstands vs. 29.2% during lowstands. Partitioning of the variance among environmental and priority-effect variables showed that purely environmental variation

($E|P$) significantly explained 8.3% ($P = 0.002$) of species variance during highstands, and 9.3% ($P = 0.002$) during lowstands. However, priority effects alone ($P|E$) explained 39.5% of species variance during highstands ($P = 0.002$) vs. only 15.5% during lowstands ($P = 0.002$). The intersection between priority effects and environmental variation ($P \cap E$) was small but positive (4.4%) for lowstands and negative for highstands (−4.1%).

Discussion

We reconstructed the repeated reassembly of an ecological community experiencing dramatic environmental change over a time span of 1800 years. The variance in community composition explained by changes in three important habitat conditions (lake depth, salinity, fish abundance) was relatively modest, and similar for lowstand and highstand periods. The priority effect, however, was much stronger during highstands than during lowstands, and explained, especially for the highstands, a much higher portion of variance in community composition than environmental change. Moreover, priority effects at the transition from highstands to lowstands were merely transient, whereas they persisted at least for 50 years from lowstands to highstands (Table 1, Fig. 3).

The observed asymmetry in the dependence of lowstand and highstand communities on priority effects confirms that priority effects are strongest when new, unoccupied habitat is colonized (Begon et al. 2006). We propose that each time the remnant pond inside the crater expanded to a large lake, the resident local community could colonize this vast, empty habitat and preempt resources at the expense of less abundant regional immigrants (Mergeay et al. 2007). Although community composition during highstands was significantly influenced by environmental variation ($E|P$) = 8.3%), it was much more influenced by the specific history of community assembly during the preceding lowstand ($P|E$) = 39.5%), and thus by priority effects.

The eventual outcome of the interplay between species sorting and priority effects operating in our study system is that priority effects interfere with species sorting when local residents colonize and saturate an empty habitat before other species arrive from elsewhere. Persistence of these priority effects results in an apparently weak response of species to major environmental variation. The three environmental gradients we reconstructed are most certainly an incomplete representation of the *Daphnia* habitat. They are nevertheless key variables in the environmental regulation of African freshwater zooplankton, and the magnitude of reconstructed local variation in at least two of them (lake depth/size and salinity) covers the full gradient of habitat conditions occupied by African *Daphnia* species (Frey 1993, Benzie 2005, Mergeay et al. 2006*a*). Priority effects were still apparent 50 years after the environmental turnover, which represents >500 generations in *Daphnia*, including one sexual generation per year. Therefore, our results underscore the importance of past (historical) habitat and community dynamics on community composition on relatively long time scales.

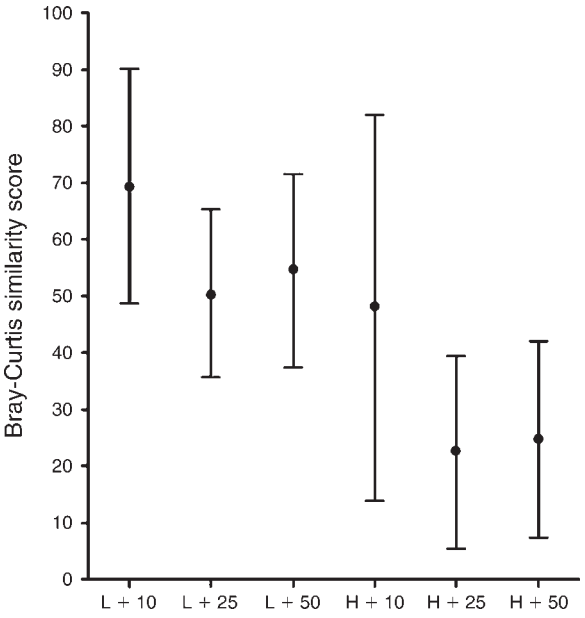

Fig. 3. Bray-Curtis similarity scores (mean and 95% confidence intervals) between Low_{end} (end of the lowstand interval) and highstand communities 10 years later (L + 10), 25 years later (L + 25), Low_{end} and 50 years later (L + 50), and between $High_{end}$ (end of the highstand interval) and lowstand communities 10 years later (H + 10), 25 years later (H + 25), and 50 years later (H + 50).

Interaction between priority effects and the storage effect

We showed that locally established communities can exert a persistent priority effect over immigrants, which in *Daphnia* disperse both in space (via wind, waterfowl, and other causes) and in time (via long-viable propagules in the local dormant egg bank). At first glance, our results seem to indicate that this priority effect acts against the storage effect (Chesson 1983, Cáceres 1997). The storage effect is the positive average growth of populations with strong temporal variation in recruitment success, achieved through overlapping generations (Chesson 1983), such as dormant propagules (seeds, dormant eggs, statoblasts, and others). In temporally variable environments, the storage effect allows dynamic coexistence of species that cannot stably coexist (Chesson 1986). The strong priority effect we observed suggests that during a lowstand to highstand transition, recruitment from the vast dormant egg bank of the main LN lake basin was numerically modest compared to the influx of animals from expanding resident CIC populations. This may be related to the fact that the lowstands lasted for several decades at least, and sometimes much longer (25–210 years; Fig. 2). Although dormant eggs can remain viable for decades (Cáceres 1998), the probability that they may be exposed to favorable

hatching conditions declines with time. In a paleogenetic study on *Daphnia barbata* from Lake Naivasha, Mergeay et al. (2007) showed that successful recolonization after ~50 years of absence happened through local recruitment from the dormant egg bank and not through immigration from elsewhere, but that nevertheless the number of hatchlings establishing this new population was very low. So whereas recruitment from the dormant egg bank must certainly have been possible after most lowstands studied here, the resident CIC community expanding into the main basin of LN typically had a very strong numerical advantage. On the other hand, the priority effect exerted by an expanding resident population may be strongly enhanced by the storage effect that is created by their own production of a new, large buffer of dormant propagules. We therefore propose that the numerical advantage of the expanding resident community during the initial phase of colonization is consolidated by the dormant propagule bank they produce, and this may have extended the impact of their priority effect in time, as observed in our data.

Local temporal vs. regional spatial priority effects

In a metacommunity context, the historical or temporal component of community variation can also be transposed to a regional component of spatial community variation, since the probability of a certain species exerting a priority effect in a new habitat is a function of different parameters. First, it depends on the relative frequency of the focal species in the regional species pool, and second, on differences in dispersal ability among species. Combined, they determine the probability that a focal species will colonize the habitat first. Third, it is affected by the overall degree of dispersal limitation of the community, determining the scope for local population growth of the first colonist before other species arrive in the habitat. Therefore, priority effects may cause strong spatial autocorrelation in the distribution of species among communities, and cause spatial patterns in the regional distribution of species that are typically interpreted as the outcome of mass effects (Cottenie 2005). The mechanisms involved in priority effects and mass effects, however, are completely different, as mass effects rely on strong immigration to compensate for negative local population growth (Leibold et al. 2004).

Perspective

Our study emphasizes the importance of priority effects in community assembly, and the need to integrate historical components of community and environmental variation in order to understand the processes determining the present-day composition of biological communities (Ricklefs 1987, Willis and Birks 2006). Studying these temporal processes in metacommunity ecology on sufficiently long time scales, however, remains a major challenge. We suggest that combining paleoecological and metacommunity approaches may be a productive method to engage in a truly comprehensive analysis of the processes regulating ecological communities. In an applied perspective, priority effects may strongly impact the response of communities to strong environmental change and thus influence community assembly in novel or heavily disturbed habitats. Conversely, priority effects could be exploited in ecological restoration projects, by selectively inducing a long-lasting priority effect of target species to buffer against successful establishment of unwanted immigrant (exotic) species. More research is needed, however, on how such manipulation of priority effects can successfully be achieved in a restoration ecology context.

Acknowledgments

Fieldwork was done with permission of the Permanent Secretary of the Ministry of Education, Science and Technology of Kenya under research permit 13/001/11C to D. Verschuren. Research was funded by the K. U. Leuven Research Fund (projects OT/04/23, GOA/2008/06 and PF/2010/07) and the Research Foundation–Flanders (project G0086.00). We thank K. Mavuti, W. Shivoga, S. Higgins, the Lake Naivasha Riparian Association, and the Lake Naivasha Yacht Club for logistic support, B. F. Cumming and K. R. Laird for sharing unpublished data, and S. Declerck, J. Kolasa, F. Van de Meutter, J. Vanoverbeke, B. Vanschoenwinkel, K. Cottingham, and several anonymous reviewers for useful comments. J. Mergeay was initially supported by fellowships from IWT-Vlaanderen, the K. U. Leuven Research Fund, and the Research Foundation–Flanders. H. Eggermont was supported by the Research Foundation–Flanders and by the Research Foundation and the Federal Science Policy of Belgium (Action 1). D. Verschuren acknowledges support by the Federal Science Policy of Belgium (project SD/BD/03 'CLANIMAE') during the writing of this paper.

Literature Cited

Begon, M., C. R. Townsend, and J. L. Harper. 2006. Ecology: from individuals to ecosystems. Fourth edition. Blackwell Science, Oxford, UK.

Belyea, L. R., and J. Lancaster. 1999. Assembly rules within a contingent ecology. Oikos 86:402–416.

Benzie, J. A. H. 2005. The genus *Daphnia* (including *Daphniopsis*) (Anomopoda: Daphniidae). Backhuys, Leiden, The Netherlands.

Borcard, D., P. Legendre, and P. Drapeau. 1992. Partialling out the spatial component of ecological variation. Ecology 73:1045–1055.

Brooks, J. L. 1965. Predation and relative helmet size in cyclomorphic *Daphnia*. Proceedings of the National Academy of Sciences USA 53:119–126.

Cáceres, C. E. 1997. Temporal variation, dormancy, and coexistence: a field test of the storage effect. Proceedings of the National Academy of Sciences USA 94:9171–9175.

Cáceres, C. E. 1998. Interspecific variation in the abundance, production, and emergence of *Daphnia* diapausing eggs. Ecology 79:1699–1710.

Carpenter, S. R., and J. F. Kitchell. 1993. The trophic cascade in lakes. Cambridge University Press, Cambridge, UK.

Chesson, P. L. 1983. Coexistence of competitors in a stochastic environment: the storage effect. Pages 188–198 *in* H. I. Friedman and C. Strobeck, editors. Population biology. Springer, New York, New York, USA.

Chesson, P. L. 1986. Environmental variation and the coexistence of species. Pages 240–256 *in* J. Diamond and T.

Case, editors. Community ecology. Harper and Row, New York, New York, USA.
Colbourne, J. K., C. C. Wilson, and P. D. N. Hebert. 2006. The systematics of Australian *Daphnia* and *Daphniopsis* (Crustacea: Cladocera): a shared phylogenetic history transformed by habitat-specific rates of evolution. Biological Journal of the Linnean Society 89:469–488.
Connell, J. H., and R. O. Slatyer. 1977. Mechanisms of succession in natural communities and their role in community stability and organization. American Naturalist 111:1119–1144.
Cottenie, K. 2005. Integrating environmental and spatial processes in ecological community dynamics. Ecology Letters 8:1175–1182.
Cottenie, K., and L. De Meester. 2004. Metacommunity structure: synergy of biotic interactions as selective agents and dispersal as fuel. Ecology 85:114–119.
De Meester, L., A. Gomez, B. Okamura, and K. Schwenk. 2002. The monopolization hypothesis and the dispersal-gene flow paradox in aquatic organisms. Acta Oecologica-International Journal of Ecology 23:121–135.
Frey, D. G. 1993. The penetration of cladocerans into saline waters. Hydrobiologia 267:233–248.
Gerla, D. J., M. Vos, B. W. Kooi, and W. M. Mooij. 2009. Effects of resources and predation on the predictability of community composition. Oikos 118:1044–1052.
Glorfeld, L. W. 1995. An improvement on Horns parallel analysis methodology for selecting the correct number of factors to retain. Educational and Psychological Measurement 55:377–393.
Hammer, U. T. 1986. Saline lake ecosystems of the world. Springer, London, UK.
Harper, D. M. 1987. The ecology and distribution of zooplankton in lakes Naivasha and Oloidien. Studies on the Lake Naivasha ecosystem 1982–1984. Report. University of Leicester, Leicester, UK.
Hemsing, J. 1987. Naivasha and the Lake Hotel. Sealpoint, Nairobi, Kenya.
Hubbell, S. P., and R. B. Foster. 1986. Biology, chance and history and the structure of tropical rain forest tree communities. Pages 314–329 *in* J. M. Diamond and T. J. Case, editors. Community ecology. Harper and Row, New York, New York, USA.
Kerfoot, W. C., and A. Sih. 1987. Predation, direct and indirect impacts on aquatic communities. University Press of New England, Hanover, New Hampshire, USA.
Kitching, R. L. 1987. Spatial and temporal variation in water-filled treeholes. Oikos 48:280–288.
Lampert, W. 1987. Feeding and nutrition in *Daphnia*. Pages 143–192 *in* R. H. Peters and R. De Bernardi, editors. Daphnia. Instituto Italiano di Idrobiologia, Verbania-Pallanza, Italy.
Law, R., and R. D. Morton. 1993. Alternative permanent states of ecological communities. Ecology 74:1347–1361.
Legendre, P., and E. Gallagher. 2001. Ecologically meaningful transformations for ordination of species data. Oecologia 129:271–280.
Legendre, P., and L. Legendre. 1998. Numerical ecology. Second edition. Elsevier Science B.V, Amsterdam, The Netherlands.
Leibold, M. A., M. Holyoak, N. Mouquet, P. Amarasekare, J. M. Chase, M. F. Hoopes, R. D. Holt, J. B. Shurin, R. Law, D. Tilman, M. Loreau, and A. Gonzalez. 2004. The metacommunity concept: a framework for multi-scale community ecology. Ecology Letters 7:601–613.
Lockwood, J. L., R. D. Powell, M. P. Nott, and S. L. Pimm. 1997. Assembling ecological communities in time and space. Oikos 80:549–553.
Louette, G., and L. De Meester. 2007. Predation and priority effects in experimental zooplankton communities. Oikos 116:419–426.
Lowndes, A. G. 1936. Scientific results of the Cambridge Expedition to the East African Lakes 1930-1. No. 16. The smaller Crustacea. Linnean Journal of Zoology 40:1–33.
Mavuti, K. M. 1990. Ecology and role of zooplankton in the fishery of lake Naivasha. Hydrobiologia 208:131–140.
Mavuti, K. M., and M. R. Litterick. 1981. Species composition and distribution of zooplankton in a tropical lake, Lake Naivasha, Kenya. Archiv für Hydrobiologie 93:52–58.
Mergeay, J., X. Aguilera, S. Declerck, A. Petrusek, T. Huyse, and L. De Meester. 2008. The genetic legacy of polyploid Bolivian *Daphnia*: the tropical Andes as a source for the North and South American *D. pulicaria* complex. Molecular Ecology 17:1789–1800.
Mergeay, J., S. Declerck, D. Verschuren, and L. De Meester. 2006*a*. Daphnia community analysis in shallow Kenyan lakes and ponds using sediment archives. Freshwater Biology 51:399–411.
Mergeay, J., J. Vanoverbeke, D. Verschuren, and L. De Meester. 2007. Extinction, recolonisation and dispersal through time in a planktonic crustacean. Ecology 88:3032–3043.
Mergeay, J., D. Verschuren, and L. De Meester. 2005. Daphnia species diversity in Kenya, and a key to the identification of their ephippia. Hydrobiologia 542:261–274.
Mergeay, J., D. Verschuren, and L. De Meester. 2006*b*. Invasion of an asexual American water flea clone throughout Africa, and rapid displacement of a native sibling species. Proceedings of the Royal Society B 273:2839–2844.
Mergeay, J., D. Verschuren, L. Van Kerckhoven, and L. De Meester. 2004. Two hundred years of a diverse Daphnia community in Lake Naivasha (Kenya): effects of natural and human-induced environmental changes. Freshwater Biology 49:998–1013.
Ricklefs, R. E. 1987. Community diversity–relative roles of local and regional processes. Science 235:167–171.
Robinson, J. F., and J. E. Dickerson. 1987. Does invasion sequence affect community structure? Ecology 68:587–595.
Shulman, M. J., J. C. Ogden, J. P. Ebersole, W. N. McFarland, S. L. Miller, and N. G. Wolf. 1983. Priority effects in the recruitment of juvenile coral fishes. Ecology 64:1508–1513.
Statsoft. 2007. Statistica v.8. Statsoft, Tulsa, Oklahoma, USA.
Ter Braak, C. J. F., and L. Smilauer. 2002. CANOCO 4.5. Biometris–Plant Research International, Wageningen, The Netherlands.
Uku, J. N., and K. M. Mavuti. 1994. Comparative limnology, species diversity and biomass relationship of zooplankton and phytoplankton in 5 freshwater lakes in Kenya. Hydrobiologia 272:251–258.
Urban, M. C., and L. De Meester. 2009. Community monopolization: local adaptation enhances priority effects in an evolving metacommunity. Proceedings of the Royal Society B 276:4129–4138.
Verschuren, D. 2001. Reconstructing fluctuations of a shallow East African lake during the past 1800 yrs from sediment stratigraphy in a submerged crater basin. Journal of Paleolimnology 25:297–311.
Verschuren, D., B. Cumming, and K. R. Laird. 2004. Quantitative reconstruction of past salinity variation in African lakes: assessment of chironomid-based inference models (Insecta: Diptera) in space and time. Canadian Journal of Fisheries and Aquatic Sciences 61:986–998.
Verschuren, D., K. R. Laird, and B. F. Cumming. 2000*a*. Rainfall and drought in equatorial east Africa during the past 1,100 years. Nature 403:410–414.
Verschuren, D., J. Tibby, K. Sabbe, and N. Roberts. 2000*b*. Effects of depth, salinity, and substrate on the benthic invertebrate community of a fluctuating tropical lake. Ecology 81:164–182.
Willis, K. J., and H. J. B. Birks. 2006. What is natural? The need for a long-term perspective in biodiversity conservation. Science 314:1261–1265.

Hydrobiologia
DOI 10.1007/s10750-011-0829-7

CLADOCERA AS INDICATORS

Distribution and faunal richness of Cladocera in western Uganda crater lakes

Bob Rumes · Hilde Eggermont · Dirk Verschuren

Received: 29 April 2011 / Accepted: 15 July 2011

Abstract In this study, we analyse the distribution and species richness of epibenthic and planktonic Cladocera (Crustacea: Branchiopoda) in 62 Uganda crater lakes, spread across the climatic gradient between the sub-humid shoulder and semi-arid floor of the East African Rift Valley. Together, these lakes cover large environmental gradients in salinity, trophic conditions and depth. In total, 36 species of Cladocera were encountered in the freshwater lakes (<1,500 μS/cm), whereas only a single species was found in the true saline lakes (>10,000 μS/cm). Cladoceran species richness in individual lakes was found to be determined primarily by the presence of a well-developed littoral belt of submerged and emergent aquatic macrophytes, pH and salinity. The highest species richness occurred in fresh but eutrophic shallow waters, with relatively low pH (6.5–7) and dense aquatic macrophyte growth. As identified by multivariate statistical analysis, the distribution of Cladocera species among the Uganda lakes was most strongly determined by nutrient availability (measured as total phosphorus), the presence and diversity of aquatic macrophyte habitat, pH, mean annual temperature and the fraction of the crater catchment that is currently under agriculture. Since Cladocera play an important role in aquatic food webs, and as such contribute to the ecological integrity of aquatic ecosystems, an increased understanding of the environmental controls underlying their distribution provides valuable information on aquatic ecosystem functioning needed for management and conservation. The significant turnover of cladoceran species composition along the sampled environmental gradients demonstrates their potential as biological indicators for water quality and ecosystem health in East African lakes. Our results suggest that changes in land use are the greatest threat to natural ecosystem functioning in these African lakes, and particularly so in the shallower lakes.

Keywords Aquatic macrophytes · Crustacea · East African Rift Valley · Environmental control · Habitat · Species distribution

Electronic supplementary material The online version of this article (doi:10.1007/s10750-011-0829-7) contains supplementary material, which is available to authorized users.

Guest editors: H. Eggermont & K. Martens / Cladocera as indicators of environmental change

B. Rumes (✉) · H. Eggermont · D. Verschuren
Limnology Unit, Department of Biology, Ghent University, K. L. Ledeganckstraat 35, 9000 Ghent, Belgium
e-mail: bob.rumes@ugent.be

H. Eggermont
e-mail: hilde.eggermont@naturalsciences.be

H. Eggermont
Freshwater Biology, Royal Belgian Institute for Natural Sciences, Vautierstraat 29, 1000 Brussels, Belgium

Published online: 02 August 2011

Introduction

The Lake Edward–George branch of the East African Rift Valley and adjacent uplands in western Uganda contain about 80 volcanic crater lakes (Melack, 1978) displaying strong variations in morphometry, mixing regime, salinity and productivity. Dramatic population increase in recent decades (UNEP, 2006) creates a growing need for arable land (Wakabi, 2006), forcing people to exploit more marginal land (especially on steep slopes) for crop cultivation, which in turn has resulted in increased soil erosion (Republic of Uganda, 2002). When these steep slopes occur within the catchment of a lake, increased soil erosion and nutrient export to the lake can enhance both lake turbidity and productivity. Studies investigating human impact on the lakes of western Uganda are still scarce. Crisman et al. (2001) showed how clearance of forest for agriculture and firewood in the drainage basin of Lake Saka, and concurrent introduction of Nile perch (*Lates niloticus*) to this shallow lake, dramatically increased its trophic status. Yet, in the absence of historical data, the individual impacts of these disturbances on the aquatic ecosystem are often difficult to assess (Smol, 2002). For example, Green (1976) was uncertain about whether the disappearance of several pelagic Cladocera species from lakes Mutanda and Bunyoni was due to eutrophication, pollution or grazing by introduced zooplanktivorous fish. One way to circumvent this limited knowledge of pre-impact conditions is to compare impacted lakes with lakes that are believed to be unaffected. For example, Bwanika et al. (2004) used lakes within Queen Elizabeth National Park as reference to determine the impact of fisheries on nearby, unprotected lakes.

Cladocera (water fleas *sensu lato*) have proven to be effective biological indicators for a wide range of environmental variables (Lotter et al., 1997; Tremel et al., 2000; Chen et al., 2010). In addition, living cladoceran communities and their fossil remains preserved in lake sediments reflect their aquatic habitat in similar ways (Kattel et al., 2006; Davidson et al., 2007). As a consequence, they are widely used as biological indicators, both for modern ecosystem monitoring and for reconstruction of past environments (Bigler et al., 2006; DeSellas et al., 2008). Previous studies on Cladocera community composition in Ugandan lakes have focused on the larger Rift lakes Victoria, Albert, Edward and George (Green, 1971; Burgis et al., 1973; Lehmann, 2002; Mutune et al., 2006), swamps (Thomas, 1961) and the zooplankton of some smaller lakes (Green, 1976, 1995; Kizito et al., 1993). In this study, we analysed the distribution and species richness of both pelagic (open-water) and littoral (epibenthic) Cladocera in 62 crater lakes and a few other permanent waters in western Uganda, to comprehensively assess the relationship of cladoceran communities in East African lakes to the physical and chemical nature of their abiotic environment and associated biological habitat characteristics.

Methods

Study area

Our 62 study sites are all located in the maar crater Lake districts of Fort Portal, Kasenda, Katwe-Kikorongo and Bunyaruguru (Melack, 1978) in southwestern Uganda (Fig. 1). These small lakes are spread along the regional Rift Valley gradient from 914 to 1,566 m elevation and from semi-arid to sub-humid climate regimes. The lakes range from 56 to 135,400 µS/cm in surface-water conductivity, from oligotrophic to hyper-eutrophic in aquatic productivity, and from shallow and unstratified to deep and permanently stratified (Table 1). Lakes on the moist shoulder of the Rift Valley are fed mainly by rain and surface runoff (and an occasional small inflowing stream) and are hydrologically open with outflow to the regional groundwater table through porous upper crater walls. Lakes on the dry Rift Valley floor are hydrologically closed, often saline, and maintained against the local moisture deficit by substantial groundwater inputs (lake numbers 38–40, 50 and 55 in Fig. 1). Water depth ranges from 0.1 to 220 m and surface area (SA) from 0.01 to 3.84 km^2 (all except one are <1 km^2). The water level of all these lakes undergoes seasonal fluctuations, modest in the hydrologically open lakes and stronger in the closed lakes. Some of the salt lakes are known to dry up seasonally or intermittently.

The natural vegetation surrounding the Uganda crater lakes mainly reflects the local rainfall regime and varies from dry grass savannah on the floor of the Rift Valley (Katwe-Kikorongo and the northern part of Bunyaruguru) to semi-deciduous lowland forest on

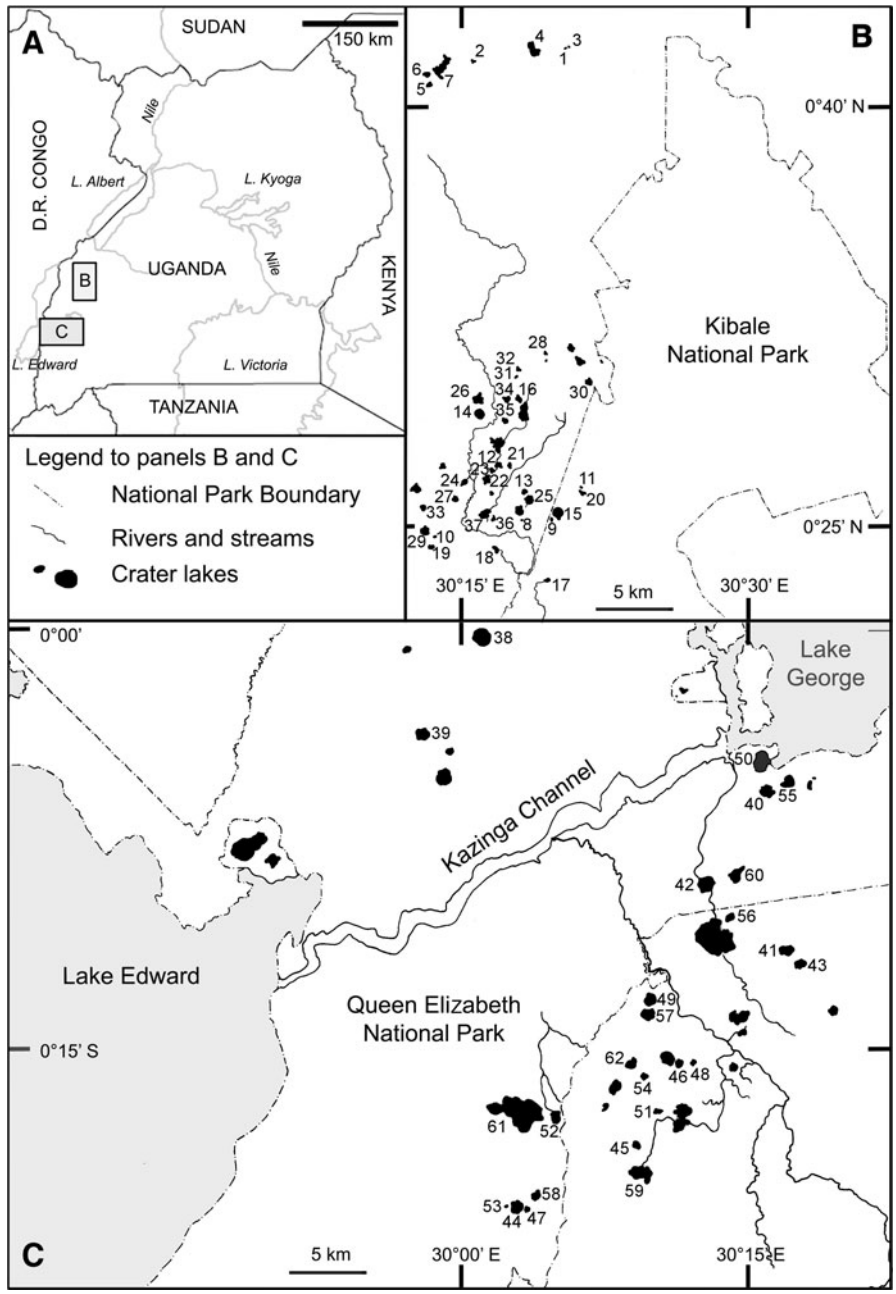

Fig. 1 Map of the study region in western Uganda showing the locations of **A** the crater lake districts in the Edward–George branch of the Rift Valley, **B** the Fort Portal (lakes 1–7) and Kasenda (lakes 8–37) districts and **C** the Kikorongo (lakes 38–39) and Bunyaruguru (lakes 40–62) districts

its shoulders (Fort Portal, Kasenda and the southern part of Bunyaruguru) (White, 1983). In most of the wetter, more densely populated areas, natural vegetation around the crater basins has now been replaced by cropland and plantations. Routine burning of secondary vegetation and intense subsistence agriculture inside gently sloping crater basins has augmented their phosphorus loading, often causing eutrophication (Kizito et al., 1993). Some lakes are situated within the boundaries of Kibale and Queen Elizabeth National Parks (Fig. 1), where human activities are limited to fishing and low-intensity exploitation of the forest.

Fieldwork

In the course of 2007 and 2008, we conducted four dry-season (January–February or August–September)

Table 1 Study lakes in western Uganda ordered by district, with data on lake surface area (SA) in km^2, maximum depth (Z_{max}) in m, elevation (Elev.) in meter asl, mean annual temperature (MAT) in °C, surface-water conductivity (Scond) in µS/cm at 25°C, surface-water pH (pH-surf), littoral habitat types (Type), Secchi depth (Secchi) in meter, total phosporous (TP) in µg/l, calcium (Ca) and magnesium (Mg) in mg/l, and the percent area of land-cover types in the lake basin: stable (forest, savannah and plantation), agriculture and fallow. Also listed are cladoceran species richness (Ntaxa) recorded at each site, and the five main types of littoral habitat (HA) as defined in the "Methods" section

	Lake/District	SA	Z_{max}	Elev	MAT	Scond	pH-surf	Secchi	TP	Ca	Mg	Stable	Agri	Fallow	Ntaxa	HA-SAND	HA-EMER	HA-SUBM	HA-FLOAT	HA-SWAMP
	Fort Portal																			
1	Ekikoto	0.02	74	1,537	20.02	497	8.29	1.80	0.01	36.0	21.2	35	25	40	5	X	X			
2	Kaitabarago	0.02	70	1,548	19.93	489	8.03	0.75	0.07	21.6	41.1	70	00	30	4	X	X	X		
3	Kayihara	0.01	66	1,537	20.02	498	8.07	1.60	0.01	30.2	15.7	70	00	30	5	X				
4	Kyaninga (South)	0.24	58	1,531	20.07	420	8.34	5.85	0.01	36.6	27.5	40	00	60	9	X	X			
5	Kyegere	0.12	53	1,566	19.79	250	8.31	2.15	0.01	13.6	5.0	01	40	59	9	X	X	X		
6	Nyabikora	0.07	7.7	1,561	19.83	188	8.31	1.20	0.02	23.2	9.1	15	50	35	8	X	X		X	
7	Saka (crater)	0.01	8.5	1,566	19.79	612	7.59	0.45	0.08	58.0	36.4	45	40	15	10	X	X		X	
	Kasenda																			
8	Kanyabutetere	0.01	5	1,188	22.85	401	8.62	0.78	2.38	42.7	12.2	00	80	20	6	X	X	X		
9	Kanyamansira	0.02	30	1,177	22.94	394	8.96	0.82	0.03	19.9	27.8	90	00	10	3	X	X	X		
10	Kanyamukali	0.02	11	1,150	23.16	920	8.60	0.65	0.40	40.3	48.7	10	70	20	6	X	X			
11	Kanyanchu	0.01	4.8	1,233	22.48	568	8.26	0.93	0.07	21.8	23.2	00	00	00	7	X	X	X	X	X
12	Kanyango	0.12	58	1,259	22.27	493	8.75	0.45	0.02	42.2	40.6	25	65	10	3	X	X		X	
13	Kasenda	0.09	13.5	1,244	22.39	312	7.63	0.83	0.04	29.7	12.3	40	05	45	4	X	X			
14	Katanda	0.37	152	1,340	21.62	419	8.51	2.00	0.04	10.1	20.0	35	50	15	3	X	X			
15	Kerere	0.27	68	1,184	22.88	263	8.04	3.63	0.02			80	00	20	9		X	X		
16	Kifuruka	0.13	3.7	1,403	21.11	411	8.33	0.82	0.08	44.4	27.1	45	45	10	9	X	X	X	X	X
17	Kisibendi	0.04	4.5	1,126	23.35	277	9.30	0.03	0.30	30.5	13.0	80	00	20	0	X	X			
18	Kitere	0.10	51	1,160	23.07	711	8.97	0.83	0.13	34.8	51.1	33	07	60	0	X	X			
19	Kyanga	0.12	54	1,146	23.19	1,112	9.11	1.40	0.11	14.5	84.0	80	15	05	1	X	X	X		
20	Kyerbwato	0.01	12.5	1,233	22.48	411	8.47	1.65	0.02	24.9	16.5	90	00	10	11	X	X	X	X	
21	Lugembe	0.08	15	1,281	22.09	407	8.30	1.35	0.05	22.4	22.7	20	60	20	5	X	X			
22	Mahuhura	0.19	154	1,254	22.31	600	8.97	5.60	0.23	35.6	47.4	38	02	60	6	X	X	X		
23	Mbajo	0.08	35	1,234	22.47	504	8.64	1.30	0.02	40.0	39.8	30	10	60	5	X	X		X	
24	Mubiro	0.16	70	1,208	22.69	718	9.02	3.20	0.02	24.0	85.4	40	15	45	4	X	X	X		
25	Murusi	0.21	57	1,226	22.54	382	8.54	1.40	0.01	29.8	26.2	35	25	40	2	X	X			
26	Mwengenyi	0.29	140	1,397	21.15	352	8.43	3.35	0.10	15.1	10.0	40	40	20	13	X	X	X	X	X
27	Njarayabana	0.12	38	1,179	22.92	857	8.84	1.20	0.81	61.6	79.4	35	15	50	0	X	X			
28	Nkuruba	0.01	34.5	1,480	20.48	370	8.31	1.01	0.06	43.3	24.6	80	00	20	2	X				
29	Ntambi	0.32	111	1,158	23.09	5,820	9.75	0.40				90	05	05	0	X		X		
30	Nyabikere	0.39	47.3	1,376	21.32	271	7.89	0.61	0.11	36.0	12.3	84	01	05	7	X	X	X		
31	Nyahirya	0.01	79	1,444	20.77	379	8.18	0.97	0.11	24.8	21.2	60	10	30	3	X			X	

Table 1 continued

	Lake/District	SA	Z_{max}	Elev	MAT	Scond	pH-surf	Secchi	TP	Ca	Mg	Stable	Agri	Fallow	Ntaxa	HA-SAND	HA-EMER	HA-SUBM	HA-FLOAT	HA-SWAMP
32	Nyamswiga	0.03	43	1,447	20.75	330	7.76	1.10	0.21	39.5	17.4	35	20	45	8	X	X	X	X	
33	Nyamugosani	0.11	37	1,234	22.47	988	8.94	1.52	0.34	49.3	58.3	10	35	55	1	X	X			
34	Nyantonde	0.12	180	1,387	21.24	501	8.76	3.10	0.01	29.1	46.0	15	60	25	6	X	X			
35	Rukwanzi	0.08	169	1,332	21.68	425	8.33	5.02	0.05	29.2	34.1	92	02	06	5	X				
36	Wandakara	0.03	10.5	1,158	23.09	1,125	8.76	0.70	0.06	22.8	42.8	02	65	33	2	X	X			
	Wandakara - swamp	0.01	0.4	1,146	23.19	1,452	8.21	0.10	0.39			10	80	10	1					X
37	Wankenzi	0.16	59	1,158	23.09	496	8.65	0.36	0.06	25.4	12.0	10	50	40	2	X	X			
	Kikorongo																			
38	Kikorongo	0.92	9.8	915	25.06	22,400	9.58	1.20		7.7	5.7	100	00	00	1	X				
39	Kitagata	0.62	8.9	914	25.07	135,400	9.63	0.05				100	00	00	0	X				
	Bunyaruguru																			
40	Bagusa	0.33	0.9	905	25.14	61,100	10.62	0.24		9.6	70.7	100	00	00	0	X				
41	Bugwagi	0.60	85	1,048	23.98	441	9.02	2.45	0.02	20.5	37.7	0.45	40	15	4	X	X			
42	Chibwera	0.76	10.5	971	24.60	457	8.91	1.35	0.06	15.3	24.3	100	00	00	11	X		X		X
43	Ibamba	0.01	1.2	1,073	23.78	104	6.55	0.35	0.15	9.0	7.1	10	75	15	21		X		X	X
44	Karolero	0.51	35	1,103	23.54	181	8.05	3.80	0.24	12.7	7.6	100	00	00	8	X			X	
45	Kako	0.17	29	1,396	21.16	89	8.18	2.30	0.01	6.5	6.0	08	85	07	3	X				
46	Kamweru	0.20	43	1,232	22.49	170	9.59	0.55	0.07	16.7	13.5	05	65	30	3	X				
47	Kacuba	0.05	14.5	1,102	23.54	148	8.75	1.49	0.05	12.6	7.8	100	00	00	13	X	X	X	X	
48	Kasirya	0.09	43	1,251	22.34	302	8.72	2.35	0.02	22.8	24.1	15	50	35	0	X	X			
49	Katinda	0.44	17	1,024	24.18	743	9.48	0.53	0.04	12.0	27.7	01	70	29	1	X	X			
50	Kibengo	0.88	4.8	914	25.07	264	9.92	0.20	0.09	25.8	11.1	100	00	00	5	X	X			
51	Kigezi	0.39	29	1,302	21.92	265	8.49	0.99	0.11	27.3	19.6	11	47	41	4	X	X	X		
52	Kyasunduka	0.50	2.1	1,004	24.34	269	8.69	0.30	0.46	19.9	15.3	60	20	20	1	X	X			
53	Kyogo	0.02	3.4	1,113	23.45	56	6.87	3.00	0.59	4.8	2.0	100	00	00	20		X	X	X	X
54	Mafura	0.16	29	1,255	22.30	259	9.29	0.65	0.02	27.6	19.7	00	80	20	2	X	X			
55	Maseche	0.32	0.2	908	25.12	68,200	10.19	0.02		7.8	6.0	100	00	00	0	X				
56	Mbugo	0.36	2.6	978	24.55	214	9.63	0.51	0.10	8.2	29.8	20	70	05	1	X	X			
57	Mirambi	0.53	22	1,077	23.75	642	9.83	0.90	0.04	9.9	27.0	00	70	30	2	X	X			
58	Murabio	0.27	15	1,098	23.58	141	8.42	2.03	0.02	11.9	8.3	100	00	00	7	X	X	X	X	
59	Nkugute	0.89	58	1,409	21.06	121	8.72	0.90	0.05	11.3	7.6	21	64	15	5	X	X		X	
60	Nshenyi	0.44	0.05	966	24.65	11,230	10.05	0.02		7.5	2.0	100	00	00	0	X				
61	Nyamusingere	3.84	4.3	978	24.55	681	9.40	0.36	0.06	11.0	30.9	99	00	00	2	X	X			
62	Nyungu	0.14	25	1,172	22.98	430	9.40	0.08	0.26	27.2	41.3	02	85	13	0	X	X			

field campaigns in western Uganda, surveying a total of 62 crater lakes. Latitude, longitude and elevation (in meter above sea level) were recorded by GPS (Garmin Csx 60). Following Eggermont et al. (2010), mean annual air temperature (MAT) was estimated using a region-specific linear relationship between elevation and temperature ($P < 0.001$, RMSE: 0.95°C) derived from the Global Historical Climatology Network (GHCN) database (monthly time series from the 1930s to 2006; 4 stations) and the Global Summary of the Day (GSOD) database (time series from 1957 to 2006; 10 stations). Maximum lake depth (Z_{max}) was determined by GPS-guided echo-sounding. Lake SA was calculated using either field-measured diameter and/or circumference (small, circular crater lakes) or by analysis of topographical maps (larger lakes, often irregular in shape). We distinguished and quantified four main types of land use per lake basin: stable ground cover (which includes natural or secondary forest, grass and wooded savannah, and tree plantations), fallow land, habitation and (subsistence or commercial) crop agriculture. Habitation occupied a significant fraction of land in only two crater basins (Kasenda and Nyabikere) and was therefore not included in statistical analyses. The other three land-cover types represent broad categories in runoff and soil erosion rates, ranging from low (natural vegetation and plantations) over intermediate (fallow land) to high (crop agriculture).

Surface-water temperature (SWT), surface and bottom pH (pH-surf, pH-bot), dissolved oxygen (DO) at 0.5 m depth (or surface when $Z_{max} < 0.5$ m) and specific conductance at 25°C (Scond, a proxy for salinity) were measured at the time of sampling with a Hydrolab Quanta multiprobe. Transparency (Secchi depth) was measured using a 22-cm diameter Secchi disk. The following chemical species were determined: major and trace cations (Ca, Mg, Na, K, Ba, Sr, Fe, Mn), anions (F, Cl, Br, NO_3, SO_4), dissolved silica (Si), dissolved phosphorus (P), dissolved inorganic carbon (DIC), total organic carbon (TOC), total phosphorus (TP) and total nitrogen (TN). Collection of water samples and analysis for cations, anions, dissolved phosphorus and dissolved inorganic carbon (DIC) followed the procedures described in Eggermont et al. (2007). Nutrients were analysed the same day using a Hach Lange DR2800 spectrophotometer. Total phosphorus (TP, in mg/l) and total nitrogen (TN, in mg/l) concentrations were determined using quartz-cuvette tests following hydrolysis. Dissolved silica (Si, in mg/l) was analysed upon return to Belgium, using inductively coupled plasma atomic emission spectrometry. Chlorophyll *a* (Chl *a*, in µg/l) concentrations were measured at the surface. Between 400 and 700 ml of water was filtered using a Nalgene filtration unit and GF5 Macherey-Nagel glass fiber filters (45 mm diameter). The filter was extracted by placing it for 24 h in a tube containing 5 ml of 90% acetone, at 4°C. The extracted solution was filtered using a syringe with encapsulated filter into a 5-cm spectrophotometric cell. The Chl *a* concentration is the absorption value at 665 nm in a DRELL 2800 spectrophotometer after zeroing with pure acetone.

The presence or absence of fish was recorded in all 56 studied freshwater lakes (Scond values <1,500 µS/cm); fish can be assumed absent in the five true saline lakes (>10,000 µS/cm) and in Lake Ntambi (5,820 µS/cm). Many lakes contain indigenous fish populations (Sato et al., 2003), but in most cases non-indigenous fish were added to increase available protein resources (Kizito et al., 1993; Crisman et al., 2001; Bwanika et al., 2004). We did not assess the relative fishing intensity in this study, as even inside national parks fish poaching is a common practice and no trustworthy information on fishing pressure is available.

Cladocera were sampled by repeatedly sweeping a 50-µm mesh net across planktonic and epibenthic habitat in near-shore (littoral) environments and in the off-shore planktonic (pelagic) environment. If habitats contained aquatic macrophytes, these were removed from the water and rinsed above the net to adequately sample the attached invertebrate fauna. Samples were instantly fixed in either formalin (5% formaldehyde) neutralized with powdered calcite or in 40% ethanol. Concurrent sampling and identification of aquatic macrophytes was carried out along transects from the lakeshore to the depth limit of aquatic plant growth. Submerged macrophytes in deeper water were sampled using a 4-m long rake. For this study, we differentiated between five main types of littoral habitat (HA): sandy or rocky shores including those with submerged parts of terrestrial vegetation (HA-sand); emergent reed-like vegetation such as *Phragmites*, *Cladium* and *Typha* (HA-emer); submerged vegetation with few or no floating parts,

such as *Ceratophyllum*, *Potamogeton* and *Chara* (HA-subm); submerged vegetation with considerable floating parts, mostly *Nymphea nouchali* (HA-float); and a swampy vegetation occurring at the edge of some lakes with *Cyperus papyrus* and *Miscanthidium violaceum* (HA-swamp). The total number of macrophyte habitat types present in a lake (#Macrophytes, ranging from 1 to 4) was used as a measure of the diversity of vegetated aquatic habitat.

Laboratory analyses

Samples were rinsed using a 50-μm mesh sieve, and retained residues were scanned with a binocular microscope at 30× magnification under a combination of incident and transmitted light. Except for some readily identifiable species, most specimens were picked and mounted in glycerine on microscope slides. Dissection of specimens was carried out when required for observation of diagnostic characters. Identifications were done with a compound microscope at 100–400× magnification, by comparison with Korovchinsky (1992) for the Sididae; Kořínek (1984) and Rey & Saint-Jean (1968, 1969) for the Daphniidae; Smirnov (1976) and Dumont et al. (1981) for the Moinidae; Smirnov (1992), Kořínek (1984) and Dumont et al. (2002) for the Macrothricidae; Fryer (1968) and Kotov & Štifter (2006) for the Ilyocryptidae; and Smirnov (1996), Kořínek (1984), Rajapaksa & Fernando (1987), Dumont & Silva-Briano (2000), Smirnov et al. (2006) and Van Damme & Dumont (2008) for the Chydoridae. To permit comparison of our results with those of Verschuren et al. (2000), who studied environmental regulation of cladoceran (and other aquatic invertebrate) communities in a shallow fluctuating lake in Kenya, Table 2 provides a list of species of which the nomenclature has been updated since that study. A sizable fraction of widely distributed species as currently recognised may consist of several cryptic species (Forró et al., 2008). We used the designation 'cf.' to distinguish between species described from Europe or South America and the morphologically similar, yet distinct, African specimens encountered in our samples.

Data analyses

Three water-chemistry variables (Br, NO_3, SO_4) were removed from the dataset because their concentrations were below detection limit (MDL) at more than half of the study sites. The remaining variables were tested for normality using Shapiro–Wilks tests (Shapiro et al., 1968). Fifteen variables were normalized using either logarithmic transformation (SA, Scond, TP, TN, Chl *a*, TOC, Na, Mn, P, S and Cl) or squared-root transformation (K, Sr, F and #Macrophytes). Relationships among the environmental variables were assessed using a Pearson's correlation matrix (Appendix A—Electronic supplementary material). Correlation matrices and normality tests were generated using the software package STATISTICA 5.5 (Statsoft, 2000).

For multivariate statistical analysis, samples were pooled per lake across all local habitat types in order to obtain a representative presence–absence dataset for each lake. For assessment of species distribution in relation to lake variables, species were recorded as present in a lake when at least two specimens were encountered in the pooled samples from that lake. In our dataset, this procedure marginally reduced the frequency of occurrence for four species (see Table 2). We retained species which were found in only one lake, since also rare species contribute ecological information to the dataset (Birks, 1995). For freshwater lakes (Scond <1,500 μS/cm), we calculated a Spearman rank correlation matrix to quantify the relationships between environmental variables and species richness, using pair-wise deletion where data on environmental parameters was incomplete. To allow meaningful comparison between lakes, species richness was evaluated using the raw number of species rather than a diversity index, because even with similar sampling effort among sites, the number of individuals collected varied by three orders of magnitude. We refrained from using rarefaction methods and rarefied species diversity indices to evaluate differences in species diversity (and evenness) between lakes, because our pooled data on Cladocera presence per lake represent equal sampling effort in each habitat type that we recognised to be present in that lake, not equal and spatially random sampling effort in each lake. We estimated total species richness in the study area using Chao's formula and two re-sampling estimators, which are based on the number of species observed only in a single location, in exactly two locations and the total number of species observed in the dataset (Colwell & Coddington, 1994).

Table 2 List of Cladocera taxa recorded in the studied Uganda crater lakes with indication of the number of lakes where the species was found and the total number of specimens across all lakes

	No. of lakes	No. of specimens
Sidoidea Ctenopoda		
Sididae Baird, 1850		
Pseudosida Herrick, 1884		
Pseudosida szalayi Daday, 1898	2	53
Diaphanosoma Fischer, 1850		
Diaphanosoma excisum Sars, 1886	2	19
Daphnioidea Anomopoda		
Bosminidae Sars, 1865		
Bosmina Baird, 1845		
Bosmina longirostris Muller, 1785	1	6
Chydoridae Dybowski & Grochowski, 1894		
Alona Baird, 1843		
Alona cambouei Guerne & Richard, 1893 (a)	18	97
Alona guttata Sars, 1862	8	196
Alona cf. *verrucosa* Sars, 1901 (b)	11	186
Alonella Sars, 1862		
Alonella exigua Lilljeborg, 1853	1	10
Alonella excisa Fischer, 1854	5	19
Chydorus Leach, 1816		
Chydorus eurynotus Sars, 1901	4	177
Chydorus parvus Daday, 1898	30	1649
Coronatella Dybowki & Grochowski, 1894		
Coronatella cf. *rectangula* Sars, 1861 (c)	1	28
Disparalona Fryer, 1968		
Disparalona hamata Birge, 1879 (d)	11	128
Dunhevedia King, 1853		
Dunhevedia crassa King, 1853	11	51
Dunhevedia serrata Daday, 1898	3	10
Ephemeroporus Frey, 1982		
Ephemeroporus barroisi Richard, 1894	4	59
Euryalona Sars, 1901		
Euryalona orientalis Daday, 1898	4	17
Graptoleberis Sars, 1862		
Graptoleberis testudinaria Fischer, 1848	2	7
Karualona Dumont & Silva-Briano, 2000		
Karualona iberica Alonso & Pretus, 1989 (e)	14	198
Kurzia Dybowski and Grochowski, 1894		
Kurzia longirostris Daday, 1898	1	2
Notoalona Rajapaksa and Fernando, 1987		
Notoalona globulosa Daday, 1898	3	85
Oxyurella Dybowski and Grochowski, 1894		
Oxyurella singalensis Daday, 1898	6	75
Pleuroxus Baird, 1843		
Pleuroxus cf. *varidentatus* Frey, 1993 (f)	14	199
Pleuroxus toumodensis Brehm, 1933	5	42

Table 2 continued

	No. of lakes	No. of specimens
Pseudochydorus Fryer, 1968		
Pseudochydorus cf. *globosus* Baird, 1843 (g)	26	90
Daphniidae Straus, 1820		
Ceriodaphnia Dana, 1853		
Ceriodaphnia cornuta Sars, 1885 (h)	28	1142
Ceriodaphnia dubia Richard, 1894	14	880
Daphnia Müller, 1785		
Daphnia barbata Weltner, 1898 (i)	1	2
Daphnia laevis Birge, 1879	3	67
Scapholeberis Schoedler, 1858		
Scapholeberis kingi Sars, 1888	1	7
Simocephalus Schoedler, 1858		
Simocephalus mesorostris Orlova-Bienkowskaja, 1995	2	69
Simocephalus vetulus Muller, 1776	11	162
Simocephalus serrulatus Koch, 1841	1	67
Ilyocryptidae Smirnov, 1976		
Ilyocryptus Sars, 1862		
Ilyocryptus spinifer Herrick, 1882	1	40
Macrothricidae Norman & Brady, 1867		
Macrothrix Baird, 1843		
Macrothrix triserialis group Brady, 1886	29	970
Moinidae Goulden, 1868		
Moina Baird, 1850		
Moina belli Gurney, 1904	1	24976
Moina micrura Kurz, 1874	17	2152
Moinodaphnia Herrick, 1887		
Moinodaphnia macleayi King, 1853	2	125

Changes in nomenclature since the study of Verschuren et al. (2000):
(a) *Alona* nr *cambouei*;
(b) *Biapertura verrucosa*;
(c) *Alona rectangula*;
(d) *Pleuroxus* nr *laevis*;
(e) *Biapertura karua*;
(f) *Pleuroxus aduncus*;
(g) *Pseudochyodorus globosus*;
(h) *Ceriodaphnia* nr *rigaudi*;
(i) *Ctenodaphnia barbata*

Multivariate analyses and analysis of beta diversity were limited to the subset of 51 of the 56 sampled freshwater lakes where Cladocera were actually found. To avoid further deletion of sites, missing Chl *a* data for Lake Mafura were replaced by the overall average value of the other freshwater lakes (cf. ter Braak, 1987). The same principle was applied for the missing water chemistry data from Kerere. The final set of 35 environmental variables, including five categorical variables representing the various types of littoral habitat, from 51 freshwater lakes was centred and standardized to allow comparison of disparate variables (ter Braak & Smilauer, 2002).

A principal component analysis (PCA) on a matrix of correlations was used to identify the principal environmental gradients that may structure the faunal dataset. Given a gradient length of 2.76 in a detrended correspondence analysis (DCA; Hill & Gauch, 1980), we used canonical correspondence analysis (CCA; ter Braak & Smilauer, 2002) to explore the relationships between the presence–absence of species and environmental variables. Rare species were down-weighted, and forward selection of environmental variables was used to identify which variables explained the greatest amount of variance in the species assemblages. In case of similar contributions, priority was given to variables with known ecological relevance. In order to determine whether the observed effect of cations and anions was not caused by their correlation to other environmental parameters, a supplementary correspondence analysis was performed without cation and anion data. We used a Monte Carlo permutation test with 499 permutations to test whether the first axis

significantly explained part of the variation in the species data (ter Braak & Verdonschot, 1995). Multivariate statistics were performed using the package CANOCO v. 4.5 (ter Braak & Smilauer, 2002). The beta diversity, the extent of species replacement or biotic change along the sampled gradients, was calculated according to Whittaker (1960), which is appropriate in ecological applications of presence–absence data (Wilson & Shmida, 1984).

Results

Environmental gradients

We found a number of correlations between MAT (or elevation) and SWT, conductivity, pH, lake depth, and local vegetation (see Appendix A—Electronic supplementary material), which all broadly reflect the regional gradient between the often large, shallow and more saline lakes of the dry, warm Rift Valley floor versus the smaller, deeper freshwater lakes of the wetter uplands. Transparency (Secchi) is positively correlated with maximal lake depth and negatively with the productivity indicators TN, Chl *a* and TOC. Scond and pH-surf are positively correlated with most cations and anions and negatively with #Macrophytes. Negative correlations between the different types of land use are evidently an artefact of our method to quantify land use in the crater basin as % land cover. The various indicators of aquatic productivity (TP, TN, TOC and Chl *a*) are all positively correlated with one another.

Our dataset of freshwater lakes with Cladocera covers a number of environmental gradients (Fig. 2). The first two PCA axes together account for 30.1% of the environmental variance in the dataset ($\lambda_1 = 0.209$ and $\lambda_2 = 0.092$; Fig. 2). PCA axis 1, which explains 20.9% of the total variation, mainly captures gradients of aquatic macrophyte habitats, conductivity and surface pH. To a lesser extent, it also reflects gradients in DIC, dissolved Si, Cl and Mg. Several types of aquatic macrophyte habitat show a strong inverse relationship with pH, reflected by their opposite positions in the ordination plot (Fig. 2; Appendix A—Electronic supplementary material). Surface-water pH in pristine freshwater lakes ranges from slightly acidic to alkaline (6.55–9.92), with the

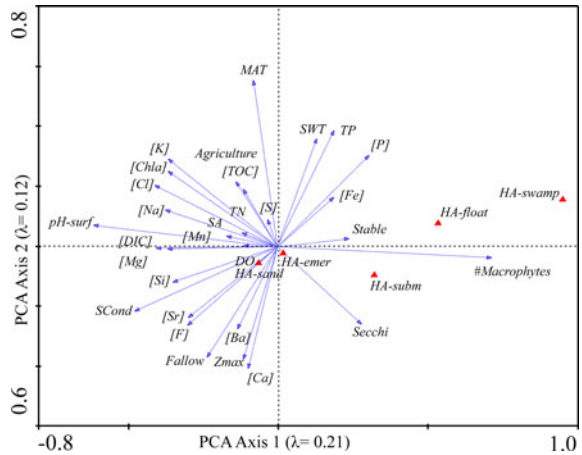

Fig. 2 Principal component analysis (PCA) of all measured environmental variables in 51 freshwater crater lakes with Cladocera in Western Uganda

slightly acidic lakes containing diverse aquatic macrophyte habitats and the alkaline lakes dominated by algae. PCA axis 2, which explains 9.2% of the total environmental variance, is mainly determined by gradients in MAT, lake depth, land use and Ca. To a lesser extent, it also reflects gradients in SWT, TP and P. The plot also illustrates the strong inverse relationship between transparency and both Chl *a* and TOC.

Faunistics

A total of 37 Cladocera species from 26 genera were found in 52 of the 62 study lakes (51 freshwater lakes and 1 salt lake, Table 2). In total, we identified and counted ~34,000 specimens. 73% of these belong to the halophilic species *Moina belli*, which occurs abundantly in the saline lake Kikorongo (22,400 µS/cm). Five other common but more widespread species (*Chydorus parvus*, *Macrothrix triserialis*, *Ceriodaphnia cornuta*, *Ceriodaphnia dubia* and *Moina micrura*) together account for 20% of our collection with between 2,192 (*M. micrura*) and 880 (*C. dubia*) specimens identified. Of the remaining 31 species, we found between 2 and 199 specimens. The most widely distributed species are *Chydorus parvus*, *Macrothrix triserialis*, *Ceriodaphnia cornuta*, *Pseudochydorus* cf. *globosus*, *Alona cambouei* and *Moina micrura*, which were the most widely distributed, being present in 30, 29, 28, 27, 18 and 17 lakes, respectively. Species richness per lake was highly

variable ranging from 0 (five lakes; see below) to 21 (Lake Ibamba). *Scapholeberis kingi*, *Pseudosida szalayi*, *Moinodaphnia macleayi*, *Ilyocryptus spinifer* and *Kurzia longirostris* were found only in the shallow, swamp-like lakes Ibamba and Kyogo. Other rare taxa that were found in only one or two lakes include *Alonella exigua*, *Coronatella* cf. *rectangula*, *Bosmina longirostris*, *Daphnia barbata*, *Diaphanosoma excisum*, *Graptoleberis testudinaria*, *Moina belli*, *Simocephalus mesorostris* and *S. serrulatus* (Table 2). *Bosmina longirostris* was encountered only in a shallow temporary swamp near Lake Wandakara. *Daphnia barbata* was found in Lake Kibengo (a satellite basin of Lake George) and in the Kazinga channel which connects lakes George and Edward (Fig. 1). Cladocerans were lacking at five freshwater lakes: Kasirya, Kitere, Kisibendi, Njarayabana and Nyungu. Both Nyungu and Kisibendi are hyper-eutrophic, while Kasirya, Kitere and Njarayabana are less productive but also lack significant submerged or floating aquatic macrophytes.

Only three cladoceran species were found at Scond values above 1,000 µS/cm: *Alonella excisa* was found in Lake Kyanga (1,112 µS/cm) and *Macrothrix* sp. in Wandakara (1,158 µS/cm). *Moina belli* is the only truly halophilic cladoceran in our dataset.

In the set of 56 freshwater lakes, species richness was positively correlated with the diversity of aquatic macrophyte habitat (#Macrophytes: $r = 0.733$, $P < 0.001$), and negatively with pH-surf ($r = -0.662$, $P < 0.001$), Chl *a* ($r = -0.369$, $P = 0.006$) and Scond ($r = -0.448$, $P = 0.001$). Chao's formula suggests a regional species richness of 42 species; the first- and second-order jack-knife estimates are 44 and 47 species, respectively. This indicates that the present survey may have missed from 5 to 10 species (12–21%) of the total regional species pool.

Species–environment relationships

Canonical correspondence analysis with forward selection retained the following variables, which together explain 21.7% of the total faunal variance: TP, MAT, #Macrophytes, pH-surf, % agriculture and Mg (Table 3). The Monte Carlo permutation test on the first CCA axis was highly significant (axis 1: $F = 3.55$, $P = 0.002$). TP, MAT, pH-surf and #Macrophytes are the most important predictors of Cladocera community composition on CCA axis 1 (Fig. 3). Besides the diversity of aquatic macrophyte habitats, the most variance along CCA axis 2 is explained by the fraction of the crater basin used for agriculture and TP. This reflects a gradient in both aquatic macrophyte diversity and lake productivity, as determined by Z_{max} and %agriculture. Lakes situated in the lower quadrants have an extensive littoral zone

Table 3 Statistics summary for a CCA of environmental variables and the presence–absence data of 36 Cladocera species in 51 Uganda crater lakes

Canonical correspondence axes	1	2	3	4	
Eigenvalues	0.21	0.12	0.09	0.08	
Species environment correlations	0.86	0.76	0.69	0.71	
Cumulative percentage of variance					
Of species data	7.5	12	15.3	18.2	
Of species–environment relationship	34.3	55	70.4	83.6	
Sum of all eigenvalues					2.74
Sum of all canonical eigenvalues					0.59
Weighted correlation coefficients of selected environmental variables					
TP	0.58	0.26	−0.09	0.01	
MAT	0.55	0.10	0.08	0.50	a
pH-surf	−0.50	0.11	0.11	0.34	a
No. of macrophytes	0.44	−0.53	−0.21	−0.14	a
Mg	−0.38	−0.14	0.48	0.25	a
Agriculture	0.15	0.27	0.43	−0.42	a

[a] Environmental variable significantly explains part of the variation after variance partitioning

with several types of submerged, floating or emergent aquatic macrophytes. They are often located in national parks (Fig. 1) and/or have crater basins with steep, uncultivated slopes. The upper quadrants include lakes located in crater basins with intensive agriculture, as well as several shallow, naturally eutrophic lakes. *Diaphanosoma*, *Moinodaphnia*, *Ilyocryptus* and *Pseudosida* seem to be associated with dilute, swampy lakes with low pH (Fig. 3B). *Ceriodaphnia*, *Alona cambouei*, *Macrothrix triserialis* and *Chydorus parvus* were encountered in a wide variety of lakes, while *Simocephalus latirostris*, *Dunhevedia crassa*, *Alona guttata* and *Pleuroxus toumodensis* seem restricted to lakes with diverse aquatic macrophyte habitat. Removal of cation and anion data did not drastically alter the resultant CCA as forward selection retained the same remaining variables, which, due to the exclusion of Mg, explain only 18.8% of the total faunal variance (Table 4).

A beta diversity of 4.95, reflecting five turnovers in Cladoceran species composition, indicates that six relatively distinct Cladoceran communities occur along the environmental gradients represented by our dataset of 56 fresh Uganda lakes.

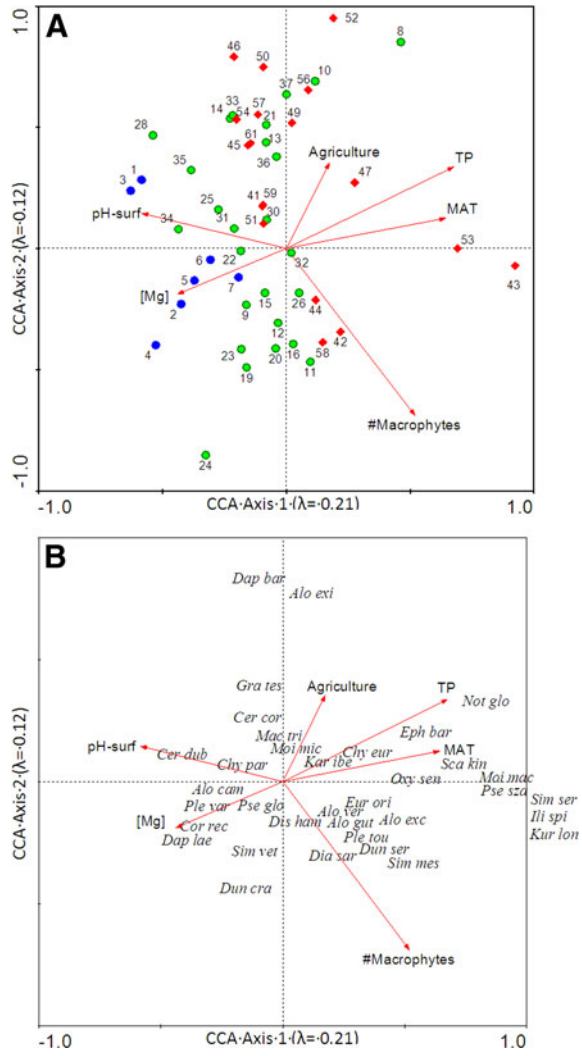

Fig. 3 Canonical correspondence analysis (CCA) of **A** the 51 study sites and **B** cladoceran presence–absence data in relation to selected environmental variables. Sites are classified according to lake disctrict: Fort Portal (*dark circles*), Kasenda (*light circles*) and Bunyaruguru (*diamonds*). Site and taxon codes are found in Tables 1 and 2, respectively. Three species (*Sim ser*, *Ili spi* and *Kur lon*) have identical scores due to a uniform distribution

Discussion

Environmental gradients

The limited number of lakes with intermediate salinities (1,500–10,000 µS/cm) in our current dataset reflects the true scarcity of such lakes in tropical Africa (Talling & Lemoalle, 1998; Verschuren et al., 2004). In our dataset, saline to hypersaline lakes are concentrated in the southern (Kikorongo and Bunyaruguru) lake clusters and are typically rather shallow and eutrophic. The freshwater lakes display a wide range of depths and trophic levels, with the shallower lakes often being polymictic and eutrophic, whereas deeper lakes are oligomictic or meromictic and oligo- to mesotrophic (Verschuren et al., 2009). Pronounced inter-annual and inter-seasonal differences in measured surface-water TP is due to cycles of stratification and mixing, as often a quite strong depth gradient in TP (and TN) occurs with nutrients accumulating in the hypolimnion during stratification (Cocquyt et al., 2010). A single surface-water TP, TN, DOC or Chl *a* measurement will therefore not always be a good measure for the average trophic status of a lake. In the PCA ordination, the fraction of land used for agriculture is aligned with both TOC and Chl *a*, suggesting a relationship between lake trophic status and land use intensity. This relationship is neither straightforward nor universal, however, since there is no significant positive correlation between % agriculture and the various indicators of lake trophic status (Appendix A—Electronic supplementary

Table 4 Statistics summary for a CCA of environmental variables (excluding anion and cation data) and the presence–absence data of 36 Cladocera species in 51 Uganda crater lakes

Canonical correspondence axes:	1	2	3	4	
Eigenvalues	0.20	0.12	0.08	0.07	
Species environment correlations	0.85	0.75	0.70	0.69	
Cumulative percentage of variance					
Of species data	7.4	11.7	14.7	17.2	
Of species–environment relationship	39.6	62.5	78.2	91.8	
Sum of all eigenvalues					2.74
Sum of all canonical eigenvalues					0.52

material). Land-use intensity influences aquatic ecosystem functioning by impacting on aquatic macrophyte development, as suggested by the negative correlation of #Macrophytes with % agriculture ($r = -0.318$, $P = 0.016$) and its positive correlation with % natural vegetation and plantations ($r = 0.396$, $P = 0.002$) in freshwater lakes. In our dataset, transparency (Secchi) is positively correlated with maximal lake depth and negatively with MAT, since most deep lakes are situated in the northern (Fort Portal and Kasenda), more elevated and thus colder lakes. This also explains the inverse relationship between MAT and transparency.

Faunistics

The species richness of Cladocera in our 62 western Uganda study lakes (37 species) is comparable to that found in a set of lowland lakes and ponds in Cameroon (35 species; Chiambeng, 2004). Due to the large number of species recorded from only one (9 species) or two (5 species) lakes, Chao's formula indicated that from 5 to 10 species were missed by this survey. More extensive sampling conducted over a longer period of time would probably reveal more species. Green (1993) had already noted that in East African freshwater lakes the long-term cumulative number of zooplankton species found could be substantially higher than the number of species sampled at any one time. We suspect that most of the species we missed are to be found in either swamp or planktonic habitats. Characteristic swamp habitat occurs at only seven of our sites and we did not encounter several of the species previously recorded from Ugandan swamps by Thomas (1961) such as *Grimaldina brazzai* and *Latonopsis fasciculata*. Also, the pelagic zone of lakes is subject to marked seasonal dynamics in algal composition (Kizito et al., 1993) which in turn is likely to result in seasonal changes in zooplankton composition.

Several cladoceran species such as *Scapholeberis kingi*, *Pseudosida szalayi* and *Moinodaphnia macleayi* were found only in dilute, but eutrophic, swampy lakes. *Pleuroxus toumodensis* and *Dunhevedia serrata* were found almost exclusively in pristine lakes with (abundant) aquatic macrophytes. At the other extreme, *Karualona iberica*, *Moina micrura* and *Macrothrix triserialis* did not exhibit clear responses to any of the measured environmental variables, indicating that these species are rather eurytopic in nature. Indeed, *Moina micrura* is considered by some to be the most successful cladoceran in tropical Africa for its widespread distribution and fast adaptation to local changes in ecological conditions (Saint-Jean & Bonou, 1994). In this study, we found this species in a wide diversity of lakes, ranging from shallow, eutrophic lakes with abundant macrophytes to very deep, oligotrophic lakes without significant littoral zone. *Alona cambouei* was often found in lakes with sandy or muddy littoral zones, while *A.* cf. *verrucosa* and *A. guttata* were more common in lakes with submerged or floating macrophytes. Different *Alona* species are known to prefer different habitats (Tremel et al., 2000) or environmental conditions (Verschuren et al., 2000; and primary references therein). *Simocephalus vetulus* was found almost exclusively in oligo- and mesotrophic lakes with submerged or emergent macrophytes. The two exceptions are Lake Ibamba and Lake Nyabikere, two eutrophic lakes with a broad reed fringe along the shore and other aquatic macrophytes in the littoral. *S. vetulus* has previously been noted to prefer dense vegetation of submerged macrophytes

(Alonso, 1996; Hann & Zrum, 1997). *Simocephalus mesorostris* was found in two shallow, pristine lakes with abundant vegetation, consistent with previous records of this species in the vegetation of warm, unpolluted water bodies with low pH and low oxygen concentrations (Orlova-Bienkowskaja, 1995). *Graptoleberis testudinaria*, a phytophilic chydorid which during feeding glides over surfaces of aquatic macrophytes like a minute snail (Fryer, 1968), was found in lakes Nyabikere and Kanyamukali. In the latter lake, we assume it must be feeding on epiphytic algae attached to submerged parts of reeds, the only aquatic macrophytes present. *Pseudochydorus* cf. *globosus* was found to be most common in oligo- and mesotrophic lakes, but it also occurred in one shallow, hyper-eutrophic lake. This species is a scavenger feeding on dead crustaceans and organic detritus (Fryer, 1968; Van Damme & Dumont, 2007). In Europe, it occurs in oligo- to slightly eutrophic waters, in association with submerged macrophytes (Flössner, 2000), but can also be the dominant cladoceran in turbid water containing little or no vegetation (Van Damme & Dumont, 2007).

Environmental regulation of Cladocera distribution in Uganda crater lakes

When considering the entire dataset, lake-water salinity (Scond) is a major factor determining Cladocera distribution among lakes, with only one species (*Moina belli*) found in the saline lakes. Having found *Moina belli* at Lake Kikorongo on several occasions since 2001, we suspect that Thomas's (1961) record of *Moina* sp. from there concerns *M. belli* as well. It has also been recorded from Lake Shala, Ethiopia, where it occurs at conductivities up to 21,000 µS (Green, 1993). Its absence from lake Nshenyi (11,230 µS/cm) in this study of the living fauna could be related to seasonal desiccation, as the samples from this lake did contain two resting eggs of *M. belli*. This low diversity in saline lakes reflects the typical freshwater association of the Cladocera, most of which are unable to tolerate conductivities above 3,000 µS/cm (Frey, 1993). Even within the freshwater range (Scond $<$ 1,500 µs/cm), cladoceran species richness was negatively correlated with conductivity. However, this pattern could be due to limited salinity tolerance of local aquatic macrophytes rather than direct physiological stress experienced by the Cladocera (Hammer, 1986; Verschuren et al., 2000).

Our CCA of cladoceran community composition in freshwater Ugandan crater lakes showed that the diversity of aquatic macrophyte habitat in a lake, TP, MAT, pH-surf, land used for crop agriculture and Mg are all important explanatory environmental variables. This result is consistent with observations that community composition in Cladocera is influenced by aquatic vegetation (Declerck et al., 2005), nutrients (Jeppesen et al., 2003; Declerck et al., 2005; Taylor et al., 2006), pH (Roff & Kwiatkowski, 1977), climate (Gyllström et al., 2005; Kamenik et al., 2007) and cations (Kamenik et al., 2007). To a certain extent, CCA axis 1 reflects broad regional differences in Mg and TP between the northern (Fort Portal and Kasenda) and southern (Bunyaruguru) lakes (Fig. 3A). CCA axis 2 distinguishes mostly pristine lakes with abundant macrophytes from those with significant human impact. The density of zooplantivorous fish, not measured in this study, may also be an important structuring force as seems to be the case in shallow European lakes (Davidson et al., 2007).

Our results match those of studies in Europe where eutrophic shallow waters, densely overgrown with macrophytes, generally support large densities of phytophilous cladocerans, including rare taxa (Gulyás, 1994; Illyová & Némethová, 2005). In this regard, it is worth noting that the species richness in Lake Kifuruka fell from 14 species in 2002 (Knockaert, 2002) to 9 in 2008 (this study), likely because macrophyte beds of *Nymphea nouchali* and *Ceratophyllum demersum* were strongly reduced by the introduction of a *Tilapia* species that feeds on aquatic macrophytes. In most tropical lakes, high transparency, low productivity, abundant aquatic macrophytes and the associated rich Cladocera fauna are maintained by wide *Phragmites australis* or *Cyperus papyrus* belts that limit terrestrial nutrient input (Dumont, 1992). Even a narrow buffer of natural vegetation along the shoreline or in the littoral zone is beneficial, particularly in shallow lakes with steep crater slopes and high soil-erosion rates. This may explain why species richness in Lake Ibamba, and to a lesser extent in Lake Nyabikora, is high compared to other shallow lakes with similar land use intensity.

Hoffmann & Dodson (2005) discuss the various ways in which land use can affect zooplankton species richness. In this study, land used for crop

agriculture is a proxy for the vulnerability of catchment soils to erosion and, therefore, also to cultural eutrophication; TP is an obvious proxy for lake trophic status at the time of sampling. In the pristine lakes we studied, species richness tended to increase with primary productivity as in Hoffman & Dodson (2005), but at the upper end of the productivity gradient Cladocera species richness drastically declined due to the absence of submerged plants. Indeed, the latter results in loss of structural habitat and food diversity (Jeppesen et al., 2003; Declerck et al., 2005). In disturbed lakes, the relationship between primary productivity and species richness was less clear, but the decline in species richness at the upper end of the productivity gradient was still obvious. This strong variation in productivity and aquatic macrophytes in shallow lakes may explain why, in contrast to Hofmann (1996), we did not find a positive correlation between cladoceran species richness and lake depth or lake size, even when limiting our dataset to relatively shallow lakes ($Z_{max} < 20$ m).

Whereas the effect of Ca concentrations on zooplankton community composition is well known (Hessen et al. 2000; Wærvågen et al., 2002; Jeziorski et al., 2008), it is unclear how Mg concentrations affect Cladocera species composition in our study region. Variation of Ca and Mg with total salinity in African lakes is controlled by carbonate precipitation in waters of higher salinity and alkalinity (Beadle, 1932). Mg carbonates will precipitate at higher alkalinities than those of Ca (Talling & Talling, 1965; Gorham et al., 1983). In our data, there was a significant correlation between Mg and both Cladocera species richness ($r = -0.387$, $P = 0.003$) and Scond ($r = 0.416$, $P = 0.001$). Additionally, among the freshwater lakes with Cladocera there is also a north–south gradient across the study region with on average higher Mg concentrations and conductivities in northern lakes than in southern lakes (Fig. 3A). We surmise that the effect of Mg on species composition can be attributed to both Scond and a north–south gradient in bedrock Mg concentrations, rather than a direct effect of Mg itself.

Conclusion

Our analysis shows that Cladocera species distribution in the crater lakes of western Uganda is most strongly determined by a number of quantifiable environmental variables such as nutrient availability (total phosphorus), the presence and diversity of aquatic macrophyte habitat, pH, mean annual temperature and the fraction of the crater catchment under agriculture. The significant turnover of cladoceran species composition along these critical environmental gradients demonstrates their potential as biological indicators for the water quality and ecosystem health of the Uganda crater lakes, as well as for palaeolimnological reconstructions of both natural and anthropogenic changes in East African lake systems. Our results suggest that, especially in the shallower Uganda crater lakes, changes in land use are the greatest threat to natural ecosystem functioning. Preservation of water quality and aquatic biodiversity in these lakes should be of primary importance.

Acknowledgments Fieldwork was conducted under Uganda National Council for Science and Technology research clearance NS 162 and Uganda Wildlife Authority Research permit UWA/TBDP/RES/50, with logistic support from Uganda Wildlife Authority. We thank Johnson Bwembale, Imke De Windt and Maureen Fagot for field assistance, Angelica Alcantara for lab assistance, Kay Van Damme for invaluable assistance with regard to the identifications, Julie Lebrun (Gembloux Agro-Bio Tech, Belgium) for data on aquatic macrophyte distribution and Lei Chou (Université Libre de Bruxelles, Belgium) and Pierre-Denis Plisnier (Royal Museum for Central Africa, Belgium) for TP and TN data. This research was sponsored by the Fund for Scientific Research of Flanders, the King Leopold III-fund for Nature Exploration and Conservation (Belgium), the Flemish Interuniversity Council, the Belgian Federal Science Policy (Action 1 project to H. Eggermont) and the Belgian Federal Science Policy in the framework of the CLANIMAE (Climate and Human Impacts on African Ecosystems) project.

References

Alonso, M., 1996. Crustacea, Branchiopoda. In Ramos, M. A., et al. (eds), Fauna Iberica, Vol. 7. Museo Nacional de Ciencias Naturales Consejo Superior de Investigaciones Cientificas, Madrid.

Beadle, L. C., 1932. Scientific results of the Cambridge Expedition to the East African Lakes, 1930–31. 4. The waters of some East African lakes in relation to their fauna and flora. Journal of the Linnean Society of London: Zoology 38: 157–211.

Bigler, C., O. Heiri, R. Krksova, A. F. Lotter & M. Sturm, 2006. Distribution of diatoms, chironomids and Cladocera in surface sediments of thirty mountain lakes in south-eastern Switzerland. Aquatic Sciences 68: 154–171.

Birks, H. J. B., 1995. Quantitative palaeoenvironmental reconstructions. In Maddy, D. & J. S. Brew (eds), Statistical Modelling of Quaternary Science Data. Technical Guide, Vol. 5. Quaternary Research Association, Cambridge.

Burgis, M. J., J. P. E. C. Darlington, I. G. Dunn, G. G. Ganf, J. J. Gwahaba & L. M. McGowan, 1973. The biomass and distribution of organisms on Lake George, Uganda. Proceedings of the Royal Society of London Series B: Biological Sciences 184: 271–298.

Bwanika, G. N., B. Makanga, Y. Kizito, L. J. Chapman & J. Balirwa, 2004. Observations on the biology of Nile tilapia, *Oreochromis niloticus* L., in two Ugandan crater lakes. African Journal of Ecology 42: 93–101.

Chen, G., C. Dalton & D. Taylor, 2010. Cladocera as indicators of trophic state in Irish lakes. Journal of Paleolimnology 44: 465–481.

Chiambeng, G. Y., 2004. Rainforest Branchiopoda (Crustacea: Anomopoda, Cetenopoda and Cyclestherida) of Cameroon, Gulf of Guinea, Central Africa. Unpublished PhD Thesis, Ghent.

Cocquyt, C., P. Plisnier, V. Gelorini, B. Rumes & D. Verschuren, 2010. Observations on the limnology and phytoplankton community of crater Lake Kyaninga (Uganda), with special attention to its diatom flora. Plant Ecology and Evolution 143: 365–377.

Colwell, R. K. & J. A. Coddington, 1994. Estimating terrestrial biodiversity through extrapolation. Philosophical Transactions of the Royal Society of London Series B: Biological Sciences 345: 101–118.

Crisman, T. L., L. J. Chapman, C. A. Chapman & J. Prenger, 2001. Cultural eutrophication of a Ugandan highland crater lake: a 25-year comparison of limnological parameters. Verhandlungen Internationalis Vereinigung Limnologie 27: 3574–3578.

Davidson, T. A., C. D. Sayer, M. R. Perrow, M. Bramm & E. Jeppesen, 2007. Are the controls of species composition similar for contemporary and sub-fossil cladoceran assemblages? A study of 39 shallow lakes of contrasting trophic status. Journal of Paleolimnology 38: 117–134.

Declerck, S., J. Vandekerkhove, L. Johannson, K. Muylaert, J. M. Conde-Porcuna, K. Van Der Gucht, C. Perze-Martinez, T. Lauridsen, K. Schwenk, G. Zwart, W. Rommens, J. Lopez-Ramos, E. Jeppesen, W. Vyverman, L. Brendonck & L. De Meester, 2005. Multi-group biodiversity in shallow lakes along gradients of phosphorous and water plant cover. Ecology 86: 1905–1915.

DeSellas, A. M., A. M. Patterson, J. N. Sweetman & J. P. Smol, 2008. Cladocera assemblages from the surface sediments of south-central Ontario (Canada) lakes and their relationships to measured environmental variables. Hydrobiologia 600: 105–119.

Dumont, H. J., 1992. The regulation of plant and animal species and communities in African shallow lakes and wetlands. Revue d'Hydrobiologie Tropicale 4: 303–346.

Dumont, H. J. & M. Silva-Briano, 2000. *Karualona* n. gen. (Anomopoda: Chydoridae), with a description of two new species, and a key to all known species. Hydrobiologia 435: 61–82.

Dumont, H. J., J. Pensaert & I. Van de Velde, 1981. The crustacean zooplankton of Mali (West Africa). Hydrobiologia 80: 161–187.

Dumont, H. J., M. Silva-Briano & K. K. Babu Subhash, 2002. Re-evaluation of the *Macrothrix rosea-triserialis* group with description of two new species (Crustacea, Anomopoda, Macrothricidae). Hydrobiologia 467: 1–44.

Eggermont, H., J. M. Russell, G. Schettler, K. Van Damme, I. Bessems & D. Verschuren, 2007. Physical and chemical limnology of alpine lakes and pools in the Rwenzori Mountains (Uganda–DR Congo). Hydrobiologia 592: 151–173.

Eggermont, H., O. Heiri, J. M. Russell, M. Vuille, L. Audenaert & D. Verschuren, 2010. Paleotemperature reconstruction in tropical Africa using fossil Chironomidae (Insecta: Diptera). Journal of Paleolimnology 43: 413–435.

Flössner, D., 2000. Die Haplopoda und Cladocera (ohne Bosminidae) Mitteleuropas. Backhuys Publishers, Leiden.

Forró, L., N. M. Korovchinsky, A. A. Kotov & A. Petrusek, 2008. Global diversity of cladocerans (Cladocera: Crustacea) in freshwater. Hydrobiologia 595: 177–184.

Frey, D. G., 1993. The penetration of cladocerans into saline waters. Hydrobiologia 267: 233–248.

Fryer, G., 1968. Evolution and adaptive radiation in the Chydoridae (Crustacea: Cladocera): a study in comparative functional morphology and ecology. Philosophical Transactions of the Royal Society of London Series B: Biological Sciences 254: 221–385.

Gorham, E., W. E. Dean & J. E. Sanger, 1983. The chemical composition of lakes in the north-central United States. Limnology and Oceanography 28: 287–301.

Green, J., 1971. Associations of Cladocera in the zooplankton of the lake sources of the White Nile. Journal of Zoology 165: 373–414.

Green, J., 1976. Changes in the zooplankton of Lakes Mutanda, Bunyoni and Mulehe (Uganda). Freshwater Biology 6: 433–436.

Green, J., 1993. Zooplankton associations in East African lakes spanning a wide salinity range. Hydrobiologia 267: 249–256.

Green, J., 1995. Altitudinal distribution of tropical planktonic Cladocera. Hydrobiologia 307: 75–84.

Gulyás, P., 1994. Studies on Rotatoria and Crustacea in the various water-bodies of Szigetköz. Limnologie Aktuell 2: 63–78.

Gyllström, M., L.-A. Hansson, E. Jeppesen, F. Garcia-Criado, E. Gross, K. Irvine, T. Kairesalo, R. Kornijow, M. R. Miracle, M. Nykänen, T. Nõges, S. Romo, D. Stephen, E. Van Donk & B. Moss, 2005. The role of climate in shaping zooplankton communities of shallow lakes. Limnology and Oceanography 50: 2008–2021.

Hammer, U. T., 1986. Saline Lake Ecosystems of the World. Junk, Dordrecht. 616 pp.

Hann, B. J. & L. Zrum, 1997. Littoral zooplankton in a prairie coastal wetland: seasonal abundance and community structure. Hydrobiologia 357: 37–52.

Hessen, D. O., L. Skardal & N. E. Wiik Alstad, 2000. Calcium limitation in *Daphnia magna*. Journal of Plankton Research 22: 553–568.

Hill, M. O. & H. G. Gauch, 1980. Detrended Correspondence analysis: an improved ordination technique. Vegetation 42: 47–58.

Hoffmann, M. D. & S. I. Dodson, 2005. Land use, primary productivity, and lake area as descriptors of zooplankton diversity. Ecology 86: 255–261.

Hofmann, W., 1996. Empirical relationships between cladocerans fauna and trophic state in thirteen northern German lakes: analysis of surficial sediments. Hydrobiologia 318: 195–201.

Illyová, M. & D. Némethová, 2005. Long-term changes in cladoceran assemblages in the Danuber floodplain area (Slovak-Hungarian stretch). Limnologica 35: 274–282.

Jeppesen, E., J. P. Jensen, C. Jensen, B. Faafeng, P. Brettum, D. Hessen, M. Søndergaard, T. Lauridsen & K. Christoffersen, 2003. The impact of nutrient state and lake depth on top-down control in the pelagic zone of lakes: study of 466 lakes from the temperate zone to the Arctic. Ecosystems 6: 313–325.

Jeziorski, A., N. D. Yan, A. M. Paterson, A. M. DeSellas, M. A. Turner, D. S. Jeffries, B. Keller, R. C. Weeber, D. K. McNicol, M. E. Palmer, K. McIver, K. Arseneau, B. K. Ginn, B. F. Cumming & J. P. Smol, 2008. The widespread threat of calcium decline in fresh waters. Science 322: 1374–1377.

Kamenik, C., K. Szeroczyńska & R. Schmidt, 2007. Relationships among recent Alpine Cladocera remains and their environment: implications for climate-change studies. Hydrobiologia 594: 33–46.

Kattel, G. R., R. W. Battarbee, A. Mackay & H. J. B. Birks, 2006. Are cladoceran fossils in lake sediment samples a biased reflection of the communities from which they are derived? Journal of Paleolimnology 38: 157–181.

Kizito, Y. S., A. Nauwerck, L. J. Chapman & W. Koste, 1993. A limnological survey of some Western Uganda Crater Lakes. Limnologica 23: 335–347.

Knockaert, A., 2002. Distribution of Crustacean Zooplankton (Cladocera) Along a Salinity Gradient of Crater Lakes in Western Uganda. Unpublished Dissertation, Master of Science in Advanced Studies in Marine and Lacustrine Sciences, Ghent.

Kořínek, V., 1984. Cladocera. Hydrobiological survey of the Lake Bangwelulu Luapula River basin. Scientific Results 13: 1–117.

Korovchinsky, N. M., 1992. Sididae and Holopedidae (Crustacea: Daphniformes). Guides to the Identification of the Microinvertebrate of the Continental Waters of the World, Vol. 3. SPB Academics, The Hague.

Kotov, A. A. & P. Štifter, 2006. Cladocera: Family Ilyocryptidae (Branchiopoda: Cladocera: Anomopoda). In Dumont, H. J. (ed.), Guides to the Identification of the Microinvertebrates of the Continental Waters of the World, Vol. 22. Backhuys Publishers, Kerkwerve.

Lehmann, J. T., 2002. Application of satellite AVHRR to water balance, mixing dynamics and chemistry of Lake Edward, East Africa. In Odada, E. & D. O. Olago (eds), The East African Great Lakes: Limnology, Paleolimnology and Biodiversity. Kluwer, Dordrecht.

Lotter, A. F., H. J. B. Birks, W. Hofmann & A. Marchetto, 1997. Modern diatom, cladocera, chironomid, and chrysophyte cyst assemblages as quantitative indicators for the reconstruction of past environmental conditions in the Alps. I. Climate. Journal of Paleolimnology 18: 395–420.

Melack, J. M., 1978. Morphometric, physical and chemical features of the volcanic crater lakes of western Uganda. Archiv für Hydrobiologie 84: 430–453.

Mutune, M. D., R. Omondi & M. Owili, 2006. Systematics and distribution of zooplankton in Lake Victoria basin, Kenya. In Odada, E. & D. O. Olago (eds), Proceedings of the 11th World Lakes Conference, Vol. 2. ILEC, Nairobi.

Orlova-Bienkowskaja, M. J., 1995. A revision of the *Simocephalus (latirostris)* species group (Crustacea: Anomopoda: Daphniidae). Hydrobiologia 36: 43–58.

Rajapaksa, R. & C. H. Fernando, 1987. Redescription and assignment of Alona globulosa Daday, 1898 to a new genus *Notoalona* and a description of *Notoalona freyi* sp. nov. Hydrobiologia 144: 131–153.

Republic of Uganda, 2002. The Second Participatory Poverty Assessment Report: Deepening the Understanding of Poverty. Ministry of Finance, Planning and Economic Development, Kampala.

Rey, J. & L. Saint-Jean, 1968. Les Cladocères (Crustacés, Branchiopodes) du Tchad. Premier note. Cahiers ORSTOM, Série Hydrobiologie 2(3–4): 79–118.

Rey, J. & L. Saint-Jean, 1969. Les Cladocères (Crustacés, Branchiopodes) du Tchad. Deuxième note. Cahiers ORSTOM. Série Hydrobiologie 3(3–4): 21–42.

Roff, J. C. & R. E. Kwiatkowski, 1977. Zooplankton and zoobenthos communities of selected northern Ontario lakes of different acidities. Canadian Journal of Zoology 55: 899–911.

Saint-Jean, L. & C. A. Bonou, 1994. Growth, production, and demography of *Moina micrura* in brackish tropical fishponds (Layo, Ivory Coast). Hydrobiologia 272: 125–146.

Sato, A., N. Takezaki, H. Tichy, F. Figueroa, W. E. Mayer & J. Klein, 2003. Origin and speciation of haplochromine fishes in east African Crater Lakes investigated by the analysis of their mtDNA, Mhc genes, and SINEs. Molecular Biology and Evolution 20: 1448–1462.

Shapiro, S. S., M. B. Wilk & H. J. Chan, 1968. A comparative study of various tests for normality. Journal of the American Statistical Association 63: 1343–1372.

Smirnov, N. N., 1976. Macrothricidae and Moindae Fauna of the world. Fauna of the U.S.S.R. Crustaceana 1(3): 1–236.

Smirnov, N. N., 1992. The Macrothricidae of the World. SPB Academic Publishing, Amsterdam.

Smirnov, N. N., 1996. Cladocera: The Chydorinae and Sayciinae (Chydoridae) of the World. Guides to the Identification of the Microinvertebrates of the Continental Waters of the World, Vol. 11. SPB Academic Publishing, Amsterdam.

Smirnov, N. N., A. A. Kotov & J. S. Coronel, 2006. Partial revision of the *aduncus*-like species of *Pleuroxus* Baird, 1943 (Chydoridae, Cladocera) from the southern hemisphere with comments on subgeneric differentiation within the genus. Journal of Natural History 40: 1617–1639.

Smol, J. P., 2002. Pollution of Lakes and Rivers: A Paleoenvironmental Perspective. Oxford University Press Inc., New York.

Statsoft Inc., 2000. Statistica for Windows. Computer Program Manual, Tulsa.

Talling, J. F. & J. Lemoalle, 1998. Ecological Dynamics of Tropical Inland Waters. Cambridge University Press, New York.

Talling, J. F. & I. B. Talling, 1965. The chemical composition of African lake waters. Internationale Revue der gesamten Hydrobiologie und Hydrographie 50(3): 421–463.

Taylor, D., C. Dalton, M. Leira, P. Jordan, G. Chen, L. Leon-Vintro, K. Irvine, H. Bennion & T. Nolan, 2006. Recent histories of six productive lakes in the Irish Ecoregion based on multiproxy palaeolimnological evidence. Hydrobiologia 571: 237–259.

Ter Braak, C. J. F., 1987. The analysis of vegetation–environment relationships by canonical correspondence analysis. Vegetatio 69: 69–77.

ter Braak, C. J. F. & P. Smilauer, 2002. CANOCO reference Manual and CanoDraw for Windows User's Guide: Software for Canonical Community Ordination (version 4.5). Microcomputer Power, Ithaca.

ter Braak, C. J. F. & P. F. M. Verdonschot, 1995. Canonical correspondence analysis and related multivariate methods in aquatic ecology. Aquatic Sciences 57: 255–289.

Thomas, I. F., 1961. The Cladocera of the Swamps of Uganda. Crustaceana 2: 108–125.

Tremel, B., S. E. Frey, N. D. Yan, K. M. Somers & T. W. Pawson, 2000. Habitat specificity of littoral Chydoridae (Crustacea, Branchiopda, Anomopoda) in Plastic Lake, Ontario, Canada. Hydrobiologia 432: 195–205.

UNEP, 2006. Africa's Lakes: Atlas of Our Changing Environment. EarthPrint.com.

Van Damme, K. & H. J. Dumont, 2007. Limb morphology of the carnivorous anomopods *Anchistropus emarginatus* Sars, 1862 and *Pseudochydorus globosus* (Baird, 1843) (Crustacea: Branchiopoda: Anomopoda). Annales de Limnologie 43: 271–284.

Van Damme, K. & H. J. Dumont, 2008. Further division of Alona Baird, 1943: separation and position of Coronatella Dybowski and Grochowski and Ovalona gen. n. (Crustacea: Cladocera). Zootaxa 1960: 1–44.

Verschuren, D., P. Plisnier, H. Hughes, J. Lebrun, V. Gelorini, C. Cocquyt & G. Mahy, 2009. CLANIMAE:Climatic and Anthropogenic Impacts on African Ecosystems. Final Report Phase 1 (2007–2008). Belspo, Brussels.

Verschuren, D., J. Tibby, K. Sabbe & N. Roberts, 2000. Effects of depth, salinity, and substrate on the invertebrate community of a fluctuating tropical lake. Ecology 81: 164–182.

Verschuren, D., B. F. Cumming & K. R. Laird, 2004. Quantitative reconstruction of past salinity variations in African lakes using fossil midges (Diptera: Chironomidae): assessment of inference models in space and time. Canadian Journal of Fisheries and Aquatic Sciences 61: 986–998.

Wærvågen, S., N. A. Rukke & D. A. Hessen, 2002. Calcium content of crustacean zooplankton and its potential role in species distribution. Freshwater Biology 47: 1866–1878.

Wakabi, W., 2006. Population growth continues to drive up poverty in Uganda. Lancet 367: 558.

White, F., 1983. The Vegetation of Africa. A Descriptive Memoir to Accompany the UNESCO/AETFAT/UNSO Vegetation Map of Africa. UNESCO, Paris.

Whittaker, R. H., 1960. Vegetation of the Siskyou Mountains, Oregon and California. Ecological Monographs 30: 279–338.

Wilson, M. V. & A. Shmida, 1984. Measuring beta diversity with presence–absence data. Journal of Ecology 72: 1055–1064.

Quaternary Research 72 (2009) 315–324

Contents lists available at ScienceDirect

Quaternary Research

journal homepage: www.elsevier.com/locate/yqres

Human impacts, climate change, and aquatic ecosystem response during the past 2000 yr at Lake Wandakara, Uganda

James M. Russell [a,*], S.J. McCoy [a], D. Verschuren [b], I. Bessems [b], Y. Huang [a]

[a] Department of Geological Sciences, Brown University, Box 1846, Providence, RI, 02912, USA
[b] Limnology Unit, Department of Biology, Ghent University, K. L. Ledeganckstraat 35, B 9000 Gent, Belgium

ARTICLE INFO

Article history:
Received 29 June 2008
Available online 21 August 2009

Keywords:
Africa
Paleoclimate
Paleolimnology
Human impacts
Holocene
Organic matter

ABSTRACT

Analyses of carbon and hydrogen isotope ratios of terrestrial leaf waxes and the carbon and nitrogen abundance, ratio, and isotopic composition of bulk sediments from Lake Wandakara, a crater lake in western Uganda, East Africa, document human and climatic controls on the aquatic system and on the surrounding terrestrial vegetation during the past two millennia. Our data indicate that Wandakara was a relatively stable, productive lake surrounded by C_3 vegetation from AD 70 to 1000. Abrupt changes in the $\delta^{13}C$ of terrestrial leaf waxes indicate a series of abrupt shifts in the relative abundance of C_3 and C_4 vegetation caused by a combination of climate change and human activities around Wandakara beginning at AD 1000. Abrupt shifts in bulk sediment organic geochemistry, particularly C/N ratios and $\delta^{15}N$, indicate that human activities at this time caused permanent changes in the limnology of Lake Wandakara, including eutrophication. Our results suggest that the biogeochemistry of Lake Wandakara was more sensitive to shifting human impacts than to climate variations during the past millennium, highlighting the importance of understanding the intensity of pre-colonial human impacts on Africa's aquatic ecosystems.

Introduction

Unraveling the causes of paleoenvironmental change is crucial to understanding the sensitivity and resilience of terrestrial and aquatic ecosystems to disturbance, as well as the complex interactions between climate, environment, and society. East African climate has fluctuated dramatically during the past two millennia, with major regional climate events registered by paleolimnological records at about AD 100, 1000, 1250, 1600 and 1800 (Verschuren et al., 2000; Alin and Cohen, 2003; Russell and Johnson, 2005, 2007). These events had an enormous impact on Africa's landscapes and lakes, including replacement of forests with grasslands during intervals of drought (Marchant and Taylor, 1998; Lamb et al., 2003), and changes in the productivity of East Africa's great lakes (e.g., Cohen et al., 2006). However, understanding the impacts of tropical African climate change must take into account large-scale use of the landscape by pre-colonial societies (Hamilton, 1972; Robertshaw et al., 2004). Complicating this issue, climate variations appear to have influenced cultural and political change in pre-colonial East African societies (Taylor, 1993; Taylor et al., 2000; Robertshaw et al., 2004), causing synergistic effects on African paleoenvironments.

A variety of factors obscure our view of the relative impacts of climate and humans on African ecosystems. First, African climate change exhibits significant regional variability (Verschuren, 2004; Russell et al., 2007; Russell and Johnson, 2007). Climate between AD 1450 and 1750, for instance, was characterized by wet conditions in eastern-most Africa (Verschuren et al., 2000; Stager et al., 2005) and drought in the western rift valley in Uganda, Tanzania, and Malawi (Russell and Johnson, 2007). Such geographic gradients invalidate the assumption that paleoclimate records can be geographically extrapolated to infer climate impacts on local ecosystems. Second, many paleoclimate reconstructions from tropical Africa are based upon biogeochemical and paleoecological analyses of lake sediments and/or palynological reconstructions of vegetation (e.g., Bonnefille and Chalié, 2000; Talbot et al., 2006). These data provide the fundamental framework for our understanding of African climate history, yet both lake biogeochemistry and terrestrial vegetation are obviously sensitive to both climate and human impacts. Characterizing the complex and interactive impacts of paleoclimatic and socio-political change thus requires multiproxy methods, including proxies exclusively sensitive to climate.

Here we apply novel, compound-specific stable isotope indicators to investigate the impacts of climate change and human land clearance on terrestrial vegetation and lacustrine biogeochemistry during the past two millennia at Lake Wandakara, a small crater lake in western Uganda (Fig. 1). This is an ideal site at which to conduct this research because the century-scale climate history of western Uganda during the past two millennia has been well characterized by investigations of

* Corresponding author.
E-mail address: James_Russell@Brown.edu (J.M. Russell).

0033-5894/$ – see front matter
doi:10.1016/j.yqres.2009.06.008

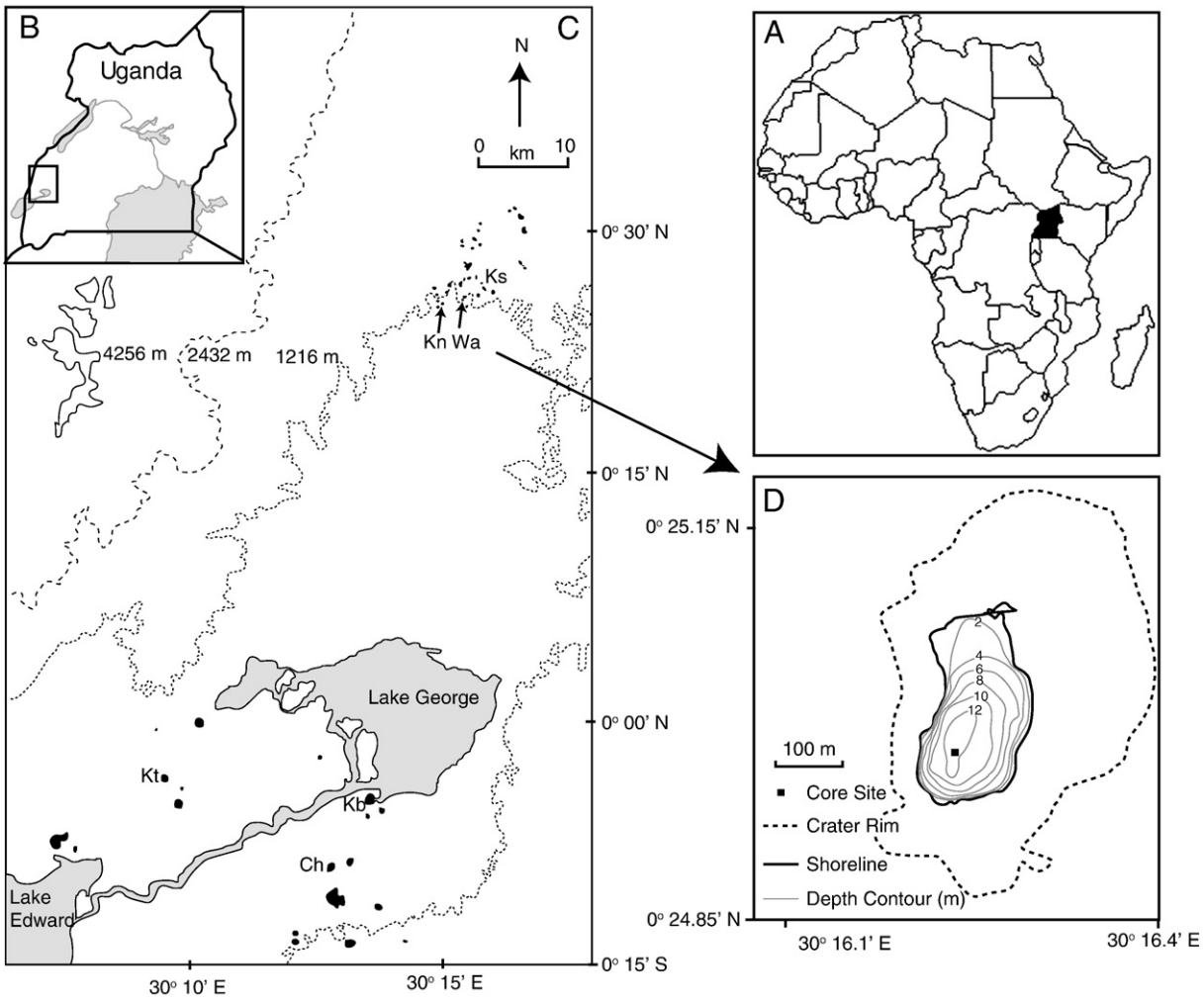

Figure 1. (A) Map of Africa with Uganda shaded. (B) Map of Uganda. The inset square inset highlights the location of the study area. (C) The crater lake district of western Uganda, modified from Melack (1978). Initials correspond to the names of lakes that have been investigated for paleoclimate studies by Bessems et al. (2008). Ks is Kasenda, Kn is Kanyamukali, Wa is Wandakara, Kt is Kitagata, Kb is Kibengo, and Ch is Chibwera. (D) Bathymetric map of Lake Wandakara with our core site.

multiple crater lakes in the region (Bessems, 2007; Bessems et al., 2008; Russell et al., 2007), as well as Lake Edward (Russell and Johnson, 2007), providing a local climate history to guide the interpretation of past ecosystem changes. Second, archaeological studies have documented substantial human interactions with the landscape in western Uganda during the past 1000 yr (Robertshaw et al., 2004; Taylor et al., 2000). Indeed, palynological investigations of Lake Wandakara indicate major changes in local vegetation in response to both climate change and pre-colonial human activities (Ssemmanda et al., 2005). Our multiproxy approach builds upon these previous studies by demonstrating that pre-colonial human landscape clearance caused substantial changes in the biogeochemistry of Lake Wandakara, and provides a new method for investigating climatic versus anthropogenic impacts on vegetation and limnological processes.

Study site

Lake Wandakara is a maar crater lake located in the Kasenda lake district of western Uganda, in the western branch of the East African rift system (Fig. 1). The lake lies within a topographically closed basin within the larger catchment area of Lake Edward to the south. It is located 1170 m above sea level, has a surface area of 4 ha, and a maximum depth of 12.25 m. The water column is seasonally stratified, with an anoxic hypolimnion, and is slightly saline with a surface conductivity of ~1060 μS/cm and a pH of 8.9. The regional climate is tropical sub-humid, with two distinct rainy seasons from March to May and from October to December (Nicholson, 1996). The annual average rainfall in western Uganda is 1300 mm, while the average annual evaporation is 1750 mm (Russell and Johnson, 2006). The lake's catchment is underlain by volcanic ash and basic volcanic rocks which have weathered to fertile soil (Bishop, 1965). This climate and soil naturally supports moist semi-deciduous forest (White, 1983); following human land clearance, however, crops such as maize, cassava, and banana are now farmed on Lake Wandakara's crater slopes.

Materials and methods

Sediment cores were taken in January 2001 and 2002 from the central, deepest part of Lake Wandakara using a single-drive piston corer for sub-recent sediments and a square-rod piston corer for deeper deposits. The topmost section containing unconsolidated sediment was sectioned upright in the field in 1-cm increments into Whirl-Pak bags to preserve physical and geochemical properties for dating. Deeper sediments were recovered in a stainless steel barrel using the square-rod piston corer, extruded in 1-m sections on site into a polyethylene sheath, and sealed in a PVC tube for transport. Multiple cores were taken to ensure overlap between adjacent core sections. Cores were shipped to Ghent University, Belgium, where they were split, macrosceopically and microscopically described, and

sampled. The 4.81-m composite core sequence recovered from Lake Wandakara consists of massive to laminated silty clays with variable calcium carbonate and organic matter concentrations; detailed lithostratigraphic information is contained in Bessems (2007).

Core chronology for late Holocene deposits was determined using ^{137}Cs, ^{210}Pb, and ^{14}C dating. ^{137}Cs activities were measured by gamma spectroscopy at Queen's University, Kingston, Canada, while ^{210}Pb activity was constrained by alpha spectrometric measurement of radiation emitted from ^{210}Po at the University of Manitoba, Winnipeg, Canada. Radiometric ages were calculated using the constant rate of supply (CRS) ^{210}Pb dating model (Appleby and Oldfield, 1978). Chronology of pre-20th century deposits was determined based on accelerator mass spectrometry (AMS) radiocarbon dates of plant macrofossils and bulk organic mud (Table 1). Our age model also includes two ^{14}C dates on terrestrial plant macrofossils from the core studied by Ssemmanda et al. (2005), which we transferred to our cores through cross-correlation of loss-on-ignition profiles and visual lithostratigraphic markers, including sediment laminations.

Samples of 0.5-mL volume were taken every 4 cm for analyses of the total organic carbon and nitrogen abundance, ratio, and isotopic composition (%OC, %N, C/N, $\delta^{13}C_{org}$ and $\delta^{15}N_{org}$). Samples were soaked in 10% HCl for 1 h to remove carbonates, followed by rinses in high-purity distilled water to remove HCl. Treated samples were freeze-dried, ground with a mortar and pestle, and analyzed using a Carlo Erba Elemental Analyzer interfaced to a Finnigan Delta Plus XL isotope-ratio mass spectrometer through a Conflo II interface. Analytical precision on internal standards was 0.3‰ for $\delta^{15}N_{org}$ and 0.07‰ for $\delta^{13}C_{org}$. All results are reported relative to air for $\delta^{15}N_{org}$ and to VPDB for $\delta^{13}C_{org}$.

We measured the hydrogen and carbon isotopic composition of leaf wax fatty acids from 27 samples taken at 10- to 20-cm intervals throughout the core. Sample preparation followed the protocol outlined by Huang et al. (2004). Briefly, sediment samples were freeze-dried and ground, and free lipids were extracted in 9:1 dichloromethane:methanol using a Dionex accelerated solvent extractor. Fatty acids were isolated using solid phase extraction (Aminopropyl Bond Elute®) in a glass column (Russell and Werne, 2007), and were methylated using anhydrous 2% HCl in methanol. Fatty acid methyl esters were purified using silica gel column chromatography prior to isotopic analysis. Ester-bound lipids were extracted from 15 of the sediment residues using saponification under reflux with 0.5 N KOH/MeOH with 2–3% water. The solution was acidified, and lipids were extracted with hexane. We then isolated, methylated, and purified the bound fatty acids using the procedure described above.

Compound identification and quantification were carried out using a gas chromatography (GC) flame ionization detector and GC–mass spectrometry prior to isotopic analysis. An HP 6890 GC–pyrolysis system stable isotope spectrometer with a high-temperature pyrolysis reactor was used for hydrogen isotopic analysis of long-chain (C_{22} and higher) free and short-chain (C_{16} and C_{18}) bound fatty acid methyl esters (FAMES). Due to variable concentrations for different fatty acids, isotope measurements focused on only two long-chain waxes, C_{28} and C_{30} *n*-acid. Carbon isotopic analyses of long-chain FAMES were performed on an HP 6890 GC with a Combustion Interface interfaced to a Finnigan Delta$^+$ XL. The precision (1-sigma) of triplicate δD measurements was ≤2‰; precision on $\delta^{13}C$ analysis was ≤0.5‰. Accuracy was checked by analysis of laboratory isotopic standards between every six injections. All δD measurements are reported in per mil (‰) notation relative to SMOW, and $\delta^{13}C$ analyses are reported in ‰ notation relative to VPDB. Values were corrected for the isotopic composition of the added methyl group by mathematically removing their isotopic contributions (Huang et al., 2004).

Results and interpretations

Our multiproxy reconstruction of environmental change at Lake Wandakara is based primarily upon five different geochemical analyses of its sedimentary organic matter: C/N, the $\delta^{13}C$ and $\delta^{15}N$ of bulk organic matter, and the $\delta^{13}C$ and δD of fatty acids. Below we briefly summarize the primary controls on each of these and discuss their interpretation in the context of our record from Lake Wandakara.

Core chronology

The sediment core spans the interval from about AD 70 to 2000 (Fig. 2). ^{137}Cs activity has a maximum value at 33-cm depth (Fig. 2A), similar to the depth recorded by Ssemmanda et al. (2005), that probably records the 1963/64 fallout maximum. Total ^{210}Pb activity shows a fairly regular and exponential decline from values of 0.94 Bq/g at the core top to a supported value of 0.15 Bq/g at 96.5-cm depth (Fig. 2B). CRS age modeling indicates an average sedimentation rate of 0.060 ± 0.021 g/cm^2/yr in the ^{210}Pb-dated interval, with an age estimate of AD 1860 for 96.5-cm depth. Paired dating of terrestrial macrofossils and bulk organic matter indicates that a substantial radiocarbon reservoir exists in Lake Wandakara. We have applied a reservoir correction of 1865 ^{14}C yr to bulk ages based upon the average age differences between paired dates across the entire core (Bessems, 2007). Four of our eleven ^{14}C dated intervals returned outlying ages that may result from either sediment reworking or incorrect assumptions regarding our reservoir correction. However, 4 dates from terrestrial macrofossils and 3 reservoir-corrected bulk organic carbon

Table 1
AMS ^{14}C from Lake Wandakara.

Depth (cm)	Lab no.	Dated material	^{14}C age ± error (yr AD)	Calibrated age (AD)	Calibrated age range (AD)
104.5	Poz-18552	OM	1655 ± 30	–	–
171	Poz-16552	OM	2150 ± 30	1548	1494–1601 (0.632)
253	Poz-16553	OM	2545 ± 35	1329	1267–1391 (1.0)
271	*Poz-18553*	*OM*	*2910 ± 35*	*986*	*938–1033 (0.877)*
351	*Poz-18629*	*OM*	*3585 ± 35*	*323*	*242–403 (1.0)*
392	Poz-5497	OM	3380 ± 35	561	502–620 (0.762)
446	Poz-19323	Leaf/stem	1740 ± 40	346	212–409 (0.988)
446	*Poz-18554*	*OM*	*2800 ± 35*	*1099*	*1022–1076 (1.0)*
462	Poz-19327	Leaf/stem	1790 ± 35	198	130–266 (0.744)
462	Poz-19325	Stem	1790 ± 35	198	130–266 (0.744)
462	Poz-19324	Leaf	1820 ± 35	190	120–259 (0.922)
462	*Poz-18578*	*OM*	*3320 ± 30*	*604*	*558–649 (0.988)*
234*	AAR-6885	Leaf	655 ± 40	1336	1276–1397 (1.0)

Samples marked by an asterisk are from Ssemmanda et al. (2005). Dated material includes organic matter (OM) and terrestrial plant leaves, stems, and twigs. Calibrated ages were obtained from Reimer et al. (2004) and Stuiver et al. (1998) after applying an 1865-yr reservoir correction to bulk organic matter dates. Calibrated age ranges are the highest probability range in the 2-sigma range, probabilities are given in parenthesis. The sample at 104.5-cm depth returned a negative range, indicating that the reservoir correction was likely too large for this sample. Samples in italic font were not included in our age model (Fig. 2) as they appeared as stratigraphic outliers.

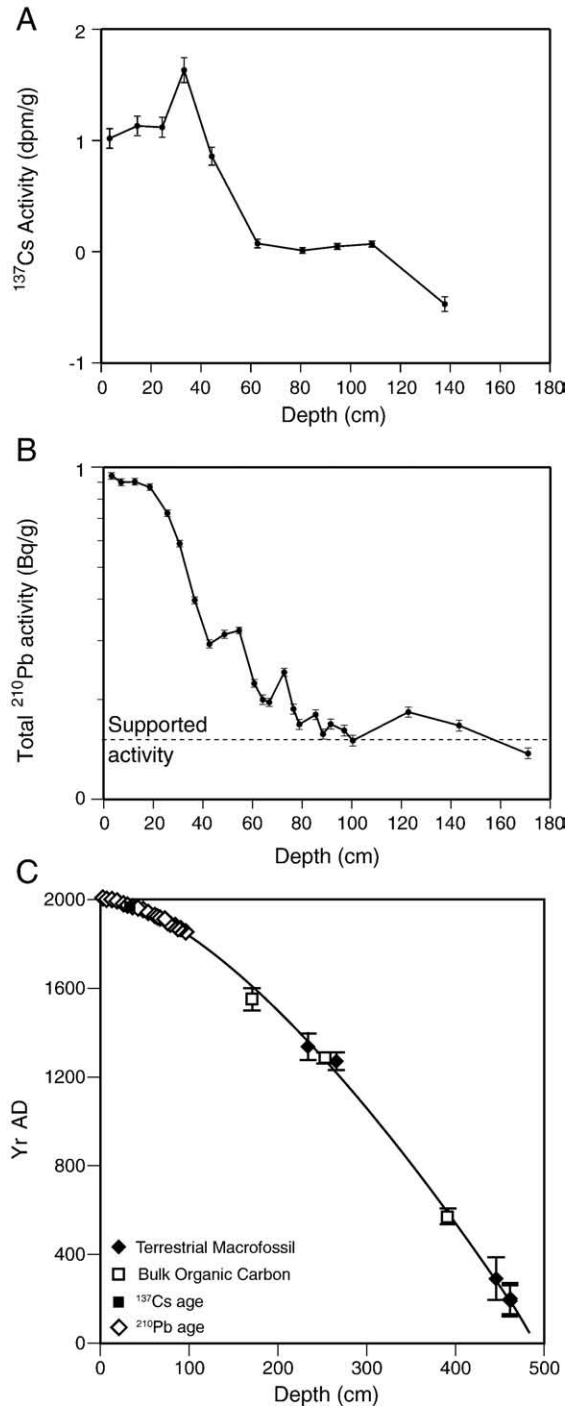

Figure 2. Year/depth model for Lake Wandakara based upon ^{137}Cs, ^{210}Pb, and AMS ^{14}C ages. The line represents a 3rd-order polynomial regression through dated intervals. ^{14}C dates on bulk organic carbon have been corrected for an 1865-yr reservoir effect. Four bulk ^{14}C dates that appeared to be stratigraphic outliers are not shown. Error bars indicate 2-sigma age ranges from Calib 5.0.2 (Reimer et al., 2004; Stuiver et al., 1998).

^{14}C dated levels fit reasonably well with our ^{210}Pb and ^{137}Cs based age models. A 3rd-order polynomial regression to these data forms the basis for our age model (Fig. 2C). Results below are reported in years AD.

C/N: organic matter sources in Lake Wandakara

Organic carbon concentrations (on a carbonate-free basis) vary between 4.7 and 48.7%, while %N varies between 0.5 and 5.6% (Fig. 3). %OC and %N values vary substantially at centennial time-scales around mean values of about 30% (%OC) and 3% (%N) until a dramatic decline centered on AD 1700. This time interval is represented by an ~35-cm-thick silt bed in our core, which Ssemmanda et al. (2005) show to have high magnetic susceptibility. In general, low %OC values reflect high siliciclastic mineral concentrations (Bessems, 2007). Following this minimum, %OC and %N return to their average values at about AD 1800.

The ratio of carbon to nitrogen has long been used to distinguish organic matter (OM) derived from phytoplankton and OM produced by terrestrial plants (Meyers, 1994; Prahl et al., 1980). Atomic C/N ratios of less than 10 are typically interpreted to reflect OM derived from phytoplankton, while C/N values greater than 20 reflect OM sourced from terrestrial plants (Talbot and Lærdal, 2000). However, selective loss of N from sedimentary organic matter during early diagenesis, as well as nitrogen limitation experienced by growing phytoplankton favor high sedimentary C/N ratios even when the OM is primarily of phytoplankton origin (Hecky et al., 1993; Talbot and Lærdal, 2000).

The C/N ratio of sedimentary OM in Lake Wandakara varies between 6.7 and 12.1 (Fig. 3), which is relatively low compared to many other East African lakes (Talbot and Lærdal, 2000). Given these low values combined with the effects of OM diagenesis and nitrogen limitation during phytoplankton growth, we interpret the C/N ratio to reflect predominantly aquatic sources of OM to the sediments in Lake Wandakara. In sediments deposited between AD 70 and 1250, the C/N of organic matter varies between 10.3 and 12.1, with a weakly rising trend and little coherent century-scale variability. These values likely represent aquatic biomass formed under relatively low N availability. The C/N ratio decreases abruptly from higher than 11 to less than 9 at AD 1250, then further declines from mean values of ~9 around AD 1400 to ~7.4 at the sediment surface, with little change in the low-organic silts deposited at about AD 1700. We interpret this decline to reflect changes in the stoichiometry of aquatic organic matter rather than a change in OM source, with the low C/N values of OM sourced predominantly from phytoplankton indicating progressively less N limitation for phytoplankton growth.

Carbon isotopes of bulk organic matter

There is a large range of possible $\delta^{13}C$ compositions of bulk sedimentary OM, due to variations in OM source, the degree of fractionation by terrestrial plants and aquatic algae, and processes that alter the isotopic composition of dissolved CO_2 in lakes. The photosynthetic pathway used by local vegetation is the dominant control on the $\delta^{13}C$ of terrestrial OM. Most plants, including trees, shrubs, and some grasses fix carbon through the C_3 pathway, and have bulk $\delta^{13}C$ values that typically lie between −30 and −25‰. In contrast, most tropical grasses as well as some crops such as maize, sugar cane, and millet, are C_4 vascular plants. C_4 plants have enriched $\delta^{13}C_{org}$ values relative to C_3, with typical values ranging from −16 to −10‰ (Meyers, 1997).

$\delta^{13}C_{org}$ in our core from Lake Wandakara averages −26.9‰ from AD 70 to 1150, with a weak positive trend towards the present (Fig. 3). From AD 1150 to present, $\delta^{13}C_{org}$ exhibits large, abrupt oscillations with peak values of −14.2‰, −13.9‰, and −15.7‰ at about AD 1300, 1450, and 1700, respectively. Intervening periods centered at AD 1400, 1550, and 1800 to the present have $\delta^{13}C_{org}$ values averaging −24‰, enriched relative to values in sediments deposited from AD 70 to 1150. The amplitude of the shifts beginning at AD 1250 is similar to the difference between end-member compositions of C_3 and C_4 plants, suggesting a control of vegetation type on $\delta^{13}C_{org}$; however, the low C/N of the sedimentary OM indicates that the dominant source of organic matter is aquatic, not terrestrial—including sediments deposited during the abrupt peaks in $\delta^{13}C_{org}$. Interestingly, much of the Wandakara sedimentary sequence falls well outside typical C/N-$\delta^{13}C_{org}$ compositional fields for freshwater algae and terrestrial plants

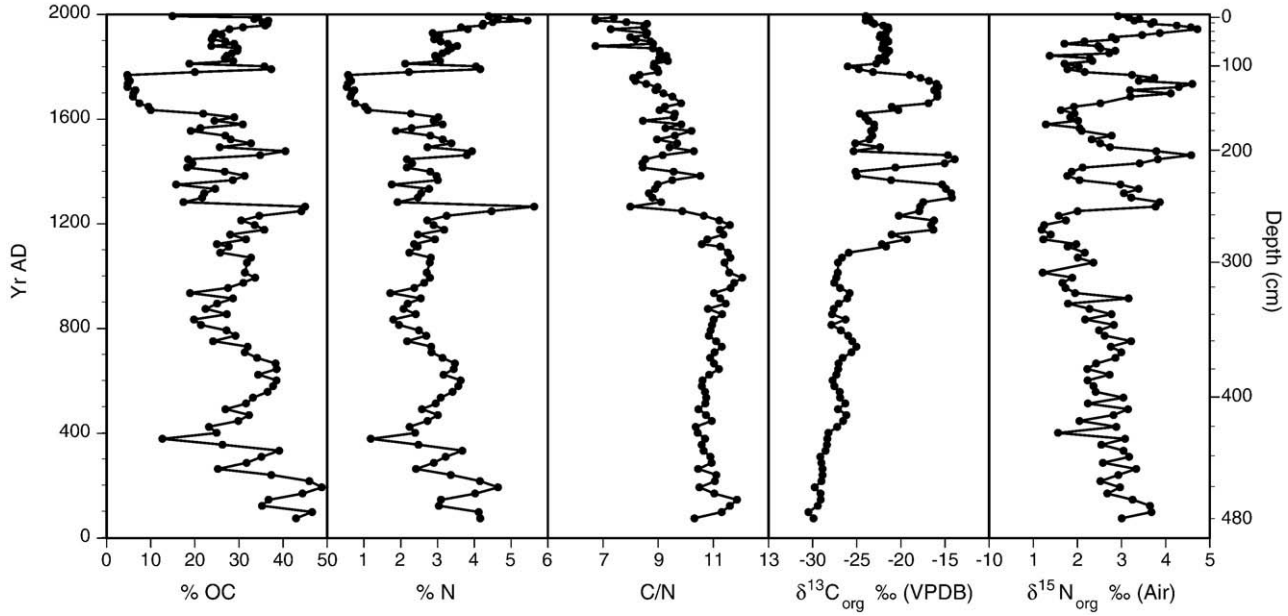

Figure 3. Bulk organic geochemical measurements, including % organic carbon, % nitrogen, atomic C/N ratio, $\delta^{13}C_{org}$, and $\delta^{15}N_{org}$ from Lake Wandakara plotted by age (at left) and depth (at right). Note the non-linear depth scale, indicating compaction of sediment with depth.

(Fig. 4) (Meyers, 1994; Meyers and Ishiwarty, 1993). A variety of limnological processes, too numerous to review here, can enrich the $\delta^{13}C$ of aquatic OM, including bacterial processing of terrestrial C4 organic matter (Hedges et al., 1997), eutrophication (Schelske and Hodell, 1995), algal metabolism (Meyers, 1994; Talbot and Johannessen, 1992), and reservoir effects on DIC (Talbot, 1990). Additional proxies are thus needed to understand the $\delta^{13}C$ variability observed in Lake Wandakara through time.

Leaf wax carbon isotopes

Long-chain fatty acids from Lake Wandakara show strong even-over-odd chain-length predominance with peak abundances near the C_{30} *n*-acid, indicating that they are primarily derived from terrestrial plants (Eglinton and Hamilton, 1967). The $\delta^{13}C$ of leaf waxes is typically depleted relative to bulk biomass (Hedges et al., 1997), but C_3 and C_4 vegetation can still be distinguished because leaf waxes from C_3 plants typically have $\delta^{13}C$ values of about −35‰, while those from C_4 plants have values of about −20‰ (Huang et al., 2000). $\delta^{13}C$ values of the C_{28} and C_{30} *n*-acids in Lake Wandakara are strongly correlated (Fig. 5A); only trends in $\delta^{13}C$ for the C_{30} *n*-acid ($\delta^{13}C_{C30}$) will be described here. $\delta^{13}C_{C30}$ varies between −33 and −28‰ between AD 70 and 1100 with a weak positive trend toward the present (Fig. 5), reflecting an originally mostly C_3 terrestrial vegetation with gradually increasing C_4 abundances. $\delta^{13}C_{C30}$ shifts abruptly toward values of ~−20‰ between AD 1200 and 1440 implying almost pure C_4 vegetation surrounding Lake Wandakara, then falls to ~−30‰ around AD 1440. $\delta^{13}C_{C30}$ remains low until AD ~1600, then rises to a peak of −20.1‰ at AD 1740, declines to −27‰ by about AD 1800, and then varies between −26 and −29.5‰ from AD 1800 to the present. These more recent values reflect mixed C_3/C_4 vegetation, as exists in the crater basin today.

Abrupt shifts in the $\delta^{13}C_{C30}$ of Lake Wandakara sediments match both the timing and amplitude of abrupt changes in $\delta^{13}C_{org}$ (Fig. 6). It is highly unlikely that lake-driven variations in $\delta^{13}C_{org}$ would match the amplitude of vegetation-driven changes in $\delta^{13}C_{C30}$. We therefore argue that the $\delta^{13}C$ of bulk organic matter is largely controlled by shifts in the vegetation surrounding Lake Wandakara, despite a predominantly aquatic source of organic matter to the sediments as indicated by low C/N. Lakes receive large subsidies of organic carbon from their watersheds, much of which is reprocessed by microbes before burial (Cole et al., 1994; Einsele et al., 2001; Meyers and Ishiwarty, 1993). This reprocessing can enrich the originally terrestrial organic matter with nitrogen while retaining the isotopic composition of terrestrial biomass (Hedges et al., 1997). Dissolved and particulate organic matter from soils bears the isotopic composition of terrestrial plants but has low C/N ratios relative to terrestrial plant OM (Meyers and Teranes, 2001), and therefore would require relatively little microbial alteration if soil OM is the predominant source of OM to lake sediments. Although the exact mechanisms are unclear, our $\delta^{13}C_{org}$ and $\delta^{13}C_{C30}$ data clearly show that vegetation type can exert a dominant control on the $\delta^{13}C$ of aquatic organic matter in tropical crater lakes. In addition, these data document large changes in the vegetation surrounding Lake Wandakara, confirming palynological evidence for substantial human and/or climatic impacts on vegetation in the region (Ssemmanda et al., 2005).

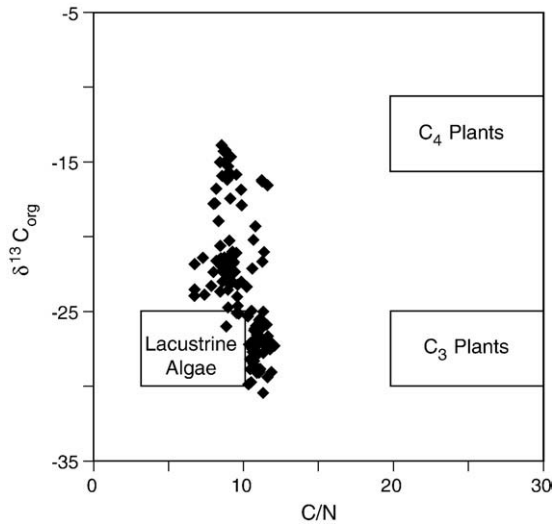

Figure 4. Crossplot of atomic C/N and ^{13}Corg values with typical compositions of lacustrine algae, C3 and C4 plants illustrated by boxes as suggested in Meyers (1997. Data from Lake Wandakara are indicated by diamonds, and do not appear consistent with typical algal or land plant compositions.

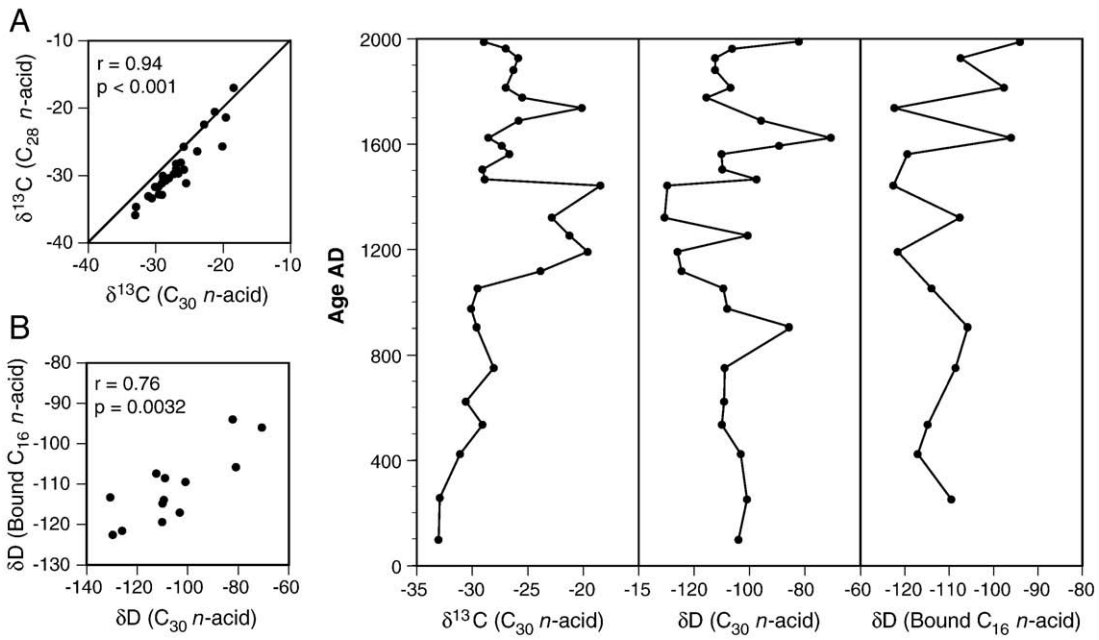

Figure 5. (A) Crossplot of δ^{13}CC30 and δ^{13}CC28 exhibiting strong correlation. (B) Crossplot of δDC30 and δDC16. At bottom, δ13CC30, δDC30, and δDC16 are plotted against age.

Fatty acid hydrogen isotopes

The δD of long-chain, terrestrially derived fatty acids is controlled by the δD of the water used by plants, transpiration from leaf surfaces, and kinetic fractionation during biosynthesis (Hou et al., 2008; Sessions et al., 1999). The δD of tropical rainfall, which forms the source water for leaf waxes, is controlled by the 'amount effect', which causes rainfall δD to become isotopically depleted as the rainfall amount increases (Dansgaard, 1964; Vuille et al., 2005). Decreased plant transpiration under more humid conditions will deplete the δD of leaf waters and the fatty acids formed from these waters, amplifying the amount effect, although growth chamber experiments have shown the transpiration effect to be relatively small (Hou et al., 2008). The amount effect and plant transpiration are typically interpreted to dominate leaf wax δD variations in tropical sediment records (e.g., Liu et al., 2005; Schefuß et al., 2005); however, vegetation type also can influence leaf wax δD through differences in D/H fractionation. C_4 and C_3 grasses appear to have broadly similar biosynthetic fractionation factors for D/H in leaf waxes (Chikaraishi and Naraoka, 2003), but field and culture experiments have shown that fatty acids produced by trees can have δD compositions enriched by ~50‰ relative to grasses from the same environment due to different apparent fractionation factors (Hou et al., 2007, 2008). However, recent surveys of long-chain fatty acids preserved in lake sediments in the American southwest have shown that interactions between humidity and vegetation type produce relatively invariant apparent fractionation between leaf wax and local rainfall δD (Hou et al., 2008). Although more arid conditions cause isotopically heavier rainfall and higher plant transpiration, increasing the δD of leaf waxes, drier environments also favor grasses, which produce isotopically depleted leaf waxes, balancing the amount and transpiration effects. Thus, although the first-order control on leaf wax δD in the tropics is the δD of meteoric waters, interactions between climate and vegetation suggest the potential for complex, non-linear responses of leaf wax δD to rainfall variability.

Considering these multiple controls on the δD of long-chain fatty acids, we also analyzed the δD of bound C_{16} fatty acid. Short-chain (C_{16}–C_{18}) fatty acids in lake sediments are derived primarily from aquatic sources (Eglinton and Hamilton, 1967; Huang et al., 2002), and the principal control on their δD is the δD of lake water (Huang et al., 2002, 2004). The δD of closed-basin tropical lakes such as Wandakara reflects the hydrologic balance of the lake, with drier conditions causing isotopically enriched lake water due to both the amount effect on precipitation and kinetic fractionation during evaporation from the lake surface, which favors the retention of deuterium relative to hydrogen in the lake water (Craig, 1961). By comparing δD_{C16} and δD_{C30}, we can thus elucidate which δD variations reflect real hydroclimatic changes, as opposed to other processes.

δD_{C30} varies between −100 and −110‰ from AD 70 to 800, peaks at −81‰ around AD 950, then varies from −131 to −124‰ from AD 1100 to 1450 (aside from a single peak at AD 1250; Fig. 5). Over this interval, δD_{C16} rises from −118‰ to 107‰ from AD 70 to 1000, then falls to values of −120‰ and lower from about AD 1200 to 1550, aside from a single peak at AD 1320. δD_{C30} rises from −130 to −70‰ between AD ~1450 and 1620, then falls to −112‰ by about 1760. δD_{C16} peaks at −97‰ at AD 1620, similar in timing to enrichments in δD_{C30}, then oscillates between values of −122 and −96‰ from AD 1700 to the present. δD_{C30} remains low from AD 1760 to 1920, then becomes more enriched toward the present. δD_{C16} and δD_{C30} are positively correlated (Fig. 5B), with intervals of isotopic enrichment centered on about AD 1000 and 1600, similar to the timing of major droughts in the region (Russell and Johnson, 2007).

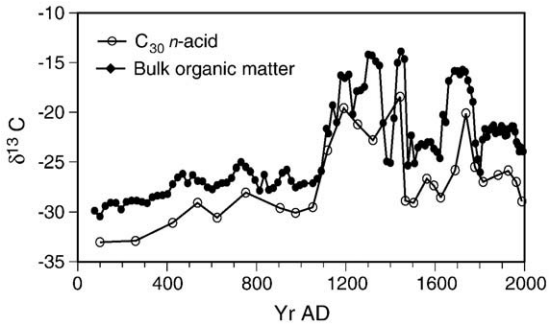

Figure 6. δ^{13}C of bulk organic matter and C_{30} n-acid plotted versus age. Note the similarity in both the timing and amplitudes of the observed changes.

If changes in vegetation surrounding Lake Wandakara were mainly driven by rainfall, $\delta^{13}C_{C30}$ and δD_{C30} should also be positively correlated: during intervals of drought shifts toward C_4 ecosystems would occur, recorded by enriched δD_{C30} values. However, $\delta^{13}C_{C30}$ and δD_{C30} are clearly negatively correlated (Fig. 5). In fact, large positive shifts in $\delta^{13}C_{C30}$ are associated with depleted δD_{C30} values, and peak $\delta^{13}C_{C30}$ from AD 1200 to 1440 occurs during an interval of regionally wet climate conditions (Russell et al., 2007, Russell and Johnson, 2007). This suggests that the abrupt shifts toward C_4 vegetation were not caused by climate but instead by human activities on the landscape, presumably forest clearance for agriculture (Ssemmanda et al., 2005).

Nitrogen isotopes of organic matter: biogeochemical impacts of forest clearance

Measured $\delta^{15}N$ values for East African vegetation range from 4 to 15‰, with no consistent differences in the $\delta^{15}N$ of trees and grasses (Muzuka, 1999). Conversion of organic matter to nitrate, which would be favored in oxic terrestrial soils, further enriches the $\delta^{15}N$ of nitrate that is transported to lakes (Meyers and Teranes, 2001). Algae typically discriminate against ^{15}N during assimilation (François et al., 1996; Talbot, 2001; Talbot and Lærdal, 2000), and the selective removal of ^{14}N during photosynthesis progressively enriches the residual nitrogen pool. Other processes that can enrich $\delta^{15}N_{org}$ include ammonia volatization (Collister and Hayes, 1991; Talbot and Johannessen, 1992), and microbial nitrification and denitrification (Talbot, 2001). On the other hand, nitrogen fixation by cyanobacteria produces OM with a $\delta^{15}N$ of ~0‰ (Talbot, 2001).

The shift in trends, variability, and values at about AD 1200 is also apparent in $\delta^{15}N_{org}$ (Fig. 5), indicating that human conversion of C_3- to C_4-dominated ecosystems surrounding Lake Wandakara strongly altered the lake's nitrogen cycle. $\delta^{15}N_{org}$ slowly declines from ~3‰ to ~1‰ from AD 400 to 1250. This shift likely indicates a gradual rise in the abundance of N-fixing cyanobacteria in the lake, perhaps related to decreasing N availability as suggested by increasing C/N (Hecky and Kling, 1987). After reaching a minimum value of 1.2‰ at AD 1170, $\delta^{15}N_{org}$ exhibits relatively large, 3‰ oscillations with enriched values at about AD 1300, 1460, 1730, and 1940. The switch in $\delta^{15}N_{org}$ variability is roughly coincident with changes in $\delta^{13}C_{org}$ and an abrupt decrease in C/N. We suggest that these variations result from an increased flux of isotopically enriched N from the landscape during conversion of forest to grassland. This hypothesis is confirmed by decreases in %OC during peaks in $\delta^{15}N_{org}$, implying dilution of %OC by clastic minerals. Interestingly, C/N values do not rise during periods of depleted $\delta^{13}C_{org}$ and $\delta^{15}N_{org}$ after AD 1250, suggesting that land clearance at that time resulted in a permanent switch toward elevated nitrogen concentrations in Lake Wandakara.

Discussion

Distinguishing human versus climatic controls on East African vegetation

Archaeological and palynological investigations provide evidence of human impact on western Ugandan landscapes beginning at about 500 BC with the arrival of Bantu people, who brought iron use and a range of different crops. Yet widespread forest clearance and environmental impacts are not suggested until about AD 1000, coincident with the appearance of large settlements, cereal agriculture, and new ceramic cultures. These populations then dispersed in the late 18th century to form pastoralist kingdoms (Robertshaw et al., 2004; Sutton, 1995, 1998; Taylor et al., 1999, 2000).

Palynological investigations of the vegetation history surrounding Lake Kasenda (~5 km from Wandakara) indicate replacement of forest by grassland by AD 1000, followed by a return to forest at both Kasenda and Wandakara at AD 1750 (Ssemmanda et al., 2005), in agreement with the documented regional human demographic changes. Yet forest clearance and regrowth at AD 1000 and 1800, respectively, in western Uganda must also have been affected by intervals of high rainfall and drought. Geochemical and stable isotopic investigations of sedimentary calcite in Lake Edward (Russell and Johnson, 2007) as well as lithostratigraphic studies of western Ugandan crater lakes (Russell et al., 2007) indicate a largely coherent hydroclimatic history for the region, with major droughts centered at about AD 100, 1100, and 1600, while AD 400, 1000, 1300, and the late 1700s were relatively wet. Geochemical data from Lake Edward indicates that the interval from AD 500 to 850 was also relatively dry (Russell and Johnson, 2005), although not all climate records in the region register changes during that time.

Because century-scale climate changes in East Africa appear linked to changes in large-scale atmospheric and oceanic circulation (Verschuren, 2004), it is highly unlikely that these climate events did not affect Lake Wandakara. Both carbonate geochemical (Bessems, 2007) and diatom-based salinity reconstructions from Lake Wandakara (Ryves et al., in revision) indicate drought conditions at ca. AD 1000 and 1600, coincident with the climate history outlined above. The effects of climate on Lake Wandakara can thus be inferred through comparison of our new data with this regional climate history.

Furthermore, we suggest that it may be possible to elucidate human versus climate impacts on vegetation using compound-specific stable isotopic data. Positive excursions in both δD_{C16} and δD_{C30} suggest drought conditions at about AD 1000 and 1600, identical in timing to major droughts during the past millennium identified at Lake Edward (Russell and Johnson, 2007). However, δD_{C30} exhibits an enormous range relative to δD_{C16}, with δD_{C30} values ranging from −70 to −130‰. The shift toward grassland at AD 1000 must therefore have influenced the δD_{C30} record due to biosynthetic fractionation differences between trees and grasses (Hou et al., 2007). Indeed, the enormous amplitude of shifts in δD_{C30} relative to δD_{C16} likely results from the replacement of forest with C_4 grasslands during wet periods—a process driven by humans rather than by climate. The amplified δD_{C30} response occurs because of a combination of the amount effect during wet periods and stronger isotopic fractionation by grasses relative to trees, both of which favor isotopically depleted δD_{C30} (Hou et al., 2008). This constitutes a novel method for detecting human impacts on vegetation, and highlights the importance of understanding the processes controlling vegetation changes when interpreting geochemical records of climate.

Human impacts on vegetation and aquatic ecosystems at Lake Wandakara

Paleolimnological investigations in tropical Africa have largely assumed that population densities prior to colonial times were too low to have significantly affected aquatic ecosystems. This contrasts with paleolimnological studies in Europe (Fritz, 1989; Renberg et al., 1993), South America (Binford et al., 1987; Abbott and Wolfe, 2003), and North America (Ekdahl et al., 2004) that document substantial prehistoric human impacts on lakes, including lake eutrophication, as well as palynological studies that indicate substantial human impacts on vegetation in East Africa (e.g., Taylor et al., 2000).

Our multiproxy dataset from Lake Wandakara, coupled with the regional paleoclimate reconstructions described above, allows us to distinguish both human impacts on vegetation as well as impacts on Lake Wandakara itself. From AD 70 until ~1000, Lake Wandakara was surrounded by C_3 vegetation. %OC, C/N and $\delta^{15}N_{org}$ data suggest a relatively productive aquatic ecosystem, with a gradually decreasing supply of dissolved N through time which perhaps resulted in increasing importance of cyanobacteria. δD_{C30} exhibits intermediate values during this interval, with a peak at AD 900 that may correlate with a minor drought, also registered by rising Mg/Ca in Lake Edward

(Fig. 7). Lake Wandakara thus appears to have been a relatively stable and resilient ecosystem during this time period, despite evidence for century-scale hydroclimatic change in western Uganda.

Lake Wandakara changed dramatically at AD 1000, when $\delta^{13}C$ data register an abrupt increase in the abundance of C_4 vegetation (Fig. 7). The $\delta^{13}C_{C30}$ signal could reflect either replacement of forest by C_4 grasses, or the local establishment of sorghum and millet farming, which have been documented in western Uganda at this time by archaeological studies (Sutton, 1995, 1998). Ssemmanda et al. (2005) interpreted grassland expansion at this time as "linked to human impact during a brief arid phase," and Taylor et al. (1999) present evidence for human forest clearance around AD 1000 at Kabata Swamp, ~10 km from Lake Wandakara. Regional paleoclimate records suggest dry conditions throughout equatorial East Africa beginning at about AD 1000 (Verschuren, 2004), yet δD_{C30} shifts towards relatively depleted values, indicating a strong control of vegetation type on δD. Although the relative importance of humans versus climate on grassland expansion at AD 1000 remains difficult to disentangle, we speculate that the negative shift in δD_{C30} despite drier conditions suggests that the primary factor influencing vegetation was humans, as climate effects typically dominate δD variability during climate-driven changes in vegetation (Hou et al., 2008).

Wet conditions returned to western Uganda from AD 1200 to 1450, yet C_4 vegetation persisted around Lake Wandakara, indicating strong human control of terrestrial vegetation. Interestingly, abrupt changes in C/N and $\delta^{15}N_{org}$ at Lake Wandakara do not occur until AD 1250, lagging changes in $\delta^{13}C_{org}$ by ~150 yr. This lag could reflect a delayed response of the lake to grassland expansion, the effects of increased rainfall during a period of intense human use of the landscape, or increasing utilization of the Wandakara watershed by humans from AD 1250 on, resulting in the eutrophication of Lake Wandakara. In support of the latter interpretation, %OC and %N decline rapidly at AD 1250, indicating increases in clastic mineral input consistent with landscape clearance. These shifts are synchronous with increasing $\delta^{15}N_{org}$ but lag shifts in $\delta^{13}C_{org}$, likely indicating that climate-induced changes in terrestrial vegetation were followed by landscape clearance, siltation, and alteration of the nitrogen cycle at Lake Wandakara during the early part of the 2nd millennium AD. Robertshaw et al. (2004) argues for an increase in the number and size of agricultural settlements in western Uganda from AD 1180 to 1400, coincident with the timing of changes in the nitrogen cycle documented at Lake Wandakara. Moreover, western Ugandan farmers are thought to have fertilized agricultural fields with cattle manure, which would provide a source of isotopically enriched N to Lake Wandakara (Teranes and Bernasconi, 2000). In any case, that the abrupt changes in C/N and $\delta^{15}N_{org}$ do not occur until clear evidence appears for human alteration of the local vegetation indicates that Lake Wandakara was more sensitive to human activities than to climate variability at this time.

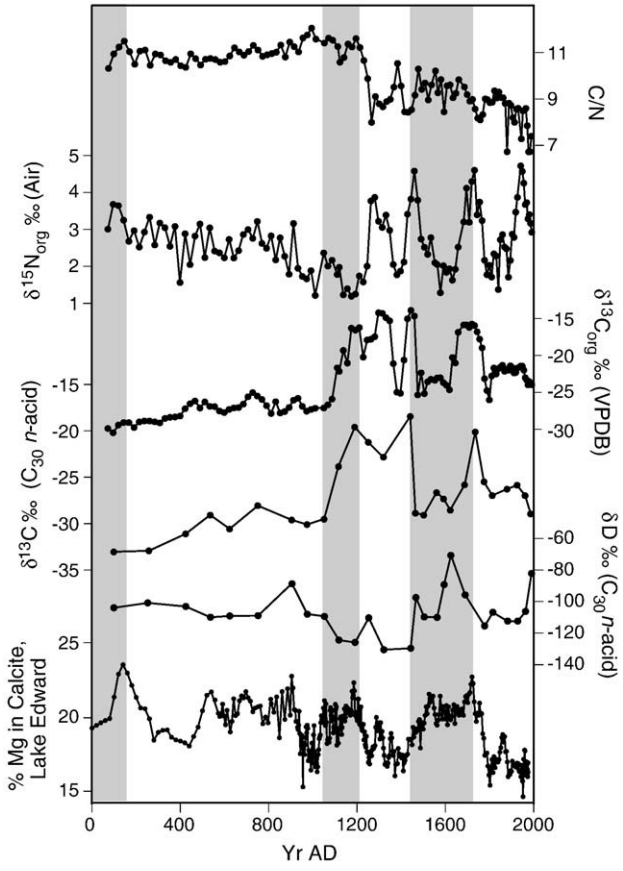

Figure 7. Key organic geochemical indicators from Lake Wandakara plotted with the % Mg in calcite from Lake Edward, an indicator of the salinity of the lake. Rising and high % Mg values in Lake Edward indicate more saline conditions and drought, while falling or low values indicate relatively wet conditions. Gray bars are droughts indicated by the Lake Edward record as well as other regional datasets discussed in the text.

Dry conditions returned to western Uganda at AD 1450 and persisted until 1750 (Russell and Johnson, 2007). $\delta^{13}C_{C30}$ values average −27‰ during this interval, indicating that a mix of C_3 and C_4 vegetation surrounded Lake Wandakara, yet palynological data suggest dominance of grassland at this time (Ssemmanda et al., 2005). Abundant C_3 grasses seem unlikely given evidence for widespread drought. An alternative explanation could be the cultivation of C_3 crops in the Wandakara watershed at this time. A brief peak in $\delta^{13}C_{C30}$ indicates the re-expansion of C_4 grassland at AD 1750, coinciding with very low %OC (Fig. 2), reflecting heavy siltation in Lake Wandakara related to a second phase of watershed clearance. This is followed by the development of a mixed C_3/C_4 ecosystem, consistent with widespread evidence for the dispersal of human populations in western Uganda and associated forest regrowth. Despite evidence for reforestation around Lake Wandakara in the late 18th century, neither C/N ratios nor $\delta^{15}N_{org}$ return to the values observed in the 1st millennium AD. Human occupation of the basin in the 11th century thus caused semi-permanent changes in the chemistry of soils in the Wandakara basin and/or in the nitrogen biogeochemistry of Lake Wandakara.

Conclusions

We document profound historical changes in the aquatic ecosystem of Lake Wandakara, western Uganda, and the terrestrial vegetation within the lake's crater basin. Wandakara was a relatively stable, productive lake surrounded by C_3 vegetation prior to human alteration of the landscape about 1200 AD. Although the relative abundance of C_3 and C_4 vegetation around Wandakara varied between AD 1000 and today due to combinations of human activities and climate, human activities from about AD 1200 appear to have caused permanent changes in the limnology of Lake Wandakara, including eutrophication, suggesting that the biotgeochemistry of this lake is far more sensitive to human impacts than to climate. Whether Lake Wandakara is archetypical or atypical in this regard will require similar studies at other lakes in the region.

Acknowledgments

We thank Hilde Eggermont for field assistance, Marcelo Alexandre for laboratory assistance, and David Ryves for discussion during the preparation of this manuscript. We thank the Ugandan National Council of Science and Technology for permission to conduct this research, funds from Brown University to JR, and the Fund for Scientific Research of Flanders and the Belgian Federal Science Policy for partial funding of the research described in this paper.

References

Abbott, M.B., Wolfe, A.P., 2003. A 1300-year record of pre-Incan metallurgy recorded by lake sediments from the Bolivian Andes. Science.

Alin, S.R., Cohen, A.S., 2003. Lake-level history of Lake Tanganyika, East Africa, for the past 2500 years based on ostracode-inferred water-depth reconstruction. Palaeogeography, Palaeoclimatology, Palaeoecology 199, 31–49.

Appleby, P.G., Oldfield, F., 1978. The calculation of ^{210}Pb dates assuming a constant rate of supply of unsupported ^{210}Pb to the sediment. Cantena 5, 1–8.

Bessems, I., 2007. Late-Holocene climatic reconstruction in equatorial East Africa: sedimentology and stable isotope geochemistry of lake deposits. Universiteit Gent.

Bessems, I., Verschuren, D., Russell, J.M., Hus, J., Cumming, B., 2008. Paleolimnological evidence for widespread late-18th century drought across equatorial East Africa. Palaeogeography, Palaeoclimatology, Palaeoecology 259, 107–120.

Binford, M.W., Brenner, M., Whitmore, T.J., Higuera-Gundy, A., Deevey, E.S., Leyden, B., 1987. Ecosystems, paleoecology, and human disturbance in subtropical and tropical America. Quaternary Science Reviews 6, 115–128.

Bishop, W.W., 1965. Quaternary geology and geomorphology in the Albertine Rift Valley, Uganda. Geologic Society of America Special Publication 48, 293–320.

Bonnefille, R., Chalié, F., 2000. Pollen-inferred precipitation time-series from equatorial mountains, Africa, the last 40 kyr BP. Global Planetary Change 26, 1257–1266.

Chikaraishi, Y., Naraoka, H., 2003. Compound-specific dD and d13C analyses of n-alkanes extracted from terrestrial and aquatic plants. Phytochemistry 63, 361–371.

Cohen, A.S., Lezzar, K.E., Cole, J., Dettman, D.L., Ellis, G.S., Eagle, M., Chorokoa, K., Plisnier, P.D., Langenberg, V., Michelo, V., Zilifi, D., 2006. Late Holocene linkages between decade-scale climate variability and productivity at Lake Tanganyika, Africa. Journal of Paleolimnology 36.

Cole, J.J., Caraco, N.F., Kling, G., Kratz, T.K., 1994. Carbon dioxide supersaturation in the surface waters of lakes. Science 265, 1568–1570.

Collister, J.W., Hayes, J.M., 1991. A preliminary study of the carbon and nitrogen isotope biogeochemistry of lacustrine sedimentary rocks from the Green River Formation, Wyoming, Utah, and Colorado. U.S. Geological Survey Bulletin A–G, C1–C16.

Craig, H., 1961. Isotopic variation in meteoric waters. Science 133, 1702–1703.

Dansgaard, W., 1964. Stable isotopes in precipitation. Tellus 16, 436–468.

Eglinton, G., Hamilton, R.J., 1967. Leaf epicuticular waxes. Science 156, 1332–1334.

Einsele, G., Yan, J., Hinderer, M., 2001. Atmospheric carbon burial in modern lake basins and its significance for the global carbon budget. Global Planetary Change 30, 167–195.

Ekdahl, E., Teranes, J.L., Guilderson, T., Turton, C.L., McAndrews, J.H., Wittkop, C., Stoermer, E.F., 2004. Prehistorical record of cultural eutrophication from Crawford Lake, Canada. Geology 32, 745–748.

François, R., Pilskaln, C.H., Altabet, M., 1996. Seasonal variation in the nitrogen isotopic composition of sediment trap materials collected in Lake Malawi. In: Johnson, T.C., Odada, E.O. (Eds.), The Limnology, Climatology, and Paleoclimatology of the East African Lakes. Gordon and Breach, Amsterdam, pp. 241–250.

Fritz, S.C., 1989. Lake development and limnological response to prehistoric and historic land-use in Diss, Norfolk, U. K. Journal of Ecology 77, 182–202.

Hamilton, A.C., 1972. The interpretation of pollen diagrams from highland Uganda. Palaeoecology of Africa 7, 45–149.

Hecky, R.E., Kling, H.J., 1987. Phytoplankton ecology in the great lakes of the rift valleys of central Africa. Archiv fur Hydrobiologie Ergebisse Limnologie 25, 3–34.

Hecky, R.E., Campbell, P., Hendzel, L.L., 1993. The stoichiometry of carbon, nitrogen, and phosphorus in particulate matter of lakes and oceans. Limnology and Oceanography 38, 1476–1481.

Hedges, J.I., Keil, R.G., Benner, R., 1997. What happens to terrestrial organic matter in the ocean? Organic Geochemistry 27, 195–212.

Hou, J., D'Andrea, W., MacDonald, D., Huang, Y., 2007. Hydrogen isotope variability in leaf waxes among terrestrial and aquatic plants around Blood Pond, Massachusetts (USA). Organic Geochemistry 38, 977–984.

Hou, J., D'Andrea, W., Huang, Y., 2008. Can sedimentary leaf waxes record D/H ratios of continental precipitation? Field, model, and experimental assessments. Geochimica et Cosmochimica Acta. 72, 3503–3517.

Huang, Y., Dupont, L., Sarnthein, M., Hayes, J.M., Eglinton, G., 2000. Mapping of C4 plant input from North West Africa into North East Atlantic sediments. Geochimica et Cosmochimica Acta 64, 3505–3513.

Huang, Y., Shuman, B., Wang, Y., Webb, T., 2002. Hydrogen isotope ratios of palmitic acid in lacustrine sediments record late-Quaternary climate variations. Geology 30, 1103–1106.

Huang, Y., Shuman, B., Wang, Y., Webb, T., 2004. Hydrogen isotope ratios of individual lipids in lake sediments as novel tracers of climatic and environmental change: a surface sediment test. Journal of Paleolimnology 31, 363–375.

Lamb, H.F., Derbyshire, I., Verschuren, D., 2003. Vegetation response to rainfall variation and human impact in central Kenya during the past 1100 years. Holocene 13, 285–292.

Liu, W., Huang, Y., An, Z., Clemens, S.C., Li, L., Prell, W.L., Ning, Y., 2005. Summer monsoon intensity controls C4/C3 plant abundance during the last 35 ka in the Chinese Loess Plateau: carbon isotope evidence from bulk organic matter and individual leaf waxes. Palaeogeography, Palaeoclimatology, Palaeoecology 220, 243–257.

Marchant, R., Taylor, D., 1998. Dynamics of montane forest in central Africa during the late Holocene: a pollen-based record from western Uganda. Holocene 8, 375–381.

Melack, J.M., 1978. Morphometric, physical, and chemical features of the volcanic crater lakes of Western Uganda. Archiv fur Hydrobiologie 85, 430–453.

Meyers, P.A., 1994. Preservation of elemental and isotopic source identification of sedimentary organic matter. Chemical Geology 144, 289–302.

Meyers, P.A., 1997. Organic geochemical proxies of paleoceanographic, paleolimnologic, and paleoclimatic processes. Organic Geochemistry 27, 213–250.

Meyers, P.A., Ishiwarty, R., 1993. Lacustrine organic geochemistry — an overview of indicators of organic matter sources and diagenesis in lake sediments. Organic Geochemistry 20, 867–900.

Meyers, P.A., Teranes, J.L., 2001. Sediment organic matter. In: Last, W.M., Smol, J.P. (Eds.), Tracking Environmental Change Using Lake Sediments. Kluwer Academic Publishers, Dordrecht.

Muzuka, A.N.N., 1999. Isotopic compositions of tropical East African flora and their potential as source indicators of organic matter in coastal marine sediments. Journal of African Earth Sciences 28, 757–766.

Nicholson, S.E., 1996. A review of climate dynamics and climate variability in Eastern Africa. In: Johnson, T.C., Odada, E.O. (Eds.), The Limnology, Climatology, and Paleoclimatology of the East African Lakes. Gordon and Breack Publishers, Amsterdamn, pp. 25–56.

Prahl, F.G., Bennett, J.T., Carpenter, R., 1980. The early diagenesis of aliphatic hydrocarbons and organic matter in sedimentary particulates from Dabob Bay, Washington. Geochimica et Cosmochimica Acta 44.

Reimer, P.J., Baillie, M.G.L., Bard, E., Bayliss, A., Beck, J.W., Bertrand, C., Blackwell, P.G., Buck, C.E., Burr, G.S., Cutler, K.B., Damon, P.E., Edwards, R.L., Fairbanks, R.G., Friedrich, M., Guilderson, T., Hogg, A.G., Hughen, K.A., Kromer, B., McCormac, F.G., Manning, S.W., Ramsey, C.B., Reimer, R.W., Remmele, S., Southon, J.R., Stuiver, M., Talamo, S., Taylor, F.W., van der Plicht, J., Weyhenmeyer, C.E., 2004. IntCal04 terrestrial radiocarbon age calibration 26–0 ka BP. Radiocarbon 46, 1029–1058.

Renberg, I., Korsman, T., Birks, H.J.B., 1993. Prehistoric increases in the pH of acid sensitive Swedish lakes caused by land-use changes. Nature 362, 824–827.

Robertshaw, P., Taylor, D., Doyle, S., Marchant, R., 2004. Famine, climate, and crisis in Western Uganda. In: Battarbee, R.W., Gasse, F., Stickley, C.E. (Eds.), Past Climate Variability through Europe and Africa, Developments Palaeoenvironmental Research, Springer, Dordrecht, pp. 535–547.

Russell, J.M., Johnson, T.C., 2005. A high-resolution geochemical record from Lake Edward, Uganda-Congo, and the timing and causes of tropical African drought during the late Holocene. Quaternary Science Reviews 24, 1375–1389.

Russell, J.M., Johnson, T.C., 2006. The water balance and stable isotope hydrology of Lake Edward, Uganda-Congo. Journal of Great Lakes Research 32, 77–90.

Russell, J.M., Johnson, T.C., 2007. Little Ice Age drought in equatorial Africa: ITCZ migrations and ENSO variability. Geology 35, 21–24.

Russell, J.M., Werne, J.P., 2007. The use of solid phase extraction columns in fatty acid purification. Organic Geochemistry 38, 48–51.

Russell, J.M., Eggermont, H.E., Verschuren, D., 2007. Spatial complexity of Little Ice Age climate in East Africa: sedimentary records from two crater lake basins in Western Uganda. Holocene 17, 183–193.

Ryves, D.B., Mills, K., Bennike, O., Brodersen, K.P., Lamb, A.L., Leng, M.J., Russell, J.M., Ssemmanda, I., in revision. Testing the coherence of paired lakes to environmental change: a late Holocene multiproxy palaeolimnological study from two crater lakes in western Uganda. Quaternary Science Reviews.

Schefuß, E., Schouten, S., Schneider, R.R., 2005. Climatic controls on central African hydrology during the past 20,000 years. Nature 437, 1003–1006.

Schelske, C.L., Hodell, D.A., 1995. Using carbon isotopes of bulk sedimentary organic matter to reconstruct the history of nutrient loading and eutrophication in Lake Erie. Limnology and Oceanography 40, 918–929.

Sessions, A.L., Burgoyne, T.W., Schimmelmann, A., Hayes, J.M., 1999. Fractionation of hydrogen isotopes in lipid biosynthesis. Organic Geochemistry 30, 1193–1200.

Ssemmanda, I., Ryves, D.B., Bennike, O., Appleby, P.G., 2005. Vegetation history in western Uganda during the last 1200 years: a sediment-based reconstruction from two crater lakes. Holocene 15, 119–132.

Stager, J.C., Ryves, D.B., Cumming, B., Meeker, L., Beer, J., 2005. Solar variability and the levels of Lake Victoria, East Africa, during the last millennium. Journal of Paleolimnology 33, 243–251.

Stuiver, M., Reimer, P.J., Bard, E., Beck, J.W., Burr, G.S., Hughen, K.A., Kromer, B., McCormac, F.G., van der Plicht, J., Spurk, M., 1998. INTCAL98 radiocarbon age calibration, 24,000–0 cal BP. Radiocarbon 40, 1041–1083.

Sutton, J.E.G., 1995. The growth of farming communities in Africa from the equator southwards. Azania 29 (/30), 1–332.

Sutton, J.E.G., 1998. Ntusi and Bigo: farmers, cattle-herders, and rulers in western Uganda, AD 1000–1500. Azania 33, 39–72.

Talbot, M.R., 2001. Nitrogen isotopes in paleolimnology. In: Last, W.M., Smol, J.P. (Eds.), Tracking Environmental Change using Lake Sediments Volume 2: Physical and Geochemical Methods. Kluwer Acadmic Publishers, Dordrecht, pp. 401–440.

Talbot, M.R., 1990. A review of the paleohydrological interpretation of carbon and oxygen isotopic ratios in primary lacustrine carbonates. Chemical Geology (Isotope Geoscience Section) 80, 261–279.

Talbot, M.R., Johannessen, T., 1992. A high resolution paleoclimatic record for the last 27,500 years in tropical West Africa from the carbon and nitrogen isotopic composition of lacustrine organic matter. Earth Planetary Sciences Letter 110, 23–37.

Talbot, M.R., Lærdal, T., 2000. The late Pleistocene–Holocene paleolimnology of Lake Victoria, East Africa, based upon elemental and isotopic analyses of sedimentary organic matter. Journal of Paleolimnology 23, 141–164.

Talbot, M.R., Jensen, N.B., Laerdal, T., Filippi, M.L., 2006. Geochemical responses to a major transgression in giant African lakes. Journal of Paleolimnology 35, 467–489.

Taylor, D., 1993. Environmental change in montane southwest Uganda: a pollen record for the Holocene from Ahakagyezi Swamp. Holocene 3, 324–332.
Taylor, D., Marchant, R., Robertshaw, P., 1999. A sediment-based history of medium altitude forest in central Africa: a record from Kabata Swamp, Ndale volcanic field, Uganda. Journal of Ecology 87, 303–315.
Taylor, D., Robertshaw, P., Marchant, R., 2000. Environmental change and political upheaval in precolonial western Uganda. Holocene 10, 527–536.
Teranes, J.L., Bernasconi, S.M., 2000. The record of nitrate utilization and productivity limitation provided by $\delta^{15}N$ values in lake organic matter — a study of sediment trap and core sediments from Baldeggersee, Switzerland. Limnology and Oceanography 45, 801–813.
Verschuren, D., 2004. Decadal and century-scale climate variability in tropical Africa during the past 2,000 years. In: Battarbee, R.W. (Ed.), Past Climate Variability Through Europe and Africa. Elsevier Paleoenvironmental Research Book Series, Amsterdam.
Verschuren, D., Laird, K.R., Cumming, B., 2000. Rainfall and drought in equatorial East Africa during the past 1,100 years. Nature 403, 410–414.
Vuille, M., Werner, M., Bradley, R.S., Keimig, F., 2005. Stable isotopes in precipitation in the Asian monsoon region. Journal of Geophysical Research 110, 108.
White, F., 1983. The Vegetation of Africa. A Descriptive Memoir to Accompany the UNESCO/AETFAT/UNSO Vegetation Map of Africa. UNESCO, Paris.

Available online at www.sciencedirect.com
ScienceDirect
Geochimica et Cosmochimica Acta 74 (2010) 4902–4918
Geochimica et Cosmochimica Acta
www.elsevier.com/locate/gca

Environmental controls on branched tetraether lipid distributions in tropical East African lake sediments

J.E. Tierney [a,b,*], J.M. Russell [a], H. Eggermont [c,d], E.C. Hopmans [e], D. Verschuren [c], J.S. Sinninghe Damsté [e,f]

[a] Brown University, Department of Geological Sciences, Box 1846, 324 Brook St., Providence, RI 02912, USA
[b] Lamont-Doherty Earth Observatory of Columbia University, 61 Route 9W, Palisades, NY 10964, USA
[c] Limnology Unit, Ghent University, K. L. Ledeganckstraat 35, B-9000 Ghent, Belgium
[d] Royal Belgian Institute of Natural Sciences, Freshwater Biology, Vautierstraat 29, 1000 Brussels, Belgium
[e] NIOZ Royal Netherlands Institute for Sea Research, Department of Marine Organic Biogeochemistry, P.O. Box 59, 1790 AB Den Burg, Texel, The Netherlands
[f] University of Utrecht, Institute of Earth Sciences, P.O. Box 80.021, 3508 TA Utrecht, The Netherlands

Received 25 October 2009; accepted in revised form 1 June 2010; available online 9 June 2010

Abstract

Quantifying past continental temperature changes is an important aspect of paleoclimate research as it allows us to constrain the amplitude of natural variability, test predictive climate models, and provide a proper context for changes that may arise in response to anthropogenically-induced climate change. The recently developed biomarker-based methylation index of branched tetraethers/cyclization ratio of branched tetraethers (MBT/CBT) proxy shows potential as a new method for continental temperature reconstruction, but thus far it has only been applied successfully in ocean margin sediments. To assess whether this proxy is also applicable to the sedimentary record in tropical lacustrine systems, we investigated the distribution of branched glycerol dialkyl glycerol tetraethers (GDGTs) in recently deposited sediments from 46 lakes in tropical East Africa. These lakes span a substantial range in surface elevation (770–4500 m above sea level), and thus also a wide gradient of mean annual temperature. We find that, saline lakes excepted, branched GDGTs are universally abundant in the lakes investigated and can be used to predict mean annual air temperature (MAAT) with a high degree of accuracy. However, the existing global MBT/CBT calibration for MAAT based on soils predicts inaccurate temperatures when applied to our African lake dataset. This observation, together with the fact that surface water pH, and to lesser extent, lake depth appear to influence the distribution of branched GDGTs among sites, leads us to conclude that *in situ* production of branched GDGTs in lakes is likely. The robust relationship between branched GDGT distribution and the temperature and pH of African freshwater lakes makes these compounds suitable for paleoenvironmental reconstruction, however we urge caution in using branched GDGTs in lake sediments to infer past temperatures, unless their exact origin can be determined.

1. INTRODUCTION

The reconstruction of past changes in continental air temperature is of utmost importance to properly constrain climatic changes of the past, as well as to provide proper context to anthropogenically-induced climate modification. However, the reconstruction of past absolute temperatures is not trivial, especially in the tropics. Tree-ring methods (Fritts, 1974) and fossil pollen preserved in lake sediments (Webb and Bryson, 1972) have long been applied to quantitatively reconstruct past temperatures in mid- to high latitude regions (e.g., Esper et al., 2002; Davis et al., 2003). Yet the use of these methods in the tropics is difficult,

* Corresponding author. Now at: Lamont-Doherty Earth Observatory of Columbia University, 61 Route 9W, Palisades, NY 10964, USA. Tel.: +1 401 863 2810.
E-mail address: tierney@ldeo.columbia.edu (J.E. Tierney).

0016-7037/$ - see front matter © 2010 Elsevier Ltd. All rights reserved.
doi:10.1016/j.gca.2010.06.002

due to the scarcity and poor preservation of trees with demonstrably annual growth rings (Dunbar and Cole, 1999) and the sensitivity of tropical plants to environmental variables other than temperature, in particular the amount and seasonality of precipitation (e.g., Vincens et al., 2007). Paleothermometry based on the distribution of aquatic biota, such as chironomid larvae, along the modern-day temperature gradient (e.g., Walker et al., 1991; Lotter et al., 1997) shows promise in tropical Africa (Eggermont et al., 2009), however chironomids are also sensitive to in-lake variables such as pH, dissolved oxygen, and lake productivity, which may or may not correlate with temperature (Velle et al., 2005). Likewise, the geochemical method of temperature reconstruction based on oxygen isotope ratios in tropical lake sediment, speleothem or ice core archives is complicated by the influence of rainfall amount and moisture source on the isotopic composition of rainfall (Barker et al., 2001; Gasse, 2002), and hence may not yield a pure temperature signal (Vuille et al., 2003).

Paleotemperature proxies based on molecular biomarkers in microorganisms such as bacteria and archaea are a promising alternative to the methods listed above. One potential advantage is that the environmental controls acting upon membrane lipid distributions in these microorganisms may be relatively uncomplicated. For example, the TEX_{86} (TetraEther IndeX of 86 carbons) paleotemperature proxy (Schouten et al., 2002; Powers et al., 2004) has been successfully used to quantitatively reconstruct past temperature change on the African continent (Powers et al., 2005; Tierney et al., 2008, 2010). Unfortunately, this proxy appears to be applicable only in large lake systems (Blaga et al., 2009; Powers et al., 2010), limiting its general use.

A newly developed molecular biomarker method, the so-called MBT/CBT (methylation index of branched tetraethers/cyclization ratio of branched tetraethers) proxy (Weijers et al., 2007a), shows considerable promise as a means to reconstruct past continental temperatures. This proxy is based on the relative abundances of branched glycerol dialkyl glycerol tetraethers (GDGTs), bacterial membrane lipids found ubiquitously in soils, peat bogs, and lake sediments (Sinninghe Damsté et al., 2000; Weijers et al., 2006a, 2007a; Blaga et al., 2009; Tierney and Russell, 2009). Weijers et al. (2007a) showed that the distribution of branched GDGTs in soils worldwide is strongly influenced by two environmental variables — local air temperature and soil pH — and used these relationships to define temperature and pH inference functions based on the MBT and CBT indices. The MBT/CBT proxy has since been successfully applied to reconstruct air temperatures from marine deltaic and near-margin environments (e.g., the Congo Fan, Weijers et al., 2007b; the North Sea, Donders et al., 2009; Rueda et al., 2009), where branched GDGTs are associated with a large influx of terrestrial soil organic matter.

Branched GDGTs are present in sediments of all lakes investigated thus far (Blaga et al., 2009; Tierney and Russell, 2009), suggesting that the MBT/CBT paleothermometer may also be applied to these systems. However, there is evidence for an autochthonous, *in situ* source of branched GDGTs in lakes in addition to an allochthonous source associated with soil organic matter (Sinninghe Damsté et al., 2009; Tierney and Russell, 2009). If this is the case, the mixture of soil-derived and lake-derived branched GDGTs in lake sediments could seriously hamper application of the MBT/CBT proxy, or limit its use to lakes where one of these sources is proved negligible.

To further explore whether the MBT/CBT proxy can be applied to lacustrine environments, we investigated the distribution of branched GDGTs in surficial sediments from 46 lakes in tropical East Africa. This region is ideal for such a study, because (1) limited seasonality in air temperature reduces possible complications arising from seasonal variation in branched GDGT production, and (2) East African lakes vary widely in size, depth, pH, and salinity, potentially allowing us to separate the specific influence of each of these environmental variables on GDGT distribution among lakes. Most importantly, the altitude range of our East African lake sites (from 770 m to 4500 m) allows us to compare branched GDGT distributions across a large gradient of mean annual air temperature (MAAT; 1–25 °C) within a relatively small geographical area.

2. MATERIALS AND METHODS

2.1. Site sampling and limnological data

We collected intact surface sediment samples (0–1 cm or 0–2 cm) from mid-lake locations in a diverse set of 46 lakes in East Africa (Fig. 1), including small maar crater lakes, large tectonic lakes, valley swamps, and high-elevation mountain lakes. Our dataset covers a wide range in elevation (770–4500 m), conductivity (8–135,000 μS/cm), depth (0.5–110 m), water-column mixing regime (shallow to permanently stratified), and sedimentary organic carbon content (0.9–49.6%). Year of collection, locations, and the specific limnological characteristics of each lake are listed in Table A1. In a few cases, local MAAT was derived directly from on-site temperature loggers (indicated with an

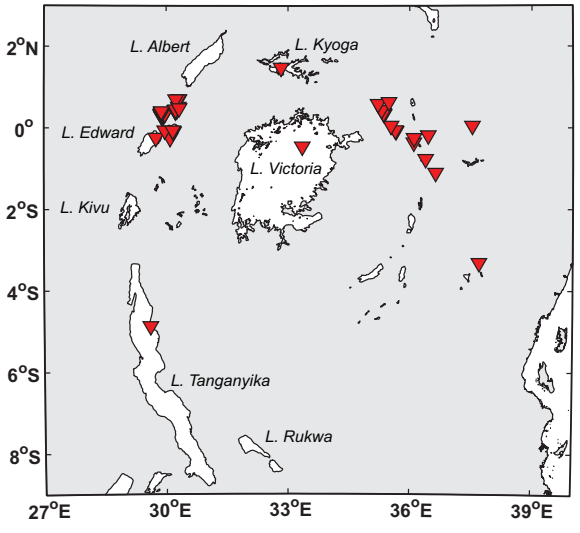

Fig. 1. Location of the 46 study lakes in equatorial East Africa.

asterisk in Table A1), but in most cases it was calculated from a region-specific tropical lapse rate model (Eggermont et al., 2009) which uses a combination of temperature logger data, Global Historical Climatology Network (GHCN) data and Global Summary of the Day (GSOD) data (for a full discussion see Eggermont et al., 2009). Given the modest root mean square error (RMSE) of this lapse-rate model (0.95 °C) compared to the regional MAAT gradient covered (1–25 °C), we refer to the model's MAAT estimates as simply 'MAAT'. Limnological data (surface and bottom water temperature and pH, surface conductivity, bottom dissolved oxygen, depth, surface area, catchment area) were collected during field surveys by the authors (usually spread over multiple seasons and years) or compiled from the published literature; data sources are indicated in Table A1.

2.2. Sediment analyses

Sediment samples were freeze-dried and then homogenized using a mortar and pestle. A small aliquot was analyzed for total organic carbon (TOC) content using a Carlo Erba Instruments NC2100 elemental analyzer (EA); samples were treated with a weak solution of HCl (0.5N) to remove any authigenic carbonate prior to EA analysis. The remaining sediment (1–6 g, depending on TOC content) was extracted with a Dionex© accelerated solvent extraction (ASE) system with a 9:1 v/v mixture of dichloromethane (DCM) and methanol (MeOH). Total lipid extracts were separated into apolar and polar fractions using Al_2O_3 column chromatography, with hexane/DCM (9:1, v/v) and DCM/MeOH (1:1, v/v) as the respective eluents. The polar fraction was dried under N_2 gas, redissolved in hexane/isopropanol (99:1, v/v) and then filtered through a PTFE 0.45 μm filter prior to analysis by high performance liquid chromatography/atmospheric pressure chemical ionization-mass spectrometry (HPLC/APCI-MS). Analysis was performed with an Agilent 1100 LC/MSD SL at the Royal Netherlands Institute for Sea Research (NIOZ), using single ion monitoring (SIM) mode of the following ions: *m/z* 1292, *m/z* 1050, *m/z* 1048, *m/z* 1046, *m/z* 1036, *m/z* 1034, *m/z* 1032, *m/z* 1022, *m/z* 1020, *m/z* 1018 and following the analytical methods of Schouten et al. (2007). Peak areas were integrated according to the method described in Weijers et al. (2007a). Quantification of GDGTs was achieved by adding a synthetic C_{46} GDGT standard (cf. Huguet et al., 2006) to the fraction containing the GDGTs prior to the filtration step. However, five lake sites used in this study were previously prepped and analyzed for GDGT composition and lacked an internal standard, thus are missing absolute concentration data. Relative abundances of each individual branched GDGT are expressed as fractions of the sum of all nine recovered compounds, and referred to as 'fractional abundances'.

The MBT and CBT indices were calculated as in Weijers et al. (2007a), with roman numerals corresponding to the structures in Fig. 2:

$$\mathrm{MBT} = \frac{([\mathrm{I}] + [\mathrm{Ib}] + [\mathrm{Ic}])}{([\mathrm{I}] + [\mathrm{Ib}] + [\mathrm{Ic}]) + ([\mathrm{II}] + [\mathrm{IIb}] + [\mathrm{IIc}]) + ([\mathrm{III}] + [\mathrm{IIIb}] + [\mathrm{IIIc}])} \quad (1)$$

$$\mathrm{CBT} = -\log\left(\frac{([\mathrm{Ib}] + [\mathrm{IIb}])}{([\mathrm{I}] + [\mathrm{II}])}\right) \quad (2)$$

The resulting MBT and CBT values were used to infer temperature and pH using the equations of Weijers et al. (2007a):

$$\mathrm{MBT} = 0.122 + 0.187 \times \mathrm{CBT} + 0.020 \times \mathrm{MAAT} \quad (3)$$

$$\mathrm{CBT} = 3.33 - 0.38 \times \mathrm{pH} \quad (4)$$

We also calculated the branched and isoprenoidal tetraether (BIT) index (Hopmans et al., 2004) as a representation

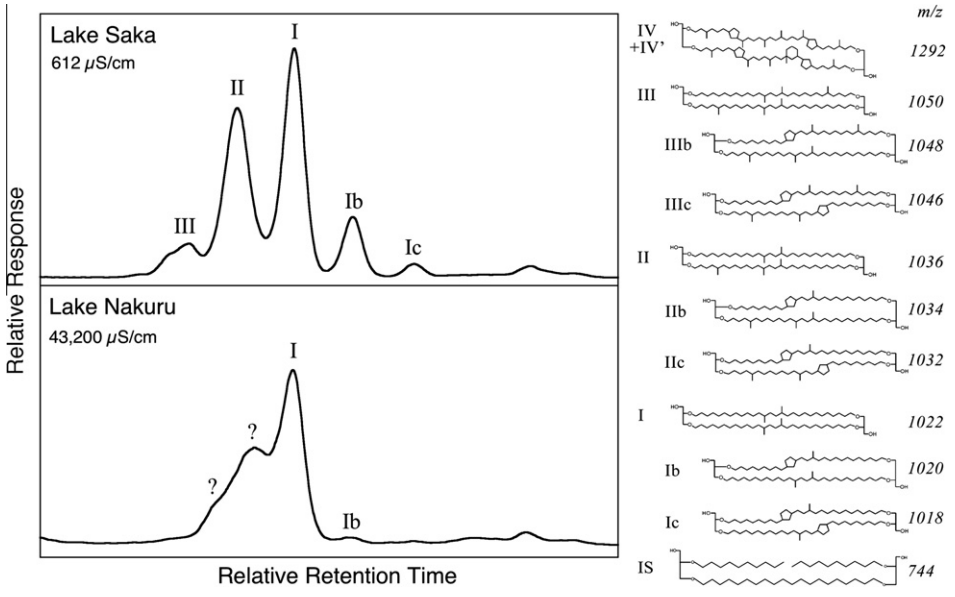

Fig. 2. Total ion current traces (including all monitored ions) of branched GDGTS from a representative freshwater lake (upper panel: Lake Saka, Uganda) and a representative saline lake (bottom panel: Lake Nakuru, Kenya). Though GDGT-I is clearly present in the Nakuru sample, GDGTs II and III are not resolved, suggesting that the GDGTs present may be structurally different. At right are the structures of branched and isoprenoidal GDGTs discussed in the text.

of the relative amount of branched and isoprenoidal GDGTs in the samples:

$$\mathrm{BIT} = \frac{([\mathrm{I}] + [\mathrm{II}] + [\mathrm{III}])}{([\mathrm{I}] + [\mathrm{II}] + [\mathrm{III}] + [\mathrm{IV}]} \quad (5)$$

The average duplicate errors for MBT, CBT, and BIT were 0.001, 0.005, and 0.001, respectively. Average concentration error was 2% of the given value, and the error on fractional abundances was 0.001.

2.3. Statistical analyses

We calculated a pair-wise correlation matrix for environmental variables and GDGT characteristics (fractional abundances, absolute concentrations, and the MBT and CBT indices) across all sites, excluding the five strongly saline (surface-water conductivity >30,000 μS/cm) lakes ($n = 41$). Some variables were log-transformed to correct for any highly skewed distributions. The significance of correlations (Pearson's coefficient, with a cut-off p value of 0.05) and root mean square error (RMSE) were assessed via one-way analysis of variance (ANOVA).

We performed principal component analysis (PCA) on the subset of 36 lakes, which excludes the saline lakes and the five lakes for which absolute GDGT concentration data are lacking. PCA assigns a loading to each environmental variable on each principal component, representing the degree by which this component is influenced by that variable (Morrison, 1976). We also performed redundancy analyses (RDA) on the same subset of 36 lakes (RDA-1) and on the set of 22 lakes for which catchment area data were available (RDA-2). Redundancy analysis is a 'constrained' version of PCA in the sense that it visualizes the variation in the GDGT data directly in relation to the environmental variables (i.e., it seeks the combination of explanatory environmental variables that best explain the variation in the dependent data matrix, in this case GDGT distributions). To assess whether a particular environmental variable explained a significant ($p < 0.05$) portion of the variation in the GDGT data, we performed a variance partitioning test, involving a series of RDAs with that variable as the sole constraining variable (999 unrestricted permutations). The unique and independent explanatory power of each variable was then assessed through a series of RDAs with that variable as the sole constraining variable and the other variables treated as co-variables.

Selected regressions were also performed. In particular, we applied the Weijers et al. (2007a) global soil calibration (Eq. (3)) to calculate MBT/CBT-inferred MAAT (Table 2) for our lake sites and then regressed these values against observed MAAT (as derived from the lapse rate model). Similarly, we applied the Weijers et al. (2007a) calibration to calculate CBT-derived pH (Eq. (4)) and then regressed these values against measured lake surface water pH. In this case, two sites with outlier values were excluded from the regression; they were identified on the basis of jack-knifed distances (greater than two standard deviations from the trend), where the distance for each observation is calculated with estimates of the mean, standard deviation, and correlation that does not include the observation itself. In addition, we performed least squares multiple regressions of the fractional abundances of nine branched GDGTs on, respectively, MAAT, surface and bottom water temperature, and surface and bottom water pH.

PCA and RDA analyses were performed using CANOCO v. 4.5 software (ter Braak and Smilauer, 2002); regression analyses were performed with JMP software.

3. RESULTS

3.1. Lipid analyses

Branched GDGTs were present in all lakes of our dataset but concentrations varied substantially from 9 to 160 μg/g TOC (Table A2). MBT values ranged from 0.16 to 0.63 and CBT values from 0.27 to 2.2 (Table A2). Branched GDGT distributions in the five strongly saline lakes (conductivity >30,000 μS/cm) differ substantially from those of all other, fresh to slightly saline lakes (up to 5900 μS/cm; see examples of GDGT distributions in

Table 1
Loadings of environmental variables on PCA axes 1 and 2, and RDA interset correlations. Values greater than 0.5 are in bold. MAAT, mean annual air temperature; SW, surface water; DO, dissolved oxygen; CA/SA, ratio of catchment area to lake surface area.

Variable	PCA loadings		RDA-1 correlations		RDA-2 correlations	
	Axis 1	Axis 2	Axis 1	Axis 2	Axis 1	Axis 2
MBT	**0.61**	**0.51**				
CBT	**−0.85**	0.07				
Log [branched GDGTs]	−0.03	0.31	−0.07	0.32	−0.27	−0.07
Log [crenarchaeol]	0.43	**−0.70**	−0.15	**−0.52**	−0.05	0.46
MAAT	**0.90**	0.39	**−0.95**	0.06	**−0.97**	0.06
SWpH	**0.88**	0.28	**−0.84**	−0.26	**−0.92**	0.20
Log conductivity	**0.79**	0.32	**−0.73**	−0.12	**−0.82**	0.23
Log depth	**0.64**	**−0.71**	−0.35	**−0.51**	−0.19	0.35
Log DO	**−0.54**	0.46	0.41	0.24	0.30	0.03
Log surface area	**0.62**	−0.15	−0.45	−0.20		
Log CA/SA					**0.69**	−0.03
Cum.% variance	45.6%	64.9%				
Cum.% variance, GDGTs			62.2%	79.0%	83.9%	89.0%
Cum.% variance, GDGT-environ.			76.5%	97.1%	91.9%	97.5%

Table 2
Results of RDA variance partitioning tests. 'None' indicates an RDA performed with the given variable as the sole constraining variable and no co-variables included, and 'all others' indicates an RDA with the given variable as the sole constraining variable and all other variables treated as co-variables.

Variable	Covariables	RDA-1% variance	RDA-2% variance
MAAT	None	60.0**	81.5 **
	All others	42.9**	41.5**
SWpH	None	49.0**	73.1**
	All others	23.3**	23.4*
Log conductivity	None	36.4**	59.1**
	All others	8.8	9.4
Log depth	None	15.6*	4.6
	All others	0.5	3.7
Log DO	None	12.7**	8
	All others	5.3	13.4
Log surface area	None	14.5*	
	All others	4.2	
Log CA/SA	None		41.0**
	All others		5.8
Log [crenarchaeol]	None	8.9*	2.8
	All others	6.8	2.6
Log [branched GDGTs]	None	3	6.5
	All others	2.1	5.6

* p value <0.05.
** p value <0.01.

Fig. 2). In sediments from these saline lakes, the shapes and retention times of the peaks eluting in the branched GDGT region of the total ion current traces suggest that some of the compounds present may be structurally distinct from known branched GDGTs (Fig. 2). Because of this, we did not calculate MBT and CBT values for the saline lakes, and also excluded these lakes from the statistical analyses.

3.2. Statistical tests

3.2.1. Correlations

The correlation matrix for our 41 non-saline East African lakes indicated that local MAAT, surface and bottom water temperature, surface and bottom water pH, surface water conductivity, and the ratio of catchment area to lake surface area (CA/SA) are all highly correlated with each other ($|r| > 0.8$ in all cases except CA/SA, where $r = -0.67$; Table A3). This is because the cold high-altitude lakes are generally more acidic than the warm low-altitude lakes and also tend to have a higher CA/SA.

The MBT and CBT indices and the fractional abundances of individual branched GDGTs are moderately to highly correlated with all the above-mentioned environmental variables (Table A3). In contrast, the fractional abundances of branched GDGTs are not significantly correlated with dissolved oxygen and the concentrations of branched GDGTs (Table A3). The fractional abundance of branched GDGTs IIc and Ic is significantly correlated with lake depth ($r = 0.52$, $p = 0.019$ and $r = 0.54$, $p = 0.011$, respectively) and with the absolute concentration of crenarchaeol ($r = 0.75$, $p < 0.0005$ and $r = 0.66$, $p = 0.001$, respectively; Table A3). Crenarchaeol concentration is also strongly correlated with lake depth ($r = 0.72$, $p < 0.0005$) but only modestly correlated with lake surface area ($r = 0.44$, $p = 0.05$; Table A3).

3.2.2. Principal components analysis

The PCA on 36 East African lakes identifies the general relationships between branched GDGT distribution and the different environmental variables, and determines the amount of variance in the dataset that is explained by these relationships. In this analysis we used the MBT and CBT indices to represent patterns in the fractional abundances of branched GDGTs, so as to examine general relationships between branched GDGT distribution and environmental variables. The absolute concentrations (per gram organic carbon) of branched GDGTs and crenarchaeol are treated as environmental variables, reasoning that the concentrations of these compounds are capable of impacting their distribution. Among the environmental variables, we excluded bottom water pH and surface and bottom water temperatures, as they correlated very strongly with surface water pH and MAAT, respectively. We also did not include the BIT index, which as a ratio of branched GDGTs to crenarchaeol is redundant with the absolute concentrations.

The first two PCA axes account for a cumulative 64.9% of the variance in our dataset, with PCA axis 1 alone accounting for 45.6% of the variance (Table 1). This axis primarily captures variance in MAAT, surface water pH, and conductivity. PCA axis 2 reflects variance in depth and crenarchaeol concentration (Table 1 and Fig. 3a). The CBT index loads primarily on the first axis, whereas the MBT index loads on both axes nearly equally. The PCA biplot (Fig. 3a) graphically depicts the distribution of individual lake sites in relation to the environmental variables, MBT and CBT. Cold, high-elevation lakes (all but one of the lakes above ~3000 m elevation) plot in the lower left quadrant, and shallow, middle-elevation (2000–3000 m) lakes from Kenya plot predominantly in the upper left quadrant. Deep lakes situated at lower elevations plot in the lower right quadrant, and more shallow low-elevation lakes plot in the upper right.

3.2.3. Redundancy analysis

We used RDA to determine the influence of each environmental variable on the distribution of branched GDGTs among lakes. In this analysis, we used the individual fractional abundances of the branched GDGTs rather than the MBT and CBT indices, to examine the impact of environmental factors on each of the nine branched GDGTs. In the first RDA on the 36-lake dataset (RDA-1), axes 1 and 2 together explain 79.5% of the branched GDGT distribution data and 97.1% of the relationship between the branched GDGTs and the environmental variables (Table 1). RDA-1 axis 1 captures the gradients in MAAT, surface water pH, and conductivity, and it alone explains 62.2% of the branched GDGT distributions and 76.5% of the relation-

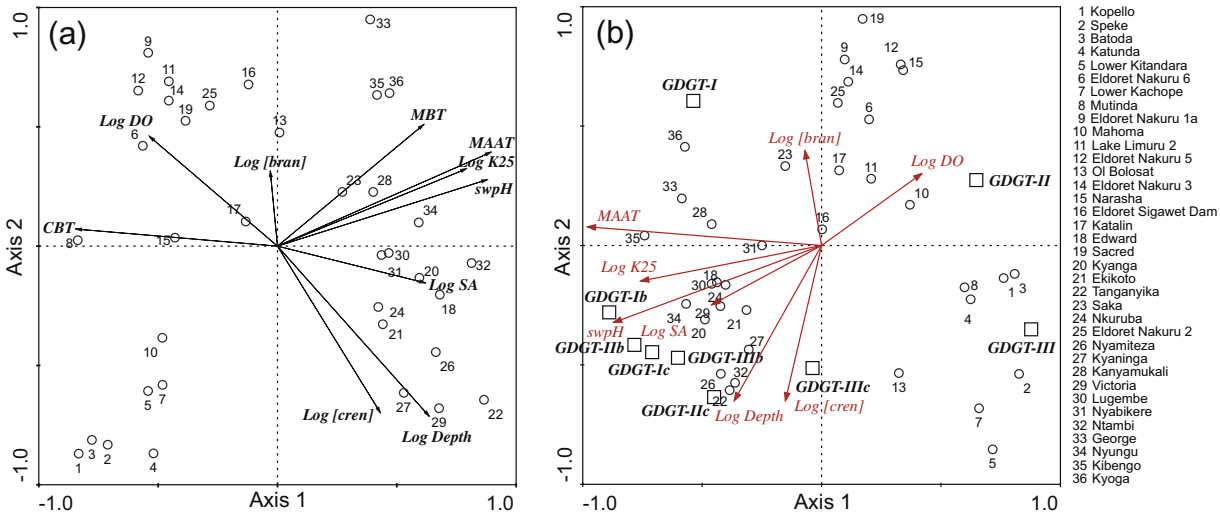

Fig. 3. (a) Principal components analysis (PCA) biplot showing relationships between environmental variables, MBT and CBT indices, absolute GDGT concentrations, and 36 East African lake sites; see number key on the right. (b) Redundancy analysis (RDA) triplot showing relationships between environmental variables, GDGT concentrations, fractional branched GDGT abundances and lake sites. Some variables were log-transformed prior to the analysis to correct for skewed distributions. DO, dissolved oxygen; [bran], branched GDGT concentration; [cren], crenarchaeol concentration; K25, conductivity; swpH, surface water pH; SA, lake surface area.

ship between the GDGTs and the environmental variables. Variance partitioning indicated that only MAAT and pH contribute significantly and independently to the variation in GDGT distribution, accounting for 42.9% and 23.3% of the variance, respectively (Table 2). The RDA-1 triplot (Fig. 3b) illustrates trends in the variance of the individual fractional abundances of branched GDGTs with respect to the environmental variables. As with the PCA, the position of individual lakes in this triplot reflects how each lake relates to the overall trends in the environmental parameters and GDGTs, as determined mostly by their MAAT and pH (axis 1) and their depth (axis 2).

We performed a second RDA on a subset of 22 lakes, adding the CA/SA ratio as environmental variable to test for changes in the ratio of soil-derived and aquatic GDGTs, reasoning that lakes with a larger catchment would likely receive more soil inputs. The results of this RDA-2 were similar to those of RDA-1. As expected, since in our dataset CA/SA is highly correlated with MAAT and pH, RDA-2 axis 1 captured gradients in MAAT, pH, conductivity and CA/SA and explains 91.9% of the relationship between branched GDGT distribution and environmental variables (Table 1). Variance partitioning indicated that CA/SA does not, however, explain a significant amount of the variance in GDGT distributions independent from the other variables (Table 2).

3.2.4. Regression analysis

The regression results reflect the capability of the distribution of branched GDGTs to predict MAAT and surface water pH. Regression of MBT/CBT-derived MAAT (using Eq. (3); Weijers et al., 2007a) against MAAT produces a high coefficient of determination ($r^2 = 0.85$, $p < 0.0001$; Fig. 4a), demonstrating that the lake GDGTs can robustly predict MAAT. However, the regression has a large y-intercept (12.6 °C) and its slope (0.75) differs significantly from 1 ($p < 0.0001$). Regression of CBT-derived pH (using Eq. (4); Weijers et al., 2007a) against measured surface water pH similarly demonstrates good prediction capability (Fig. 4b). This regression has a slope significantly greater than 1 ($p < 0.0001$), but the positive y-intercept of 0.2 pH units is not significantly different from 0 ($p = 0.64$).

Least squares multiple linear regression of the nine branched GDGT fractional abundances demonstrates excellent prediction of MAAT, with a very high coefficient of determination ($r^2 = 0.96$) and low RMSE (2.0 °C; Fig. 4c). Coefficients of determination for multiple regressions of the nine GDGT fractional abundances against surface and bottom water temperatures (not shown) are only slightly lower ($r^2 = 0.91$ and $r^2 = 0.90$). Multiple regression of the nine branched GDGT fractional abundances against surface water pH also shows good predictability, although its coefficient of determination ($r^2 = 0.85$) is not as high as with MAAT (Fig. 4d). Regression with bottom water pH (not shown) resulted in a much lower coefficient of determination ($r^2 = 0.69$).

4. DISCUSSION

Branched GDGTs were first identified in peats and soils (Sinninghe Damsté et al., 2000; Weijers et al., 2006a), and are generally considered to be terrestrial in origin (Hopmans et al., 2004). However, several recent investigations of branched GDGTs in lacustrine environments concluded that *in situ* production of these compounds in lakes is also possible (Tierney and Russell, 2009; Sinninghe Damsté et al., 2009). In their study of Lake Towuti, a large lake in Indonesia, Tierney and Russell (2009) found that branched GDGTs in surface sediments had much lower MBT and CBT index values than soils from the lake

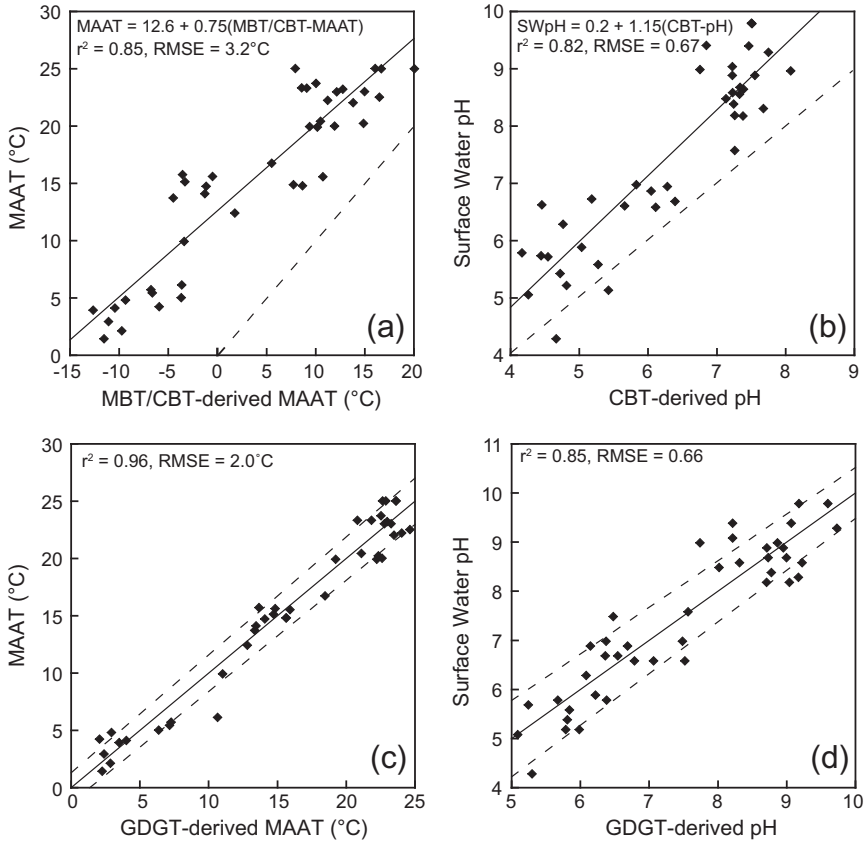

Fig. 4. (a) Regression of MBT/CBT-derived MAAT versus local MAAT (as estimated from a regional lapse rate model; see text), when applying the Weijers et al. (2007a) global calibration for soils to our African lake-sediment samples. (b) Regression of CBT-derived pH versus measured surface water pH. Dotted lines in (a) and (b) represent the one-to-one relationship. (c) Multiple regression of fractional branched GDGT abundances and MAAT. (d) Multiple regression of fractional branched GDGT abundances and surface water pH. Dotted lines in (c) and (d) represent 95% confidence intervals.

catchment. When these MBT and CBT indices were used to estimate temperature with the Weijers et al. (2007a) global soil calibration, the lake sediments and soils differed by ~10 °C. The substantially different branched GDGT compositions of catchment soils and lake sediment observed by these authors implied that there were two sources of branched GDGTs: the soils, and production in the lake itself. On the other hand, in a study of Lake Challa, a crater lake in Kenya, Sinninghe Damsté et al. (2009) showed that, although branched GDGTs in soils and lake sediments appeared to have slightly different MBT and CBT values, on a flux basis most of the branched GDGTs in the lake could be accounted for by terrestrial run-off. This implied that although *in situ* production could not be ruled out, most of the branched GDGTs in Lake Challa were soil-derived.

As both these studies focused on individual lakes, differences between the findings can potentially be due to site-specific conditions and processes. The extensive lake dataset used in this study allows us to identify the major environmental controls on branched GDGT distribution among lakes, and to consider the possibility of *in situ* production of branched GDGTs within a variety of lake environments.

4.1. Influence of temperature

Our RDA results clearly identify temperature (here represented by MAAT) as the most important environmental variable affecting GDGT distributions in East African lakes: MAAT independently explains nearly half of the variance in branched GDGT fractional abundances (Table 2). Multiple regression of the nine branched GDGTs against MAAT also demonstrates the excellent ability of these compounds to predict temperature (Fig. 4c). However, when we applied the Weijers et al. (2007a) global soil calibration to the MBT and CBT index values, we found a notable difference between GDGT-calculated MAAT and observed MAAT. Specifically, the large y-intercept of the regression (Fig. 4a) indicates that, when applying the global soil calibration, East African lake sediments predict cooler-than-expected MAAT. This implies that the relationship of lake sediment GDGTs with MAAT is significantly different from that of soil GDGTs with MAAT.

The difference in MBT/CBT-inferred MAAT between soils and lake sediments is also apparent if we compare our lake data to data from an altitude transect of soils on Mt. Kilimanjaro (Sinninghe Damsté et al., 2008) (Fig. 5a).

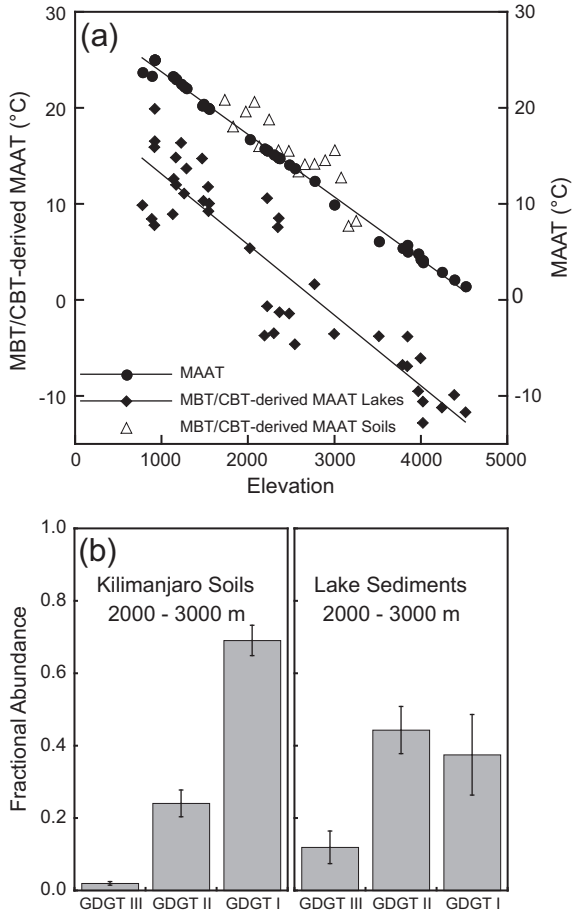

Fig. 5. (a) Lapse rate modelled MAAT, Mt. Kilimanjaro soil MBT/CBT-derived MAAT (Sinninghe Damsté et al., 2008) and African lake sediment MBT/CBT-derived MAAT (this study) plotted versus surface elevation. (b) Bar plots of average branched GDGT distributions ($n = 12$, with 1σ errors) of Mt. Kilimanjaro soil samples (Sinninghe Damsté et al., 2008) and lake surface sediments (this study) between 2000 and 3000 m surface elevation.

When plotted against elevation, the Mt. Kilimanjaro soils and MAAT agree nicely, validating the Weijers et al. (2007a) calibration for prediction of MAAT from African soil GDGTs (Fig. 5a). In contrast, lake branched GDGT-derived MAAT estimates plot well below soil branched GDGT-derived MAAT and actual MAAT. Clearly, the Weijers et al. (2007a) calibration is not applicable to African lake sediments. The observed 'cold bias' in our lake sediment data is consistent with the observation by Tierney and Russell (2009) that lake sediment GDGTs inferred colder-than-observed MAAT in Lake Towuti, Indonesia. What could explain this difference? One could conclude that a new, regional soil calibration is needed. Indeed, there are no East African soils in the Weijers et al. (2007a) calibration dataset, and hence Sinninghe Damsté et al. (2008) proposed an alternative calibration for their Mt. Kilimanjaro soils. However, Mt. Kilimanjaro soils do track MAAT relatively well using the Weijers et al. (2007a) calibration (Fig. 5a). Rather, a distinct and consistent difference occurs between branched GDGT distributions in soils and those in lakes.

Comparison between the fractional abundances of major branched GDGTs (I, II, and III) in Mt. Kilimanjaro soils (Sinninghe Damsté et al., 2009) and in African lake sediments situated at a comparable altitude range (between 2000 and 3000 m, in our dataset mostly from lakes in the central Kenya highlands) reveals that the lake sediments have, on average, sixfold higher fractional abundances of GDGT III, twofold higher fractional abundances of GDGT II, and only half as much GDGT I (Fig. 5b). Although there are notable differences in the distribution of all major GDGT compounds, most of the bias in predicted temperature can be explained by the high fractional abundance of GDGT III in lake sediments, which is the GDGT with the most methyl groups and is more abundant at lower temperatures in soils (Weijers et al., 2007a). This particular GDGT is clearly important in driving the relationship between branched GDGT distribution and temperature in lake sediments: of all the branched GDGTs, the fractional abundance of GDGT III has the highest correlation with MAAT ($r = -0.96$; Table A3), and it loads prominently on RDA axis 1 (Fig. 3b).

The 'excess' GDGT III in lake sediments is unlikely to have a soil origin, because all branched GDGTs are structurally similar and thus should be transported to the lake with no significant changes in distribution. It is also unlikely, given the diversity in the size and mean slope of drainage basins surrounding the sampled lakes, that lake sediment GDGTs are consistently derived from soils at much higher elevations than the lake itself; the elevation gradient within most lake catchments is simply too small to account for the observed cold bias. The most reasonable explanation for the high fractional abundance of GDGT III in lake sediments (Fig. 5b) is that branched GDGTs with a different composition than that in catchment soils are produced in the lake.

If in-lake production were the only source of branched GDGTs in lake sediments, the relationship between GDGT distribution and lake temperature (surface or bottom, depending on where the branched GDGT-producing bacteria reside) would likely be stronger than a relationship with MAAT. In our dataset we cannot discriminate between these relationships because both surface and bottom water temperatures are highly correlated with MAAT ($r > 0.99$ in both cases; Table A3). Therefore, based on temperature data alone we cannot determine whether the branched GDGTs are recording water (as would be the case given *in situ* production) or air temperatures (as would be the case given soil production) or a combination of both. Our regression analyses show slightly lower coefficients of determination between branched GDGT distribution and surface ($r^2 = 0.91$) or bottom ($r^2 = 0.90$) water temperatures than between the GDGTs and MAAT ($r^2 = 0.96$), but these lower values most likely reflect our low measurement frequency of lake temperatures in relation to daily and seasonal variability. In contrast, the MAAT data used to construct the lapse rate model (Eggermont et al., 2009) are based on continuous on-site monitoring of MAAT with loggers or on largely continuous regional temperature data-

sets. Inaccurate estimation of average surface and bottom water temperatures due to infrequent sampling is a common problem in limnology, and for this reason Livingstone et al. (1999) argued that quantitative lake-based models for temperature reconstruction should always calibrate to MAAT rather than lake temperatures. We thus continue to compare our GDGT distributions to MAAT, even though we assume that if branched GDGTs are produced in the lake, they are most likely recording lake water temperatures.

4.2. Influence of pH

In our East African dataset, lake water pH is highly correlated with MAAT ($r = 0.94$ and $r = 0.88$ for surface and bottom pH, respectively; Table A3), but RDA analysis and variance partitioning shows that surface water pH does account for a significant amount (23.3%) of the variance in branched GDGT distribution independent of other variables including MAAT. Consequently, pH is the second most important environmental variable controlling branched GDGT distribution in lakes. Most of the cyclic GDGT compounds previously identified as driving the relationship with pH (e.g., GDGT Ib, GDGT IIb, GDGT Ic; Weijers et al., 2007a) plot close to surface water pH in our RDA triplot (Fig. 3b). Moreover, multiple regression of the fractional GDGT abundances adequately predicts pH (Fig. 4d). Use of the Weijers et al. (2007a) global soil calibration predicts observed surface water pH imperfectly (Fig. 4b) but the offset is not nearly as large as with the MAAT transfer function. This corroborates our argument (Section 4.1) that the bias in lake sediment MBT/CBT-inferred MAAT is largely due to the dominance of GDGT III, since GDGT III is not included in the CBT calculation (Eq. (2)).

We did not measure soil pH within our lakes' drainages, therefore we cannot assess whether the correlation between GDGT fractional abundances and surface water pH is due to correlation of lake water pH with local soil pH. Indeed, the high-elevation lakes in our dataset are generally surrounded by acidic soils, and some low-elevation lakes are situated in carbonaceous terrain. However, the high pH values (pH > 9) predicted by the GDGT distribution in low-altitude lakes using a least-squares multiple regression model (Fig. 4d) would seem to suggest an aquatic influence. Such high pH values are not commonly found in soils (Batjes, 1997), but are typical of productive tropical lake environments, where CO_2 removal by intense algal photosynthesis increases surface water pH (Talling and Lemoalle, 1998). This also fits with the finding that, in terrain where soil pH and lake pH are different, lake sediment branched GDGTs infer lake and not soil pH values (Tierney and Russell, 2009).

The coefficient of determination between GDGT distribution and bottom water pH is notably lower ($r^2 = 0.69$) than between GDGT distribution and surface pH ($r^2 = 0.85$). This difference would seem to suggest that the branched GDGTs, if produced *in situ*, are likely produced in the upper water column, rather than in bottom waters. This may explain the observation that branched GDGT flux in a sediment trap suspended near the base of the surface mixed layer in Lake Challa is equivalent to the accumulation rate of branched GDGTs in recent sediments at 92 m depth (Sinninghe Damsté et al., 2009).

4.3. Influence of depth

If branched GDGTs are produced within the lake environment, one might expect limnological variables other than temperature and pH, such as salinity, dissolved oxygen and depth, to also influence the distribution and concentration of these compounds. Our RDA analyses suggest that the latter environmental variables do not account for a significant amount of variance on their own. Nevertheless, axis 2 of both the PCA and RDA represents variance in branched GDGT distribution associated predominantly with depth and the concentration of crenarchaeol (Fig. 3). Furthermore, the large spread of lake sites and certain GDGTs along this ordination axis suggests that although depth does not explain a significant amount of the total variance, for some GDGTs it may be an influential factor. Specifically, depth seems to influence the fractional abundances of cyclic GDGTs containing two cyclopentane rings: GDGT Ic, GDGT IIc, and GDGT IIIc. The fractional abundance of GDGT Ic and GDGT IIc among lakes is significantly correlated with depth (Section 3.2.1), and GDGT IIc also plots very close to depth in the RDA triplot (Fig. 3b). GDGT IIIc is not correlated with depth ($r = 0.19$) but does plot almost exclusively on RDA axis 2 (Fig. 3b). From the perspective of individual lake sites, depth may particularly influence the distribution of GDGTs in shallow, mid-elevation lakes in Kenya, which plot in the upper right quadrant of the RDA triplot (Fig. 3b). These lakes have low concentrations of the cyclic GDGTs associated with depth (GDGT Ic, IIc, and IIIc) as well as the monocyclic GDGTs (GDGT IIb, GDGT Ib) that contribute to the CBT index (Eq. (2)).

The relationship between depth and this particular group of branched GDGTs may suggest that these compounds have a separate, or additional source from that of the other branched GDGTs. Strong correlations between GDGT Ic, GDGT IIc and crenarchaeol (see Section 3.2.1), the latter also plotting close to RDA axis 2, could provide a hint. The strong positive relationship between crenarchaeol concentration and lake depth in our dataset is compelling evidence that lacustrine crenarchaeota thrive in deep (but not necessarily large) African lakes. We speculate that this is because mesophilic crenarchaeota are most likely ammonium oxidizers (Könneke et al., 2005), and thus are more productive in stratified lakes with a deep mixed layer, where ammonium availability near the oxycline is high and competition from photoautotrophs is low. The as-yet unknown microorganisms producing the minor cyclic branched GDGTs may have a similar ecological niche.

4.4. Concentrations of GDGTs and the BIT index

Our PCA and RDA results show no evidence of a significant environmental influence on the total, absolute concentrations of branched GDGTs. It is somewhat surprising that there is no obvious relationship with pH, as previous

studies suggested that branched GDGTs are typically more abundant in acidic peats and soils (Weijers et al., 2006b, 2007a). Our data suggest that lake pH does not impact productivity of the microorganisms that synthesize these compounds in lacustrine environments. We do observe, however, a significant correlation between the summed absolute concentration of branched GDGTs and both catchment area ($r = 0.55$, $p = 0.01$) and lake surface area ($r = 0.50$, $p = 0.02$). The correlation with catchment area could indicate that there is a larger flux of terrestrial GDGTs in larger catchments, but the positive correlation with lake surface area is less easy to explain, given the context that there is a strong decrease in terrestrial GDGT fluxes with distance from shore in marine environments (Hopmans et al., 2004). In our dataset, the relationship between surface area and branched GDGT concentration is probably an artefact of catchment area and lake surface area being highly correlated ($r = 0.94$); this could also explain why there is no significant relationship between branched GDGT concentration and the CA/SA ratio ($r = 0.20$, $p = 0.38$).

In contrast with the concentrations of branched GDGTs, the concentration of crenarchaeol is strongly correlated with lake depth, which as already mentioned in Section 4.4 may be an indication of the preferred habitat of mesophilic crenarchaeota. It is also noteworthy that the BIT index is significantly correlated with crenarchaeol concentration ($r = -0.85$, $p < 0.0005$) but not with branched GDGT concentration ($r = 0.03$, $p = 0.9$). This indicates that, at least across the full gradient of African lake environments, the BIT index (i.e., the ratio between the two types of GDGTs) is mostly a proxy for crenarchaeol concentration rather than terrestrial GDGT flux, as originally suggested by Hopmans et al. (2004) for marine settings, and by Verschuren et al. (2009) and Sinninghe Damsté et al. (2009) in the case of Lake Challa in Kenya. In their study of the Congo Fan, Weijers et al. (2009) also concluded that the BIT index predominantly reflects crenarchaeol concentration.

4.5. New functions to infer temperature and pH from GDGT distributions

As discussed in Sections 4.2 and 4.3, although the soil calibrations for MAAT and pH (Weijers et al., 2007a) are not suitable for our African lake dataset, the branched GDGT distributions in these lakes can still accurately predict MAAT and pH. For these applications we formulate new equations, using the MBT and CBT indices in the manner of Weijers et al. (2007a):

$$\mathrm{MAAT} = 11.84 + 32.54 \times \mathrm{MBT} - 9.32 \times \mathrm{CBT} \quad (6)$$

$r^2 = 0.89$, RMSE = 3.0 °C (excluding two jack-knifed outliers).

$$\mathrm{pH} = 10.32 - 3.03 \times \mathrm{CBT} \quad (7)$$

$r^2 = 0.83$, RMSE = 0.66 pH units (excluding two jack-knifed outliers).

The two outliers are lakes Limuru and Eldoret-Nakuru 1, two shallow ponds from the Kenyan lakes subgroup, which as described in Section 4.4 have CBT values that are compromised by the relationship between the minor cyclic GDGTs and lake depth.

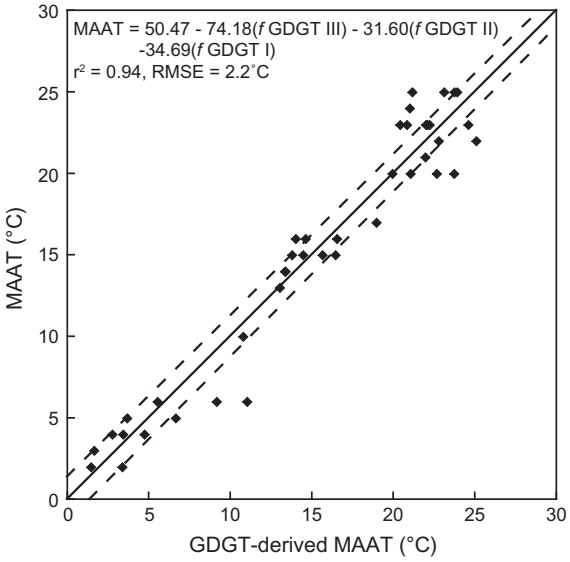

Fig. 6. New MAAT inference model, based on multiple regression of the fractional abundances of three major branched GDGT compounds (GDGTs I, II, and III) in African lake sediments.

The new CBT function (Eq. (7)) for pH compares favorably with the multiple regression results (Fig. 4d). The MBT-CBT derived function for MAAT (Eq. (6)) is less accurate than the multiple regression (Fig. 4c), likely because it makes use of the CBT index and accordingly includes variance associated with pH. We therefore propose an alternate approach which employs a three-component regression consisting of only the three major branched GDGTs (GDGTs I, II, and III):

$$\mathrm{MAAT} = 50.47 - 74.18 \times \mathrm{f\ GDGT\ III} - 31.60 \times \mathrm{f\ GDGT\ II} - 34.69 \times \mathrm{f\ GDGT\ I} \quad (8)$$

$r^2 = 0.94$, RMSE = 2.2 °C (Fig. 6).

This function excludes the cyclic GDGT compounds, which, although they may also relate to temperature, are thought to be a physiological adaptation to pH (Weijers et al., 2007a). Eq. (8) produces excellent prediction of MAAT in our African lake dataset and is easy to apply. In effect, this function is similar to a linear regression involving the MBT index, as it takes into account the fractional abundances of the three major branched GDGTs. Regression of MBT directly against MAAT has a significantly lower coefficient of determination ($r^2 = 0.67$), however. By giving each of the three major branched GDGTs its own coefficient, prediction of MAAT is greatly improved.

5. SUMMARY AND CONCLUSIONS

Our survey of branched GDGTs in the surficial bottom sediments of 46 East African lakes suggests that variations

in the distribution of these compounds are primarily related to temperature and secondarily to lake pH. No other environmental variable explains a significant amount of the total variance, except that depth may influence the fractional abundance of GDGTs with two cyclopentane moieties. We also find that the concentration of crenarchaeol is strongly related with lake depth, and that the BIT index primarily reflects the production of crenarchaeol rather than the flux of branched GDGTs. This result highlights the importance of quantifying both branched GDGTs and crenarchaeol to understand environmental controls on, and interpretation of, the BIT index.

We further demonstrate that branched GDGT distributions in lakes can be used to predict temperature and pH with a high degree of accuracy, and derive new functions with which this can be accomplished. However, the distinct differences between soil and lake sediment GDGT distributions, good correlation of the latter with lake surface pH, the need for different MAAT and pH calibrations than those previously established by Weijers et al. (2007a), and the influence of depth on GDGT distribution all indicate that branched GDGTs are produced within lake systems as well as in catchment soils. This introduces a number of complications. For one, lacustrine GDGTs should record lake temperature rather than air temperature. In tropical lakes, both surface and bottom water temperatures are highly correlated with mean annual air temperature (Lewis, 1973), which allows us to infer MAAT based on branched GDGT distributions. In subtropical and temperate-region lakes, however, summer/winter surface temperatures are related to summer/winter air temperatures while bottom temperature year-round is determined by the lowest wintertime air temperature (with a minimum of 4 °C). Thus, depending on where in the water column the branched GDGTs are produced, and on the magnitude of seasonal variation in GDGT production, GDGT signatures of lake temperature in extratropical lakes will be more disconnected from local MAAT.

In their study of Lake Challa in Kenya, Sinninghe Damsté et al. (2009) suggested that if GDGTs are produced in both soils and lakes, GDGTs in lake sediments likely represent a variable mixture of allochthonous and autochthonous GDGT distributions. However, in our 46-lake dataset spanning the complete regional temperature gradient across East Africa (as determined by site elevation), any scatter in GDGT-inferred MAAT that these variable mixtures may induce does not prevent good prediction of MAAT from the lake sediment GDGT distributions. We also do not find any conclusive evidence that the catchment area explains variance in the dataset independent from other variables. It may be that the concentrations of autochthonous branched GDGTs in these tropical lakes far exceed those of allochthonous GDGTs, such that the lake signal is dominant; Tierney and Russell (2009) previously found that the concentrations of lacustrine GDGTs were an order-of-magnitude higher than the concentrations in the watershed soils. We therefore recommend that future studies involving lacustrine GDGTs examine the relative and absolute concentrations of branched GDGTs both within the lake of interest and in surrounding catchment soils to determine the source of the compounds and the environmental signal they reflect.

Branched GDGTs show considerable promise as a lacustrine paleothermometer, but unanswered questions hinder the application of these compounds towards this purpose. For one, if branched GDGTs are produced within the lake system, are they produced in the upper water column, lower water column, or in the sediments? A recent study from a fjord environment in Svalbard, Norway suggests that branched GDGTs may be produced within the marine sediment column (Peterse et al., 2009); if this is the case for the branched GDGTs in lakes as well, then the temperatures they record could be bottom water temperatures. In addition, without knowledge of the metabolism or ecological niche of the microorganisms producing branched GDGTs, we cannot fully understand how or why the lipid distributions of these organisms respond to environmental influences. We conclude that a branched-GDGT based temperature proxy can be used in tropical lake environments, but adequate constraints on the local sources of these compounds need to be established before it can be applied with confidence as a paleothermometer at individual sites.

ACKNOWLEDGMENTS

The fieldwork for this study was conducted with research permits of the Uganda National Council for Science and Technology, the Uganda Wildlife Authority, the Kenya Wildlife Service and the Kenya Ministry of Education, Science & Technology to J. Russell, D. Verschuren and H. Eggermont. We thank two anonymous reviewers, L. Schwark and J. Werne for helpful suggestions that greatly improved this manuscript. This research was supported by ACS-PRF# 45337-G to J. Russell and National Defense Science and Engineering Graduate Fellowship to J. Tierney.

Appendix A

Table A1
Geographical and limnological data for the 46 lakes studied, including country (UG, Uganda; DRC, DR Congo; KN, Kenya; TZ, Tanzania), year of sediment collection, latitude (Lat.) and longitude (Long.), lake depth (Depth), surface area (S. Area), catchment area (C. Area), catchment area/surface area (CA/SA) ratio, near-bottom dissolved oxygen concentration (DO), surface elevation (Elev.), mean annual air temperature (MAAT), surface water temperature (SW Temp), bottom water temperature (BW Temp), surface water pH (SW pH), bottom water pH (BW pH), conductivity (Conduct.), and percent total organic carbon of sampled sediments (%TOC). MAAT values marked with an asterisk were measured with an on-site temperature logger; the rest were estimated from a lapse rate model, see the main text. Data sources listed in the last column are as follows: a, Eggermont et al. (2009); b, Eggermont et al. (2007); c, Mergeay et al. (2005, 2006); d, Lehman (2002); e, this study; f, Descy et al. (2005); g, Talling and Talling (1965); h, Mungoma (1988); j, Viner (1969); k, Viner and Smith (1973); l, Bugenyi and Magumba (1996); m, Gasse et al. (1983).

Lake name	Country	Collection year	Lat.	Long.	Depth (m)	S. Area (m^2)	C. Area (m^2)	CA/SA ratio	DO (mg/L)	Elev. (m)	MAAT (°C)	SW Temp. (°C)	BW Temp. (°C)	SW pH	BWpH	Conduct. (μS/cm)	%TOC	Data sources
Kopello	UG	2007	0.310	29.892	14.3	3.01E+04	2.69E+06	89.6	2.39	4017	4.0*	7.6	5.7	5.1	4.9	10	25.6	a, b
Kamsongi's Pool	UG	2007	0.372	29.883	0.5	3.00E+01			13.77	4509	1.5	2.1	2.1	5.4	5.4	8		a, b
Speke	DRC	2006	0.405	29.881	18.0	3.91E+04	1.06E+06	27.1	3.09	4235	3.0*	5.8	5.3	5.9	5.2	13	16.3	a, b
Batoda	UG	2006	0.300	29.883	16.0	9.53E+04	2.51E+06	26.4	3.66	4017	4.2*	7.5	6.1	5.2	5.0	11	19.2	a, b
Marsh Pool II	UG	2007	0.334	29.873	1.0	3.00E+01			12.58	4380	2.2	5.1		5.7	5.7	11		a, b
Upper Kachope	UG	2007	0.332	29.893	12.0	4.59E+04			3.45	3961	4.9*	7.8	6.4	6.7	6.2	20	18.5	a, b
Nsuranja	UG	2007	0.293	29.908	12.5	2.16E+04	1.75E+06	81.3	2.34	3834	5.8	8.8	6.8	4.3	4.3	11	24.0	a, b
Katunda	UG	2006	0.280	29.895	10.5	3.77E+04	7.96E+06	211.4	0.00	3782	5.5	8.0	7.5	5.2	5.2	14	30.2	a, b
Lower Kitandara	UG	2006	0.349	29.887	12.0	2.86E+04	4.15E+06	145.0	4.60	3989	4.3*	6.4	5.9	7.0	6.5	30	21.2	a, b
Eldoret Nakuru 6	KN	2005	−0.082	35.658	1.0	2.00E+03			4.02	2536	13.8	24.9	24.9	6.6	6.6	117	2.4	c
Lower Kachope	UG	2006	0.334	29.872	13.0	8.12E+03			3.09	3841	5.1	8.4	7.4	6.7	6.0	22	26.4	a, b
Mutinda	UG	2006	0.274	29.928	1.5	3.00E+01			12.41	3507	6.2	7.7		6.3	6.3	18	8.3	a, b
Eldoret Nakuru 1a	KN	2005	0.440	35.305	1.0	1.00E+03			2.79	2185	15.8	14.1	14.1	6.9	6.9	196	8.4	c
Mahoma	UG	2008	0.346	29.968	13.2	4.76E+04	2.05E+05	4.3	0.53	2990	10.0*	14.2	12.5	5.8	5.1	21	49.6	a, b
Lake Limuru 2	KN	2005	−1.106	36.630	2.5	2.50E+05			12.16	2294	15.2	23.1	23.1	7.5	7.5	155	9.8	c
Eldoret Nakuru 5	KN	2005	−0.060	35.640	1.0	1.00E+02			19.39	2471	14.2	20.8	20.8	6.6	6.6	204	5.6	c
Ol Bolosat	KN	2003	−0.183	36.450	2.0	2.00E+07			15.71	2358	14.8	20.6		9.0		1960	5.2	a
Eldoret Nakuru 3	KN	2005	0.333	35.365	1.0	3.00E+02			8.02	2214	15.7	16.3	16.3	7.0	7.0	221	1.9	c
Narasha	KN	2003	0.050	35.533	7.2	2.00E+06			3.90	2764	12.5	16.0		5.6		34	14.9	a
Eldoret Sigawet Dam	KN	2005	0.585	35.218	1.5	5.00E+04			12.62	2014	16.8	22.5	22.5	8.5	8.2	214	0.9	c

(*continued on next page*)

Table A1 (*continued*)

Lake name	Country	Collection year	Lat.	Long.	Depth (m)	S. Area (m^2)	C. Area (m^2)	CA/SA ratio	DO (mg/L)	Elev. (m)	MAAT (°C)	SW Temp. (°C)	BW Temp. (°C)	SW pH	BWpH	Conduct. (μS/cm)	%TOC	Data sources
Katalin	KN	2003	0.633	35.483	4.5	1.50E+05			0.40	2337	14.9	19.5		6.6		78	4.7	a
Edward	UG	2001	−0.246	29.750	29.0	2.33E+09	1.58E+10	6.8	2.45	910	25.1	26.8	25.8	8.9	8.1	840	14.1	d, e
Challa	KN	2003	−3.317	37.698	92.0	4.20E+06	5.57E+06	1.3	0.00	880	23.4	24.6	22.0	8.9	7.3	355		a, c, e
Sacred	KN	1999	0.050	37.533	5.0	5.10E+05				2350	14.9	16.7	16.7	5.8	5.8	25	47.2	c
Kyanga	UG	2001	0.400	30.233	57.0	1.18E+05	1.15E+05	1.0	0.14	1122	23.4	26.9	24.1	9.4	7.3	1055	10.6	e
Ekikoto	UG	2002	0.700	30.317	72.0	1.60E+04			0.00	1537	20.0	24.0	21.7	8.6	7.1	464	20.7	a, e
Tanganyika (Kigoma)	TZ	2005	−4.872	29.617	110.0	3.26E+10	1.98E+11	6.1	2.34	773	23.8	25.7	24.5	9.1	8.8	680	5.8	f
Saka	UG	2007	0.700	30.233	8.0	5.24E+05			0.00	1543	20.0	22.7	20.7	7.6	6.3	612	38.0	e
Nkuruba	UG	2002	0.517	30.300	34.0	1.32E+04	4.80E+04	3.6	0.00	1480	20.5	23.8	22.1	8.4	6.6	352	14.9	a, e
Eldoret Nakuru 2	KN	2005	0.361	35.351	1.5	5.00E+02			6.89	2217	15.6	14.5	14.5	6.9	6.9	171	0.4	c
Nyamiteza	UG	2002	0.433	30.217	34.0	3.36E+05	2.98E+05	0.9	0.00	1254	22.3	26.0	23.2	9.0	8.2	1057	8.2	e
Kyaninga	UG	2002	0.700	30.300	58.0	2.40E+05	1.85E+05	0.8	0.40	1531	20.1	23.8	21.8	8.3	6.7	407	14.2	a, e
Kanyamukali	UG	2008	0.400	30.233	10.2	2.28E+04	2.48E+04	1.1	0.82	1161	23.1	26.6	25.0	8.7	8.1	958	9.3	e
Victoria	UG	1996	−0.460	33.350	76.0	6.88E+10	1.95E+11	2.8	1.70	1133	23.3	25.5	24.5	8.2	7.9	110	14.5	l, m
Lugembe	UG	2002	0.433	30.267	18.0	7.98E+04	2.40E+05	3.0	0.51	1280	22.1	24.9	22.6	8.7	7.3	395	21.5	a, e
Nyabikere	UG	2001	0.480	30.320	45.0	3.95E+05	5.15E+05	1.3	0.40	1463	20.3	25.1	22.4	8.2	6.8	270	21.5	a, e
Ntambi	UG	2001	0.450	30.233	42.0	3.24E+05	2.83E+05	0.9	0.00	1158	23.1	27.2	24.4	9.4	9.3	5900	7.3	e
George	UG	2003	−0.083	30.177	4.0	2.50E+08	9.98E+09	39.9	7.72	910	25.1	28.5	25.2	9.8	8.8	230	27.6	e, j, k
Nyungu	UG	2008	−0.250	30.100	26.0	1.44E+05	3.39E+05	2.4	0.00	1220	22.6	24.7	22.3	9.3	7.6	452	8.4	e
Kibengo	UG	2001	−0.067	30.167	6.0	8.81E+05	1.16E+06	1.3	2.20	914	25.1	27.7	26.5	9.8	9.3	220	11.4	a, e
Kyoga	UG	1998	1.480	32.828	5.7	1.72E+09	7.50E+10	43.6		914	25.1	28.0	26.7	8.6	8.3	128	4.3	e, g, h
Kitagata	UG	2001	−0.067	29.967	9.0	6.20E+05				944	24.8	28.0		9.6	9.3	135,000	4.1	e
Bogoria	KN	2001	−0.250	36.100	9.0	3.40E+07				993	22.7	28.7	26.1	10.0	9.9	68,400	3.4	e, g, m
Bagusa	UG	2000	−0.100	30.183	0.9	3.28E+05				925	25.0	31.8	24.9	10.8	10.7	61,100	12.0	e
Nakuru	KN	2001	−0.361	36.094	0.8	4.00E+07				1770	18.2	23.8	23.4	10.0	10.0	43,200	3.9	e, g, m
Elementaita	KN	2001	−0.767	36.383	0.6	1.80E+07				1786	18.1	30.2	18.4	10.7	10.1	32,200	2.8	e, g, m

Table A2
Fractional abundances (f) of the nine major branched GDGT compounds, absolute concentrations of summed branched GDGTs (μg/g TOC), absolute concentrations of crenarchaeol (ng/g TOC), calculated indices BIT, MBT and CBT (see main text for description), and the CBT-derived pH and MBT/CBT-derived temperature (°C) estimates when applying the Weijers et al. (2007a) calibration.

Lake name	f GDGT III	f GDGT IIIb	f GDGT IIIc	f GDGT II	f GDGT IIb	f GDGT IIc	f GDGTI	f GDGT Ib	f GDGT Ic	Branched GDGTs (μg/g TOC)	Crenarchaeol (ng/g TOC)	BIT	MBT	CBT	CBT-pH	MBT/ CBT-T
Kopello	0.364	0.001	0.001	0.433	0.009	0.004	0.184	0.003	0.002	12	1084	0.91	0.19	1.72	4.2	−12.7
Kamsongi's Pool	0.411	0.001	0.000	0.398	0.011	0.001	0.172	0.005	0.000			0.87	0.18	1.54	4.7	−11.6
Speke	0.414	0.002	0.001	0.404	0.013	0.002	0.156	0.008	0.001	15	651	0.95	0.16	1.42	5.0	−11.2
Batoda	0.339	0.002	0.001	0.449	0.014	0.003	0.186	0.006	0.001	9	471	0.94	0.19	1.50	4.8	−10.5
Marsh Pool II	0.362	0.001	0.000	0.401	0.009	0.001	0.219	0.007	0.001			0.90	0.23	1.61	4.5	−9.8
Upper Kachope	0.369	0.002	0.001	0.420	0.017	0.004	0.178	0.009	0.001			0.95	0.19	1.36	5.2	−9.4
Nsuranja	0.234	0.001	0.001	0.463	0.015	0.007	0.269	0.005	0.004			0.93	0.28	1.56	4.7	−6.8
Katunda	0.332	0.003	0.001	0.412	0.022	0.005	0.211	0.011	0.004	140	8849	0.93	0.23	1.27	5.4	−6.7
Lower Kitandara	0.420	0.004	0.001	0.353	0.037	0.005	0.155	0.020	0.004	9	524	0.94	0.18	0.95	6.3	−6.0
Eldoret Nakuru 6	0.123	0.001	0.000	0.530	0.008	0.000	0.325	0.012	0.001	41	142	1.00	0.34	1.64	4.4	−4.6
Lower Kachope	0.340	0.003	0.001	0.393	0.042	0.005	0.180	0.029	0.007	54	2089	0.96	0.22	0.90	6.4	−3.8
Mutinda	0.187	0.001	0.001	0.460	0.013	0.006	0.319	0.010	0.004	81	5395	0.93	0.33	1.52	4.8	−3.7
Eldoret Nakuru 1a	0.092	0.000	0.000	0.489	0.006	0.000	0.409	0.005	0.000	57	13	1.00	0.41	1.95	3.6	−3.6
Mahoma	0.184	0.002	0.000	0.441	0.010	0.003	0.350	0.008	0.003	36	302	0.99	0.36	1.65	4.4	−3.5
Lake Limuru 2	0.075	0.001	0.000	0.459	0.002	0.000	0.459	0.004	0.000	86	246	1.00	0.46	2.18	3.0	−3.4
Eldoret Nakuru 5	0.150	0.003	0.000	0.505	0.024	0.001	0.287	0.027	0.001	55	153	1.00	0.32	1.18	5.6	−1.4
Ol Bolosat	0.201	0.005	0.001	0.473	0.076	0.003	0.198	0.039	0.005	27	340	0.98	0.24	0.77	6.7	−1.2
Eldoret Nakuru 3	0.130	0.003	0.000	0.514	0.032	0.002	0.288	0.028	0.004	54	124	1.00	0.32	1.12	5.8	−0.6
Narasha	0.141	0.003	0.000	0.425	0.026	0.001	0.391	0.013	0.001	58	208	1.00	0.40	1.33	5.3	1.7
Eldoret Sigawet Dam	0.115	0.006	0.001	0.419	0.107	0.005	0.280	0.059	0.008	65	160	1.00	0.35	0.62	7.1	5.4
Katalin	0.091	0.003	0.001	0.398	0.042	0.001	0.424	0.038	0.002	77	411	0.99	0.46	1.01	6.1	7.7
Edward	0.121	0.006	0.000	0.371	0.117	0.020	0.249	0.096	0.020	163	47,765	0.70	0.37	0.46	7.5	7.9
Challa	0.094	0.006	0.000	0.399	0.092	0.006	0.302	0.088	0.012			0.62	0.40	0.59	7.2	8.5
Sacred	0.047	0.003	0.000	0.320	0.008	0.001	0.611	0.009	0.002	131	86	1.00	0.62	1.75	4.2	8.6
Kyanga	0.077	0.007	0.002	0.379	0.133	0.007	0.304	0.084	0.007	25	583	0.97	0.40	0.50	7.5	9.0
Ekikoto	0.097	0.009	0.002	0.363	0.108	0.011	0.311	0.083	0.017	31	1053	0.95	0.41	0.55	7.3	9.3
Tanganyika (Kigoma)	0.100	0.006	0.001	0.355	0.088	0.019	0.313	0.084	0.034	53	158,726	0.19	0.43	0.59	7.2	9.9
Saka	0.110	0.010	0.001	0.346	0.096	0.006	0.331	0.083	0.018	60	143	1.00	0.43	0.58	7.2	10.1
Nkuruba	0.065	0.008	0.001	0.375	0.105	0.007	0.341	0.083	0.015	52	4238	0.90	0.44	0.58	7.2	10.4
Eldoret Nakuru 2	0.085	0.000	0.000	0.349	0.033	0.004	0.478	0.043	0.007	7	75	0.99	0.53	1.04	6.0	10.7
Nyamiteza	0.091	0.013	0.001	0.296	0.193	0.011	0.267	0.112	0.015	13	6892	0.52	0.39	0.27	8.1	11.2
Kyaninga	0.075	0.007	0.001	0.338	0.130	0.012	0.304	0.115	0.018	16	22,537	0.32	0.44	0.42	7.7	11.8
Kanyamukali	0.067	0.006	0.000	0.354	0.102	0.007	0.354	0.099	0.012	18	638	0.95	0.47	0.55	7.3	12.1
Victoria	0.066	0.004	0.000	0.359	0.083	0.006	0.354	0.107	0.023	32	55,951	0.29	0.48	0.57	7.3	12.7
Lugembe	0.061	0.005	0.000	0.328	0.103	0.008	0.370	0.104	0.021	24	2265	0.88	0.50	0.53	7.4	13.7
Nyabikere	0.057	0.006	0.001	0.322	0.091	0.005	0.386	0.118	0.013	43	375	0.99	0.52	0.53	7.4	14.8
Ntambi	0.055	0.012	0.000	0.301	0.068	0.007	0.463	0.074	0.020	10	2856	0.71	0.56	0.73	6.8	14.9
George	0.045	0.007	0.001	0.295	0.116	0.004	0.406	0.116	0.010	75	62	1.00	0.53	0.48	7.5	16.0
Nyungu	0.053	0.005	0.000	0.315	0.100	0.003	0.346	0.169	0.009	40	648	0.98	0.52	0.39	7.7	16.4
Kibengo	0.040	0.006	0.001	0.294	0.111	0.005	0.414	0.122	0.009	12	48	0.99	0.54	0.48	7.5	16.6
Kyoga	0.031	0.005	0.001	0.248	0.076	0.007	0.496	0.117	0.019	129	406	1.00	0.63	0.59	7.2	20.0

Table A3

Correlation matrix of GDGT distributions and environmental variables for 41 East African lake sites, including correlation coefficients and p values.

	fGDGTIII	fGDGTIIIb	fGDGT IIIc	fGDGT II	fGDGTIIb	fGDGTIIc	fGDGT I	fGDGT Ib	fGDGTIc	SW pH	BW pH	SW Temp	BW Temp	MAAT	Log K25	Log Depth	Log DO	Log SA	Log CA	Log CA/SA	Log [branc]	Log [cren]	MBT	CBT	BIT
f GDGT III	1.0000	−.6338	.0464	.6885	−.7520	−.3216	−.8638	−.8766	−.6556	−.8587	−.7661	−.9734	−.9647	−.9591	−.8021	−.2206	.3585	−.3872	−.1114	.7375	−.2933	−.0700	−.9458	.8118	.2210
	p = —	p = .002	p = .842	p = .001	p = .000	p = .155	p = .000	p = .000	p = .001	p = .000	p = .000	p = .000	p = .000	p = .000	p = .000	p = .337	p = .111	p = .083	p = .631	p = .000	p = .197	p = .763	p = .000	p = .000	p = .336
fGDGT IIIb	−.6338	1.0000	.2760	−.6635	.7893	.3821	.4710	.5758	.4745	.7531	.7107	.6946	.6691	.6701	.8542	.2894	−.4040	.0750	−.1410	−.5845	−.0780	.1190	.5572	−.7315	−.2664
	p = .002	p = —	p = .226	p = .001	p = .000	p = .087	p = .031	p = .006	p = .030	p = .000	p = .000	p = .000	p = .001	p = .001	p = .000	p = .203	p = .069	p = .747	p = .542	p = .005	p = .737	p = .608	p = .009	p = .000	p = .243
f GDGT IIIc	.0464	.2760	1.0000	−.0764	.2907	.1780	−.1805	−.0255	.0141	.0859	−.0396	.0010	−.0083	−.0087	.0184	.1854	.0141	−.0371	−.0127	.0892	−.0324	.0430	−.1331	−.1529	−.1469
	p = .842	p = .226	p = —	p = .742	p = .201	p = .440	p = .434	p = .913	p = .952	p = .711	p = .865	p = .996	p = .971	p = .970	p = .937	p = .421	p = .951	p = .873	p = .956	p = .700	p = .889	p = .853	p = .565	p = .508	p = .525
fGDGT II	.6885	−.6635	−.0764	1.0000	−.6481	−.1774	−.7096	−.8007	−.5116	−.8026	−.8200	−.7359	−.7345	−.7388	−.6310	.0969	.0564	−.3453	−.2056	.3238	−.1314	.1294	−.8035	.7910	.0874
	p = .001	p = .001	p = .742	p = —	p = .001	p = .442	p = .000	p = .000	p = .018	p = .000	p = .000	p = .000	p = .000	p = .000	p = .002	p = .676	p = .808	p = .125	p = .371	p = .152	p = .570	p = .576	p = .000	p = .000	p = .706
fGDGT IIb	−.7520	.7893	.2907	−.6481	1.0000	.4920	.3994	.8111	.5273	.8344	.6898	.8152	.8029	.8140	.7929	.2875	−.3051	.2359	−.0082	−.6513	.1045	.1870	.5932	−.9126	−.3338
	p = .000	p = .000	p = .201	p = .001	p = —	p = .023	p = .073	p = .000	p = .014	p = .000	p = .001	p = .000	p = .000	p = .000	p = .000	p = .206	p = .179	p = .303	p = .972	p = .001	p = .652	p = .417	p = .005	p = .000	p = .139
fGDGT IIc	−.3216	.3821	.1780	−.1774	.4920	1.0000	.0254	.2884	.7534	.4033	.4267	.4351	.4627	.4667	.5343	.5170	−.0419	.5302	.4037	−.2747	.3267	.7486	.1653	−.4666	−.6867
	p = .155	p = .087	p = .440	p = .442	p = .023	p = —	p = .913	p = .205	p = .000	p = .070	p = .054	p = .049	p = .035	p = .033	p = .013	p = .016	p = .857	p = .013	p = .070	p = .228	p = .148	p = .000	p = .474	p = .033	p = .001
fGDGT I	−.8638	.4710	−.1805	−.7096	.3994	.0254	1.0000	.6715	.5018	.6819	.6906	.8044	.7967	.7794	.5897	−.0636	−.2296	.3349	.1441	−.4985	.2632	−.1914	.9589	−.5452	.0208
	p = .000	p = .031	p = .434	p = .000	p = .073	p = .913	p = —	p = .001	p = .020	p = .001	p = .001	p = .000	p = .000	p = .000	p = .005	p = .784	p = .317	p = .138	p = .533	p = .021	p = .249	p = .406	p = .000	p = .011	p = .929
fGDGT Ib	−.8766	.5758	−.0255	−.8007	.8111	.2884	.6715	1.0000	.5767	.8763	.7602	.8859	.8827	.8947	.7297	.1780	−.2419	.3770	.1407	−.6193	.2501	.0479	.8509	−.9165	−.2050
	p = .000	p = .006	p = .913	p = .000	p = .000	p = .205	p = .001	p = —	p = .006	p = .000	p = .000	p = .000	p = .000	p = .000	p = .000	p = .440	p = .291	p = .092	p = .543	p = .003	p = .274	p = .837	p = .000	p = .000	p = .373
fGDGT Ic	−.6556	.4745	.0141	−.5116	.5273	.7534	.5018	.5767	1.0000	.6304	.6728	.7016	.7259	.7257	.6732	.5412	−.1389	.6751	.4838	−.4456	.3056	.6585	.6114	−.6546	−.7149
	p = .001	p = .030	p = .952	p = .018	p = .014	p = .000	p = .020	p = .006	p = —	p = .002	p = .001	p = .000	p = .000	p = .000	p = .001	p = .011	p = .548	p = .001	p = .026	p = .043	p = .178	p = .001	p = .003	p = .001	p = .000
SW pH	−.8587	.7531	.0859	−.8026	.8344	.4033	.6819	.8763	.6304	1.0000	.9206	.9281	.9249	.9382	.8847	.1984	−.1447	.3965	.1529	−.6332	.1491	.0352	.8181	−.9236	−.2213
	p = .000	p = .000	p = .711	p = .000	p = .000	p = .070	p = .001	p = .000	p = .002	p = —	p = .000	p = .000	p = .000	p = .000	p = .000	p = .389	p = .532	p = .075	p = .508	p = .002	p = .519	p = .879	p = .000	p = .000	p = .335
BW pH	−.7661	.7107	−.0396	−.8200	.6898	.4267	.6906	.7602	.6728	.9206	1.0000	.8598	.8699	.8787	.8126	.0931	.0057	.5454	.3420	−.4846	.1325	.0832	.7862	−.8103	−.2973
	p = .000	p = .000	p = .865	p = .000	p = .001	p = .054	p = .001	p = .000	p = .001	p = .000	p = —	p = .000	p = .000	p = .000	p = .000	p = .688	p = .980	p = .011	p = .129	p = .026	p = .567	p = .720	p = .000	p = .000	p = .191
SW Temp	−.9734	.6946	.0010	−.7359	.8152	.4351	.8044	.8859	.7016	.9281	.8598	1.0000	.9961	.9952	.8655	.2336	−.2556	.4717	.2008	−.7038	.2943	.1155	.9108	−.8740	−.2659
	p = .000	p = .000	p = .996	p = .000	p = .000	p = .049	p = .000	p = .000	p = .000	p = .000	p = .000	p = —	p = 0.00	p = .000	p = .000	p = .308	p = .263	p = .031	p = .383	p = .000	p = .195	p = .618	p = .000	p = .000	p = .244
BW Temp	−.9647	.6691	−.0083	−.7345	.8029	.4627	.7967	.8827	.7259	.9249	.8699	.9961	1.0000	.9973	.8533	.2328	−.2350	.5082	.2407	−.6889	.3207	.1485	.9058	−.8783	−.2880
	p = .000	p = .001	p = .971	p = .000	p = .000	p = .035	p = .000	p = .000	p = .000	p = .000	p = .000	p = 0.00	p = —	p = 0.00	p = .000	p = .310	p = .305	p = .019	p = .293	p = .001	p = .156	p = .521	p = .000	p = .000	p = .206
MAAT	−.9591	.6701	−.0087	−.7388	.8140	.4667	.7794	.8947	.7257	.9382	.8787	.9952	.9973	1.0000	.8580	.2339	−.2222	.5160	.2536	−.6737	.3233	.1522	.8980	−.8891	−.2893
	p = .000	p = .001	p = .970	p = .000	p = .000	p = .033	p = .000	p = .000	p = .000	p = .000	p = .000	p = 0.00	p = 0.00	p = —	p = .000	p = .308	p = .333	p = .017	p = .267	p = .001	p = .153	p = .510	p = .000	p = .000	p = .203
Log K25	−.8021	.8542	.0184	−.6310	.7929	.5343	.5897	.7297	.6732	.8847	.8126	.8655	.8533	.8580	1.0000	.4174	−.4202	.2297	−.0454	−.7454	.0661	.2484	.7056	−.8291	−.3266
	p = .000	p = .000	p = .937	p = .002	p = .000	p = .013	p = .005	p = .000	p = .001	p = .000	p = .000	p = .000	p = .000	p = .000	p = —	p = .060	p = .058	p = .316	p = .845	p = .000	p = .776	p = .278	p = .000	p = .000	p = .148
Log Depth	−.2206	.2894	.1854	.0969	.2875	.5170	−.0636	.1780	.5412	.1984	.0931	.2336	.2328	.2339	.4174	1.0000	−.4240	.2270	.0327	−.5263	−.0740	.7274	.0518	−.2784	−.7234
	p = .337	p = .203	p = .421	p = .676	p = .206	p = .016	p = .784	p = .440	p = .011	p = .389	p = .688	p = .308	p = .310	p = .308	p = .060	p = —	p = .055	p = .322	p = .888	p = .014	p = .750	p = .000	p = .823	p = .222	p = .000
Log DO	.3585	−.4040	.0141	.0564	−.3051	−.0419	−.2296	−.2419	−.1389	−.1447	.0057	−.2556	−.2350	−.2222	−.4202	−.4240	1.0000	.4011	.5693	.5438	−.0302	−.2425	−.2523	.2403	.0756
	p = .111	p = .069	p = .951	p = .808	p = .179	p = .857	p = .317	p = .291	p = .548	p = .532	p = .980	p = .263	p = .305	p = .333	p = .058	p = .055	p = —	p = .072	p = .007	p = .011	p = .897	p = .290	p = .270	p = .294	p = .745
Log SA	−.3872	.0750	−.0371	−.3453	.2359	.5302	.3349	.3770	.6751	.3965	.5454	.4717	.5082	.5160	.2297	.2270	.4011	1.0000	.9389	−.0182	.5034	.4353	.4058	−.3697	−.5454
	p = .083	p = .747	p = .873	p = .125	p = .303	p = .013	p = .138	p = .092	p = .001	p = .075	p = .011	p = .031	p = .019	p = .017	p = .316	p = .322	p = .072	p = —	p = .000	p = .938	p = .020	p = .049	p = .068	p = .099	p = .011
Log CA	−.1114	−.1410	−.0127	−.2056	−.0082	.4037	.1441	.1407	.4838	.1529	.3420	.2008	.2407	.2536	−.0454	.0327	.5693	.9389	1.0000	.3259	.5496	.3608	.1791	−.1378	−.4005
	p = .631	p = .542	p = .956	p = .371	p = .972	p = .070	p = .533	p = .543	p = .026	p = .508	p = .129	p = .383	p = .293	p = .267	p = .845	p = .888	p = .007	p = .000	p = —	p = .149	p = .010	p = .108	p = .437	p = .551	p = .072
Log CA/SA	.7375	−.5845	.0892	.3238	−.6513	−.2747	−.4985	−.6193	−.4456	−.6332	−.4846	−.7038	−.6889	−.6737	−.7454	−.5263	.5438	−.0182	.3259	1.0000	.2004	−.1415	−.5897	.5971	.3166
	p = .000	p = .005	p = .700	p = .152	p = .001	p = .228	p = .021	p = .003	p = .043	p = .002	p = .026	p = .000	p = .001	p = .001	p = .000	p = .014	p = .011	p = .938	p = .149	p = —	p = .384	p = .541	p = .005	p = .004	p = .162
Log [branc]	−.2933	−.0780	−.0324	−.1314	.1045	.3267	.2632	.2501	.3056	.1491	.1325	.2943	.3207	.3233	.0661	−.0740	−.0302	.5034	.5496	.2004	1.0000	.2491	.2888	−.2165	.0282
	p = .197	p = .737	p = .889	p = .570	p = .652	p = .148	p = .249	p = .274	p = .178	p = .519	p = .567	p = .195	p = .156	p = .153	p = .776	p = .750	p = .897	p = .020	p = .010	p = .384	p = —	p = .276	p = .204	p = .346	p = .904
Log [cren]	−.0700	.1190	.0430	.1294	.1870	.7486	−.1914	.0479	.6585	.0352	.0832	.1155	.1485	.1522	.2484	.7274	−.2425	.4353	.3608	−.1415	.2491	1.0000	−.0750	−.1935	−.8467
	p = .763	p = .608	p = .853	p = .576	p = .417	p = .000	p = .406	p = .837	p = .001	p = .879	p = .720	p = .618	p = .521	p = .510	p = .278	p = .000	p = .290	p = .049	p = .108	p = .541	p = .276	p = —	p = .747	p = .401	p = .000
MBT	−.9458	.5572	−.1331	−.8035	.5932	.1653	.9589	.8509	.6114	.8181	.7862	.9108	.9058	.8980	.7056	.0518	−.2523	.4058	.1791	−.5897	.2888	−.0750	1.0000	−.7390	−.1017
	p = .000	p = .009	p = .565	p = .000	p = .005	p = .474	p = .000	p = .000	p = .003	p = .000	p = .000	p = .000	p = .000	p = .000	p = .000	p = .823	p = .270	p = .068	p = .437	p = .005	p = .204	p = .747	p = —	p = .000	p = .661
CBT	.8118	−.7315	−.1529	.7910	−.9126	−.4666	−.5452	−.9165	−.6546	−.9236	−.8103	−.8740	−.8783	−.8891	−.8291	−.2784	.2403	−.3697	−.1378	.5971	−.2165	−.1935	−.7390	1.0000	.3147
	p = .000	p = .000	p = .508	p = .000	p = .000	p = .033	p = .011	p = .000	p = .001	p = .000	p = .000	p = .000	p = .000	p = .000	p = .000	p = .222	p = .294	p = .099	p = .551	p = .004	p = .346	p = .401	p = .000	p = —	p = .165
BIT	.2210	−.2664	−.1469	.0874	−.3338	−.6867	.0208	−.2050	−.7149	−.2213	−.2973	−.2659	−.2880	−.2893	−.3266	−.7234	.0756	−.5454	−.4005	.3166	.0282	−.8467	−.1017	.3147	1.0000
	p = .336	p = .243	p = .525	p = .706	p = .139	p = .001	p = .929	p = .373	p = .000	p = .335	p = .191	p = .244	p = .206	p = .203	p = .148	p = .000	p = .745	p = .011	p = .072	p = .162	p = .904	p = .000	p = .661	p = .165	p = —

REFERENCES

Barker P. A., Street-Perrott F. A., Leng M. J., Greenwood P. B., Swain D. L., Perrott R. A., Telford R. J. and Ficken K. J. (2001) A 14,000-year oxygen isotope record from diatom silica in two alpine lakes on Mt. Kenya. *Science* **22**, 2307–2310.

Batjes N. H. (1997) A world dataset of derived soil properties by FAO-UNESCO soil unit for global modelling. *Soil Use Manage.* **13**, 9–16.

Blaga C. I., Reichart G.-J., Heiri O. and Sinninghe Damsté J. S. (2009) Tetraether membrane lipid distributions in water-column particulate matter and sediments: a study of 47 European lakes along a north-south transect. *J. Paleolimnol.* **41**, 523–540.

Bugenyi F. W. B. and Magumba K. M. (1996) The present physicochemical ecology of Lake Victoria, Uganda. In *The Limnology, Climatology, and Paleoclimatology of the East African Lakes* (eds. T. C. Johnson and E. O. Odada). Gordon and Breach, Amsterdam, The Netherlands, pp. 141–153.

Davis B. A. S., Brewer S., Stevenson A. C., Guiot J. and Data Contributors (2003) The temperature of Europe during the Holocene reconstructed from pollen data. *Quatern. Sci. Rev.* **22**, 1701–1716.

Descy J. P., Plisnier P. D., Leporcq B., Stenuite S., Pirlot S., Stimart J., Gosselain V., Andre L., Alleman L., Langlet D., Vyverman W., Cocquyt C., De Wever A., Stoyneva M. P., Deleersnijder E., Naithani J., Chitamwebwa D., Chande A., Kimirei I., Sekadende B., Mwaitega S., Muhoza S., Sinyenza D., Makasa L., Lukwessa C., Zulu I. and Phiri H. (2005) Climlake: climate variability as recorded in Lake Tanganyika. Final report (2001–2005). In *FSPO — Global Change, Ecosystems, and Biodiversity* (eds. P. D. Plisnier and J. P. Descy) Brussels, Belgium. pp. 104.

Donders T. H., Weijers J. W. H., Musterman M., Kloosterboer-van Hoeve M. L., Buckles L. K., Pancost R. D., Schouten S., Sinninghe Damsté J. S. and Brinkhuis H. (2009) Strong climate coupling of terrestrial and marine environments in the Miocene of northwest Europe. *Earth Planet. Sci. Lett.* **281**, 215–225.

Dunbar R. B. and Cole J. E. (1999) Annual Records of Tropical Systems (ARTS). *PAGES Workshop Rep. Ser.* **99**, 72.

Eggermont H., Russell J. M., Schetter G., Vandamme K. and Verschuren D. (2007) Physical and chemical limnology and climate sensitivity of alpine lakes and pools in the Rwenzori Mountains Uganda-Congo. *Hydrobiologia* **592**, 151–173.

Eggermont H., Heiri O., Russell J., Vuille M., Audenaert L. and Verschuren D. (2009) Paleotemperature reconstruction in tropical Africa using fossil Chironomidae (Insecta: Diptera). *J. Paleolimnol.*. doi:10.1007/s10933-009-9339-2.

Esper J., Cook E. R. and Schweingruber F. H. (2002) Low-frequency signals in long tree-ring chronologies for reconstructing past temperature variability. *Science* **295**, 2250–2253.

Fritts H. C. (1974) Relationships of ring widths in arid-site conifers to variations in monthly temperature and precipitation. *Ecol. Monogr.* **44**, 411–440.

Gasse F. (2002) Diatom-inferred salinity and carbonate oxygen isotopes in Holocene waterbodies of the western Sahara and Sahel (Africa). *Quat. Sci. Rev.* **7**, 737–767.

Gasse F., Talling J. F. and Kilham P. (1983) Diatom assemblages in East Africa: classification, distribution and ecology. *Rev. Hydrobiol. Trop.* **16**, 3–34.

Hopmans E. C., Weijers J. W. H., Schefuß E., Herfort L., Sinninghe Damsté J. S. and Schouten S. (2004) A novel proxy for terrestrial organic matter in sediments based on branched and isoprenoid tetraether lipids. *Earth Planet. Sci. Lett.* **224**, 107–116.

Huguet C., Hopmans E. C., Febo-Ayala W., Thompson D. H., Sinninghe Damsté J. S. and Schouten S. (2006) An improved method to determine the absolute abundance of glycerol dibiphytanyl glycerol tetraether lipids. *Org. Geochem.* **37**, 1036–1041.

Könneke M., Bernhard A. E., de la Torre J. R., Walker C. B., Waterbury J. B. and Stahl D. A. (2005) Isolation of an autotrophic ammonia-oxidizing marine archaeon. *Nature* **437**, 543–546.

Lehman J. (2002) Application of AVHRR to water balance, mixing dynamics, and water chemistry of Lake Edward, East Africa. In *The East African Great Lakes: Limnology, Palaeolimnology, Biodiversity* (eds. E. O. Odada and D. Olgao). Kluwer Academic Publishers, Dordrecht, The Netherlands, pp. 235–260.

Lewis, Jr., W. M. (1973) The thermal regime of Lake Lanao (Philippines) and its theoretical implications for tropical lakes. *Limnol. Oceanogr.* **18**, 200–217.

Livingstone D. M., Lotter A. F. and Walker I. R. (1999) The decrease in summer surface water temperature with altitude in Swiss alpine lakes: a comparison with air temperature lapse rates. *Arctic Antarct. Alpine Res.* **31**, 341–352.

Lotter A. F., Birks H. J. B., Hofmann W. and Marchetto A. (1997) Modern diatom, cladoceran, chironomid, and chrysophyte cyst assemblages as quantitative indicators for reconstruction of past environmental conditions in the Alps. I. Climate. *J. Paleolimnol.* **18**, 395–420.

Mergeay J., Verschuren D. and De Meester L. (2005) *Daphnia* species diversity in Kenya, and a key to the identification of their ephippia. *Hydrobiologia* **542**, 261–274.

Mergeay J., Declerck S., Verschuren D. and De Meester L. (2006) *Daphnia* community analysis in shallow Kenyan lakes and ponds using dormant eggs in surface sediments. *Freshwater Biol.* **51**, 399–411.

Morrison D. F. (1976) *Multivariate Statistical Models*. McGraw-Hill, New York.

Mungoma S. (1988) Horizontal differentiation in the limnology of a tropical river-lake (Lake Kyoga, Uganda). *Hydrobiologia* **162**, 89–96.

Peterse F., Kim J.-H., Schouten S., Kristensen D. K., Koç N. and Sinninghe Damsté J. S. (2009) Constraints on the application of the MBT/CBT palaeothermometer at high latitude environments (Svalbard, Norway). *Org. Geochem.* **40**, 692–699.

Powers L. A., Werne J. P., Johnson T. C., Hopmans E. C., Sinninghe Damsté J. S. and Schouten S. (2004) Crenarchaeotal membrane lipids in lake sediments: a new paleotemperature proxy for continental paleoclimate reconstruction? *Geology* **32**, 613–616.

Powers L. A., Johnson T. C., Werne J. P., Castañeda I. S., Hopmans E. C., Sinninghe Damsté J. S. and Schouten S. (2005) Large temperature variability in the southern African tropics since the Last Glacial Maximum. *Geophys. Res. Lett.* **32**. doi:10.1029/2004GL022014.

Powers L., Werne J. P., Vanderwoude A. J., Sinninghe Damsté J. S., Hopmans E. C. and Schouten S. (2010) Applicability and calibration of the TEX_{86} paleothermometer in lakes. *Org. Geochem.* **41**, 404–413.

Rueda G., Rosell-Melé A., Escala M., Gyllencreutz R. and Backman J. (2009) Comparison of instrumental and GDGT-based estimates of sea surface and air temperatures from the Skagerrak. *Org. Geochem.* **40**, 287–291.

Schouten S., Hopmans E. C., Schefuß E. and Sinninghe Damsté J. S. (2002) Distributional variations in marine crenarchaeotal membrane lipids: a new tool for reconstructing ancient sea water temperatures? *Earth Planet. Sci. Lett.* **204**, 265–274.

Schouten S., Huguet C., Hopmans E. C., Kienhuis M. V. M. and Sinninghe Damsté J. S. (2007) Analytical methodology for TEX_{86} paleothermometry by high-performance liquid

chromatography/atmospheric pressure chemical ionization–mass spectrometry. *Anal. Chem.* **79**, 2940–2944.

Sinninghe Damsté J. S., Hopmans E. C., Pancost R. D., Schouten S. and Geenevasen J. A. J. (2000) Newly discovered non-isoprenoid dialkyl diglycerol tetraether lipids in sediments. *J. Chem. Soc. Chem. Commun.* **17**, 1683–1684.

Sinninghe Damsté J. S., Ossebaar J., Schouten S. and Verschuren D. (2008) Altitudinal shifts in the branched tetraether lipid distribution in soil from Mt. Kilimanjaro (Tanzania): implications for the MBT/CBT continental palaeothermometer. *Org. Geochem.* **39**, 1072–1076.

Sinninghe Damsté J. S., Ossebaar J., Abbas B., Schouten S. and Verschuren D. (2009) Fluxes and distribution of tetraether lipids in an equatorial African lake: constraints on the application of the TEX_{86} paleothermometer and BIT index in lacustrine settings. *Geochim. Cosmochim. Acta* **73**, 4232–4249.

Talling J. F. and Talling I. B. (1965) The chemical composition of African lake waters. *Int. Rev. Gesamten Hydrobiol.* **50**, 421–463.

Talling J. F. and Lemoalle J. (1998) *Ecological Dynamics of Tropical Inland Waters*. Cambridge University Press, Cambridge, UK.

ter Braak C. J. F. and Smilauer P. (2002) CANOCO reference manual and Canodraw for Windows Users Guide: software for canonical community ordination (version 4.5). Microcomputer Power, Ithaca, NY, USA. 500 pp.

Tierney J. E., Mayes M. T., Meyer N., Johnson C., Swarzenski P. W., Cohen A. S. and Russell J. M. (2010) Late-twentieth-century warming in Lake Tanganyika unprecedented since AD 500. *Nat. Geosci.* **3**, 422–425.

Tierney J. E., Russell J. M., Huang Y., Sinninghe Damsté J. S., Hopmans E. C. and Cohen A. S. (2008) Northern hemisphere controls on tropical Southeast African climate during the past 60,000 years. *Science* **322**, 252–255.

Tierney J. E. and Russell J. M. (2009) Distributions of branched GDGTs in a tropical lake system: implications for lacustrine application of the MBT/CBT paleoproxy. *Org. Geochem.* **40**, 1032–1036.

Velle G., Brooks S. J., Birks H. J. B. and Willassen E. (2005) Chironomids as a tool for inferring Holocene climate: an assessment based on six sites in Southern Scandinavia. *Quatern. Sci. Rev.* **24**, 1429–1462.

Vincens A., Garcin Y. and Buchet G. (2007) Influence of rainfall seasonality on African lowland vegetation during the Late Quaternary: pollen evidence from Lake Masoko, Tanzania. *J. Biogeogr.* **34**, 1274–1288.

Viner A. B. (1969) The chemistry of the water of Lake George. *Verh. Int. Ver. Theor. Angew. Limnol.* **17**, 289–296.

Viner A. B. and Smith I. B. (1973) Geographical, physical, and historical aspects of Lake George. *Proc. Roy. Soc. Lond. B. Biol.* **184**, 235–270.

Vuille M., Bradley R. S., Healy R., Werner M., Hardy D. R., Thompson L. G. and Keimig F. (2003) Modeling δ^{18} O in precipitation over the tropical Americas: 2. Simulation of the stable isotope signal in Andean ice cores. *J. Geophys. Res.* **108**. doi:10.1029/2001JD002039.

Walker I. R., Smol J. P., Engstrom D. R. and Birks H. J. B. (1991) An assessment of Chrinonomidae as quantitative indicators of past climatic change. *Can. J. Fish. Aquat. Sci.* **48**, 975–987.

Webb, III, T. W. and Bryson R. A. (1972) Late- and post-glacial climatic change in the northern Midwest, U.S.A.: quantitative estimates derived from fossil pollen spectra by multivariate statistical analysis. *Quatern. Res.* **2**, 70–115.

Weijers J. W. H., Schouten S., Spaargaren O. C. and Sinninghe Damsté J. S. (2006a) Occurrence and distribution of tetraether membrane lipids in soils: implications for the use of the TEX_{86} proxy and the BIT Index. *Org. Geochem.* **37**, 1680–1693.

Weijers J. W. H., Schouten S., Hopmans E. C., Geenevasen J. A. J., David O. R. P., Coleman J. M., Pancost R. D. and Sinninghe Damsté J. S. (2006b) Membrane lipids of mesophilic anaerobic bacteria thriving in peats have typical archaeal traits. *Environ. Microbiol.* **8**, 648–657.

Weijers J. W. H., Schouten S., van den Donker J. C., Hopmans E. C. and Sinninghe Damsté J. S. (2007a) Environmental controls on bacterial tetraether membrane lipid distribution in soils. *Geochim. Cosmochim. Acta* **71**, 703–713.

Weijers J. W. H., Schefuß E., Schouten S. and Sinninghe Damsté J. S. (2007b) Coupled thermal and hydrological evolution of tropical Africa over the last deglaciation. *Science* **315**, 1701–1704.

Weijers J. W. H., Schouten S., Schefuß E., Schneider R. R. and Sinninghe Damsté J. S. (2009) Disentangling marine, soil and plant organic carbon contributions to continental margin sediments: a multi-proxy approach in a 20,000 year sediment record from the Congo deep-sea fan. *Geochim. Cosmochim. Acta* **73**, 119–132.

Associate editor: Josef Werne

tions have been completed (Stebich et al., 2009), and b) the late Holocene with geochemical (Schettler et al., 2006b) and minerogenic analyses (Chu et al., 2009). For the late Glacial in particular, short cold/dry spells were recorded that are perfectly correlated with events reported from the Greenland ice core records. Such synchronicity in abrupt climate shifts demonstrates that the North Atlantic and East Asian regions were strongly coupled via atmospheric teleconnections. The varve-based chronologies that have been established from several lakes also enabled precise determination of the age of several tephra layers preserved in the sediment records, thereby providing a much improved chronology of volcanic eruptions in northeastern China (Liu et al., 2009).

Outlook

In addition to the research topics outlined above, lake sediment records are also used to investigate the history of eutrophication, especially in the large and shallow floodplain lakes of the middle and lower reaches of the Yangtze River, which is one of the most densely populated and industrialized areas in China. Paleolimnological research on these lakes mainly relies upon diatom-based reconstructions of total phosphorus concentrations in lake water (Yang et al., 2008; Dong et al., 2008). The multi-proxy record from Lake Erhai in Yunnan, southern China, is also an excellent example of how to use lake sediment records to reconstruct climate-human-environment interactions during the Holocene (Dearing et al., 2008).

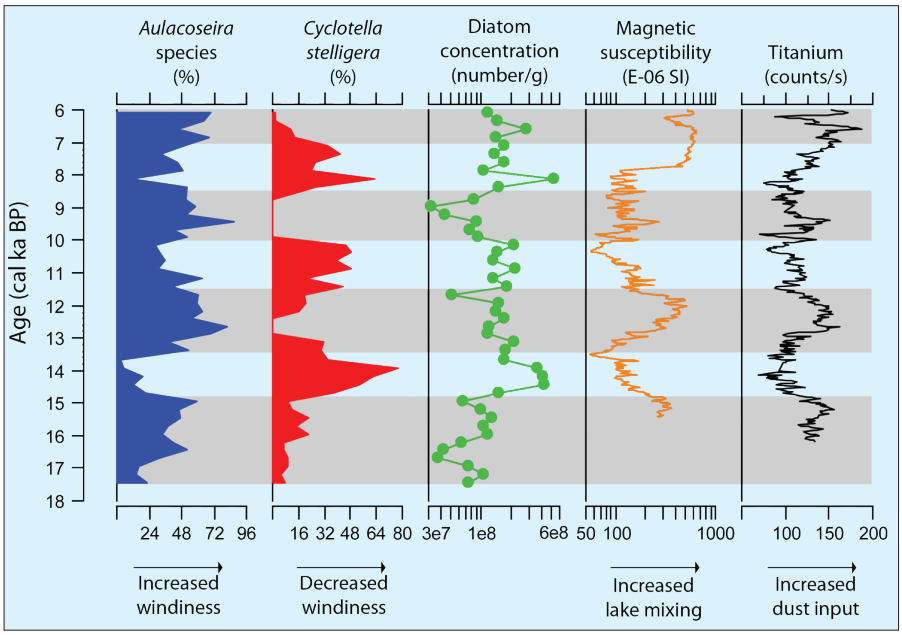

Figure 2: Comparison of the diatom data; % abundances of the planktonic centric taxa Aulacoseira *spp. (**blue**) and* Cyclotella stelligera *(**red**), as well as diatom concentration (**green**) (Wang et al., 2008), with the titanium (Ti) content (**black**) and magnetic susceptibility records (**orange**) (Yancheva et al., 2007) from the Huguang maar lake (South China). High abundances of* Aulacoseira *spp. are indicative of periods of turbulent water column mixing due to strong winds, while increased abundance of* C. stelligera *suggests thermally stratified, weak wind conditions. The seasonal change in relative abundance of these taxa can, therefore, be used as a proxy of the strength of winter monsoon winds. Ti and magnetic susceptibility are proxies for dust input and lake mixing, respectively.*

Acknowledgements

The authors would like to thank the financial support from the National Science Foundation of China (grants # 4050 21018, 4087 2113 and 10572107) and the Chinese Academy of Sciences (grant # kzcx2-yw-119-02).

References

Chen, F. et al., 2008: Holocene moisture evolution in arid central Asia and its out-of-phase relationship with Asian monsoon history, *Quaternary Science Reviews*, **27**: 351-364.

Chu, G., Sun, Q., Gu, Z., Rioual, P., Liu, Q., Wang, K., Han, J. and Liu, J., 2009: Dust records from varved lacustrine sediments of two neighboring lakes in northeastern China over the last 1400 years, *Quaternary International*, **194**: 108-118.

Colman, S.M., Yu, S.-Y., An, Z.S., Shen, J. and Henderson, A.C.G., 2007: Late Cenozoic climate changes in China's western interior: a review of research on Lake Qinghai and comparison with other records, *Quaternary Science Reviews*, **26**: 2281-2300.

Wang, L. et al., 2008: Diatom-based inference of variations in the strength of Asian winter monsoon winds between 17,500 and 6000 calendar years B.P., *Journal of Geophysical Research*, **113**: D21101, doi:10.1029/2008JD010145.

Yancheva, G. et al., 2007: Influence of the intertropical convergence zone on the East Asian monsoon, *Nature*, **445**: 74-77.

For full references please consult:

www.pages-igbp.org/products/newsletters/ref2009_3.html

Paleolimnology of African lakes: Beyond the exploration phase

Dirk Verschuren[1] and James M. Russell[2]

[1]Limnology Unit, Department of Biology, Ghent University, Belgium; dirk.verschuren@UGent.be
[2]Department of Geological Sciences, Brown University, Providence, USA

Longstanding research questions on tropical climate-human-ecosystem interactions can be tackled by combining novel and traditional paleoenvironmental proxies from high-quality sediment archives in African lakes.

Paleolimnology of African lakes: Something particular

African lakes have had a special allure to paleolimnologists ever since pioneering work by Dan Livingstone and his students revealed their potential for tropical paleoecology and paleoclimatology. However, it took time before their particularities (e.g., methane-charged muds, unstable sedimentary environments associated with fluctuating lake level) and logistical challenges no longer hampered application of the modern paleolimnological techniques that were developed in Europe and North America during the 1980s. Given the scarcity of annually resolved African lake records, progress in African paleolimnology depends on well-constrained radiometric chronologies. This is often challenging, because lakes with the hydrological sensitivity required to register decade- to century-scale climate variability tend to display significant variability in sedimentation rates and radiocarbon reservoir age, with complicating effects on the age-depth relationship that cannot easily be resolved by ^{210}Pb/^{14}C-based age models. As for the reconstructions themselves, the principal issues are that, firstly, past human impacts on African lakes and the surrounding landscapes cannot be determined without accounting for major climatic influence on ecosystem dynamics at

all timescales; and secondly, the pressing need for quantitative temperature proxies, and for hydrological proxies unaffected by lake-groundwater interactions and temperature effects on evaporation. Basin-specific hydrological modeling is one solution, exemplified by work on Rift Valley lakes in Ethiopia (Legesse et al., 2004) and Kenya (Bergner et al., 2003; Duhnforth et al., 2006). Other methodological advances have come from the development of regional calibration datasets that constrain the ecological indicator value of in-lake biological proxies (e.g., Rumes et al., 2005; Eggermont et al., 2006; 2009), and application of new organic biomarker proxies for temperature and moisture balance to African lake records.

Resolving African climate history

Reconstructions of African climate history using these improved techniques testify to the global teleconnection of climate variability at glacial-interglacial, orbital and shorter time scales but also reveal distinct tropical climate processes. For example, results of ICDP-sponsored drilling in Lake Malawi (southeastern tropical Africa) and Lake Bosumtwi (tropical West Africa) show that tropical African climate history differs from the characteristic 100-ka saw-tooth pattern of continental ice-sheet growth and decay. Most importantly, tropical aridity during the Last Glacial Maximum (MIS2) paled in comparison with megadroughts recurring at ~21-ka intervals during MIS5 and MIS4, when high eccentricity strengthened precessional insolation forcing (Scholz et al., 2007; Cohen et al., 2007). Penetrating a sub-lacustrine ridge in Lake Tanganyika with Kullenberg-coring methods, Felton et al. (2007) recovered a continuous climate record back to the base of MIS3. Analyses of organic biomarker proxies for past temperature (the TEX_{86} index of crenarchaeotal membrane lipids) and moisture balance (the δD of leaf waxes) by Tierney et al. (2008) revealed that millennial MIS3 drought episodes in southeastern tropical Africa coincide with Heinrich events (Fig. 1), suggesting northern high-latitude influence on sea-surface temperature in the western Indian Ocean. This study also confirmed the result of Powers et al. (2005) from Lake Malawi, which showed that postglacial warming started ~20 ka BP, i.e., coincident with the start of major continental ice-sheet melting, but well before the rise in atmospheric CO_2. A moisture balance reconstruction from Lake Malawi based on the C3/C4 vegetation ratio incorporated in the $\delta^{13}C$ of leaf wax alkanes (Castañeda et al., 2007) supports evidence for early Holocene drought in southern tropical Africa (Nash et al., 2006; Garcin et al., 2007), associated with the rapid resumption of Intertropical Convergence Zone (ITCZ) migration far into the Northern Hemisphere at the end of the Younger Dryas (Talbot et al., 2007). Reviewing all relevant lake (and nearshore marine) paleoclimate records/patterns across southern Africa, Gasse et al. (2008) report progress in resolving the longstanding conflict between evidence for a dry LGM (and Younger Dryas) in Lake Malawi (e.g., Johnson et al., 2002) vs. wet conditions during those times recorded in nearby Lake Masoko (Garcin et al., 2006). Another issue of longstanding debate has been whether Holocene retreat of the northernmost summer-time position of the ITCZ caused a gradual or abrupt mid-Holocene weakening of the West African monsoon over North Africa, and thus a gradual or abrupt mid-Holocene desiccation of the Sahara desert. Multiple-proxy analyses on the uniquely continuous sediment record of a groundwater-fed lake in northern Chad (Kröpelin et al., 2008) revealed that, while the aquatic ecosystem responded to deteriorating moisture balance with a threshold response to hydrological closure of the lake basin, the surrounding terrestrial ecosystem evolved gradually from a grass savannah to Saharian scrubland to hyper-arid desert, between 5.6 and 2.7 ka.

Until recently, reconstructions of Holocene climate history in sub-Saharan Africa showed affinity with either Northern or Southern Hemisphere summer insolation forcing. A new 25-ka lake record from Lake Challa near Mt. Kilimanjaro, just south of the equator in East Africa, promises to reveal the history of hydrological change in the western Indian Ocean domain, where latitudinal ITCZ migration far north and south of the equator generates a markedly bimodal pattern of seasonal rainfall (Verschuren et al., ESF EuroCLIMATE project CHALLACEA). However, because the north-south trending Congo Air Boundary, where moisture from the Atlantic and Indian Ocean meet, is situated near ~33-35°E above the East African plateau, the climate history of much of tropical Africa bears a strong signature of variation in Atlantic Ocean circulation. This is particularly evident during the main phase of the Little Ice Age (LIA; 1400-1750 AD), when drought in western tropical Africa (Shanahan et al., 2009) and central equatorial Africa including western portions of the East African plateau (e.g, Russell and Johnson, 2007) contrasted with above-average rainfall over the eastern half of the plateau (Verschuren et al. 2000a). Lake Victoria

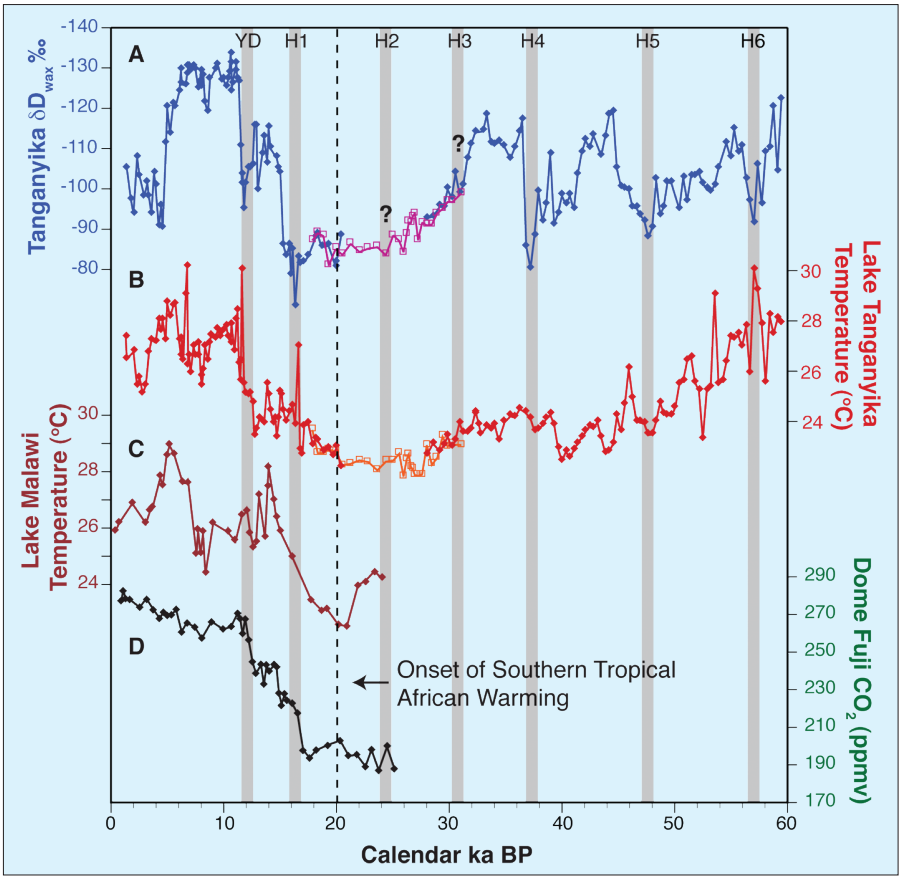

*Figure 1: Comparison of Lake Tanganyika $\delta D_{leaf\ wax}$-inferred regional moisture balance (**A**; blue and purple lines) and TEX_{86}-inferred temperature (**B**; red and orange lines) with the Lake Malawi TEX_{86}-inferred temperature (**C**; brown line; Powers et al., 2005), and glacial-to-Holocene record of atmospheric CO_2 in Dome Fuji ice (**D**; black line; Kawamura et al., 2007). Gray bars indicate the Younger Dryas (YD) and Heinrich events H1 to H6; H2 and H3 are not apparent in Tanganyika basin hydrology. Figure modified after Tierney et al. (2008).*

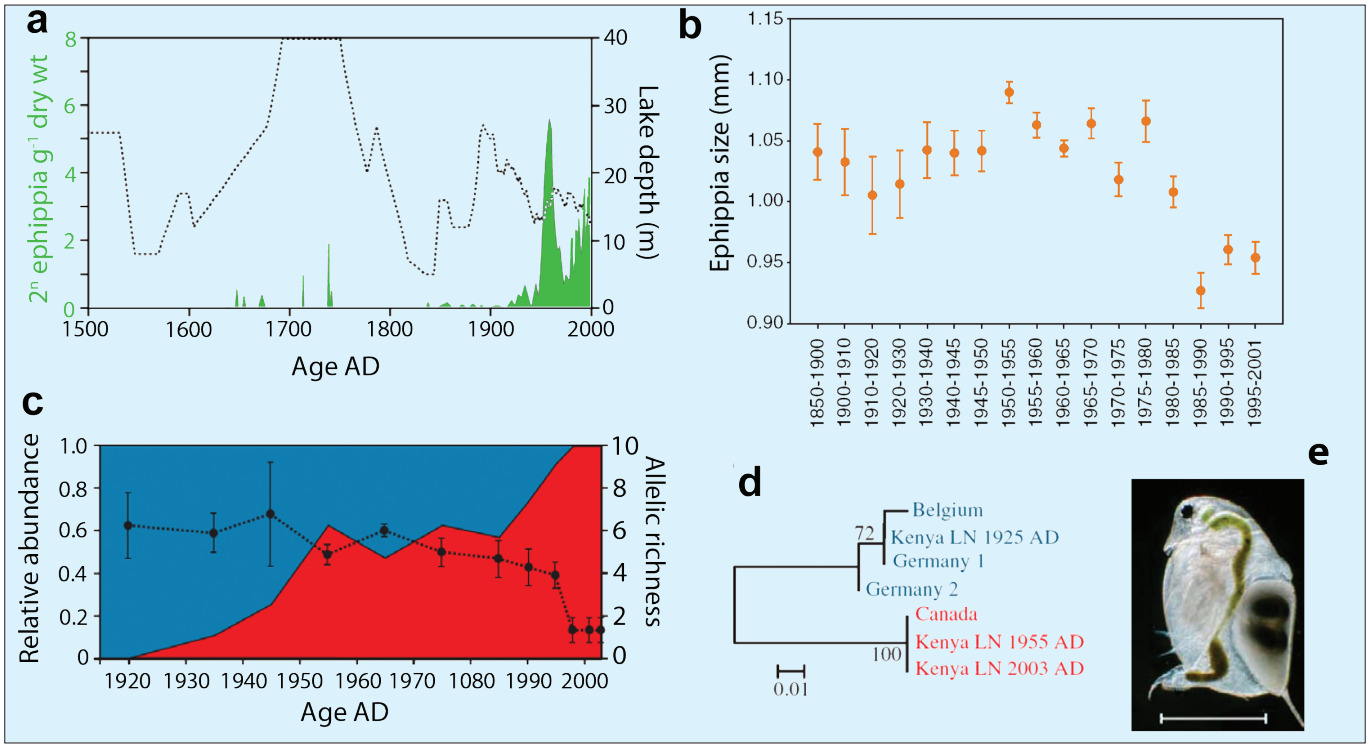

Figure 2: History of the water flea Daphnia pulex *population in Lake Naivasha (Kenya) reconstructed from the sediment record of its fossil resting eggs (ephippia).* ***a****) Population abundance through time (green area) in relation to historical lake-level fluctuations (dotted line), showing the relative scarcity of this species prior to the 1940s. 2^n = ephippia abundance on base 2 logarithmic scale.* ***b****) Evolution of mean water-flea body size since the mid-19th century derived from measurements of fossil ephippia. This indicates i) lowered size-selective fish predation in the 1950s due to fishery collapse associated with the mid-20th-century lowstand, and ii) recently increasing fish predation attributed to the disappearance of submerged aquatic macrophytes, which has resulted from anthropogenic siltation and eutrophication.* ***c****) Relative abundance of the asexual American genotype (red) and the indigenous African genotypes (blue) of* D. pulex *in Lake Naivasha since the inadvertent introduction of the American* D. pulex *variant during a fish-stocking effort in the 1920s, based on genetic analysis of multiple individual fossil ephippia in each sediment level; also shown is the associated loss in the local population's genetic diversity through time (allelic richness: dotted line with 95% confidence intervals).* ***d****) Phylogenetic tree based on a mitochondrial gene fragment showing the relationship of Lake Naivasha* D. pulex *in 1925, 1955 and 2003 to populations from Belgium and Germany ('Old World' genotypes, including Africa) and Canada ('New World' genotypes). The scale bar indicates genetic distance, i.e., the number of base substitutions between the different gene variants (haplotypes).* ***e****)* D. pulex *with eggs visible inside the ephippium. The scale bar is 1 mm. Figures a, c and d are from Mergeay et al. (2006), b is from Mergeay et al. (2004).*

(Stager et al., 2005) and central Ethiopia (Lamb et al., 2007) display intermediate LIA rainfall anomalies, reminiscent of the regional patterns of modern ENSO teleconnections (Verschuren and Charman, 2008).

Resolving human impact on African ecosystems

Lake Tanganyika, buffered against the immediate impact of catchment disturbance by great depth and permanent stratification, produced the first paleolimnological evidence of African lake-ecosystem response to anthropogenic climate change (O'Reilly et al., 2003). This would be much harder to demonstrate in records from shallower African lakes, of which the aquatic communities show continuous species turnover due to habitat restructuring associated with lake-level and salinity fluctuations (Verschuren et al., 1999; 2000b). Paleolimnological studies on the population genetics of water fleas in such lakes show that their genotypic identity is stable through time as long as episodes of ecological crisis (such as lake desiccation) do not exceed the few decades during which resting eggs remain viable in bottom muds (Mergeay et al., 2007). Another paleogenetic study (Mergeay et al., 2006) revealed that an asexual American variant of the common water flea *Daphnia pulex*, introduced accidentally to Lake Naivasha in Kenya in the 1920s, has since outcompeted the indigenous, sexually reproducing variant of the same species not only locally, but throughout sub-Saharan Africa (Fig. 2).

Outlook of paleolimnology in African lakes

With the spatial patterns of past hydrological change across tropical Africa now better constrained, studies of climate-human-environment interactions can start to make rigorous distinction between climate-driven and anthropogenic impacts on the long-term dynamics of vegetation, fire and lake-water quality. Although today's profound landscape modification has mostly resulted from rapidly increasing demographic and agricultural pressure during the 20th century (Verschuren et al., 2002; Fleitmann et al., 2007), significant vegetation disturbance by indigenous agriculturalists extends to the late 18th century near Lake Tanganyika (Cohen et al., 2005), the 17th century in the Kenya highlands (Lamb et al., 2003), and at least the 10-11th century in western Uganda (Ssemmanda et al., 2005; Lejju, 2009; Russell et al., 2009). In western tropical Africa, landscape disturbance is thought to have started ~2400 BP when climate-induced drying opened up the rainforest for farming (Ngomanda et al., 2009). Future studies will paint an increasingly comprehensive picture of the timing and relative magnitude of indigenous human impact on the African landscape. Focusing on the highest-quality lake-sediment records and through innovative use of both traditional and novel proxies, African paleolimnology will no doubt continue to make significant contributions to our understanding of past tropical climate dynamics and climate-human-ecosystem interaction.

References

Gasse, F., Chalié, F., Vincens, A., Williams, M.A.J. and Williamson, D., 2008: Climatic patterns in equatorial and southern Africa from 30,000 to 10,000 years ago reconstructed from terrestrial and near-shore proxy data, *Quaternary Science Reviews*, **27**: 2316-2340.

Kröpelin, S. et al., 2008: Climate-driven ecosystem succession in the Sahara: the past 6000 years, *Science*, **320**: 765-768.

Mergeay, J., Verschuren, D. and De Meester, L., 2006: Invasion of an asexual American water flea clone throughout Africa and rapid displacement of a native sibling species, *Proceedings of the Royal Society London B*, **273**: 2839-2844.

Scholz, C.A., et al., 2007: East African mega-droughts between 135 and 75 thousand years ago and bearing on early-modern human origins, *Proceedings of the National Academy of Scienes USA*, **104**: 16416-16421.

Tierney, J.E., Russell, J.M., Huang, Y.S. and Cohen, A.S., 2008: Northern Hemisphere controls on tropical Southeast African climate during the last 60,000 years, *Science*, **322**: 252-255.

For full references please consult:

www.pages-igbp.org/products/newsletters/ref2009_3.html

Full Reference List:

Bergner, A.G.N., Trauth, M.H. and Bookbagen, B., 2003: Paleoprecipitation estimates for the Lake Naivasha basin (Kenya) during the last 175 ky using a lake-balance model, *Global and Planetary Change*, **36**: 117-136.

Castañeda, I.S., Werne, J.P. and Johnson, T.C., 2007: Wet/arid phases in the southeast African tropics since the Last Glacial Maximum, *Geology*, **35**, 823-826.

Cohen, A.S., Palacios-Fest, M.R., Msaky, E.S., Alin, S.R., McKee, B.A., O'Reilly, C.M., Dettman, D.L., Nkotagu, H., and Lezzar, K.E., 2005: Paleolimnological investigations of anthropogenic environmental change in Lake Tanganyika: IX. Summary of paleorecords of environmental change and catchment deforestation at Lake Tanganyika and impacts on the Lake Tanganyika ecosystem, *Journal of Paleolimnology,* **34**: 125-145.

Cohen, A.S, et al., 2007: Ecological consequences of early Late Pleistocene mega-droughts in tropical Africa, *Proceedings of the National Academy of Science USA*, **104**: 16422-16427.

Duhnforth, M., Bergner, A.G.N. and Trauth, M.H., 2006: Early holocene water budget of the Nakuru-Elmenteita Basin, Central Kenya Rift, *Journal of Paleolimnology,* **36**: 281-294.

Eggermont, H., Heiri, O. M., Russell, J. M., Vuille, M., Audenaert, L. and Verschuren, D., 2009: Paleotemperature reconstruction in tropical Africa using fossil Chironomidae (Insecta: Diptera), *Journal of Paleolimnology*, doi 10.1007/s10933-009-9339-2.

Eggermont, H., Heiri, O. M. and Verschuren, D., 2006: Subfossil Chironomidae (Insecta: Diptera) as quantitative indicators of past salinity variation in African lakes, *Quaternary Science Reviews,* **25**: 1966-1994.

Felton, A.A., et al., 2007: Paleolimnological evidence for the onset and termination of glacial aridity from Lake Tanganyika, Tropical East Africa, *Palaeogeography, Palaeoclimatology, Palaeoecology*, **252**: 405-423.

Fleitmann, D., Dunbar, R.B., McCulloch, M., Mudelsee, M., Vuille, M., McClanahan, T., Andrews, C. and Mucciarone, D.A., 2007: East African soil erosion recorded in a 300-year old coral colony from Kenya, *Geophysical Research Letters,* **34**: L04401.

Garcin, Y., Vincens, A., Williamson, D., Guiot, J. and Buchet, G., 2006: Wet phases in tropical southern Africa during the last glacial period, *Geophysical Research Letters*, **33**: L07703.

Garcin, Y., Vincens, A., Williamson, D., Buchet, G. and Guiot, J., 2007: Abrupt resumption of the African Monsoon at the Younger Dryas-Holocene climatic transition, *Quaternary Science Reviews,* **26**: 690-704.

Gasse, F., Chalié, F., Vincens, A., Williams, M.A.J. and Williamson, D., 2008: Climatic patterns in equatorial and southern Africa from 30,000 to 10,000 years ago reconstructed from terrestrial and near-shore proxy data, *Quaternary Science Reviews,* **27**: 2316-2340.

Johnson, T.C., Brown, E.T., McManus, J., Barry, S., Barker, P. and Gasse, F., 2002: A high-resolution paleoclimate record spanning the past 25,000 years in southern East Africa, *Science*, **296**: 113-116.

Kawamura, K. et al., 2007: Northern hemisphere forcing of climatic cycles in Antarctica over the past 360,000 years, *Nature*, **448**: 912-916.

Kröpelin, S. et al., 2008: Climate-driven ecosystem succession in the Sahara: the past 6000 years, *Science,* **320**: 765-768.

Lamb, H., Darbyshire, L. and Verschuren, D., 2003: Vegetation response to rainfall variation and human impact in central Kenya during the past 1100 years, *The Holocene*, **13**: 285-292.

Lamb, H.F., Leng, M.J., Telford, R.J., Ayenew, T. and Umer, M., 2007. Oxygen and carbon isotope, composition of authigenic carbonate from an Ethiopian lake: a climate record of the last 2000 years, *The Holocene*, **17**, 517-526.

Legesse, D., Vallet-Coulomb, C. and Gasse, F., 2004: Analysis of the hydrological response of a tropical terminal lake, Lake Abiyata (Main Ethiopian Rift Valley) to changes in climate and human activities, *Hydrological Processes*, **18**, 487-504.

Lejju, J.B., 2009: Vegetation dynamics in western Uganda during the last 1000 years: climate change or human induced environmental degradation? *African Journal of Ecology,* **47**: 21-29.

Mergeay, J., Verschuren, D., Van Kerckhoven, L. and De Meester, L., 2004: Two hundred years of a diverse *Daphnia* community in Lake Naivasha (Kenya): effects of natural and human-induced environmental changes, *Freshwater Biology,* **49**: 998-1013.

Mergeay, J., Verschuren, D. and De Meester, L., 2006: Invasion of an asexual American water flea clone throughout Africa and rapid displacement of a native sibling species, *Proceedings of the Royal Society London B*, **273**: 2839-2844.

Mergeay, J., Vanoverbeke, J., Verschuren, D. and De Meester, L., 2007: Extinction, re-colonization, and dispersal through time in a planktonic crustacean, *Ecology*, **88**: 3032-3043.

Nash, D.J., Meadows, M.E. and Gulliver, V.L., 2006: Holocene environmental change in the Okavango Panhandle, northwest Botswana, *Quaternary Science Reviews,* **25**: 1302-1322.

Ngomanda, A., Neumann, K., Schweizer, A. and Maley, J., 2009: Seasonality change and the third millennium BP rainforest crisis in southern Cameroon (Central Africa), *Quaternary Research*, **71**: 307-318.

O'Reilly, C.M., Alin, S.R., Plisnier, P.D., Cohen, A.S. and McKee, B.A., 2003: Climate change decreases aquatic ecosystem productivity of Lake Tanganyika, Africa, *Nature*, **424**: 766-768.

Powers, L. A., Johnson, T.C., Werne, J.P., Castañeda, I.S., Hopmans, E.F., Sinninghe Damsté, J.S. and Schouten, S., 2005: Large temperature variability in the southern African tropics since the Last Glacial Maximum, *Geophysical Research Letters,* **32**: L08706.

Rumes, B., Eggermont, H. and Verschuren, D., 2005: Subfossil representation of aquatic invertebrate communities in a salinity gradient of western Uganda crater lakes, *Hydrobiologia*, **542**: 297-314.

Russell, J.M. and Johnson, T.C., 2007. Little Ice Age drought in equatorial Africa: ITCZ migrations and ENSO variability, *Geology*, **35**: 21-24.

Russell, J.M., McCoy S.J., Verschuren, D., Bessems, I., Blaauw, M. and Huang, Y., 2009: Human impacts, climate change, and aquatic ecosystem response during the past 2,000 years at Lake Wandakara, Uganda, *Quaternary Research*, doi 10.1016/j.yqres.2009.06.008.

Scholz, C.A., et al., 2007: East African mega-droughts between 135 and 75 thousand years ago and bearing on early-modern human origins, *Proceedings of the National Academy of Scienes USA,* **104**: 16416-16421.

Ssemmanda, I., Ryves, D.B., Bennike, O. and Appleby, P.G., 2005: Vegetation history in western Uganda during the last 1200 years: a sediment-based reconstruction from two crater lakes, *The Holocene*, **15**: 119-132.

Shanahan, T.M., Overpeck, J.T., Anchukaitis, K.J., Beck, J.W., Cole, J.E., Dettman, D.L., Peck, J.A., Scholz, C.A. and King, J.W., 2009: Atlantic forcing of persistent drought in West Africa, *Science*, **324**: 377-380.

Stager, J.C., Ryves, D., Cumming, B.F., Meeker, L.D. and Beer, J., 2005: Solar variability and the levels of Lake Victoria, East Africa, during the last millennium, *Journal of Paleolimnology*, **33**: 243-251.

Talbot, M.R., Filippi, M.L., Jensen, N.B. and Tiercelin, J.-J., 2007: An abrupt change in the African monsoon at the end of the Younger Dryas, *Geochemistry, Geophysics, Geosystems,* **8**: Q03005.

Tierney, J.E., Russell, J.M., Huang, Y.S. and Cohen, A.S., 2008: Northern Hemisphere controls on tropical Southeast African climate during the last 60,000 years, *Science*, **322**: 252-255.

Verschuren, D. and Charman, D., 2008: Latitudinal linkages in late-Holocene moisture-balance variation. In: Battarbee, R.W. et al. (Eds), *Natural climate variability and global warming,* Blackwell, 189-231.

Verschuren, D., Tibby, J., Leavitt, P.R. and Roberts, C.N., 1999: The environmental history of a climate-sensitive lake in the former 'White Highlands' of central Kenya, *Ambio*, **28**: 494-501.

Verschuren, D., Laird, K.R. and Cumming, B.F., 2000a: Rainfall and drought in equatorial East Africa during the past 1100 years, *Nature*, **403**: 410-414.

Verschuren, D., Tibby, J., Sabbe, K. and Roberts, N., 2000b: Effects of lake level, salinity and substrate on the invertebrate community of a fluctuating tropical lake, *Ecology* **81**: 164-182.

Verschuren, D., Johnson, T.C., Kling, H.J., Edgington, D.N., Leavitt, P.R., Brown, E.T., Talbot, M.R. and Hecky, R.E., 2002: History and timing of human impact on Lake Victoria, East Africa, *Proceedings of the Royal Society London B,* **269**: 289-294.